Molecular Determinants of Tbx20 Activity during Cardiac Development

Erin Kaltenbrun

A dissertation submitted to the faculty of the University of North Carolina at Chapel Hill in partial fulfillment of the requirements for the degree of Doctor of Philosophy in the Department of Biology.

Chapel Hill

2013

Approved by:

Frank Conlon

Kenneth Poss

Jason Lieb

Robert Duronio

Stephen Crews

ABSTRACT

ERIN KALTENBRUN: Molecular Determinants of Tbx20 Activity during Cardiac Development
(Under the direction of Dr. Frank L. Conlon)

The formation of the heart is a complex process that requires the combinatorial activity of a number of critical cardiogenic transcription factors that function to drive distinct gene subprograms in the developing heart. Tbx20 is a potent activator of cardiac gene expression, and has also been shown to act as a transcriptional repressor in the heart. Precise regulation of Tbx20 expression levels and activity is crucial for normal heart development, as alterations in Tbx20 levels and activity lead to a spectrum of cardiac defects in humans and in animal models. Despite the importance of Tbx20 in heart development, very little is known about how *Tbx20* expression is regulated in the heart. Further, the mechanisms by which Tbx20 acts to regulate its target genes are not understood. Here we explore the Tbx20 transcription network, both at the gene and protein level, to identify critical determinants of Tbx20 activity during heart development.

We have identified a crucial role for BMP signaling in maintaining *Tbx20* cardiac expression during cardiac chamber maturation. This regulation is mediated by a minimal 334 bp regulatory element that is sufficient to drive cardiac expression

of *Tbx20* in *Xenopus*, zebrafish, and mouse, indicating that this regulatory pathway is evolutionarily conserved among vertebrates. To begin to decipher how Tbx20 regulates its target genes, we have undertaken a proteomic screen of Tbx20 transcription complexes, both in human cells and mouse embryonic stem cell-derived cardiomyocytes. These studies resulted in the identification of a broad chromatin remodeling network that includes both co-activators and co-repressors. Specifically, Tbx20 directly recruits a Groucho/TLE and histone deacetylase repressor complex through an N-terminal eh1 domain. Additionally, Tbx20 recruits multiple chromatin remodelers including components of the SWI/SNF complex, the NuRD complex, and the INO80 complex. Collectively, these studies suggest that Tbx20 controls gene expression in the developing heart through selective association with distinct chromatin remodeling complexes. This work provides insight into how Tbx20 activity is regulated during cardiac development.

Acknowledgments

There are many people that have been critical to the success of my graduate studies. I would first like to thank current and past members of the Conlon Lab for helpful discussions, advice, support, and technical know-how: Elizabeth Mandel, Kathleen Christine, Chris Showell, Panna Tandon, Lauren Kuchenbrod, Lauren Waldron, Nirav Amin, Stephen Sojka, Kerry Dorr, Marta Charpentier, Chris Slagle, Michelle Villasmil, and Leslie Kennedy. Special thanks to Kathleen Christine and Chris Showell for being excellent mentors and friends my first few years in the lab, and to Kerry Dorr for being my lab BFF for the last five years. This experience would not have been the same without her friendship and unyieldingly positive attitude.

I cannot thank or acknowledge Frank Conlon enough. He has been so supportive of my career. He has been enthusiastic when I was down, always available when I needed to bounce ideas around, and has allowed me an enormous amount of independence. This mentoring has helped me to grow as a scientist and a professional and for that I am extremely grateful. It is also a joy to work for someone that truly cares about the people in his lab, not only from a scientific perspective, but also on a personal level. For this reason, the morale in the Conlon Lab is extremely

high and there is a lot of camaraderie, qualities that have made coming to work a pleasure even when science wasn't going so well.

I would also like to thank my committee members Bob Duronio, Jason Lieb, Steve Crews, and Ken Poss. One of the things that drew me to UNC was the faculty commitment to good training, and my committee has demonstrated this commitment throughout my graduate training. I am grateful for their insights and helpful discussions on my work.

Finally, I would like to thank my family and friends for their support, encouragement, and friendship. I would especially like to thank my father, who passed away before I started graduate school but would have been so thrilled to be a part of this journey. I also need to thank my partner, Riley, whose companionship, honesty, wisdom, tolerance, and love have uplifted me every day that we have been together.

Table of Contents

List of Figures

List of Tables

Table

List of Abbreviations

Affinity Purification- Mass Spectrometry	AP-MS
Alpha-cardiac Myosin Heavy Chain 6	Myh6
Alpha/Beta-Myosin Heavy Chain	α/β-MHC
Amino Enhancer of Split	Aes
Atrial Natriuretic Factor	ANF
Atrial Septal Defects	ASD
Avitag	Avi
Axenfeld-Rieger Syndrome	ARS
B-type Natriuretic Peptide	BNP
basic Helix Loop Helix	bHLH
Bone Morphogenetic Protein	BMP
BRG1-Associated Factor	BAF
Cardiac alpha-actin	αCA
Cardiac Troponin T	cTnT
Coloboma, Heart Defects, choanal Atresia, Retarded growth and development, Genital abnormalities, and Ear anomalies	CHARGE
Congenital Heart Disease	CHD
Connexin	Cx
DiGeorge Syndrome	DGS
Embryoid Bodies	EBs
Embryonic day	E
Embryonic Stem Cell	ESC

Engrailed Homology 1	eh1
Epicardium-derived cells	EPDCs
Fibroblast Growth Factor	FGF
Groucho	Gro
Histone Deacetylase	HDAC
Histone Methyltranserase	HMT
Holt-Oram Syndrome	HOS1
Human Embryonic Kidney	HEK
Lymphoid Enhancer Binding Factor	LEF
Metastasis-associated Protein	MTA
Methyl-CpG Binding Domain Protein 3	MBD3
Morpholino	MO
Myocyte Enhancer Factor 2	MEF2
Neuromancer	nmr
Nucleolin	NCL
Nucleophosmin	NPM1
Nucleosome Remodeling and Deacetylase	NuRD
Outflow Tract	OFT
Polybromo- and BAF-containing	PBAF
Pro-epicardium	PEO
Restriction Enzyme Mediated Integration	REMI
Serum Response Factor	SRF
SWItch/Sucrose NonFermentable	SWI/SNF

T-box containing protein	Tbx
Transcription Factor 3	TCF3
Transducin-like enhancer of split	TLE
Transforming Growth Factor Beta	TGFβ
Ventricular Septal Defects	VSD
Wolf-Hirschorn Syndrome	WHS
Xenopus Brachyury	Xbra
Xenopus Dorsal Marginal Zone	DMZ
Xenopus Ventral Marginal Zone	VMZ

Chapter 1

Introduction

The heart is one of the first structures to form during embryonic development, and cardiac precursor cells are among the first cells of the epiblast to ingress during gastrulation. Fate-mapping studies in mice have determined that prospective heart mesoderm is localized in the anterior portion of the primitive streak (Lawson et al., 1991; Parameswaran and Tam, 1995). In the early to mid-streak stages, heart mesoderm progenitors begin to migrate from the anterior primitive streak to the anterior proximal region of the epiblast (future anterior ventral midline of the embryo) and come to lie underneath the head folds, forming a structure known as the cardiac crescent (Parameswaran and Tam, 1995; Tam et al., 1997). By the late primitive streak stages (E7-7.5), cells of the cardiac crescent begin to express the first markers of heart mesoderm including *Nkx2.5*, *Gata4/5*, *Tbx5*, and *Tbx20* (Arceci et al., 1993; Komuro and Izumo, 1993; Horb and Thomsen, 1999; Carson et al., 2000).

Myocardial precursor cells undergo a number of sequential, but overlapping processes to become terminally differentiated cardiomyocytes. Studies have demonstrated important roles for a number of signaling families in early cardiac

specification including the BMP, FGF, Hedgehog, and Wnt families (Reifers et al., 2000; Zhang et al., 2001; Gadue et al., 2006; Foley et al., 2007; Kattman et al., 2011). Integration of these signals by prospective cardiac precursors during gastrulation and anterolateral migration triggers heart field patterning and commitment to a myocardial fate. Expression of *Mesp1*, a bHLH transcription factor, is transiently expressed in prospective cardiac mesoderm and is thought to act as a molecular switch during cardiac specification by activating many of the key genes within the core cardiac transcription network and repressing genes that promote early mesoderm and endoderm cell fates (Bondue et al., 2008). Combinatorial expression of the transcription factors *Nkx2.5*, *Gata4/5*, *Tbx5*, and *Tbx20* within the early heart field marks cardiac progenitors. Recent work in this field supports the idea that these transcription factors are core components of a large regulatory network that drives myocardial lineage development and morphogenesis of the early embryonic heart. Additionally, the importance of *Nkx2.5*, *Gata4/5*, *Tbx5*, and *Tbx20* as critical modifiers of cardiac cell fate and morphogenesis is underscored by the identification of mutations within these genes that are associated with a variety of congenital heart malformations in humans (Basson et al., 1997; Schott et al., 1998; Pehlivan et al., 1999; Kirk et al., 2007). Therefore, it is critical to identify and understand the protein-protein interactions, transcriptional targets, and upstream regulators of these core cardiac transcription factors.

Here, we investigate the molecular regulators of Tbx20 expression and function during cardiac development. Within this cohort of core cardiac transcription

factors, Tbx20 is unique in that it is expressed uniformly throughout all layers (epicardium, myocardium, and endocardium) of the forming heart during development and adulthood. Additionally, this expression pattern is conserved from flies to humans implying a fundamental role for Tbx20 in proper heart development and function (Ahn et al., 2000; Griffin et al., 2000; Meins et al., 2000; Iio et al., 2001; Brown et al., 2003; Huang et al., 2012; Sakabe et al., 2012). We provide evidence that BMP signaling is required to maintain Tbx20 expression in the heart during cardiac chamber formation, suggesting a critical role for the BMP pathway in driving proper regionalization of cardiac chambers (Mandel et al., 2010). We also show that Tbx20 interacts with a unique transcription repression network that includes components of both the Nucleosome Remodeling and Deacetylase (NuRD) complex and Groucho/TLE co-repressors. We predict that the Tbx20 repression network is essential to prevent inappropriate gene activation within the developing heart. Finally, we have developed a novel approach to identify endogenous cardiac-specific Tbx20 interaction partners over the course of cardiomyocyte development, which has resulted in the discovery of new components of the Tbx20 regulatory network. First, I will introduce the current understanding of relationships within the core cardiac transcription factor network, highlighting the roles of critical activating and repressing transcription factor protein complexes in specifying and maintaining cardiac cell fate.

A CORE CARDIAC TRANSCRIPTION FACTOR NETWORK

In addition to the core factors Mesp1, Nkx2.5, Tbx5, Tbx20, and Gata4, other transcription factors are expressed and have critical functions during cardiogenesis. In particular, MEF2 factors and SRF, additional T-box proteins including Tbx1, Tbx2, Tbx3, and Tbx18, as well as the homeodomain protein Isl1 have each been shown to be important for proper heart development (Lin et al., 1997; Wang et al., 2001a; Vitelli et al., 2002; Cai et al., 2003; Harrelson et al., 2004; Hoogaars et al., 2004; Christoffels et al., 2006). Collectively, these transcription factors act in interconnected pathways to regulate the expression of each other, as well as downstream gene targets to control heart development. The transcription factors Nkx2.5, Tbx5, Tbx20, Gata4, and Mef2C also physically interact with each other, implying that the transcriptional control of heart development is directed by cardiogenic transcription factors that are linked genetically and biochemically via large multimeric protein complexes (Figure 1.1) (Morin et al., 2000; Hiroi et al., 2001; Sepulveda et al., 2002; Stennard et al., 2003; Vincentz et al., 2008; Munshi et al., 2009; Junion et al., 2012).

Positive regulation of cardiac cell fate: Evidence for a Transcription Factor Collective

Over the last two decades, studies regarding the relationships between cardiac transcription factors support the notion that core cardiac transcription factors promote specification, proliferation, and differentiation of cardiac precursor cells, as well as morphogenetic movements of the primitive heart tube, via protein-protein interactions with other transcription factors (Figures 1.2, 1.3, 1.4, and 1.5). These

protein-protein interactions appear to be critical to ensure activation of multiple cardiac genes, and thus point to a “transcription factor collective” model in which cardiogenic transcription factors bind to and activate cardiac enhancers cooperatively. I present the following examples in support of this model:

Nkx2.5

Nkx2.5 encodes a homeobox transcription factor that was originally cloned from *Drosophila* (*msh-2, tinman*) in a screen looking for new mesoderm-specific homeobox genes (Bodmer et al., 1990). *Tinman* is expressed in mesoderm primordium in the early embryo; however, expression later becomes restricted to the visceral mesoderm and the heart (Bodmer et al., 1990). *Drosophila* embryos with mutant *tinman* lack both heart precursor cells and differentiated heart cells indicating a role for *tinman* in heart precursor specification (Bodmer, 1993). The vertebrate homolog of tinman, *Nkx2.5* (*Csx*), was independently cloned in the mouse, chick, fish, and frog. In all species examined, *Nkx2.5* is expressed in early cardiomyocyte precursors (Komuro and Izumo, 1993; Lints et al., 1993; Tonissen et al., 1994; Schultheiss et al., 1995; Chen and Fishman, 1996). Targeted deletion of *Nkx2.5* in the embryonic heart arrests heart tube morphogenesis and looping, resulting in embryonic death at E9-10 (Lyons et al., 1995). Additional studies in *Xenopus* demonstrate that *XNkx2.5* overexpression results in an enlarged heart, consistent with a critical role for Nkx2.5 in maintenance of the heart fields (Cleaver et al., 1996). Interestingly, co-injection of dominant negative repressor derivatives of XNkx2.3 and XNkx2.5 into *Xenopus* embryos causes a more severe cardiovascular phenotype

than repression of XNkx2.5 alone with a complete loss of differentiated myocardium (Fu et al., 1998; Grow and Krieg, 1998). This finding suggests that there may be some functional redundancy among the NK/tinman family members and helps to explain why *Nkx2.5* knockout mice are able to generate a primitive heart tube. Early studies defined Nkx2.5 as a transcriptional activator capable of binding novel homeodomain sites as well as sites that resemble serum response elements (Chen and Schwartz, 1995), which serve as binding sites for the MADs box transcription factor SRF (Treisman, 1986).

Initial studies on Nkx2.5-mediated transcriptional regulation revealed that Nkx2.5 interacts with a number of factors to regulate gene expression in the heart. Nkx2.5 interacts with Gata4 and SRF to activate *cardiac alpha-actin* (αCA) gene expression (Chen and Schwartz, 1996; Sepulveda et al., 1998; Sepulveda et al., 2002) and interacts with Gata4 to activate *atrial natriuretic factor* (*ANF*) expression (Durocher et al., 1997; Lee et al., 1998; Sepulveda et al., 1998). A recent study demonstrated that Nkx2.5 interacts directly with the MADs box transcription factor Mef2c (Vincentz et al., 2008). Interestingly, allele inactivation of *Mef2c* results in a similar phenotype to *Nkx2.5* deficient animals, with arrested heart looping and defective cardiomyocyte differentiation (Lin et al., 1997; Vong et al., 2006). *Mef2c* and *Nkx2.5* also genetically interact; compound deletion of both genes results in a global loss of ventricular markers relative to the single mutants indicating a role for this complex in promoting ventricular identity (Vincentz et al., 2008). Additionally, Nkx2.5 has been shown to interact with the bHLH transcription factor Hand2 to

promote ventricular differentiation (Yamagishi et al., 2001). *Nkx2.5*$^{-/-}$; *Hand2*$^{-/-}$ mutants have a single atrial chamber, and expression of *Irx4*, a ventricle-specific gene, is completely abolished, thereby suggesting that Nkx2.5 and Hand2 promote ventricle differentiation in part through cooperative regulation of *Irx4* (Yamagishi et al., 2001). Aside from its role in promoting normal differentiation and morphogenesis of chamber myocardium, Nkx2.5 is also critical for development of the cardiac conduction system. *Nkx2.5* dosage is directly proportional to the number of cells in the cardiac conduction system pointing to a role for Nkx2.5 in promoting the genetic conduction program (Jay et al., 2004). Nkx2.5 was later found to promote specification of ventricular myocytes into ventricular conduction system cells through a genetic interaction with *Tbx5*, which together cooperatively regulate *Id2* and other conduction system genes (Moskowitz et al., 2007). Collectively, these studies demonstrate that interaction of Nkx2.5 with other cardiogenic transcription factors is critical for proper regulation of downstream cardiac genes, and subsequent activation of the appropriate cardiac gene program (Figure 1.2). The choice of protein co-factor may also provide an additional level of specificity for Nkx2.5-mediated gene regulation.

The importance of Nkx2.5 function in establishing the early heart field is underscored by identification of mutations in human *NKX2.5* that are associated with non-syndromic atrial septal defects (ASD), atrioventricular conduction abnormalities, ventricular septal defects (VSD), tetralogy of Fallot, double-outlet right ventricle, and valve diseases (Schott et al., 1998; Benson et al., 1999). All mutations characterized

thus far, most of which are truncations or missense mutations in the homeodomain, are predicted to augment DNA binding. These data suggest that the principal determinant of the congenital heart defects associated with *NKX2.5* mutations is the total dosage of *NKX2.5* capable of binding to DNA (Schott et al., 1998; Kasahara et al., 2000; Kasahara and Benson, 2004).

Gata4

Gata4 is a member of the GATA transcription factor family, which contains two zinc fingers that are required for binding to the GATA binding sequence [(A/T)GATA(A/G)] (Molkentin, 2000). *Gata4* was identified in a screen of a mouse embryo cDNA library searching for new GATA-binding factors and was enriched in heart tissue (Arceci et al., 1993). A second group independently identified *Gata4* in a *Xenopus* tadpole liver cDNA library and demonstrated that *Gata4* is expressed in presumptive cardiac ventral mesoderm (Kelley et al., 1993). In the primitive heart, *Gata4* is expressed in the developing atria and ventricles, as well as the endocardium. Expression in the heart persists through gestation and after birth (Kelley et al., 1993; Heikinheimo et al., 1994). Early studies in cell culture models of cardiac differentiation suggest that Gata4 plays a role in cardiomyocyte differentiation (Grepin et al., 1995; Grepin et al., 1997). However, *Gata-4* null mice form relatively normal differentiated myocardium leading to hypotheses about the possible redundancy of Gata4 with other Gata factors (*Gata5/6* are also expressed in the developing heart) or with other cardiac transcription factors (Kuo et al., 1997; Molkentin et al., 1997). Though *Gata4*$^{-/-}$ cardiac precursors undergo differentiation,

the cardiomyocytes fail to migrate to the ventral midline and instead generate cardiac structures in the dorsolateral regions of the embryo indicating that Gata4 is essential for migration of the presumptive heart fields (Kuo et al., 1997; Molkentin et al., 1997).

Gata4 acts as a potent transactivator of cardiac genes (Figure 1.3). Gata4 physically interacts with Gata6 in the myocardium to cooperatively activate *ANF/Nppa* and *B-type natriuretic peptide* (*BNP*) transcription, providing at least one example in which Gata4 and Gata6 act in the same transcriptional pathway (Charron et al., 1999). As previously described, Gata4 interacts with Nkx2.5 on the *αCA* and *ANF/Nppa* promoters (Durocher et al., 1997; Shiojima et al., 1999; Small and Krieg, 2003). Synergistic activation of *ANF/Nppa* by Nkx2.5 and Gata4 relies on an Nkx2.5-binding element in the *ANF/Nppa* promoter, suggesting that Nkx2.5 recruits Gata4 to the promoter (Shiojima et al., 1999). Similarly, Gata4 has been shown to interact with Tbx5 and Mef2C to activate the *ANF/Nppa* promoter. Gata4-Isl1 complexes activate *Mef2c* expression in the second heart field, a region of cardiogenic mesoderm that resides anterior to the primary heart field and gives rise to the outflow tract and portions of the right ventricle (Morin et al., 2000; Garg et al., 2003; Dodou et al., 2004). Gata4 and Tbx5 also cooperatively activate expression of *connexin 30.2* (*Cx30.2*), a gap junction protein required for atrioventricular node delay, in the conduction system (Munshi et al., 2009). Interestingly, a heterozygous missense mutation in human *GATA4* that is associated with cardiac septal defects disrupts the physical interaction between Gata4 and Tbx5, underscoring the

importance of the GATA4-TBX5 interaction in human heart development and supporting the idea that disruption of the core cardiac transcription factor network leads to major cardiac anomalies (Garg et al., 2003). *GATA4* haploinsufficiency also leads to congenital heart defects in humans: patients with monosomy 8p23.1 (deletion of the distal arm of chromosome 8p) and congenital heart disease were found to have deletions at the *GATA4* locus (Pehlivan et al., 1999). A del(8)(p23.1) patient who lacked cardiac anomalies did not have a *GATA4* deletion, indicating that *GATA4* deficiency directly contributes to congenital heart disease (Pehlivan et al., 1999).

Tbx5

TBX5, a member of the T-box family of transcription factors [*Brachyury (T)* gene family], was originally identified as a gene mutated in Holt-Oram syndrome (HOS1) patients (Basson et al., 1997; Li et al., 1997). HOS1 is an autosomal dominant disorder that is characterized by cardiac and skeletal defects including upper limb defects, ASD, VSD, and tetralogy of Fallot (Hurst et al., 1991). Detailed mapping of the genomic region responsible for HOS1 revealed mutations in *TBX5*. *TBX5* was subsequently found to be expressed in the human embryonic heart and limbs (Li et al., 1997). Interestingly, different *TBX5* mutations result in distinct HOS1 clinical features. Null mutations in *TBX5* lead to defects in both the limbs and heart, whereas missense mutations can produce significant cardiac defects with minor skeletal defects or minor cardiac abnormalities with extensive limb malformations (Basson et al., 1999). Structural analyses of the location of *TBX5* missense

mutations revealed that different mutations are predicted to perturb distinct target DNA interactions (binding to the major groove of DNA versus the minor groove), indicating that *TBX5* may interact with DNA differently in the developing heart compared to the limbs (Basson et al., 1999). In vitro binding assays have identified an octamer sequence [AGGTGTG(A/G)] to which Tbx5 binds that is part of the Brachyury consensus half site (Ghosh et al., 2001; Macindoe et al., 2009). Tbx5 can also bind the full palindromic *Brachyury* binding site indicating there is some flexibility in Tbx5 target sequence grammar (Ghosh et al., 2001).

The precise role of Tbx5 in heart development was first assessed in *Xenopus*, where *Tbx5* is expressed throughout the early heart field and within the forming heart tube in all but the most anterior region, the bulbus cordis (Horb and Thomsen, 1999). Inhibition of XTbx5 using a dominant negative repressor version of the protein results in a dose-dependent block in heart formation, highlighting a global role for Tbx5 in heart formation (Horb and Thomsen, 1999). In the mouse and chick, *Tbx5* is expressed uniformly throughout the cardiac crescent. However, upon formation of the heart tube, *Tbx5* expression becomes graded with stronger expression at the posterior end (Bruneau et al., 1999). In the looped heart, *Tbx5* is expressed in the left ventricle, but not the right ventricle or the outflow tract (Bruneau et al., 1999). Heterozygous *Tbx5*$^{+/-}$ mice phenocopy defects seen in HOS1 patients; homozygous deletion of *Tbx5* in the mouse results in severe hypoplasia within the posterior region of the heart and reduced expression of *ANF/Nppa* and *connexin 40* (*Cx40*) (Bruneau et al., 2001). In agreement with these studies, Tbx5 physically binds Nkx2.5 and

Gata4 to synergistically promote *ANF/Nppa* expression (Bruneau et al., 2001; Hiroi et al., 2001; Garg et al., 2003) and modulates *Cx40* expression in combination with Nkx2.5 and Gata4 (Linhares et al., 2004). Additionally, *Tbx5* and *Gata4* genetically interact; mice heterozygous for both alleles have atrioventricular septal defects and myocardial thinning, defects distinct from the isolated ASD observed in *Tbx5* heterozygotes (Maitra et al., 2009). Tbx5 also forms a complex with Mef2C on the *alpha-cardiac myosin heavy chain* (*Myh6*) promoter to drive *Myh6* expression and normal heart patterning (Ghosh et al., 2009). Collectively, these studies have identified Tbx5 as a crucial node within the cardiac transcription network (Figure 1.4). Recent studies have continued to investigate the functions of Tbx5 in different cardiac cell populations. This work has revealed an essential function for Tbx5 in directing ventricular and atrial septation (Takeuchi et al., 2003; Xie et al., 2012), specifying the proepicardium (Liu and Stainier, 2010), patterning of the conduction system (Moskowitz et al., 2004; Moskowitz et al., 2007), and regulating cardiac cell cycle progression (Goetz et al., 2006). Further studies are required to explore how Tbx5 intersects with other transcription factor pathways to regulate these diverse processes.

Tbx20

Tbx20 (*H15, Tbx12, HrT*) was independently identified in human, mouse, zebrafish, and *Drosophila* as a novel T-box gene expressed in the heart (Ahn et al., 2000; Carson et al., 2000; Griffin et al., 2000; Meins et al., 2000). Shortly thereafter, *Tbx20* was identified in *Xenopus* and chick (Iio et al., 2001; Brown et al., 2003). In all

of these species, *Tbx20* transcipts are enriched in the anterior lateral plate mesoderm and gradually become restricted to the cardiac primordial prior to ventral migration. Expression is maintained in the primary heart field throughout the process of migration, looping, and cardiac chamber formation. Thus, *Tbx20* is expressed at the same time, and in many of the same regions as the transcription factors *Tbx5*, *Nkx2.5*, and *Gata4*. Morpholino knockdown of the Tbx20 protein in *Xenopus* embryos results in a loss of cardiomyocytes and unlooped hearts, but cardiac specification and migration proceeds normally (Brown et al., 2005). In agreement with these studies, deletion of *Tbx20* in mice also results in a loss of cardiomyocytes, failure to loop, and defects in cardiomyocyte maturation and chamber specialization (Cai et al., 2005; Singh et al., 2005; Stennard et al., 2005; Takeuchi et al., 2005). Moreover, the role of Tbx20 in heart formation appears to be evolutionarily ancient, with *Drosophila* having two Tbx20 orthologues, *neuromancer* (*nmr1*) and *neuromancer2* (*nmr2*), which are also referred to as *H15* and *midline*, respectively. Like *Tbx20,* this pair of genes is required for proper development of the dorsal vessel, a structure thought to be homologous to the vertebrate heart (Miskolczi-McCallum et al., 2005; Qian et al., 2005; Reim et al., 2005).

Recent studies have identified a number of patients with dilated cardiomyopathy, ASD, or mitral valve disease that carry mutations in *TBX20*. Additionally, upregulated *TBX20* gene expression has been linked to tetralogy of Fallot (Kirk et al., 2007; Hammer et al., 2008; Qian et al., 2008; Posch et al., 2010). Of the 12 mutant forms of *TBX20* associated with congenital heart disease, eight are

missense mutations within the T-box domain, and two are identical mutations in unrelated individuals. Of the remaining four *TBX20* mutations, one is a missense mutation leading to truncation of *TBX20* in the T-box domain and the other three are missense mutations mapping to two different regions of unknown function. Interestingly, one of the missense mutations in the T-box domain is a gain-of-function mutation that enhances transcriptional activity and increases occupancy of DNA (Posch et al., 2010). These genetic studies imply that precise regulation of both TBX20 expression and transcriptional activity is critical for normal heart development.

Similar to Tbx5, the optimal binding site for Tbx20 corresponds to a T-half-site (Macindoe et al., 2009). The Tbx20 binding site differs from that of Tbx5 in that it does not display any variation in the last nucleotide position (AGGTGTGA). Additionally, Tbx5 and Tbx20 exhibit different binding affinities and kinetics on T-half-sites, thus implying that there may be some degree of T-box competition on cardiac gene promoters (Macindoe et al., 2009).

Although T-box binding elements may predominantly control localization of Tbx20 to sites within the genome, the function of Tbx20 as a transcriptional activator or repressor likely relies on protein-protein interactions with transcription factor partners. A number of studies suggest that Tbx20 physically interacts with Isl1, Nkx2.5, and Gata4 to positively regulate cardiac genes including *ANF/Nppa* (Stennard et al., 2003; Takeuchi et al., 2005; Singh et al., 2009). Further, Tbx20

transcriptional activity is enhanced in the presence of Gata4/5 and Nkx2.5 (Posch et al., 2010) Consistent with these data, a recent study identified GATA and NKX binding motifs in Tbx20-bound genomic regions. Further, these binding motifs were over-represented in Tbx20-bound regions associated with genes that were down-regulated in *Tbx20* knockout hearts, indicating that these genes represent targets of Tbx20-mediated activation (Sakabe et al., 2012). Tbx20 also interacts with Tbx5, and this interaction may be important for the regulation of genes associated with cell polarity or adhesion as depletion of Tbx20 and Tbx5 protein from *Xenopus* embryos results in severe cardiac defects compared to single morphants but cardiomyocyte marker expression is maintained (Brown et al., 2005). The effect of protein-protein interactions on Tbx20 transcriptional activity appears to be context- and dose-dependent. For instance, in the presence of Nkx2.5 and Gata4, Tbx20 activates the *ANF/Nppa* promoter; however, in the presence of Tbx5, Tbx20 appears to repress *ANF/Nppa* activation by Tbx5 in a dose-dependent manner. These results suggest that Tbx20 functions as both a co-activator and co-repressor of cardiac transcription factors (Figure 1.5), and this decision may be based on local levels of Tbx20 as well as on protein partner choice (Plageman and Yutzey, 2004; Brown et al., 2005). More studies are needed to shed light on this discussion. In particular, very little is known about the role of Tbx20 as a transcriptional repressor.

The frequent occurrence of collaborative transcription factor interactions in heart development points to several different models for how transcription factors complexes bind to and activate target genes. The first model, known as the

“enhanceosome model” suggests that transcription factors are recruited and bind to the enhancer as an intact complex. In this model, the exact positioning of bound transcription factors within the complex is important, as the complex must bind to a very specific motif grammar within the enhancer (Arnosti and Kulkarni, 2005). The second model, called the “billboard model” presupposes that each transcription factor is recruited independently to the cardiac enhancer and binds to its own sequence motif. This model predicts that cardiac enhancers will contain individual binding motifs for all bound transcription factors (Arnosti and Kulkarni, 2005). A recent study assessed genome-wide cardiac transcription factor binding in cardiomyocytes, specifically examining regions bound by the factors Nkx2.5, Gata4, Tbx5, SRF, and Mef2A (He et al., 2011). The authors found that regions bound by one transcription factor were often highly enriched for binding motifs of factors that are known to interact with the first transcription factor. Of the chromatin regions bound by multiple transcription factors, many were enriched for genes that are expressed in a cardiac-specific manner and represent bona fide cardiac enhancers, confirming that binding of multiple cardiac transcription factors is predictive of cardiac-specific transcription (He et al., 2011). A similar study assessed genome-wide binding sites in *Drosophila* dorsal mesoderm of the factors Tin (an NKX factor), Doc (a T-box factor), Pnr (a GATA factor), dTCF (an effector of Wnt signaling), and pMad (an effector of TGF-β signaling) (Junion et al., 2012). These investigators found that the most prominent binding signature within cardiac enhancers is the simultaneous recruitment of all five transcription factors. However, when they evaluated the motif content within the enhancers occupied by these transcription

factors, they found much higher enrichment of Doc and Pnr motifs compared to the other transcription factor motifs. These data indicate that Doc and Pnr may bind in a sequence-specific manner and other cardiac transcription factors may be recruited independently of sequence grammar (Junion et al., 2012). These studies have led to the development of a third enhancer model, the “transcription factor collective model”. This model suggests that cardiogenic transcription factors cooperatively activate cardiac enhancers; however, binding of the cohort of factors does not require a specific sequence motif. This model suggests that it may not be necessary for all of the factors to directly bind the enhancer. Instead, it may suffice for a subset of the transcriptions factors to bind their sequence motifs, which results in recruitment of the rest of the complex via protein-protein interactions with the DNA-bound transcription factors.

Collectively, these studies reveal the complexity of transcription factor pathways within the cardiac regulatory network. Mutations in many of the core transcription factors in this network have been identified in humans, and these mutations have been linked to a variety of cardiac malformations (reviewed in Table A1.1). These data emphasize the importance of understanding how these transcription factor pathways intersect to promote normal heart development. Additionally, the idea that the cooperative activity of multiple cardiac transcription factors promotes cardiac gene expression holds great promise for regenerative medicine. Heart failure is a leading cause of death worldwide, due largely to the inability of the human heart to regenerate damaged myocardium after infarct.

Though recent studies have demonstrated that the adult heart retains some regenerative capacity, this capacity is extremely limited, and a large portion of adult cardiomyocytes are quiescent and incapable of generating new cardiomyocytes to replace injured myocardium (Bergmann et al., 2009; Kajstura et al., 2010; Walsh et al., 2010; Senyo et al., 2013). Recent work has demonstrated that the addition of Gata4, Mef2c, and Tbx5 to adult cardiac fibroblasts is sufficient to reprogram these cells to cardiomyocytes, in vitro and in vivo (Ieda et al., 2010; Qian et al., 2012). This provides additional evidence that cardiac cell fate is driven by the combinatorial activities of multiple core transcription factors and highlights the human health applications if the relationships between these factors are precisely defined.

Cardiac transcription factors and chromatin remodelers: Regulation at the chromatin level

Cardiac transcription factors interact with a number of chromatin remodeling and histone-modifying factors to regulate gene expression in the developing heart. These interactions may promote a more accessible chromatin configuration, allowing transcription factors to bind and recruit activators to the locus; alternately, they result in recruitment of histone-modifying enzymes that alter histone-DNA contacts to promote a more “closed” chromatin configuration. Here, I will review some examples of how these types of interactions are critical for proper transcriptional regulation of cardiac development.

BAF Complexes

The SWI/SNF ATP-dependent chromatin remodeling complexes PBAF and BAF are large protein complexes that share eight common subunits. The PBAF complex is distinguished from BAF by the presence of the unique subunit Baf180 (Xue et al., 2000), whereas BAF complexes contain Baf250 (Nie et al., 2000). SWI/SNF complexes facilitate chromatin remodeling through nucleosome mobilization and allow transcription factors to access the DNA template (Kwon et al., 1994). Both SWI/SNF complexes have been demonstrated to be required for proper heart development (Lickert et al., 2004; Wang et al., 2004). Ablation of the PBAF subunit Baf180 results in hypoplastic ventricles and ventricular septal defects indicating that the PBAF complex is required for ventricular chamber development (Wang et al., 2004). Similarly, knockdown of Baf60c, a subunit common to both BAF complexes, results in impaired expansion of the early heart fields and defects in cardiomyocyte maturation (Lickert et al., 2004). Interestingly, expression of Baf60c with Tbx5, Nkx2.5, and Gata4 increased *ANF/Nppa* reporter activity compared to control in the presence of just the transcription factors, suggesting that BAF complexes may potentiate transcription factor activation of *ANF/Nppa* (Lickert et al., 2004). This potentiation requires the presence of the ATPase subunit of BAF, Brg1, which was shown to interact with Tbx5, Nkx2.5, and Gata4 in the presence of Baf60c. Finally, a combination of Baf60c, Gata4, and Tbx5 can direct mouse mesoderm into beating cardiomyocytes, again suggesting that BAF complexes permit binding of transcription factors to cardiac genes (Takeuchi and Bruneau, 2009). BAF complexes therefore interact with cardiac transcription factors to activate

cardiac genes, leading to the hypothesis that interactions between transcription factors and chromatin remodeling complexes may be a common feature of heart-specific chromatin activation.

Several groups have characterized the role of Brg1 in cardiac gene regulation (Stankunas et al., 2008; Hang et al., 2010; Takeuchi et al., 2011). Endocardial-specific deletion of Brg1 leads to trabeculation defects that arise as a result of derepression of the secreted matrix metalloproteinase, *ADAMTS1* (Stankunas et al., 2008). This study suggests that BAF complexes may be involved in both activation and repression of gene expression in the heart. Indeed, a later study examining the role of Brg1 in the myocardium found that Brg1 directly represses *α-MHC*, the *MHC* isoform that is predominantly expressed in adult heart, thereby maintaining myocardial cells in an embryonic state (Hang et al., 2010). The authors also showed that Brg1 interacts with and requires HDACs and PARPs to transcriptionally repress *α-MHC*. Interestingly, Brg1 also activates *β-MHC*, the *MHC* isoform present in embryonic myocardium, indicating that Brg1 regulates parallel pathways to control *MHC* isoform expression (Hang et al., 2010). It is unclear precisely how BAF/HDAC/PARP complexes are recruited to the MHC promoter; however, one potential mechanism is recruitment by DNA sequence-specific cardiac transcription factors. One recent study supports this hypothesis and demonstrated a genetic interdependence between cardiac transcription factors and BAF complexes. Compound heterozygous mice for *Brg1* and either *Tbx5*, *Nkx2.5* or *Tbx20* all display profound cardiac defects compared to any of the single heterozygous mice

(Takeuchi et al., 2011). Additionally, Brg1 occupancy at the *ANF/Nppa* and *Gja* promoters was markedly reduced in a *Tbx5* heterozygous background, and further reduced in a *Tbx5; Brg1* double heterozygous background, indicating that BAF complex occupancy of cardiac promoters relies on interactions with cardiac transcription factors on the target promoter (Takeuchi et al., 2011).

INO80 Complex

The INO80 chromatin remodeling complex is a very large protein complex with 11 to 16 members including the ATP-dependent helicases Ino80 and SRCAP, the DNA helicases Pontin (Ruvbl1, Tip49, Tip49a) and Reptin (Ruvbl2, Tip48, Tip49b), actin, and various actin-related proteins (Arp4, Arp5, Arp8, β-actin, Arp7, Arp9) (Shen et al., 2000; Jin et al., 2005). The INO80 complex alters chromatin accessability resulting in activation or repression of target genes (Cai et al., 2007; Ford et al., 2007; Klopf et al., 2009). Two members of the complex, Pontin and Reptin, have opposing acitivities within the INO80 complex, and this antagonistic relationship has been shown to play a role in cardiac growth in zebrafish (Rottbauer et al., 2002). An ENU-induced mutation in *Reptin* leads to cardiac hyperplasia and embryonic lethality. This mutation is an activating mutation in *Reptin*, increasing the ATPase activity of Reptin complexes, thus overriding Pontin diminution of Reptin activity, and increasing the transcriptional repressor activity of the complex. Mutant zReptin was subsequently shown to have a stronger repressive effect on β-catenin/TCF-mediated transactivation, leading to the hypothesis that Pontin/Reptin complexes regulate β-catenin-mediated activation of cell cycle genes such as cyclin

D and c-Myc to control the balance between proliferation and differentiation in the developing zebrafish heart (Rottbauer et al., 2002). Further studies are needed to investigate the role of the INO80 complex in mammalian heart development and to determine how Pontin, Reptin, or other members of the INO80 complex might intersect with additional transcription factor pathways in the heart.

Histone Deacetylases

HDACs are a class of histone-modifying enzymes that promote chromatin condensation by removing acetyl groups from conserved lysine residues of histone tails, resulting in transcriptional repression (Vidal and Gaber, 1991; Vidal et al., 1991; Rundlett et al., 1996; Hassig et al., 1997; Rundlett et al., 1998). HDACs interact with a variety of DNA-binding transcription factors and are often components of larger repression complexes (Ayer et al., 1995; Heinzel et al., 1997; Zhang et al., 1997; Wade et al., 1998). HDACs are divided into 3 classes based on their homology with the 3 yeast HDACs: class I HDACs consist of HDAC1, -2, -3, and-8, class II HDACs include HDAC4, -5, -7, and -9, and class III HDACs, which are termed sirtuins (Ekwall, 2005; Haberland et al., 2009). Several HDAC proteins have been shown to be critical for transcription repression during normal heart development (Zhang et al., 2002; Chang et al., 2004; Montgomery et al., 2007; Montgomery et al., 2008; Trivedi et al., 2008; Trivedi et al., 2010).

HDAC1 and HDAC2 have partially redundant roles in developing cardiomyocytes. Myocardium deletion of either *HDAC1* or *-2* does not result in a

cardiac phenotype; however, mice mutant for both *HDAC1* and *-2* die neonatally of cardiac arrhythmias and dilated cardiomyopathy (Montgomery et al., 2007). Heart failure in these mice likely results from upregulation of calcium channel and contractile genes, indicating that HDAC1 and -2 function to negatively regulate genes involved in calcium flux and contraction. Additional studies are needed to address the mechanism by which HDAC1 and -2 are targeted to cardiac genes. Interestingly, HDAC2 also regulates Gata4 transcriptional activity via deacetylation its lysine resides, suggesting that Gata4 is a non-histone target of HDAC2 in the heart (Trivedi et al., 2010). HDAC2 deacetylation of Gata4 requires the adaptor protein Hopx and results in a suppression of Gata4-dependent transactivation of *cyclinD2* and *cdk4*. Consistent with the requirement for HDAC2 in Gata4-mediated regulation of cell cycle genes, *HDAC2; Hopx* knockout hearts display increased cardiomyocyte proliferation indicating that HDAC2, Hopx, and Gata4 interact to regulate myocyte proliferation (Trivedi et al., 2010). It will be interesting to determine if HDACs are responsible for deacetylating other transcription factors in the heart.

Myocardium-specific deletion of *HDAC3* results in lethality at 3-4 months of age due to cardiac hypertrophy and severe defects in cardiac metabolism, suggesting the HDAC3 has an independent role from HDAC1/2 in cardiac function (Montgomery et al., 2008). *HDAC3* mutant hearts display significantly upregulated expression of genes involved in myocardial energetics as a result of aberrant activation of PPARα gene targets. These data indicate that HDAC3 is recruited by PPARs to the promoters of metabolic genes to facilitate transcriptional repression.

HDAC3 may also be important for promoting postnatal cardiomyocyte proliferation, as myocardium-specific overexpression of *HDAC3* results in increased cardiomyocyte proliferation and inhibition of cyclin-dependent kinase inhibitors (Trivedi et al., 2008). Interestingly, the effects of *HDAC3* overexpression on cardiomyocyte proliferation are limited to birth until 2 months of age, when proliferation returns to normal. It is unclear whether this occurs because the neonatal cardiomyocytes are no longer competent to respond to proliferation cues, or is a result of temporal HDAC3 activity on cell cycle genes. The mechanism by which HDAC3 activity in the heart is regulated has yet to be determined; however, it is likely that HDAC3 exists as part of a larger repressive complex that is recruited temporally in a tissue-restricted manner by tissue-specific DNA-binding factors.

Similar to the coordinated functions of HDAC1/2, the class II HDACs HDAC5 and -9 redundantly regulate embryonic cardiac growth and hypertrophy. Mouse embryos that are double null for *HDAC5* and *HDAC9* begin to die at E15.5 with ventricular septal defects and thinned ventricular walls, highlighting a role for these HDACs in cardiac growth (Chang et al., 2004). Mice lacking only *HDAC5* or *HDAC9* are born in normal Mendelian ratios but go on to display age-dependent hypertrophy indicating a defect in the cardiac stress response (Zhang et al., 2002; Chang et al., 2004). Indeed, mice mutant for either *HDAC5* or *-9* develop enlarged hearts in response to various forms of cardiac stress suggesting that HDAC5/9 are involved in regulating the transcriptional program governing cardiac hypertrophy. Interestingly, class II HDACs have been demonstrated to interact with MEF2 transcription factors

and these interactions result in the recruitment of HDACs to MEF2 target genes (McKinsey et al., 2002). In particular, one isoform of HDAC9 termed MEF2-interacting transcription repressor (MITR) encodes a truncated form of HDAC9 that does not have HDAC activity but inhibits MEF2 target genes by association with other HDACs and transcriptional repressors (McKinsey et al., 2002). The precise role that HDAC-MEF2 complexes play in embryonic heart development is unclear and warrants investigation.

Histone Methyltransferases

The effect of histone methylation on gene expression is context dependent and can both activate and repress target genes. Histone methyltransferases (HMTs) catalyze the transfer of methyl groups to lysine and arginine residues of histones (Strahl et al., 1999; Wang et al., 2001b). Typically, methylation of K4, K36, and K79 of histone H3 results in transcriptional activation (Strahl et al., 1999; Rao et al., 2005; Vakoc et al., 2006), whereas methylation of K9 and K27 is associated with transcriptional repression (Nielsen et al., 2001; Vakoc et al., 2006). Several HMTs have been implicated in heart development as both targets and functional partners of cardiac transcription factors (Gottlieb et al., 2002; Sims et al., 2002; Phan et al., 2005; Tan et al., 2006; Nimura et al., 2009; Park et al., 2010).

The HMT Smyd1 (mBop, Bop) contains a SET domain for methyltransferase activity and a MYND domain, which is involved in recruitment of HDACs to mediate transcriptional repression (Gottlieb et al., 2002). Global knockdown of Smyd1 results

in embryonic death with defects in cardiomyocyte differentiation and right ventricular development (Gottlieb et al., 2002). Additional studies in zebrafish conclude that Smyd1 is required for myofibril organization and skeletal and cardiac muscle contraction (Tan et al., 2006). Subsequent work has placed *Smyd1* expression downstream of Mef2c, thereby suggesting that Mef2c induction of *Smyd1* is necessary for development of the second heart field, which gives rise to the outflow tract and right ventricle (Phan et al., 2005). In the heart, Smyd1 interacts with the muscle-specific transcription factor skNAC to regulate the transcriptional program governing ventricular identity (Sims et al., 2002; Park et al., 2010). Interestingly, expression of the Smyd1-dependent gene *Hand2* is unaffected in *skNAC* null hearts. These results imply that Smyd1 regulates *Hand2* and possibly other cardiac genes in an skNAC-independent manner, likely through interactions with other cardiac transcription factors.

A second HMT with implications in heart development, WHSC1 (MMSET), is associated with the dominant disorder Wolf-Hirschorn syndrome (WHS) (Wright et al., 1997; Marango et al., 2008). WHS is characterized by a constellation of symptoms that include growth deficiency, mental retardation, craniofacial abnormalities, midline closure defects, skeletal defects, and atrial and ventricular septal defects (Wright et al., 1997). WHSC1 has been characterized as a SET domain-containing HMT that trimethylates K36 of histone H3 (H3K36me3) and is deleted in WHS (Nimura et al., 2009). A recent study determined that allele inactivation of *Whsc1* in the mouse recapitulates the developmental defects,

including congenital heart defects, observed in WHS patients (Nimura et al., 2009). Additionally, Whsc1 physically interacts with Nkx2.5 in embryonic hearts to transcriptionally repress the Nkx2.5 targets *Pdgfra*, *Igfbp5*, and *Isl1*, presumably via H3K36 trimethylation (Nimura et al., 2009). A functional interaction between Whsc1 and Nkx2.5 was also confirmed genetically. Mice double heterozygous for *Whsc1* and *Nkx2.5* display atrial and ventricular septal defects, providing additional evidence that Whsc1-Nkx2.5 complexes negatively modulate cardiac transcriptional networks.

DISSERTATION GOALS

The interconnectivity of core cardiac transcription factors, as well as the interface between these transcription factors and the chromatin remodeling machinery of the cell represent critical relationships that ensure the proper specification, differentiation, and morphogenesis of cardiac cells. Therefore, defining the precise interactions and mechanisms of action for each core transcription factor is critical for a full understanding of the entire transcription network. Although mutation or misregulation of *Tbx20* leads to a variety of cardiac defects in humans, mice, X*enopus*, and *Drosophila*, very little is known about the upstream signaling pathways that regulate *Tbx20* cardiac expression or the protein-protein interactions that specify Tbx20 transcriptional activity in the heart. For this reason, I sought to identify and characterize novel determinants of Tbx20 cardiac expression and activity. In Chapter 2, we identify an evolutionarily conserved cardiac enhancer that is necessary to direct *Tbx20* expression in the heart during cardiac chamber

maturation. We go on to show that this enhancer is downstream of BMP signaling and directly bound by phospho-Smad1/5/8. Because Tbx20 is required to ensure proper regionalization of the chambers, this work implies a critical role for BMP signaling in this process. To identify and characterize Tbx20 protein-protein interactions that are important in Tbx20-mediated gene regulation, Chapter 3 focuses on a proteomics-based approach to isolate Tbx20 transcription complexes using Human Embryonic Kidney 293 (HEK 293) cells as a model system. Here, we demonstrate that Tbx20 interacts with a unique transcription repression network that includes chromatin remodelers, Groucho/TLE co-repressors, and the cardiac T-box transcription factor Tbx18. In Chapter 4, we develop a method to isolate endogenous Tbx20 protein complexes from mouse embryonic stem cell (ESC)-derived cardiomyocytes and show that Tbx20 interacts with a broad chromatin remodeling network in cardiac progenitor cells. In the future, this methodology will be used to characterize the temporal and tissue-specific components of Tbx20 transcription complexes. Collectively, this work will enhance the understanding of the Tbx20 transcription network during cardiac development.

Figure 1.1. The core cardiac transcription factor network. The core cardiac transcription factors Tbx20, Tbx5, Nkx2.5, Gata4, Mef2C, and Isl1 control early heart development through multiple protein-protein interactions with each other. These interactions are necessary to ensure proper transcriptional regulation of other factors within the network and of a variety of downstream cardiac genes (not shown).

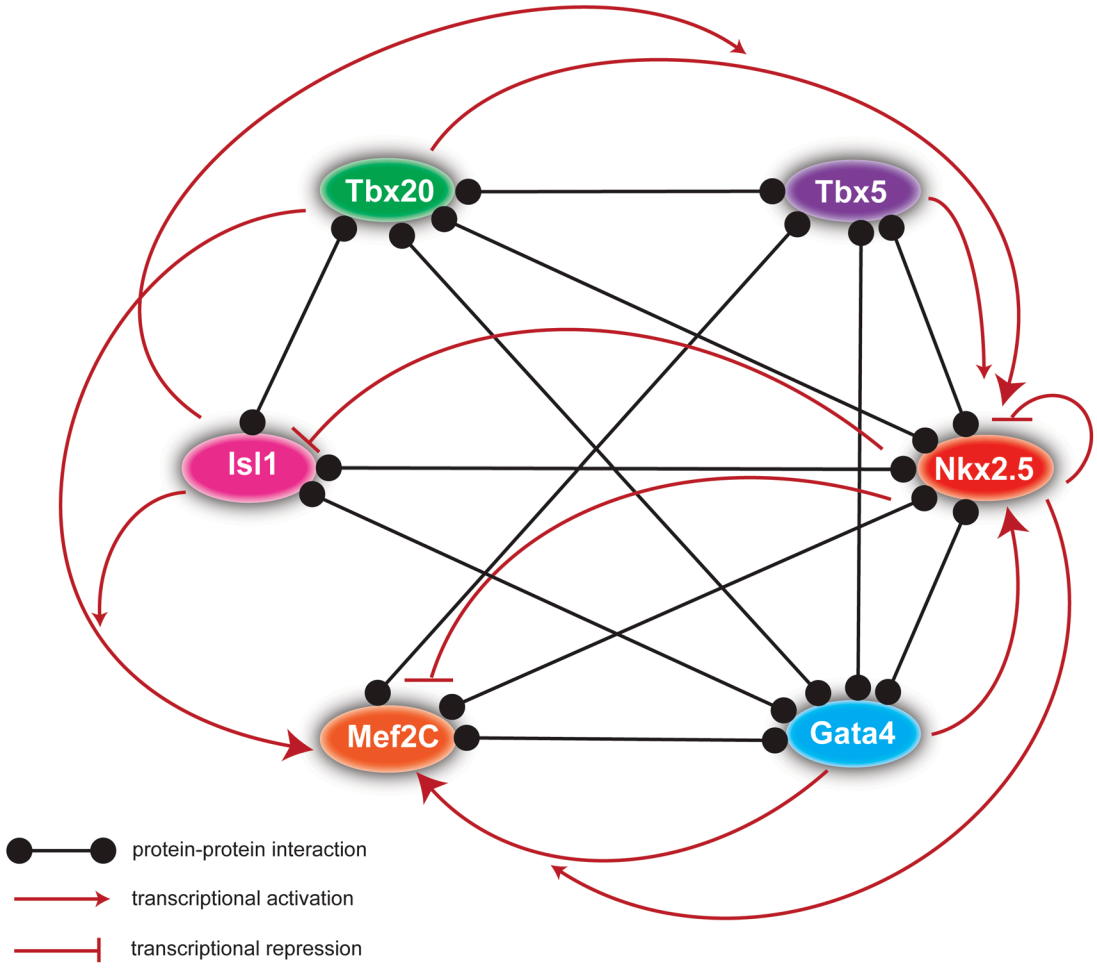

Figure 1.2. The Nkx2.5 transcription network.

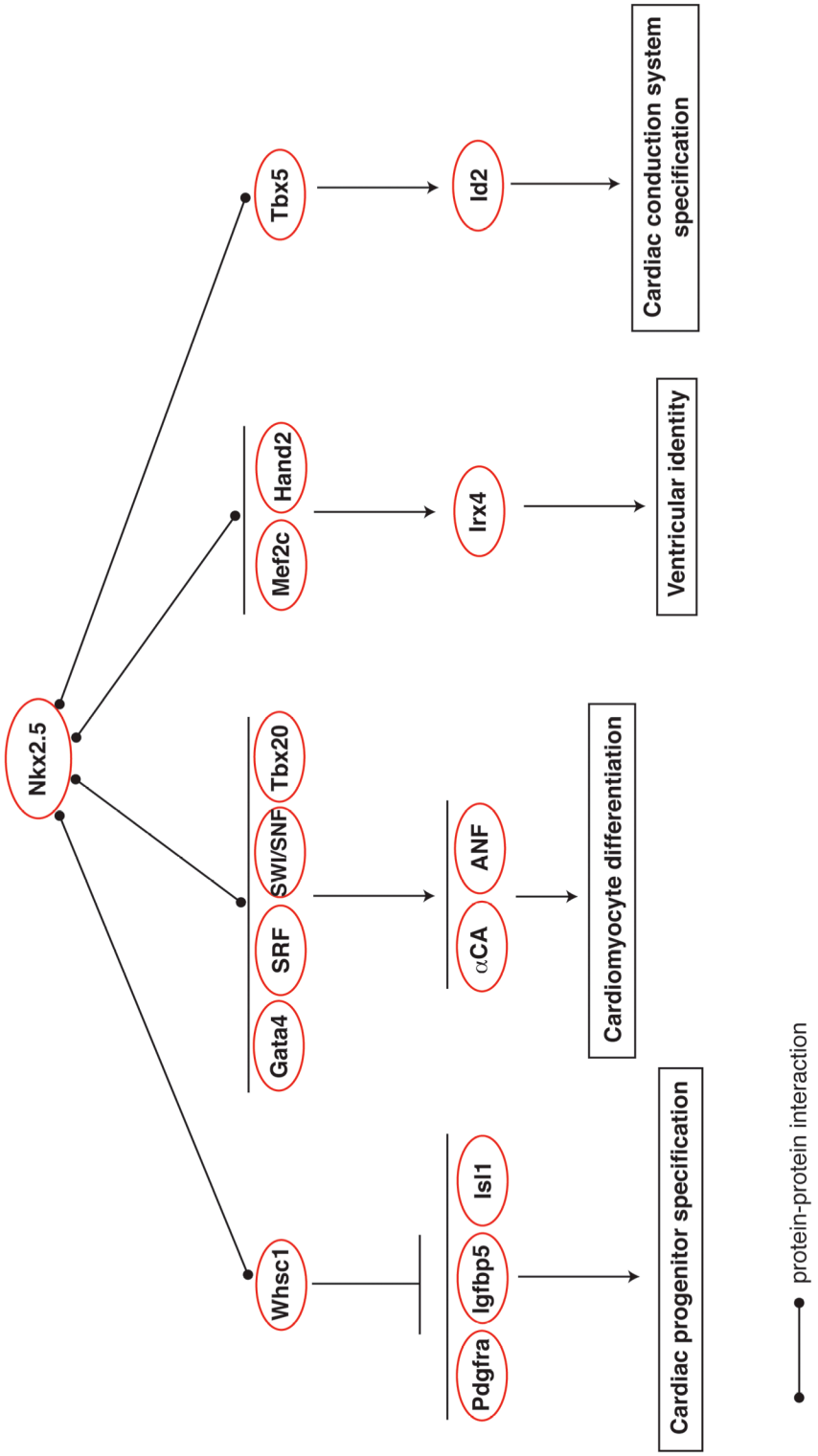

Figure 1.3. The Gata4 transcription network.

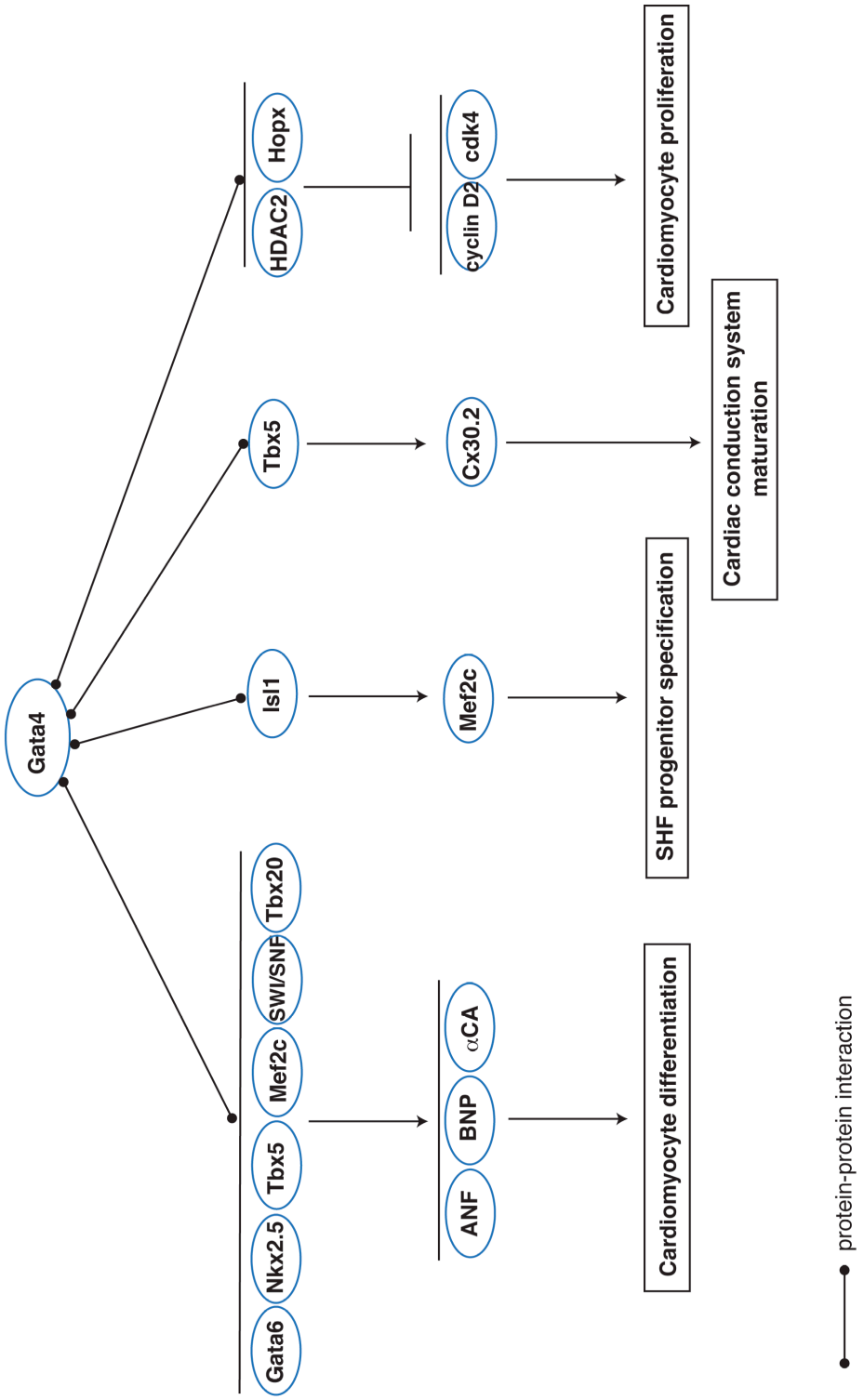

Figure 1.4. The Tbx5 transcription network.

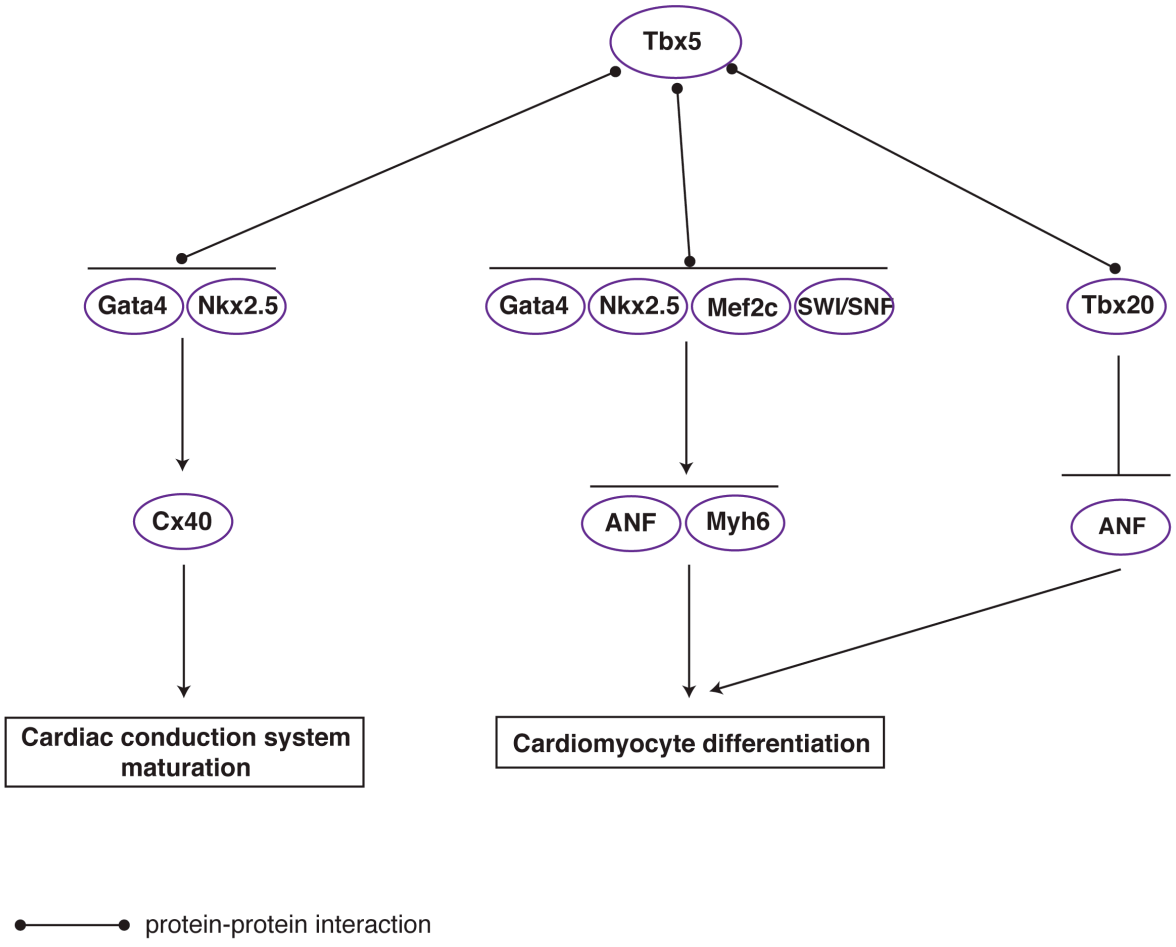

Figure 1.5. The Tbx20 transcription network.

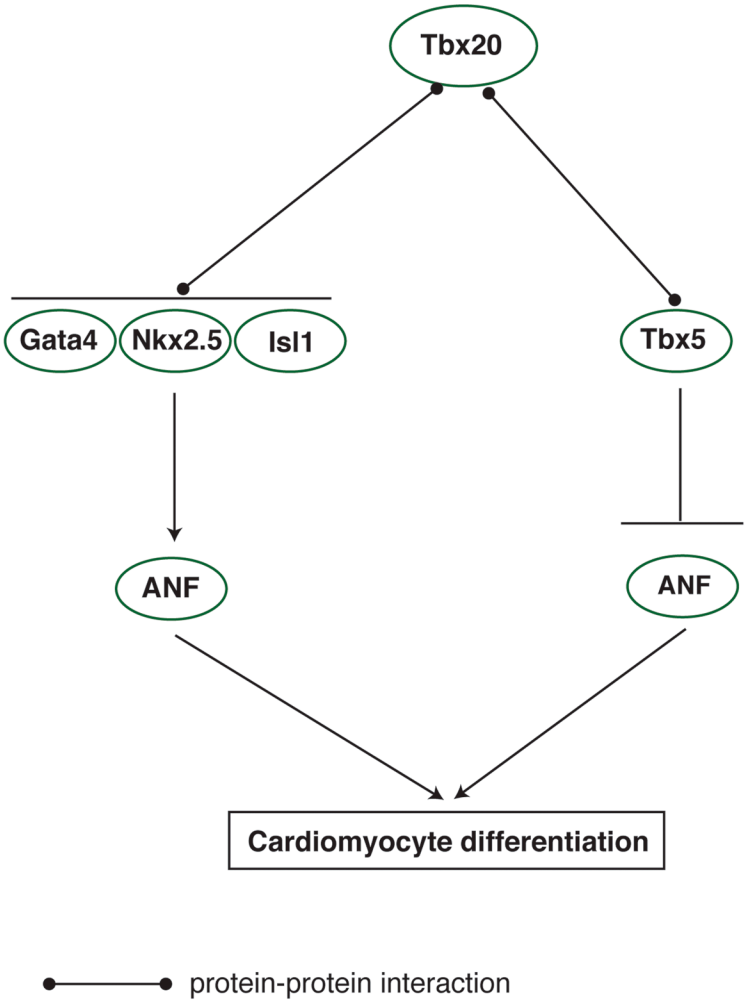

REFERENCES

Ahn, D. G., Ruvinsky, I., Oates, A. C., Silver, L. M. and Ho, R. K. (2000) 'tbx20, a new vertebrate T-box gene expressed in the cranial motor neurons and developing cardiovascular structures in zebrafish', *Mechanisms of development* 95(1-2): 253-8.

Arceci, R. J., King, A. A., Simon, M. C., Orkin, S. H. and Wilson, D. B. (1993) 'Mouse GATA-4: a retinoic acid-inducible GATA-binding transcription factor expressed in endodermally derived tissues and heart', *Molecular and cellular biology* 13(4): 2235-46.

Arnosti, D. N. and Kulkarni, M. M. (2005) 'Transcriptional enhancers: Intelligent enhanceosomes or flexible billboards?', *Journal of cellular biochemistry* 94(5): 890-8.

Ayer, D. E., Lawrence, Q. A. and Eisenman, R. N. (1995) 'Mad-Max transcriptional repression is mediated by ternary complex formation with mammalian homologs of yeast repressor Sin3', *Cell* 80(5): 767-76.

Basson, C. T., Bachinsky, D. R., Lin, R. C., Levi, T., Elkins, J. A., Soults, J., Grayzel, D., Kroumpouzou, E., Traill, T. A., Leblanc-Straceski, J. et al. (1997) 'Mutations in human TBX5 [corrected] cause limb and cardiac malformation in Holt-Oram syndrome', *Nature genetics* 15(1): 30-5.

Basson, C. T., Huang, T., Lin, R. C., Bachinsky, D. R., Weremowicz, S., Vaglio, A., Bruzzone, R., Quadrelli, R., Lerone, M., Romeo, G. et al. (1999) 'Different TBX5 interactions in heart and limb defined by Holt-Oram syndrome mutations', *Proceedings of the National Academy of Sciences of the United States of America* 96(6): 2919-24.

Benson, D. W., Silberbach, G. M., Kavanaugh-McHugh, A., Cottrill, C., Zhang, Y., Riggs, S., Smalls, O., Johnson, M. C., Watson, M. S., Seidman, J. G. et al. (1999) 'Mutations in the cardiac transcription factor NKX2.5 affect diverse cardiac developmental pathways', *The Journal of clinical investigation* 104(11): 1567-73.

Bergmann, O., Bhardwaj, R. D., Bernard, S., Zdunek, S., Barnabe-Heider, F., Walsh, S., Zupicich, J., Alkass, K., Buchholz, B. A., Druid, H. et al. (2009) 'Evidence for cardiomyocyte renewal in humans', *Science* 324(5923): 98-102.

Bodmer, R. (1993) 'The gene tinman is required for specification of the heart and visceral muscles in Drosophila', *Development* 118(3): 719-29.

Bodmer, R., Jan, L. Y. and Jan, Y. N. (1990) 'A new homeobox-containing gene, msh-2, is transiently expressed early during mesoderm formation of Drosophila', *Development* 110(3): 661-9.

Bondue, A., Lapouge, G., Paulissen, C., Semeraro, C., Iacovino, M., Kyba, M. and Blanpain, C. (2008) 'Mesp1 acts as a master regulator of multipotent cardiovascular progenitor specification', *Cell stem cell* 3(1): 69-84.

Brown, D. D., Binder, O., Pagratis, M., Parr, B. A. and Conlon, F. L. (2003) 'Developmental expression of the Xenopus laevis Tbx20 orthologue', *Development genes and evolution* 212(12): 604-7.

Brown, D. D., Martz, S. N., Binder, O., Goetz, S. C., Price, B. M., Smith, J. C. and Conlon, F. L. (2005) 'Tbx5 and Tbx20 act synergistically to control vertebrate heart morphogenesis', *Development* 132(3): 553-63.

Bruneau, B. G., Logan, M., Davis, N., Levi, T., Tabin, C. J., Seidman, J. G. and Seidman, C. E. (1999) 'Chamber-specific cardiac expression of Tbx5 and heart defects in Holt-Oram syndrome', *Developmental biology* 211(1): 100-8.

Bruneau, B. G., Nemer, G., Schmitt, J. P., Charron, F., Robitaille, L., Caron, S., Conner, D. A., Gessler, M., Nemer, M., Seidman, C. E. et al. (2001) 'A murine model of Holt-Oram syndrome defines roles of the T-box transcription factor Tbx5 in cardiogenesis and disease', *Cell* 106(6): 709-21.

Cai, C. L., Liang, X., Shi, Y., Chu, P. H., Pfaff, S. L., Chen, J. and Evans, S. (2003) 'Isl1 identifies a cardiac progenitor population that proliferates prior to differentiation and contributes a majority of cells to the heart', *Developmental cell* 5(6): 877-89.

Cai, C. L., Zhou, W., Yang, L., Bu, L., Qyang, Y., Zhang, X., Li, X., Rosenfeld, M. G., Chen, J. and Evans, S. (2005) 'T-box genes coordinate regional rates of proliferation and regional specification during cardiogenesis', *Development* 132(10): 2475-87.

Cai, Y., Jin, J., Yao, T., Gottschalk, A. J., Swanson, S. K., Wu, S., Shi, Y., Washburn, M. P., Florens, L., Conaway, R. C. et al. (2007) 'YY1 functions with INO80 to activate transcription', *Nature structural & molecular biology* 14(9): 872-4.

Carson, C. T., Kinzler, E. R. and Parr, B. A. (2000) 'Tbx12, a novel T-box gene, is expressed during early stages of heart and retinal development', *Mechanisms of development* 96(1): 137-40.

Chang, S., McKinsey, T. A., Zhang, C. L., Richardson, J. A., Hill, J. A. and Olson, E. N. (2004) 'Histone deacetylases 5 and 9 govern responsiveness of the heart to a subset of stress signals and play redundant roles in heart development', *Molecular and cellular biology* 24(19): 8467-76.

Charron, F., Paradis, P., Bronchain, O., Nemer, G. and Nemer, M. (1999) 'Cooperative interaction between GATA-4 and GATA-6 regulates myocardial gene expression', *Molecular and cellular biology* 19(6): 4355-65.

Chen, C. Y. and Schwartz, R. J. (1995) 'Identification of novel DNA binding targets and regulatory domains of a murine tinman homeodomain factor, nkx-2.5', *The Journal of biological chemistry* 270(26): 15628-33.

Chen, C. Y. and Schwartz, R. J. (1996) 'Recruitment of the tinman homolog Nkx-2.5 by serum response factor activates cardiac alpha-actin gene transcription', *Molecular and cellular biology* 16(11): 6372-84.

Chen, J. N. and Fishman, M. C. (1996) 'Zebrafish tinman homolog demarcates the heart field and initiates myocardial differentiation', *Development* 122(12): 3809-16.

Christoffels, V. M., Mommersteeg, M. T., Trowe, M. O., Prall, O. W., de Gier-de Vries, C., Soufan, A. T., Bussen, M., Schuster-Gossler, K., Harvey, R. P., Moorman, A. F. et al. (2006) 'Formation of the venous pole of the heart from an Nkx2-5-negative precursor population requires Tbx18', *Circulation research* 98(12): 1555-63.

Cleaver, O. B., Patterson, K. D. and Krieg, P. A. (1996) 'Overexpression of the tinman-related genes XNkx-2.5 and XNkx-2.3 in Xenopus embryos results in myocardial hyperplasia', *Development* 122(11): 3549-56.

Dodou, E., Verzi, M. P., Anderson, J. P., Xu, S. M. and Black, B. L. (2004) 'Mef2c is a direct transcriptional target of ISL1 and GATA factors in the anterior heart field during mouse embryonic development', *Development* 131(16): 3931-42.

Durocher, D., Charron, F., Warren, R., Schwartz, R. J. and Nemer, M. (1997) 'The cardiac transcription factors Nkx2-5 and GATA-4 are mutual cofactors', *The EMBO journal* 16(18): 5687-96.

Ekwall, K. (2005) 'Genome-wide analysis of HDAC function', *Trends in genetics : TIG* 21(11): 608-15.

Foley, A. C., Korol, O., Timmer, A. M. and Mercola, M. (2007) 'Multiple functions of Cerberus cooperate to induce heart downstream of Nodal', *Developmental biology* 303(1): 57-65.

Ford, J., Odeyale, O., Eskandar, A., Kouba, N. and Shen, C. H. (2007) 'A SWI/SNF- and INO80-dependent nucleosome movement at the INO1 promoter', *Biochemical and biophysical research communications* 361(4): 974-9.

Fu, Y., Yan, W., Mohun, T. J. and Evans, S. M. (1998) 'Vertebrate tinman homologues XNkx2-3 and XNkx2-5 are required for heart formation in a functionally redundant manner', *Development* 125(22): 4439-49.

Gadue, P., Huber, T. L., Paddison, P. J. and Keller, G. M. (2006) 'Wnt and TGF-beta signaling are required for the induction of an in vitro model of primitive streak formation using embryonic stem cells', *Proceedings of the National Academy of Sciences of the United States of America* 103(45): 16806-11.

Garg, V., Kathiriya, I. S., Barnes, R., Schluterman, M. K., King, I. N., Butler, C. A., Rothrock, C. R., Eapen, R. S., Hirayama-Yamada, K., Joo, K. et al. (2003) 'GATA4 mutations cause human congenital heart defects and reveal an interaction with TBX5', *Nature* 424(6947): 443-7.

Ghosh, T. K., Packham, E. A., Bonser, A. J., Robinson, T. E., Cross, S. J. and Brook, J. D. (2001) 'Characterization of the TBX5 binding site and analysis of mutations that cause Holt-Oram syndrome', *Human molecular genetics* 10(18): 1983-94.

Ghosh, T. K., Song, F. F., Packham, E. A., Buxton, S., Robinson, T. E., Ronksley, J., Self, T., Bonser, A. J. and Brook, J. D. (2009) 'Physical interaction between TBX5 and MEF2C is required for early heart development', *Molecular and cellular biology* 29(8): 2205-18.

Goetz, S. C., Brown, D. D. and Conlon, F. L. (2006) 'TBX5 is required for embryonic cardiac cell cycle progression', *Development* 133(13): 2575-84.

Gottlieb, P. D., Pierce, S. A., Sims, R. J., Yamagishi, H., Weihe, E. K., Harriss, J. V., Maika, S. D., Kuziel, W. A., King, H. L., Olson, E. N. et al. (2002) 'Bop encodes a muscle-restricted protein containing MYND and SET domains and is essential for cardiac differentiation and morphogenesis', *Nature genetics* 31(1): 25-32.

Grepin, C., Nemer, G. and Nemer, M. (1997) 'Enhanced cardiogenesis in embryonic stem cells overexpressing the GATA-4 transcription factor', *Development* 124(12): 2387-95.

Grepin, C., Robitaille, L., Antakly, T. and Nemer, M. (1995) 'Inhibition of transcription factor GATA-4 expression blocks in vitro cardiac muscle differentiation', *Molecular and cellular biology* 15(8): 4095-102.

Griffin, K. J., Stoller, J., Gibson, M., Chen, S., Yelon, D., Stainier, D. Y. and Kimelman, D. (2000) 'A conserved role for H15-related T-box transcription factors in zebrafish and Drosophila heart formation', *Developmental biology* 218(2): 235-47.

Grow, M. W. and Krieg, P. A. (1998) 'Tinman function is essential for vertebrate heart development: elimination of cardiac differentiation by dominant inhibitory mutants of the tinman-related genes, XNkx2-3 and XNkx2-5', *Developmental biology* 204(1): 187-96.

Haberland, M., Montgomery, R. L. and Olson, E. N. (2009) 'The many roles of histone deacetylases in development and physiology: implications for disease and therapy', *Nature reviews. Genetics* 10(1): 32-42.

Hammer, S., Toenjes, M., Lange, M., Fischer, J. J., Dunkel, I., Mebus, S., Grimm, C. H., Hetzer, R., Berger, F. and Sperling, S. (2008) 'Characterization of TBX20 in human hearts and its regulation by TFAP2', *Journal of cellular biochemistry* 104(3): 1022-33.

Hang, C. T., Yang, J., Han, P., Cheng, H. L., Shang, C., Ashley, E., Zhou, B. and Chang, C. P. (2010) 'Chromatin regulation by Brg1 underlies heart muscle development and disease', *Nature* 466(7302): 62-7.

Harrelson, Z., Kelly, R. G., Goldin, S. N., Gibson-Brown, J. J., Bollag, R. J., Silver, L. M. and Papaioannou, V. E. (2004) 'Tbx2 is essential for patterning the atrioventricular canal and for morphogenesis of the outflow tract during heart development', *Development* 131(20): 5041-52.

Hassig, C. A., Fleischer, T. C., Billin, A. N., Schreiber, S. L. and Ayer, D. E. (1997) 'Histone deacetylase activity is required for full transcriptional repression by mSin3A', *Cell* 89(3): 341-7.

He, A., Kong, S. W., Ma, Q. and Pu, W. T. (2011) 'Co-occupancy by multiple cardiac transcription factors identifies transcriptional enhancers active in heart', *Proceedings of the National Academy of Sciences of the United States of America* 108(14): 5632-7.

Heikinheimo, M., Scandrett, J. M. and Wilson, D. B. (1994) 'Localization of transcription factor GATA-4 to regions of the mouse embryo involved in cardiac development', *Developmental biology* 164(2): 361-73.

Heinzel, T., Lavinsky, R. M., Mullen, T. M., Soderstrom, M., Laherty, C. D., Torchia, J., Yang, W. M., Brard, G., Ngo, S. D., Davie, J. R. et al. (1997) 'A complex containing N-CoR, mSin3 and histone deacetylase mediates transcriptional repression', *Nature* 387(6628): 43-8.

Hiroi, Y., Kudoh, S., Monzen, K., Ikeda, Y., Yazaki, Y., Nagai, R. and Komuro, I. (2001) 'Tbx5 associates with Nkx2-5 and synergistically promotes cardiomyocyte differentiation', *Nature genetics* 28(3): 276-80.

Hoogaars, W. M., Tessari, A., Moorman, A. F., de Boer, P. A., Hagoort, J., Soufan, A. T., Campione, M. and Christoffels, V. M. (2004) 'The transcriptional repressor Tbx3 delineates the developing central conduction system of the heart', *Cardiovascular research* 62(3): 489-99.

Horb, M. E. and Thomsen, G. H. (1999) 'Tbx5 is essential for heart development', *Development* 126(8): 1739-51.

Huang, G. N., Thatcher, J. E., McAnally, J., Kong, Y., Qi, X., Tan, W., DiMaio, J. M., Amatruda, J. F., Gerard, R. D., Hill, J. A. et al. (2012) 'C/EBP transcription factors mediate epicardial activation during heart development and injury', *Science* 338(6114): 1599-603.

Hurst, J. A., Hall, C. M. and Baraitser, M. (1991) 'The Holt-Oram syndrome', *Journal of medical genetics* 28(6): 406-10.

Ieda, M., Fu, J. D., Delgado-Olguin, P., Vedantham, V., Hayashi, Y., Bruneau, B. G. and Srivastava, D. (2010) 'Direct reprogramming of fibroblasts into functional cardiomyocytes by defined factors', *Cell* 142(3): 375-86.

Iio, A., Koide, M., Hidaka, K. and Morisaki, T. (2001) 'Expression pattern of novel chick T-box gene, Tbx20', *Development genes and evolution* 211(11): 559-62.

Jay, P. Y., Harris, B. S., Maguire, C. T., Buerger, A., Wakimoto, H., Tanaka, M., Kupershmidt, S., Roden, D. M., Schultheiss, T. M., O'Brien, T. X. et al. (2004) 'Nkx2-5 mutation causes anatomic hypoplasia of the cardiac conduction system', *The Journal of clinical investigation* 113(8): 1130-7.

Jin, J., Cai, Y., Yao, T., Gottschalk, A. J., Florens, L., Swanson, S. K., Gutierrez, J. L., Coleman, M. K., Workman, J. L., Mushegian, A. et al. (2005) 'A mammalian chromatin remodeling complex with similarities to the yeast INO80 complex', *The Journal of biological chemistry* 280(50): 41207-12.

Junion, G., Spivakov, M., Girardot, C., Braun, M., Gustafson, E. H., Birney, E. and Furlong, E. E. (2012) 'A transcription factor collective defines cardiac cell fate and reflects lineage history', *Cell* 148(3): 473-86.

Kajstura, J., Gurusamy, N., Ogorek, B., Goichberg, P., Clavo-Rondon, C., Hosoda, T., D'Amario, D., Bardelli, S., Beltrami, A. P., Cesselli, D. et al. (2010) 'Myocyte turnover in the aging human heart', *Circulation research* 107(11): 1374-86.

Kasahara, H. and Benson, D. W. (2004) 'Biochemical analyses of eight NKX2.5 homeodomain missense mutations causing atrioventricular block and cardiac anomalies', *Cardiovascular research* 64(1): 40-51.

Kasahara, H., Lee, B., Schott, J. J., Benson, D. W., Seidman, J. G., Seidman, C. E. and Izumo, S. (2000) 'Loss of function and inhibitory effects of human CSX/NKX2.5 homeoprotein mutations associated with congenital heart disease', *The Journal of clinical investigation* 106(2): 299-308.

Kattman, S. J., Witty, A. D., Gagliardi, M., Dubois, N. C., Niapour, M., Hotta, A., Ellis, J. and Keller, G. (2011) 'Stage-specific optimization of activin/nodal and BMP signaling promotes cardiac differentiation of mouse and human pluripotent stem cell lines', *Cell stem cell* 8(2): 228-40.

Kelley, C., Blumberg, H., Zon, L. I. and Evans, T. (1993) 'GATA-4 is a novel transcription factor expressed in endocardium of the developing heart', *Development* 118(3): 817-27.

Kirk, E. P., Sunde, M., Costa, M. W., Rankin, S. A., Wolstein, O., Castro, M. L., Butler, T. L., Hyun, C., Guo, G., Otway, R. et al. (2007) 'Mutations in cardiac T-box factor gene TBX20 are associated with diverse cardiac pathologies, including defects of septation and

valvulogenesis and cardiomyopathy', *American journal of human genetics* 81(2): 280-91.

Klopf, E., Paskova, L., Sole, C., Mas, G., Petryshyn, A., Posas, F., Wintersberger, U., Ammerer, G. and Schuller, C. (2009) 'Cooperation between the INO80 complex and histone chaperones determines adaptation of stress gene transcription in the yeast Saccharomyces cerevisiae', *Molecular and cellular biology* 29(18): 4994-5007.

Komuro, I. and Izumo, S. (1993) 'Csx: a murine homeobox-containing gene specifically expressed in the developing heart', *Proceedings of the National Academy of Sciences of the United States of America* 90(17): 8145-9.

Kuo, C. T., Morrisey, E. E., Anandappa, R., Sigrist, K., Lu, M. M., Parmacek, M. S., Soudais, C. and Leiden, J. M. (1997) 'GATA4 transcription factor is required for ventral morphogenesis and heart tube formation', *Genes & development* 11(8): 1048-60.

Kwon, H., Imbalzano, A. N., Khavari, P. A., Kingston, R. E. and Green, M. R. (1994) 'Nucleosome disruption and enhancement of activator binding by a human SW1/SNF complex', *Nature* 370(6489): 477-81.

Lawson, K. A., Meneses, J. J. and Pedersen, R. A. (1991) 'Clonal analysis of epiblast fate during germ layer formation in the mouse embryo', *Development* 113(3): 891-911.

Lee, Y., Shioi, T., Kasahara, H., Jobe, S. M., Wiese, R. J., Markham, B. E. and Izumo, S. (1998) 'The cardiac tissue-restricted homeobox protein Csx/Nkx2.5 physically associates with the zinc finger protein GATA4 and cooperatively activates atrial natriuretic factor gene expression', *Molecular and cellular biology* 18(6): 3120-9.

Li, Q. Y., Newbury-Ecob, R. A., Terrett, J. A., Wilson, D. I., Curtis, A. R., Yi, C. H., Gebuhr, T., Bullen, P. J., Robson, S. C., Strachan, T. et al. (1997) 'Holt-Oram syndrome is caused by mutations in TBX5, a member of the Brachyury (T) gene family', *Nature genetics* 15(1): 21-9.

Lickert, H., Takeuchi, J. K., Von Both, I., Walls, J. R., McAuliffe, F., Adamson, S. L., Henkelman, R. M., Wrana, J. L., Rossant, J. and Bruneau, B. G. (2004) 'Baf60c is essential for function of BAF chromatin remodelling complexes in heart development', *Nature* 432(7013): 107-12.

Lin, Q., Schwarz, J., Bucana, C. and Olson, E. N. (1997) 'Control of mouse cardiac morphogenesis and myogenesis by transcription factor MEF2C', *Science* 276(5317): 1404-7.

Linhares, V. L., Almeida, N. A., Menezes, D. C., Elliott, D. A., Lai, D., Beyer, E. C., Campos de Carvalho, A. C. and Costa, M. W. (2004) 'Transcriptional regulation of the murine Connexin40 promoter by cardiac factors Nkx2-5, GATA4 and Tbx5', *Cardiovascular research* 64(3): 402-11.

Lints, T. J., Parsons, L. M., Hartley, L., Lyons, I. and Harvey, R. P. (1993) 'Nkx-2.5: a novel murine homeobox gene expressed in early heart progenitor cells and their myogenic descendants', *Development* 119(3): 969.

Liu, J. and Stainier, D. Y. (2010) 'Tbx5 and Bmp signaling are essential for proepicardium specification in zebrafish', *Circulation research* 106(12): 1818-28.

Lyons, I., Parsons, L. M., Hartley, L., Li, R., Andrews, J. E., Robb, L. and Harvey, R. P. (1995) 'Myogenic and morphogenetic defects in the heart tubes of murine embryos lacking the homeo box gene Nkx2-5', *Genes & development* 9(13): 1654-66.

Macindoe, I., Glockner, L., Vukasin, P., Stennard, F. A., Costa, M. W., Harvey, R. P., Mackay, J. P. and Sunde, M. (2009) 'Conformational stability and DNA binding specificity of the cardiac T-box transcription factor Tbx20', *Journal of molecular biology* 389(3): 606-18.

Maitra, M., Schluterman, M. K., Nichols, H. A., Richardson, J. A., Lo, C. W., Srivastava, D. and Garg, V. (2009) 'Interaction of Gata4 and Gata6 with Tbx5 is critical for normal cardiac development', *Developmental biology* 326(2): 368-77.

Mandel, E. M., Kaltenbrun, E., Callis, T. E., Zeng, X. X., Marques, S. R., Yelon, D., Wang, D. Z. and Conlon, F. L. (2010) 'The BMP pathway acts to directly regulate Tbx20 in the developing heart', *Development* 137(11): 1919-29.

Marango, J., Shimoyama, M., Nishio, H., Meyer, J. A., Min, D. J., Sirulnik, A., Martinez-Martinez, Y., Chesi, M., Bergsagel, P. L., Zhou, M. M. et al. (2008) 'The MMSET protein is a histone methyltransferase with characteristics of a transcriptional corepressor', *Blood* 111(6): 3145-54.

McKinsey, T. A., Zhang, C. L. and Olson, E. N. (2002) 'MEF2: a calcium-dependent regulator of cell division, differentiation and death', *Trends in biochemical sciences* 27(1): 40-7.

Meins, M., Henderson, D. J., Bhattacharya, S. S. and Sowden, J. C. (2000) 'Characterization of the human TBX20 gene, a new member of the T-Box gene family closely related to the Drosophila H15 gene', *Genomics* 67(3): 317-32.

Miskolczi-McCallum, C. M., Scavetta, R. J., Svendsen, P. C., Soanes, K. H. and Brook, W. J. (2005) 'The Drosophila melanogaster T-box genes midline and H15 are conserved regulators of heart development', *Developmental biology* 278(2): 459-72.

Molkentin, J. D. (2000) 'The zinc finger-containing transcription factors GATA-4, -5, and -6. Ubiquitously expressed regulators of tissue-specific gene expression', *The Journal of biological chemistry* 275(50): 38949-52.

Molkentin, J. D., Lin, Q., Duncan, S. A. and Olson, E. N. (1997) 'Requirement of the transcription factor GATA4 for heart tube formation and ventral morphogenesis', *Genes & development* 11(8): 1061-72.

Montgomery, R. L., Davis, C. A., Potthoff, M. J., Haberland, M., Fielitz, J., Qi, X., Hill, J. A., Richardson, J. A. and Olson, E. N. (2007) 'Histone deacetylases 1 and 2 redundantly regulate cardiac morphogenesis, growth, and contractility', *Genes & development* 21(14): 1790-802.

Montgomery, R. L., Potthoff, M. J., Haberland, M., Qi, X., Matsuzaki, S., Humphries, K. M., Richardson, J. A., Bassel-Duby, R. and Olson, E. N. (2008) 'Maintenance of cardiac energy metabolism by histone deacetylase 3 in mice', *The Journal of clinical investigation* 118(11): 3588-97.

Morin, S., Charron, F., Robitaille, L. and Nemer, M. (2000) 'GATA-dependent recruitment of MEF2 proteins to target promoters', *The EMBO journal* 19(9): 2046-55.

Moskowitz, I. P., Kim, J. B., Moore, M. L., Wolf, C. M., Peterson, M. A., Shendure, J., Nobrega, M. A., Yokota, Y., Berul, C., Izumo, S. et al. (2007) 'A molecular pathway including Id2, Tbx5, and Nkx2-5 required for cardiac conduction system development', *Cell* 129(7): 1365-76.

Moskowitz, I. P., Pizard, A., Patel, V. V., Bruneau, B. G., Kim, J. B., Kupershmidt, S., Roden, D., Berul, C. I., Seidman, C. E. and Seidman, J. G. (2004) 'The T-Box transcription factor Tbx5 is required for the patterning and maturation of the murine cardiac conduction system', *Development* 131(16): 4107-16.

Munshi, N. V., McAnally, J., Bezprozvannaya, S., Berry, J. M., Richardson, J. A., Hill, J. A. and Olson, E. N. (2009) 'Cx30.2 enhancer analysis identifies Gata4 as a novel regulator of atrioventricular delay', *Development* 136(15): 2665-74.

Nie, Z., Xue, Y., Yang, D., Zhou, S., Deroo, B. J., Archer, T. K. and Wang, W. (2000) 'A specificity and targeting subunit of a human SWI/SNF family-related chromatin-remodeling complex', *Molecular and cellular biology* 20(23): 8879-88.

Nielsen, S. J., Schneider, R., Bauer, U. M., Bannister, A. J., Morrison, A., O'Carroll, D., Firestein, R., Cleary, M., Jenuwein, T., Herrera, R. E. et al. (2001) 'Rb targets histone H3 methylation and HP1 to promoters', *Nature* 412(6846): 561-5.

Nimura, K., Ura, K., Shiratori, H., Ikawa, M., Okabe, M., Schwartz, R. J. and Kaneda, Y. (2009) 'A histone H3 lysine 36 trimethyltransferase links Nkx2-5 to Wolf-Hirschhorn syndrome', *Nature* 460(7252): 287-91.

Parameswaran, M. and Tam, P. P. (1995) 'Regionalisation of cell fate and morphogenetic movement of the mesoderm during mouse gastrulation', *Developmental genetics* 17(1): 16-28.

Park, C. Y., Pierce, S. A., von Drehle, M., Ivey, K. N., Morgan, J. A., Blau, H. M. and Srivastava, D. (2010) 'skNAC, a Smyd1-interacting transcription factor, is involved in cardiac development and skeletal muscle growth and regeneration', *Proceedings of the National Academy of Sciences of the United States of America* 107(48): 20750-5.

Pehlivan, T., Pober, B. R., Brueckner, M., Garrett, S., Slaugh, R., Van Rheeden, R., Wilson, D. B., Watson, M. S. and Hing, A. V. (1999) 'GATA4 haploinsufficiency in patients with interstitial deletion of chromosome region 8p23.1 and congenital heart disease', *American journal of medical genetics* 83(3): 201-6.

Phan, D., Rasmussen, T. L., Nakagawa, O., McAnally, J., Gottlieb, P. D., Tucker, P. W., Richardson, J. A., Bassel-Duby, R. and Olson, E. N. (2005) 'BOP, a regulator of right ventricular heart development, is a direct transcriptional target of MEF2C in the developing heart', *Development* 132(11): 2669-78.

Plageman, T. F., Jr. and Yutzey, K. E. (2004) 'Differential expression and function of Tbx5 and Tbx20 in cardiac development', *The Journal of biological chemistry* 279(18): 19026-34.

Posch, M. G., Gramlich, M., Sunde, M., Schmitt, K. R., Lee, S. H., Richter, S., Kersten, A., Perrot, A., Panek, A. N., Al Khatib, I. H. et al. (2010) 'A gain-of-function TBX20 mutation causes congenital atrial septal defects, patent foramen ovale and cardiac valve defects', *Journal of medical genetics* 47(4): 230-5.

Qian, L., Huang, Y., Spencer, C. I., Foley, A., Vedantham, V., Liu, L., Conway, S. J., Fu, J. D. and Srivastava, D. (2012) 'In vivo reprogramming of murine cardiac fibroblasts into induced cardiomyocytes', *Nature* 485(7400): 593-8.

Qian, L., Liu, J. and Bodmer, R. (2005) 'Neuromancer Tbx20-related genes (H15/midline) promote cell fate specification and morphogenesis of the Drosophila heart', *Developmental biology* 279(2): 509-24.

Qian, L., Mohapatra, B., Akasaka, T., Liu, J., Ocorr, K., Towbin, J. A. and Bodmer, R. (2008) 'Transcription factor neuromancer/TBX20 is required for cardiac function in Drosophila with implications for human heart disease', *Proceedings of the National Academy of Sciences of the United States of America* 105(50): 19833-8.

Rao, B., Shibata, Y., Strahl, B. D. and Lieb, J. D. (2005) 'Dimethylation of histone H3 at lysine 36 demarcates regulatory and nonregulatory chromatin genome-wide', *Molecular and cellular biology* 25(21): 9447-59.

Reifers, F., Walsh, E. C., Leger, S., Stainier, D. Y. and Brand, M. (2000) 'Induction and differentiation of the zebrafish heart requires fibroblast growth factor 8 (fgf8/acerebellar)', *Development* 127(2): 225-35.

Reim, I., Mohler, J. P. and Frasch, M. (2005) 'Tbx20-related genes, mid and H15, are required for tinman expression, proper patterning, and normal differentiation of cardioblasts in Drosophila', *Mechanisms of development* 122(9): 1056-69.

Rottbauer, W., Saurin, A. J., Lickert, H., Shen, X., Burns, C. G., Wo, Z. G., Kemler, R., Kingston, R., Wu, C. and Fishman, M. (2002) 'Reptin and pontin antagonistically regulate heart growth in zebrafish embryos', *Cell* 111(5): 661-72.

Rundlett, S. E., Carmen, A. A., Kobayashi, R., Bavykin, S., Turner, B. M. and Grunstein, M. (1996) 'HDA1 and RPD3 are members of distinct yeast histone deacetylase complexes that regulate silencing and transcription', *Proceedings of the National Academy of Sciences of the United States of America* 93(25): 14503-8.

Rundlett, S. E., Carmen, A. A., Suka, N., Turner, B. M. and Grunstein, M. (1998) 'Transcriptional repression by UME6 involves deacetylation of lysine 5 of histone H4 by RPD3', *Nature* 392(6678): 831-5.

Sakabe, N. J., Aneas, I., Shen, T., Shokri, L., Park, S. Y., Bulyk, M. L., Evans, S. M. and Nobrega, M. A. (2012) 'Dual transcriptional activator and repressor roles of TBX20 regulate adult cardiac structure and function', *Human molecular genetics* 21(10): 2194-204.

Schott, J. J., Benson, D. W., Basson, C. T., Pease, W., Silberbach, G. M., Moak, J. P., Maron, B. J., Seidman, C. E. and Seidman, J. G. (1998) 'Congenital heart disease caused by mutations in the transcription factor NKX2-5', *Science* 281(5373): 108-11.

Schultheiss, T. M., Xydas, S. and Lassar, A. B. (1995) 'Induction of avian cardiac myogenesis by anterior endoderm', *Development* 121(12): 4203-14.

Senyo, S. E., Steinhauser, M. L., Pizzimenti, C. L., Yang, V. K., Cai, L., Wang, M., Wu, T. D., Guerquin-Kern, J. L., Lechene, C. P. and Lee, R. T. (2013) 'Mammalian heart renewal by pre-existing cardiomyocytes', *Nature* 493(7432): 433-6.

Sepulveda, J. L., Belaguli, N., Nigam, V., Chen, C. Y., Nemer, M. and Schwartz, R. J. (1998) 'GATA-4 and Nkx-2.5 coactivate Nkx-2 DNA binding targets: role for regulating early cardiac gene expression', *Molecular and cellular biology* 18(6): 3405-15.

Sepulveda, J. L., Vlahopoulos, S., Iyer, D., Belaguli, N. and Schwartz, R. J. (2002) 'Combinatorial expression of GATA4, Nkx2-5, and serum response factor directs early cardiac gene activity', *The Journal of biological chemistry* 277(28): 25775-82.

Shen, X., Mizuguchi, G., Hamiche, A. and Wu, C. (2000) 'A chromatin remodelling complex involved in transcription and DNA processing', *Nature* 406(6795): 541-4.

Shiojima, I., Komuro, I., Oka, T., Hiroi, Y., Mizuno, T., Takimoto, E., Monzen, K., Aikawa, R., Akazawa, H., Yamazaki, T. et al. (1999) 'Context-dependent transcriptional cooperation

mediated by cardiac transcription factors Csx/Nkx-2.5 and GATA-4', *The Journal of biological chemistry* 274(12): 8231-9.

Sims, R. J., 3rd, Weihe, E. K., Zhu, L., O'Malley, S., Harriss, J. V. and Gottlieb, P. D. (2002) 'm-Bop, a repressor protein essential for cardiogenesis, interacts with skNAC, a heart- and muscle-specific transcription factor', *The Journal of biological chemistry* 277(29): 26524-9.

Singh, M. K., Christoffels, V. M., Dias, J. M., Trowe, M. O., Petry, M., Schuster-Gossler, K., Burger, A., Ericson, J. and Kispert, A. (2005) 'Tbx20 is essential for cardiac chamber differentiation and repression of Tbx2', *Development* 132(12): 2697-707.

Singh, R., Horsthuis, T., Farin, H. F., Grieskamp, T., Norden, J., Petry, M., Wakker, V., Moorman, A. F., Christoffels, V. M. and Kispert, A. (2009) 'Tbx20 interacts with smads to confine tbx2 expression to the atrioventricular canal', *Circulation research* 105(5): 442-52.

Small, E. M. and Krieg, P. A. (2003) 'Transgenic analysis of the atrialnatriuretic factor (ANF) promoter: Nkx2-5 and GATA-4 binding sites are required for atrial specific expression of ANF', *Developmental biology* 261(1): 116-31.

Stankunas, K., Hang, C. T., Tsun, Z. Y., Chen, H., Lee, N. V., Wu, J. I., Shang, C., Bayle, J. H., Shou, W., Iruela-Arispe, M. L. et al. (2008) 'Endocardial Brg1 represses ADAMTS1 to maintain the microenvironment for myocardial morphogenesis', *Developmental cell* 14(2): 298-311.

Stennard, F. A., Costa, M. W., Elliott, D. A., Rankin, S., Haast, S. J., Lai, D., McDonald, L. P., Niederreither, K., Dolle, P., Bruneau, B. G. et al. (2003) 'Cardiac T-box factor Tbx20 directly interacts with Nkx2-5, GATA4, and GATA5 in regulation of gene expression in the developing heart', *Developmental biology* 262(2): 206-24.

Stennard, F. A., Costa, M. W., Lai, D., Biben, C., Furtado, M. B., Solloway, M. J., McCulley, D. J., Leimena, C., Preis, J. I., Dunwoodie, S. L. et al. (2005) 'Murine T-box transcription factor Tbx20 acts as a repressor during heart development, and is essential for adult heart integrity, function and adaptation', *Development* 132(10): 2451-62.

Strahl, B. D., Ohba, R., Cook, R. G. and Allis, C. D. (1999) 'Methylation of histone H3 at lysine 4 is highly conserved and correlates with transcriptionally active nuclei in Tetrahymena', *Proceedings of the National Academy of Sciences of the United States of America* 96(26): 14967-72.

Takeuchi, J. K. and Bruneau, B. G. (2009) 'Directed transdifferentiation of mouse mesoderm to heart tissue by defined factors', *Nature* 459(7247): 708-11.

Takeuchi, J. K., Lou, X., Alexander, J. M., Sugizaki, H., Delgado-Olguin, P., Holloway, A. K., Mori, A. D., Wylie, J. N., Munson, C., Zhu, Y. et al. (2011) 'Chromatin remodelling complex

dosage modulates transcription factor function in heart development', *Nature communications* 2: 187.

Takeuchi, J. K., Mileikovskaia, M., Koshiba-Takeuchi, K., Heidt, A. B., Mori, A. D., Arruda, E. P., Gertsenstein, M., Georges, R., Davidson, L., Mo, R. et al. (2005) 'Tbx20 dose-dependently regulates transcription factor networks required for mouse heart and motoneuron development', *Development* 132(10): 2463-74.

Takeuchi, J. K., Ohgi, M., Koshiba-Takeuchi, K., Shiratori, H., Sakaki, I., Ogura, K., Saijoh, Y. and Ogura, T. (2003) 'Tbx5 specifies the left/right ventricles and ventricular septum position during cardiogenesis', *Development* 130(24): 5953-64.

Tam, P. P., Parameswaran, M., Kinder, S. J. and Weinberger, R. P. (1997) 'The allocation of epiblast cells to the embryonic heart and other mesodermal lineages: the role of ingression and tissue movement during gastrulation', *Development* 124(9): 1631-42.

Tan, X., Rotllant, J., Li, H., De Deyne, P. and Du, S. J. (2006) 'SmyD1, a histone methyltransferase, is required for myofibril organization and muscle contraction in zebrafish embryos', *Proceedings of the National Academy of Sciences of the United States of America* 103(8): 2713-8.

Tonissen, K. F., Drysdale, T. A., Lints, T. J., Harvey, R. P. and Krieg, P. A. (1994) 'XNkx-2.5, a Xenopus gene related to Nkx-2.5 and tinman: evidence for a conserved role in cardiac development', *Developmental biology* 162(1): 325-8.

Treisman, R. (1986) 'Identification of a protein-binding site that mediates transcriptional response of the c-fos gene to serum factors', *Cell* 46(4): 567-74.

Trivedi, C. M., Lu, M. M., Wang, Q. and Epstein, J. A. (2008) 'Transgenic overexpression of Hdac3 in the heart produces increased postnatal cardiac myocyte proliferation but does not induce hypertrophy', *The Journal of biological chemistry* 283(39): 26484-9.

Trivedi, C. M., Zhu, W., Wang, Q., Jia, C., Kee, H. J., Li, L., Hannenhalli, S. and Epstein, J. A. (2010) 'Hopx and Hdac2 interact to modulate Gata4 acetylation and embryonic cardiac myocyte proliferation', *Developmental cell* 19(3): 450-9.

Vakoc, C. R., Sachdeva, M. M., Wang, H. and Blobel, G. A. (2006) 'Profile of histone lysine methylation across transcribed mammalian chromatin', *Molecular and cellular biology* 26(24): 9185-95.

Vidal, M. and Gaber, R. F. (1991) 'RPD3 encodes a second factor required to achieve maximum positive and negative transcriptional states in Saccharomyces cerevisiae', *Molecular and cellular biology* 11(12): 6317-27.

Vidal, M., Strich, R., Esposito, R. E. and Gaber, R. F. (1991) 'RPD1 (SIN3/UME4) is required for maximal activation and repression of diverse yeast genes', *Molecular and cellular biology* 11(12): 6306-16.

Vincentz, J. W., Barnes, R. M., Firulli, B. A., Conway, S. J. and Firulli, A. B. (2008) 'Cooperative interaction of Nkx2.5 and Mef2c transcription factors during heart development', *Developmental dynamics : an official publication of the American Association of Anatomists* 237(12): 3809-19.

Vitelli, F., Morishima, M., Taddei, I., Lindsay, E. A. and Baldini, A. (2002) 'Tbx1 mutation causes multiple cardiovascular defects and disrupts neural crest and cranial nerve migratory pathways', *Human molecular genetics* 11(8): 915-22.

Vong, L., Bi, W., O'Connor-Halligan, K. E., Li, C., Cserjesi, P. and Schwarz, J. J. (2006) 'MEF2C is required for the normal allocation of cells between the ventricular and sinoatrial precursors of the primary heart field', *Developmental dynamics : an official publication of the American Association of Anatomists* 235(7): 1809-21.

Wade, P. A., Jones, P. L., Vermaak, D. and Wolffe, A. P. (1998) 'A multiple subunit Mi-2 histone deacetylase from Xenopus laevis cofractionates with an associated Snf2 superfamily ATPase', *Current biology : CB* 8(14): 843-6.

Walsh, S., Ponten, A., Fleischmann, B. K. and Jovinge, S. (2010) 'Cardiomyocyte cell cycle control and growth estimation in vivo--an analysis based on cardiomyocyte nuclei', *Cardiovascular research* 86(3): 365-73.

Wang, D., Chang, P. S., Wang, Z., Sutherland, L., Richardson, J. A., Small, E., Krieg, P. A. and Olson, E. N. (2001a) 'Activation of cardiac gene expression by myocardin, a transcriptional cofactor for serum response factor', *Cell* 105(7): 851-62.

Wang, H., Huang, Z. Q., Xia, L., Feng, Q., Erdjument-Bromage, H., Strahl, B. D., Briggs, S. D., Allis, C. D., Wong, J., Tempst, P. et al. (2001b) 'Methylation of histone H4 at arginine 3 facilitating transcriptional activation by nuclear hormone receptor', *Science* 293(5531): 853-7.

Wang, Z., Zhai, W., Richardson, J. A., Olson, E. N., Meneses, J. J., Firpo, M. T., Kang, C., Skarnes, W. C. and Tjian, R. (2004) 'Polybromo protein BAF180 functions in mammalian cardiac chamber maturation', *Genes & development* 18(24): 3106-16.

Wright, T. J., Ricke, D. O., Denison, K., Abmayr, S., Cotter, P. D., Hirschhorn, K., Keinanen, M., McDonald-McGinn, D., Somer, M., Spinner, N. et al. (1997) 'A transcript map of the newly defined 165 kb Wolf-Hirschhorn syndrome critical region', *Human molecular genetics* 6(2): 317-24.

Xie, L., Hoffmann, A. D., Burnicka-Turek, O., Friedland-Little, J. M., Zhang, K. and Moskowitz, I. P. (2012) 'Tbx5-hedgehog molecular networks are essential in the second heart field for atrial septation', *Developmental cell* 23(2): 280-91.

Xue, Y., Canman, J. C., Lee, C. S., Nie, Z., Yang, D., Moreno, G. T., Young, M. K., Salmon, E. D. and Wang, W. (2000) 'The human SWI/SNF-B chromatin-remodeling complex is related to yeast rsc and localizes at kinetochores of mitotic chromosomes', *Proceedings of the National Academy of Sciences of the United States of America* 97(24): 13015-20.

Yamagishi, H., Yamagishi, C., Nakagawa, O., Harvey, R. P., Olson, E. N. and Srivastava, D. (2001) 'The combinatorial activities of Nkx2.5 and dHAND are essential for cardiac ventricle formation', *Developmental biology* 239(2): 190-203.

Zhang, C. L., McKinsey, T. A., Chang, S., Antos, C. L., Hill, J. A. and Olson, E. N. (2002) 'Class II histone deacetylases act as signal-responsive repressors of cardiac hypertrophy', *Cell* 110(4): 479-88.

Zhang, X. M., Ramalho-Santos, M. and McMahon, A. P. (2001) 'Smoothened mutants reveal redundant roles for Shh and Ihh signaling including regulation of L/R symmetry by the mouse node', *Cell* 106(2): 781-92.

Zhang, Y., Iratni, R., Erdjument-Bromage, H., Tempst, P. and Reinberg, D. (1997) 'Histone deacetylases and SAP18, a novel polypeptide, are components of a human Sin3 complex', *Cell* 89(3): 357-64.

Chapter 2

The BMP pathway acts to directly regulate *Tbx20* in the developing heart

Preface

This work was published as a co-first author publication in the journal *Development*. Graduate student Elizabeth Mandel carried out the initial identification and characterization of the *Tbx20* cardiac enhancer by *Xenopus* transgenesis and performed all of the cell culture transcription assays in collaboration with the Wang lab. Elizabeth also performed the PHERAstar protein-DNA binding assay. I generated the *XTbx20*-EGFP transgenic mice and performed all of the BMP-inhibition assays in *Xenopus* embryos and explants. I also performed the phospho-Smad1/5/8 chromatin immunoprecipitation in *Xenopus tropicalis* embryos. The zebrafish experiments were carried out in Deborah Yelon's lab. The project was conceived by Frank Conlon, and the manuscript was written with contributions by myself, Elizabeth, Frank, and Deborah Yelon.

Mandel E.M.[#] , Kaltenbrun E.[#], Callis, T.E., Zeng X.X.I., Marques S.R., Yelon D., Wang D.Z., and Conlon F.L. (2010) The BMP pathway acts to directly regulate *Tbx20* in the developing heart. *Development* Jun 137(11):1919-29. [#] These authors contributed equally to this work.

ABSTRACT

TBX20 has been shown to be essential for vertebrate heart development. Mutations within the *Tbx20* coding region are associated with human congenital heart disease, and the loss of *Tbx20* in a wide variety of model systems leads to cardiac defects and eventually heart failure. Despite the critical role of TBX20 in a range of cardiac cellular processes, the signal transduction pathways that act upstream of *Tbx20* remain unknown. Here we have identified and characterized a conserved 334bp *Tbx20* cardiac regulatory element that is directly activated by the BMP/SMAD1 signaling pathway. We demonstrate that this element is both necessary and sufficient to drive cardiac-specific expression of *Tbx20* in *Xenopus* and that blocking SMAD1 signaling in vivo specifically abolishes *Tbx20* transcription, but not that of other cardiac factors such as *Tbx5* and MHC, in the developing heart. We further demonstrate that activation of *Tbx20* by SMAD1 is mediated by a set of novel, non-canonical, high-affinity SMAD-binding sites located within this regulatory element and that phospho-SMAD1 directly binds a non-canonical SMAD1 site in vivo. Finally, we show that these non-canonical sites are necessary and sufficient for *Tbx20* expression in *Xenopus* and that reporter constructs containing these sites are expressed in a cardiac-specific manner in zebrafish and mouse. Collectively,

our findings define *Tbx20* as a direct transcriptional target of the BMP/SMAD1 signaling pathway during cardiac maturation.

INTRODUCTION

A series of clinical studies has provided direct evidence of a role for T-box genes in heart development and human disease, as mutations in at least three T-box genes, *Tbx1, Tbx5*, and *Tbx20*, have been linked to human congenital heart disease (CHD) (Kirk et al., 2007; Hammer et al., 2008; Liu et al., 2008; Qian et al., 2008). Specifically, mutations in *Tbx20* have been associated with a wide array of congenital abnormalities, including dilated cardiomyopathy (DCM), atrial septal defects (ASD), and mitral valve disease. Moreover, upregulation of *Tbx20* has been reported in patients with tetralogy of Fallot (Kirk et al., 2007; Hammer et al., 2008; Liu et al., 2008; Qian et al., 2008). These findings are consistent with studies of *Tbx20* orthologues in a wide range of model systems including mouse (*Tbx12/20*) (Carson et al., 2000; Kraus et al., 2001), zebrafish (*Tbx20/HrT*) (Ahn et al., 2000; Griffin et al., 2000), chick (Iio et al., 2001), and *Xenopus* (Brown et al., 2003; Showell et al., 2006), which have shown a requirement for *Tbx20* in a number of cardiac cellular processes. The effects of loss of *Tbx20* appear to be in part mediated through its endogenous role in restricting expression of *Tbx2*, a T-box containing protein required for the repression of chamber specific genes (Singh et al., 2009). Despite the essential role of *Tbx20* in cardiac development, little is known about the signal transduction pathways that function upstream to regulate *Tbx20* expression in the developing heart.

Members of the bone morphogenetic protein (BMP) family and their downstream mediators, the SMADs, have also been shown to be required for many cellular events in early heart development, including cardiac progenitor specification, proliferation, and differentiation. The role of BMPs in cardiac development is evidenced by the cardiac-associated defects in mouse mutants for components of the BMP pathway and by the observation that SMAD proteins, mediators of BMP signaling, are upregulated in response to cardiac stress or injury. However, identification of a specific cellular role for any single component of the BMP pathway in cardiac development is frequently confounded by genetic redundancy within the BMP and SMAD families and temporal and spatial differences in the activities of individual pathway components (reviewed in Klaus and Birchmeier, 2009; Euler-Taimor and Heger, 2006; Wijk et al., 2007). An alternative means of dissecting the roles of BMPs in early heart development would be to identify the direct transcriptional targets of BMP signaling; however, the cardiac targets of the BMP pathway remain poorly characterized.

In efforts to define the direct targets of growth factor pathways in heart development, we have identified a 334bp regulatory element that is both necessary and sufficient for *Tbx20* expression during cardiac chamber formation in *Xenopus*. We further show that the *Tbx20* cardiac element is a direct transcriptional target of the BMP/SMAD1 arm of the transforming growth factor-β (TGF-β) pathway and that its activation is independent of the TGF-β/activin/nodal/SMAD3 pathway. We further

demonstrate that *Tbx20* is co-expressed with nuclear SMAD1 in cardiomyocytes during cardiac chamber formation and that blocking SMAD1 activity in vivo leads to a specific loss of cardiac *Tbx20* but not other markers of cardiac tissue. We go on to demonstrate that the minimal cardiac *Tbx20* element contains four critical non-canonical, high-affinity SMAD-binding sites, which are directly bound by phospho-SMAD1 and are necessary for proper combinatorial regulation of *Tbx20*. Finally, we demonstrate that the ability to recognize the non-canonical SMAD1 sites is not specific to *Xenopus* by showing that reporter constructs containing these elements are expressed in a cardiac-specific manner in zebrafish and mouse. Collectively, our studies define a direct target of the BMP/SMAD1 signaling pathways in heart development and imply a role for BMP signaling in cardiac maturation.

MATERIALS AND METHODS

BAC Library Screen, RLM-RACE

The ISB-1 *X. tropicalis* bacterial artificial chromosome (BAC) library (Children's Hospital Oakland Research Institute (CHORI)) was screened with the 5' terminus of the *X. laevis Tbx20* coding region, and BAC DNA prepared according to CHORI. DNA was initially characterized by field inversion gel electrophoresis (FIGE) and Southern blot analysis using a panel of *Tbx20* specific probes. The transcriptional start site of *X. tropicalis Tbx20* was identified using the First Choice RLM-RACE Kit (Ambion) and 5' RLM-RACE as described by the manufacturer using whole *X. tropicalis* embryos (N=25) as well as brain-enriched and heart-enriched

tissues (approximately 250 embryos for each) at stage 28. Primer sequences and details available upon request.

Tbx20-EGFP and *Xenopus* Transgenesis

Tbx20-EGFP reporter constructs were generated by introducing EGFP in-frame into exon 1 of *Tbx20* at position +142. A *Tbx20*-EGFP deletion series was generated by substituting elements of *Tbx20* ranging from 471-2106bp, each containing a 5' EcoRI linker and a 3' BamHI linker, for the original 2601bp of the *Tbx20*-EGFP construct. Details and primer sequences available upon request. All *Tbx20* reporter constructs were linearized by KpnI and transgenesis performed according to Kroll and Amaya (Kroll and Amaya, 1996). For each construct greater than 10 EGFP-positive embryos were examined from at least three independent sets of injections.

XTbx20-EGFP Transgenic Mice

The *XTbx20*(-2464)-EGFP plasmid was prepared for microinjection by digestion with SacII and KpnI to release the linear transgene. The transgene DNA was purified by agarose gel electrophoresis and injected into the pronuclei of C57BL/6 x DBA2 hybrid embryos at the UNC Animal Model core facility. Fertilized ovum were subsequently implanted into pseudo-pregnant females and offspring were analyzed for the presence of the transgene. Founders were identified by PCR analysis of tail DNA, using the following primers: 5' CCCTATTTGATCAGCAAACG 3' and 5' CACTTCCATGGGCTGATGCT 3'. Embryos resulting from timed matings

between one of the male founders and a wild-type C57Bl6 female were screened for EGFP expression on a Leica MZ16F stereomicroscope. Animal care and animal experiments were in accordance with the Animal Care Committee at the University of North Carolina-Chapel Hill.

Xenopus Embryo and Explant Culture

Xenopus embryos were obtained and staged according to Nieuwkoop and Faber (Nieuwkoop and Faber, 1967). For tissue explants, tissue posterior to the cement gland and including the heart field was excised at stage 35/36 and cultured in 1X MBS (Chemicon) at 23°C until stage 40. The cardiac explants include overlying pharyngeal endoderm and some foregut endoderm. Anterior regions of whole embryos were excised and cultured in identical conditions as cardiac explants. Explants were treated at stage 40 with either 7μM DMSO or 5μM dorsomorphin (also referred to as Compound C; Calbiochem) in 1X MBS for 6 hours at 23°C (Hao et al., 2008; Yu et al., 2008). Explants were then fixed for 2 hours at room temperature in either Dent's Fix (80% MeOH in DMSO) for whole-mount antibody staining, MEMFA for in situ hybridization, or 4% PFA for immunohistochemistry.

Zebrafish Embryo Culture and Transgenesis

For transient expression in zebrafish, the *Tbx20*(-334) reporter construct was flanked by Tol2 arms in a pT2 vector for Tol2 transposase-mediated transgenesis (Fisher et al., 2006). Embryos were injected at the 10cell stage with 100pg of

capped mRNA encoding Tol2 transposase and 50-100pg of the transgene plasmid. Injected embryos were examined and photographed at 48 hours post-fertilization (hpf) on Zeiss M2Bio and Axioplan microscopes.

Cell Culture and Luciferase Assays

Transient transfections were conducted as previously described (Wang et al., 2001). Each assay conducted in triplicate at least two times in 12-well plates using the following expression plasmids: Myocardin (Wang et al., 2001), SRF(Wang et al., 2001), Mef2c (Wang et al., 2001), SMAD3 (Feng et al., 2000), SMAD4 (Feng et al., 2000), pRK5 N-Flag Smad1 (Liu et al., 1996), pGL3-Nkx2.5 (Lien et al., 2002), Gata4 (Oh et al., 2004), and SM22 (Li et al., 1996). Fold induction was calculated as induction compared to that of reporter alone, and error bars refer to the standard deviation of fold induction.

In Situ Hybridization and Immunohistochemistry

In situ hybridization and immunohistochemistry were conducted as previously described (Goetz et al., 2006) with the following addition: anti-Phospho-Smad1(Ser463/465)/ Smad5(Ser463/465)/ Smad8(Ser426/428) (1: 100; Cell Signaling).

Protein-DNA Binding Assays

For 2X coverage of the *Tbx20*(-334) regulatory element, 21 double-stranded, 30 basepair, 5'-FAM oligos were designed to overlap by 15 bases beginning from

base -1 (Figure 2.6A) and *XVent* and SRF binding site oligos were designed as positive and negative controls respectively, based on previously published work (Henningfeld et al., 2000; Chang et al., 2001). All fluorescence polarization experiments were performed in a PHERAstar microplate reader (BMG Labtechnologies) with reactions performed in a 50μL volume containing 250nM 5'-FAM oligo and increasing concentrations of GST-SMAD1 (0-7416.67nM, information available upon request) in 10mM Tris-HCl, pH 8.0, 100mM NaCl. Each assay was performed in triplicate at 25^{o}C. Anisotropy was measured by excitation with vertically polarized light, using 490nm excitation and 520nm emission filters with the gain optimized for maximum signal and normalized to "no protein" controls. Data analysis was performed using SigmaPlot 8.0 software, and dissociation constants (K_d) determined for each oligo using the single rectangular I, 3 parameter equation $y=y_o + ax/(b+x)$ where b is equal to K_d.

Chromatin Immunoprecipitation in *Xenopus tropicalis* Embryos

Stage 41 embryos (n=30) were cross-linked in 1% Formaldehyde in PBS for 60 minutes and washed in 0.125M Glycine for 10minutes and then three times in PBS. Embryos were homogenized in 500μL Cell Lysis Buffer (50mM Tris-HCl pH8, 2mM EDTA, 0.1% NP-40, 10% glycerol, and protease/phosphatase inhibitors), centrifuged, and the pellet rinsed twice in cold PBS. Nuclei were lysed in 200μL Nuclei Lysis Buffer (50mM Tris-HCl pH8, 10mM EDTA, 1% SDS, and protease/phosphatase inhibitors) and nuclear extracts were diluted in 400μL IP Dilution Buffer (20mM Tris-HCl pH8, 2mM EDTA, 150mM NaCl, 1% Triton X-100,

and protease/phosphatase inhibitors). ChIP extracts were sonicated three times for 30 seconds on ice, centrifuged, and supernatants were precleared with 50μL Protein A/G Agarose beads (Santa Cruz Biotechnology) at 4°C for 1.5 hours. Precleared ChIP extracts were diluted in 400μL IP Dilution Buffer and incubated with 2μg antibody on a rotating wheel at 4°C overnight. 50μL of Protein A/G Agarose beads was added to the ChIP samples for 2 hours at 4°C, and beads were subsequently washed in IP Dilution Buffer, ChIP Wash Buffer (10mM Tris-HCl pH8, 1mM EDTA, 1% sodium deoxycholate, 1% NP-40, 0.25M LiCl, and protease/phosphatase inhibitors), IP Dilution Buffer, and TE Buffer (10mM Tric-HCl pH8 and 1mM EDTA). The material was eluted in Elution Buffer (50mM Tris-HCl pH8, 10mM EDTA, and 1% SDS) at 65°C, digested with RNase A for 3 hours at 37°C, and incubated in 0.3M NaCl overnight at 65°C to reverse cross links. ChIP samples were subsequently digested with proteinase K for 4 hours at 55°, phenol extracted, and precipitated, and the recovery of specific DNA sequences was determined by quantitative PCR using SYBR Green PCR reagents (Sigma) and an Applied Biosystems 7900 HT Fast Real-Time PCR machine. Anti-Phospho-Smad1(Ser463/465)/ Smad5(Ser463/465)/ Smad8(Ser426/428) (Cell Signaling) antibody was used. As a control for this procedure, ChIP was also performed on stage 9 *Xenopus laevis* embryos (n=50) with a rabbit anti-β-catenin antibody (Cocalico Laboratories; Reamstown, PA) as previously reported (Blythe et al., 2009). Fold enrichment relative to a no antibody control was calculated using the comparative C_T method (ΔΔCt). See Table S2.1 for primer sequences.

RESULTS

A *Tbx20*-EGFP transgene recapitulates endogenous expression of *Tbx20* in mid-tadpole stage embryos

Given the evolutionarily conserved role for *Tbx20* in heart development and its role in human congenital heart disease we sought to determine the regulatory pathways that are required for the proper spatial and temporal expression pattern of *Tbx20*. To this end, we mapped the cardiac transcriptional start site of *Tbx20* and inserted an EGFP reporter cassette in-frame with the TBX20 translational start site (see Materials and Methods) in a 4116bp fragment corresponding to the 5-prime end of the *Xenopus tropicalis* (*X. tropicalis*) *Tbx20* locus (Figure 2.1A, B). Based on our observations that *Tbx20* is expressed in an identical pattern in *X. tropicalis* and *X. laevis* (Brown et al., 2003; Showell et al., 2006), we introduced the *Tbx20*(-2464)-EGFP reporter into *Xenopus laevis* (*X. laevis*) embryos by restriction enzyme-mediated integration (REMI) transgenesis. Consistent with endogenous *Tbx20* expression, the *Tbx20* reporter directed expression of EGFP to the developing heart and cement gland, (≥5 rounds of injections; n≥20 EGFP-expressing embryos per experiment; Figure 2.1C-F and Figure S2.1). Specifically, EGFP expression was first observed in the cement gland at stage 24 and in the heart at stage 32. Identical to endogenous *Tbx20* expression, as the cells of the cement gland began to undergo apoptosis, expression of EGFP decreased and was completely absent by late tadpole stages (stages 48). In contrast, EGFP expression in the heart was maintained through chamber differentiation and heart looping and continued to be expressed until later stages of cardiac development (>stage 46; Figure 2.1C-F; data not shown). We did not observe EGFP expression in the heart prior to early tadpole

stages (stage 32) nor in any other tissue types including those which endogenously express *Tbx20* such as the hindbrain and eye.

A 334bp of regulatory element is sufficient for cardiac *Tbx20* expression

To define the minimal regulatory element necessary to drive *Tbx20* cardiac-specific expression, we generated transgenic embryos with a panel of 5-prime deletion constructs. Results from these injections showed that -2464bp, -1483bp, and -334bp *Tbx20* reporters (≥3 rounds of injections; ≥20 EGFP-expressing embryos per experiment; Figure 2.2A-J) all recapitulated endogenous *Tbx20* expression in cardiac tissue and the cement gland at stage 46 (8/8 EGFP-expressing embryos per construct; Figure 2.2K-P). Collectively, these data show that sequences 334bp upstream of the *Tbx20* transcriptional start site contain elements that function to regulate *Tbx20* cardiac expression at this stage of heart development.

***Tbx20* reporter expression is conserved in mouse and regulated by SMAD1/SMAD4 but not SMAD3**

We observed that offspring from a mouse transgenic founder carrying the *Xenopus Tbx20*(-2464)-EGFP reporter shows an expression pattern analogous to that observed in *Xenopus* with strong EGFP expression throughout the developing heart but not in other tissues where *Tbx20* is endogenously expressed in the mouse, such as the hindbrain and the lateral plate mesoderm (Fig. 3A-D). Based on these findings we determined whether a set of murine cardiac transcription factors identified in the minimal 334bp *Tbx20* regulatory element by ConSite, Jaspar, and

Transfac software, including SRF, NKX2.5, MEF2C, GATA4, SMAD1, and TBX5, were capable of activating *Xenopus* cardiac-specific *Tbx20* reporters (Fig. 3E-G). Of the potential transcription factors, SMAD1, SRF, and the SRF co-factor myocardin were found to be capable of activating *Tbx20* (Fig. 3E-G). We further note that the 334bp reporter has a greater response to SMAD1 and SRF than the 1483bp or 2464bp elements, suggesting sequences upstream of the 334bp element can attenuate the response to SMAD1 and SRF. Although SRF and myocardin were able to induce *Tbx20*, upon further analysis we found that *Tbx20* reporters did not respond to myocardin or SRF in a dose-dependent fashion and mutation of putative SRF binding sites had no effect on the temporal or spatial expression of the *Tbx20* reporter in vivo (data not shown). Although we cannot formally rule out a role for SRF or myocardin in the regulation of *Tbx20* expression, we did not analyze the effects of SRF or myocardin on *Tbx20* expression in greater detail.

To also characterize the activation of *Tbx20* in response to the TGF-β family of signaling molecules, we tested the ability of SMAD1, a mediator of BMP signaling, SMAD3, a mediator of TGF-β/activin/nodal signaling, and the common SMAD, SMAD4, to activate *Tbx20* luciferase reporters. We observed a dose-dependent activation of both the largest (-2464) and smallest (-334) *Tbx20* regulatory elements with increasing amounts of SMAD1 and SMAD4 (Figure 2.3H, I, K, L). Further deletions of the *Tbx20* upstream region to -251 and -81 greatly decreased the responsiveness to SMAD4 and led to an increase in EGFP in non-specific regions in *Xenopus* transgenics (Figure S2.2).

We further observed that SMAD3 failed to activate any *Tbx20* reporter though it did induce expression of the SMAD3 control reporter SM22 (Figure 2.3J) (Qiu et al., 2003). Consistent with these findings, treatment of cells with the TGF-β/activin/nodal small molecule inhibitor SB431542 had no effect on the induction of *Tbx20* in response to SMAD4 (Figure 2.3M). Taken together, these results suggest that *Tbx20* cardiac activation occurs in a SMAD1-dependent, SMAD3-independent manner which is at least in part, mediated by sequences that lie between -81bp and -334bp upstream of the *Tbx20* cardiac transcriptional start site.

Tbx20 and SMAD1 are co-localized during cardiac chamber formation

Upon activation of the BMP signaling pathway, SMAD1 is phosphorylated and translocates to the nucleus where it binds DNA and regulates transcription of neighboring genes (reviewed in (Kretzschmar and Massague, 1998; Massague et al., 2005)). To determine if SMAD1 is nuclear localized and co-expressed with *Tbx20* in cardiac tissue and therefore, could function endogenously to regulate *Tbx20* expression, we serial sectioned *X. laevis* hearts (stage 46) and examined *Tbx20* expression by in situ hybridization. On adjacent sections we examined phospho-SMAD1 expression and its cellular localization by immuno-histochemistry. Our results demonstrate that at these stages *Tbx20* and phospho-SMAD1 are co-expressed throughout the myocardium of the developing heart including the ventricle, the atria, the outflow tract, and the truncus arteriosus (Figure 2.4A-F).

SMAD signaling is required for the maintenance of *Tbx20* expression in vivo

To verify that BMP signaling regulates *Tbx20* expression in vivo we determined the effects of inhibiting SMAD1 activation on *Tbx20* expression. In order to bypass the requirements for SMAD1 during the early stages of embryogenesis we made use of the SMAD1 inhibitor Dorsomorphin and a tissue explant assay (Langdon et al., 2007; Hao et al., 2008; Yu et al., 2008; Fukuda et al., 2009). As reported for tissue culture cells (Langdon et al., 2007; Hao et al., 2008; Yu et al., 2008; Fukuda et al., 2009), treatment of stage 40 anterior explants with Dorsomorphin clearly show that Dorsomorphin blocks the nuclear localization of SMAD1 (Figure 2.5A-F; A'-F') and completely inhibits the expression of *Tbx20* in the developing heart as compared to controls (Figure 2.5G, H, K, L). Moreover, the effects of blocking SMAD1 are specific to the cardiac expression of *Tbx20* as we see little change in expression of *Tbx20* in the hindbrain (Figure 2.5I, J). Furthermore, SMAD1 inhibition has little to no effect on other cardiac markers including MHC, tropomyosin, and *Tbx5* (Figure 2.5M-P; Figure S2.3). Taken together these results strongly imply that the BMP pathway signals through SMAD1 to directly regulate the cardiac expression of *Tbx20* in vivo.

SMAD activation of *Tbx20* occurs through direct binding of SMAD1

To identify the specific endogenous SMAD1 binding sites within the minimal 334bp *Tbx20* cardiac regulatory element, and to accurately determine the binding affinity of SMAD1 to the respective elements, we used fluorescence polarization assays. Double stranded, 30bp, 5' carboxyfluorescein-labeled oligos overlapping by

15bp were designed across the 334bp *Tbx20* cardiac regulatory element for full 2x coverage (Figure 2.6A). Based on the premise that oligos tumble more slowly in solution when bound by protein as compared to unbound oligos, we combined fluorescent oligos with increasing concentrations of GST-SMAD1 fusion protein to evaluate the changes in light depolarization, as anisotropy. From the anisotropy data, we plotted binding curves and calculated dissociation constants (K_d(mM)) for each oligo interaction with SMAD1 and as controls, the binding of GST-SMAD1 to oligos containing known SMAD1 binding sequences (*XVent*) or known SRF binding sequences (Figure 2.6B, Table S2.2) (Henningfeld et al., 2000; Chang et al., 2001). SMAD1 bound oligo 8, covering bases -105 to -135, with the highest affinity (K_d=2.078 mM). However, SMAD1 bound six additional oligos (2, 6, 9, 13, 16, 19) with affinities that are equal to or greater than twice that of *XVent* (K_d=2.078 mM to K_d=3.758 mM) (Figure 2.6B, Table S2.2). Results from these studies show that SMAD1 binds the *Tbx20* cardiac regulatory element at 7 individual sites with an affinity at least twice that of the *XVent* control oligo (Kd= 7.829 mM), suggesting that the seven sites are high affinity SMAD1 binding sites (Figure 2.6C). Sequence analysis of the oligos bound by SMAD1 reveal two conserved, consensus SMAD binding sites with the sequences GTCT and CAGAC in oligos 16 and 8, respectively. We also observed that one region containing a putative binding site failed to bind SMAD1 protein in vitro. From this, we propose the presence of non-traditional SMAD binding elements between bases -15 and -45 (oligo 2), -75 and -105 (oligo 6), -120 and -150 (oligo 8/9), -180 and -210 (oligo 13), and -270 and -300 (oligo 19). We

further note that SMAD1 is capable of binding non-canonical sites with affinities equal to that of canonical sites.

The ability of SMAD1 protein to bind non-canonical sites within the *Tbx20* 334bp cardiac regulatory element suggests the presence of a common SMAD1 motif within these oligos. Accordingly, sequence analysis by MEME software revealed a novel SMAD1 binding site with the sequence AGGA/CA/TG within oligos 19, 13, 9, 6, and 2. (Figure 2.6D). Of the oligos containing the non-canonical SMAD site, SMAD1 bound oligo 6, containing the binding site AGGCAG, with the highest affinity (Figure 2.6B; Table S2.2). To determine if SMAD1 directly binds a portion of the *Tbx20* cardiac element containing both canonical and non-canonical SMAD1 sites in vivo, we performed ChIP on stage 41 *X. tropicalis* tadpoles with a phospho-SMAD1/5/8 antibody (Figure 2.6C). In parallel and as a positive control, we tested the occupancy of β-catenin on the *Xnr6* locus in stage 9 *X. laevis* embryos, as *Xnr6* has been demonstrated by others to be a direct target of β-catenin by ChIP in *Xenopus* (Blythe et al., 2009). A 6.8-fold enrichment above background of phospho-SMAD1 was observed on the endogenous SMAD1 sites within the *Tbx20* cardiac element (Figure 2.6E, Amplicon 1). We next tested the occupancy of endogenous phospho-SMAD1 on a single non-canonical SMAD1 site within the *Tbx20* cardiac element (Figure 2.6C, Amplicon 2). Strikingly, phospho-SMAD1 was enriched 9.4-fold above background on the non-canonical SMAD1 site, which is comparable to the enrichment of β-catenin we see at the *Xnr6* locus (10.6-fold; Figure 2.6E). This

data is consistent with SMAD1 directly binding a novel non-canonical site within the *Tbx20* cardiac element in vivo.

Canonical SMAD sites alone are not sufficient for *Tbx20* activation by SMAD1

To determine which SMAD1 binding sites are critical for cardiac specific expression of *Tbx20*, we mutated the two consensus SMAD1 binding sites alone or in combination, in the context of the *Tbx20*(-2464)-EGFP or –luc reporter constructs (Figure 2.7A, B), and the *Tbx20*(-334)-EGFP or –luc constructs (Figure 2.7C, D). Results from these assays show that constructs lacking SMAD1 consensus sites are still SMAD1 responsive. Thus, these data strongly imply that SMAD1 responsiveness is mediated by non-canonical SMAD1 binding sites. Finally, if we delete the 334bp minimal element in the context of the original *Tbx20*(-2464) cardiac reporter, both the response to SMAD1/4 in tissue culture assays and EGFP expression are greatly reduced (Figure 2.7E,F, data not shown). Together, these data show that the 334bp region directly upstream of the *Tbx20* start site is necessary and sufficient for cardiac expression of *Tbx20* and that *Tbx20* cardiac expression is dependent on SMAD1/4 activity.

***Xenopus Tbx20* reporter constructs are expressed in a cardiac-specific fashion in zebrafish**

As a further test if *Tbx20* is a general target of the BMP/SMAD1 pathway we analyzed expression of *Tbx20* in zebrafish mutant for the BMP receptor alk8. Consistent with our findings in *Xenopus*, we observe a significant reduction in *Tbx20* expression in zebrafish *alk8* (*lost-a-fin*) mutants (Figure 2.8A,B). Zygotic *alk8*

mutants are weakly dorsalized, exhibiting the effects of a mild disruption of BMP signaling (Bauer et al., 2001; Mintzer et al., 2001). Correspondingly, *Tbx20* expression is diminished in the bilateral heart fields (Figure 2.8B).

The observation that the BMP/SMAD1 pathway directly regulates the cardiac expression of *Tbx20* through a set of non-canonical SMAD1 binding sites, and the observation that *Tbx20* is downregulated in alk8 mutants, led us to question whether recognition of the canonical and non-canonical SMAD1 binding sites is specific to *Xenopus* or if these sites can serve as a general response to BMP/SMAD1 signaling in other vertebrates. To address these issues, we generated a *Tbx20*(-334)-EGFP fusion construct flanked by Tol2 transposase sites and injected this transgene together with Tol2 transposase RNA into zebrafish. Injection of reporter constructs in this fashion yields relatively efficient, yet highly mosaic, transgene expression (Fisher et al., 2006). The *Tbx20*(-334)-EGFP transgene was highly efficient at driving EGFP expression in the zebrafish heart (Figure 2.8C-E). 93% (92/99) of the injected embryos expressed the transgene, and 100% (92/92) of the expressing embryos displayed mosaic EGFP expression in the heart. As with *Xenopus*, expression outside the heart was inconsistent and appeared as irreproducible ectopic expression of EGFP. In summary, our data demonstrate that the 334bp element from the *Xenopus Tbx20* locus is sufficient for cardiac-specific in *Xenopus* and zebrafish.

DISCUSSION

Studies of cardiac gene regulation have suggested that heart-specific transcription is regulated temporally and spatially via a set of distinct modular cis-acting elements (Schwartz and Olson, 1999). Here we report that SMAD signaling is required in vivo for expression of *Tbx20* during cardiac chamber formation. We have also identified a 334bp element in *Xenopus* that contains a series of seven high-affinity SMAD1/4-binding sites that are necessary and sufficient for the evolutionarily conserved cardiac expression of *Tbx20* in mouse and zebrafish. Complementary to this finding, we have identified additional sequences that attenuate the BMP/SMAD1 response. Collectively, our studies demonstrate a distinct temporal requirement for BMP signaling during heart development in which BMP signaling is required during the early phases of vertebrate heart development for the establishment of the cardiac lineage and a second, later role during cardiac chamber formation and maturation through the direct transcriptional regulation of *Tbx20*.

Tbx20 cardiac expression requires canonical and non-canonical SMAD1 binding sites

Our data demonstrate a requirement for a set of high-affinity, canonical and non-canonical SMAD-binding sites in the regulation of *Tbx20* expression. Sequence analysis of regions within the 334bp *Tbx20* cardiac element that were demonstrated to bind SMAD1 reveals two conserved consensus SMAD-binding sites containing the sequences GTCT and CAGAC, as well as a novel non-canonical SMAD binding motif containing the sequence AGGA/CA/TG. We observed that SMAD1 occupies a combination of these sites in vivo during cardiac maturation. We have demonstrated

that mutation of SMAD1/4 canonical binding sites, either singly or in combination, has little effect on the expression of *Tbx20* either in vitro or in vivo, implying that it is the complement of canonical and non-canonical SMAD1-binding sites that is required for cardiac expression of *Tbx20*. Further, our results suggest that the ability of SMAD1 to bind to DNA is not based on sequence alone. This hypothesis is supported by our observation that a region of the *Tbx20* minimal element containing a putative SMAD1/4-binding site failed to bind to SMAD1 in vitro. Taken together, our data support a model in which *Tbx20* expression is regulated during the later stages of heart development by BMP signaling. In this model, the BMP pathway acts through a combinatorial set of unique SMAD-binding elements, the individual elements of which differ in their contributions to the response to growth factor signaling, and therefore, to transcriptional output.

Our finding that a complement of SMAD1/4-binding sites is required for *Tbx20* cardiac expression is broadly consistent with the results of studies on two other BMP-responsive genes, *XVent* and *Nkx2.5*. Early mesodermal expression of *XVent* is dependent on five putative SMAD1/4-binding sites, while cardiac expression of *Nkx2.5* is dependent on twelve individual SMAD1/4-binding sites (Henningfeld et al., 2000; Liberatore et al., 2002; Lien et al., 2002). Similar to our findings, point mutations or deletions in multiple SMAD1/4-binding sites in the *XVent* promoter has no effect on SMAD responsiveness (Henningfeld et al., 2000). However, regulation of cardiac-specific expression of *Nkx2.5* appears to be unique in that cardiac tissue-specific expression of *Nkx2.5* is mediated by a direct interaction of a

SMAD1/SMAD4 complex and a member of the GATA transcription factor family (Liberatore et al., 2002; Caban et al., 2004). Although we have identified a GATA consensus site within the minimal *Tbx20* cardiac element, none of the *Tbx20* reporters respond to GATA4 (Fig. 3) and deletion of the GATA site has no effect on the cardiac-specific expression of *Tbx20* (Fig. 7D). Thus, tissue-specific expression of *Tbx20*, unlike that of *Nkx2.5*, appears to occur through a GATA-independent mechanism. The activation of cardiac gene expression via BMP signaling has also been shown to be dependent on additional cardiac transcription factors. For example, the myocardin-dependent expression of cardiac genes is synergistically activated by the direct interaction of SMAD1 with myocardin (Callis et al., 2005). However, data we obtained using a large panel of cardiac transcription factors demonstrate that, with the exception of SRF, none of these factors significantly induce *Tbx20* expression in transient transcriptional assays. While we cannot formally rule out a potential role of SRF in *Tbx20* expression, mutation of the SRF-binding site had no effect on the temporal or spatial expression of *Tbx20* reporter constructs in vivo (data not shown).

Cardiac-specific *Tbx20* expression

What, then, is the mechanism underlying the cardiac-specific expression of *Tbx20*? We note that nuclear localization of SMAD1 during heart development is temporally regulated. Based on this observation and the results of reporter analyses, we favor a model in which the complement of SMAD1/4-binding sites directs a pattern of broad temporal expression of *Tbx20* in the embryo and this

temporal expression pattern is further spatially refined by restriction of expression to the developing cardiac tissue as a result of the action of as yet unidentified transcriptional repressors. This idea is supported by our observations that 1), the response of *Tbx20* reporters to SMAD1 and SMAD4 is enhanced by deletion of regions both outside and within the 334bp element; and 2), upon reduction of the 334bp *Tbx20* regulatory element to 81bp, reporter expression substantially increased in non-cardiac tissues in *X. laevis* transgenic animals. These findings are consistent with studies that have demonstrated that the BMP arm of the SMAD signaling pathway is associated with the regulation of genes involved in early heart development, while the TGF-β/activin/nodal arm of the SMAD pathway appears to drive cardiac regulation of factors associated with fibrotic, apoptotic, and anti-hypertrophic events related to progression to heart failure (reviewed in (Euler-Taimor and Heger, 2006)). Further, it has been suggested that BMP signals act as long-range diffusible morphogens originating from multiple locations in the embryo including the endoderm, ectoderm, or cardiac cells themselves (Schultheiss et al., 1997; Schlange et al., 2000). It is therefore interesting to speculate that the regulation of the novel 334bp *Tbx20* cardiac element during late cardiogenesis is a result of a continued or second wave of BMP signaling from the underlying endoderm or from the myocardial cells, mediated by SMAD1/4.

Although the SMAD1/4-binding sites are critical for expression of *Tbx20* during cardiac chamber formation, the regulatory element described here does not activate endogenous expression of *Tbx20* in other regions of the embryo. Thus, our

minimal *Tbx20* element does not comprise all of the information necessary for the complete expression of *Tbx20* and elements regulating early cardiac and neural expression of *Tbx20* remain to be identified. Based on this observation and on the modular nature of the BMP/SMAD response elements described here, it appears that, as for regulation of *Nkx2.5* expression, regulation of *Tbx20* occurs in a modular manner. Finally, taking into consideration 1), that the minimal element we have identified is required for expression of *Tbx20* during cardiac chamber formation and 2), established correlation between mutations in *Tbx20* and human congenital heart disease, and 3), that not all human mutations that map to *Tbx20* occur in the coding region of the gene (Kirk et al., 2007; Hammer et al., 2008; Liu et al., 2008; Qian et al., 2008), it will be interesting to determine if an association exists between mutations in the *Tbx20* minimal element and congenital heart disease and/or cardiac hypertrophy.

ACKNOWLEDGMENTS

We thank Dr. Shoko Ishibashi, Dr. Enrique Amaya, Scott A. Lujan, Dr. Laura M. Guogas and Dr. Matthew R. Redinbo for technical assistance, and Dr. Christopher Showell for critical reading of the manuscript and helpful suggestions. We would also like to thank Dr. Yonqin Wu and the UNC *In Situ* Hybridization Core Facility for valuable assistance. We would like to thank N.A. Thomas for her contributions to the zebrafish work and Lauren Waldron for her technical assistance with *Xenopus* transgenesis. The tropomyosin antibody developed by J.-C. Lin was obtained from the Developmental Studies Hybridoma Bank developed under the

auspices of the NICHD and maintained by the University of Iowa, Department of Biological Sciences, Iowa City, IA 52242.

Sources of Funding

This work is supported by grants to F.L.C. from the NIH/NHLBI and the American Heart Association and an award from the UNC Medical Alumni Association. E.M.M. was supported by a National Science Foundation Graduate Research Fellowship and a UNC Graduate School Dissertation Completion Fellowship. E.K. was supported by the UNC Developmental Biology Training Grant and an award from American Heart Association. Work in the Yelon lab was supported by grants from the National Institutes of Health, American Heart Association, and March of Dimes. Work in the Wang lab was supported by the NIH/NHLBI and the American Heart Association.

Figure 2.1. A regulatory element 5' to the *Tbx20* genomic locus is sufficient to drive gene expression in the cement gland and heart. (A) Schematic representation of the *X. tropicalis Tbx20* genomic locus. *X. tropicalis Tbx20* consists of 8 exons spanning approximately 20 kB. The *Tbx20* transcriptional start site is located 287bp upstream of the transcriptional start site in exon 1. A putative cardiac regulatory element is located at the 5' end of the *Tbx20* locus (dashed box). (B) Schematic representation of the 2464bp region of the 5' end of *Tbx20* cloned in frame to the EGFP reporter to examine its regulatory capacity in *X. laevis* transgenics. (C-F), As with endogenous *Xenopus Tbx20* expression of the *Tbx20* EGFP reporter is expressed in the cement gland and heart of living *X. laevis* transgenic embryos. (C), Ventral view of the anterior end of stage 46 sibling non-transgenic (left) or transgenic (right) embryos. (D), Fluorescent view of siblings in (C, E, and F), Magnified view of the EGFP expression driven by the *Tbx20* regulatory element in the cement gland (E) and heart (F) of the transgenic embryo in (D).

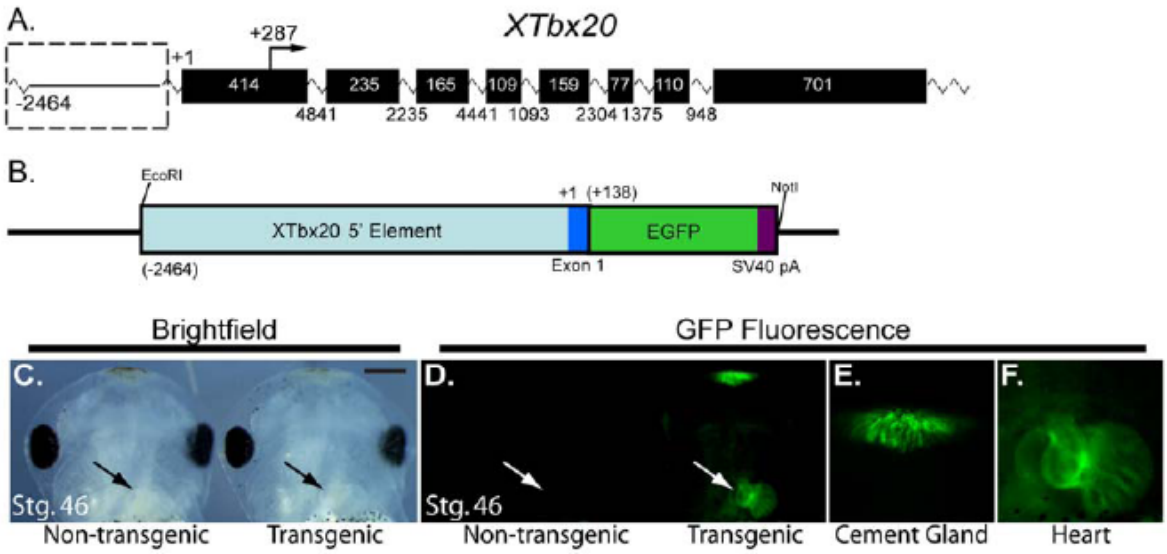
A.
XTbx20
+287
+1
-2464
414
235
165
109
159
77
110
701
4841
2235
4441
1093
2304
1375
948
B.
EcoRI
+1 (+138)
NotI
XTbx20 5' Element
EGFP
(-2464)
Exon 1
SV40 pA
Brightfield
GFP Fluorescence
C.
D.
E.
F.
Stg. 46
Stg. 46
Non-transgenic
Transgenic
Non-transgenic
Transgenic
Cement Gland
Heart

Figure 2.2. A 334bp regulatory element recapitulates the endogenous expression of *Tbx20* throughout the *X. laevis* heart. A deletion series of the 5' regulatory element was created to determine a reduced element sufficient to drive EGFP transgene expression. (A), Schematic representation of the deletion series of *Tbx20* elements fused to EGFP for *X. laevis* transgenesis. (B, E, H), Ventral view of the anterior regions of living stage 46 (late tadpole) *X. laevis* embryos (left) and siblings transgenic for constructs shown in (A) (right) under white light. (C, F, I) Embryos as viewed under fluorescent light. Green autofluorescence in the gut can be noted in both control and transgenic embryos. (D, G, I), Magnified views of the EGFP-expressing hearts of embryos in (C, F, and I) demonstrating that EGFP expression in the heart is maintained under the control of a *Tbx20*(-334) element. Transverse sections were cut through the embryos expressing *Tbx20*-EGFP shown in (B-J), and expression of the *Tbx20(-2459)*-EGFP (K, L), *Tbx20(-1483)*-EGFP (M, N), and *Tbx20(-334)*-EGFP (O, P) transgenes is demonstrated by antibody staining for EGFP. Anterior (K, M, O) and posterior (L, N, P) sections show EGFP transgene expression throughout the heart. *TA – truncus arteriosis, OFT – outflow tract, CA – carotid arch, V – ventricle, T – trabeculae, EC – endocardial cushion, PA – pulmocutaneous arch, SA – systemic arch, LA – left atrium, RA – right atrium*

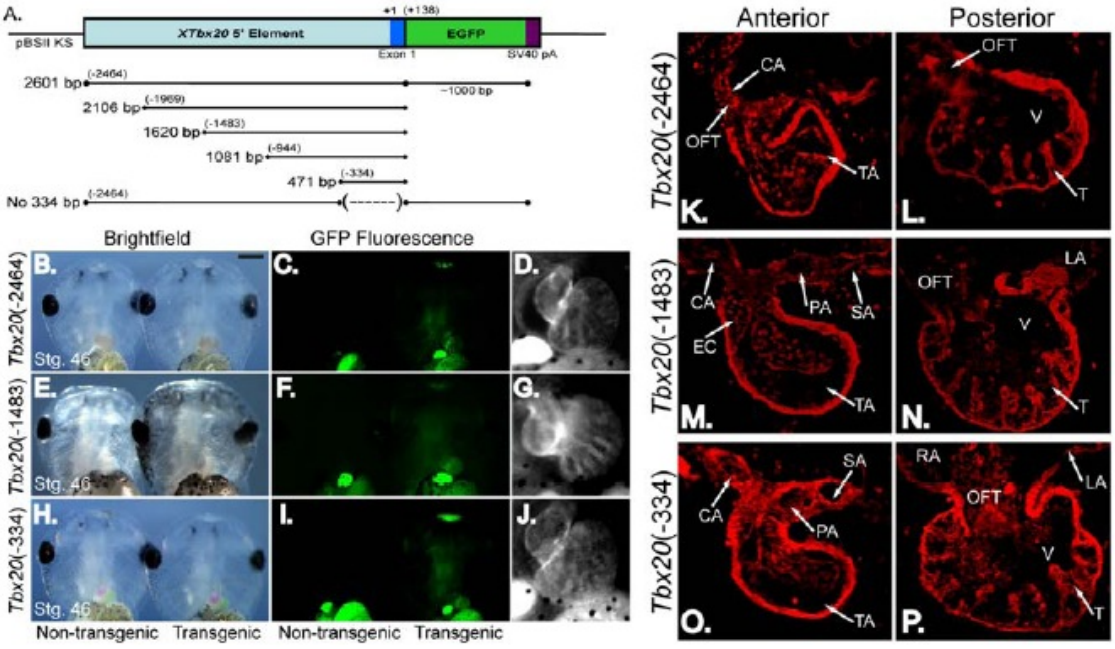
A.
+1 (+138)
pBSII KS
XTbx20 5' Element
EGFP
Exon 1
SV40 pA
2601 bp (-2464)
~1000 bp
2106 bp (-1969)
1620 bp (-1483)
1081 bp (-944)
471 bp (-334)
No 334 bp (-2464)
Brightfield
GFP Fluorescence
Tbx20(-2464)
Tbx20(-1483)
Tbx20(-334)
B.
C.
D.
E.
F.
G.
H.
I.
J.
Stg. 46
Non-transgenic
Transgenic
Non-transgenic
Transgenic
Anterior
Posterior
K.
L.
M.
N.
O.
P.
CA
OFT
TA
V
T
EC
PA
SA
LA
RA

Figure 2.3. *XTbx20* 5' regulatory elements are activated by TGF-β/BMP signaling via SMAD1 and SMAD4 but not SMAD3. (A,B), The *Xenopus XTbx20* 5' element is expressed in a cardiac-specific manner in E10.5 mouse embryos derived from a transgenic mouse founder expressing the *XTbx20*(-2464) fragment. (C,D), Magnified view of EGFP fluorescence in the heart of *XTbx20*(-2464)$^{+/-}$ mouse embryo. (E-G), Luciferase reporters controlled by three *Tbx20* deletion elements were transfected into COS7 cells with a panel of cardiac factor expression plasmids. Both the *Tbx20*(-2464) (H,I) and *Tbx20*(-334) (K,L) reporters are activated by SMAD1 and SMAD4 in a dose-dependent manner when transfected with increasing amounts of SMAD expression plasmid. (J), SMAD3 transfection does not induce the *Tbx20*(-2464) reporter, though the control SM22 reporter is dramatically induced. (M), Treatment of COS7 cells with increasing doses of a small molecule inhibitor of activin signaling SB431542 does not affect the activation of the *Tbx20*(-334) plasmid by SMAD4. Values are the fold-increase in luciferase activity relative to that driven by the reporter alone. Error bars represent the standard of fold induction for three trials. *LV- left ventricle, RV- right ventricle, OFT- outflow tract.* Scale bars: 1mm in (A-D).

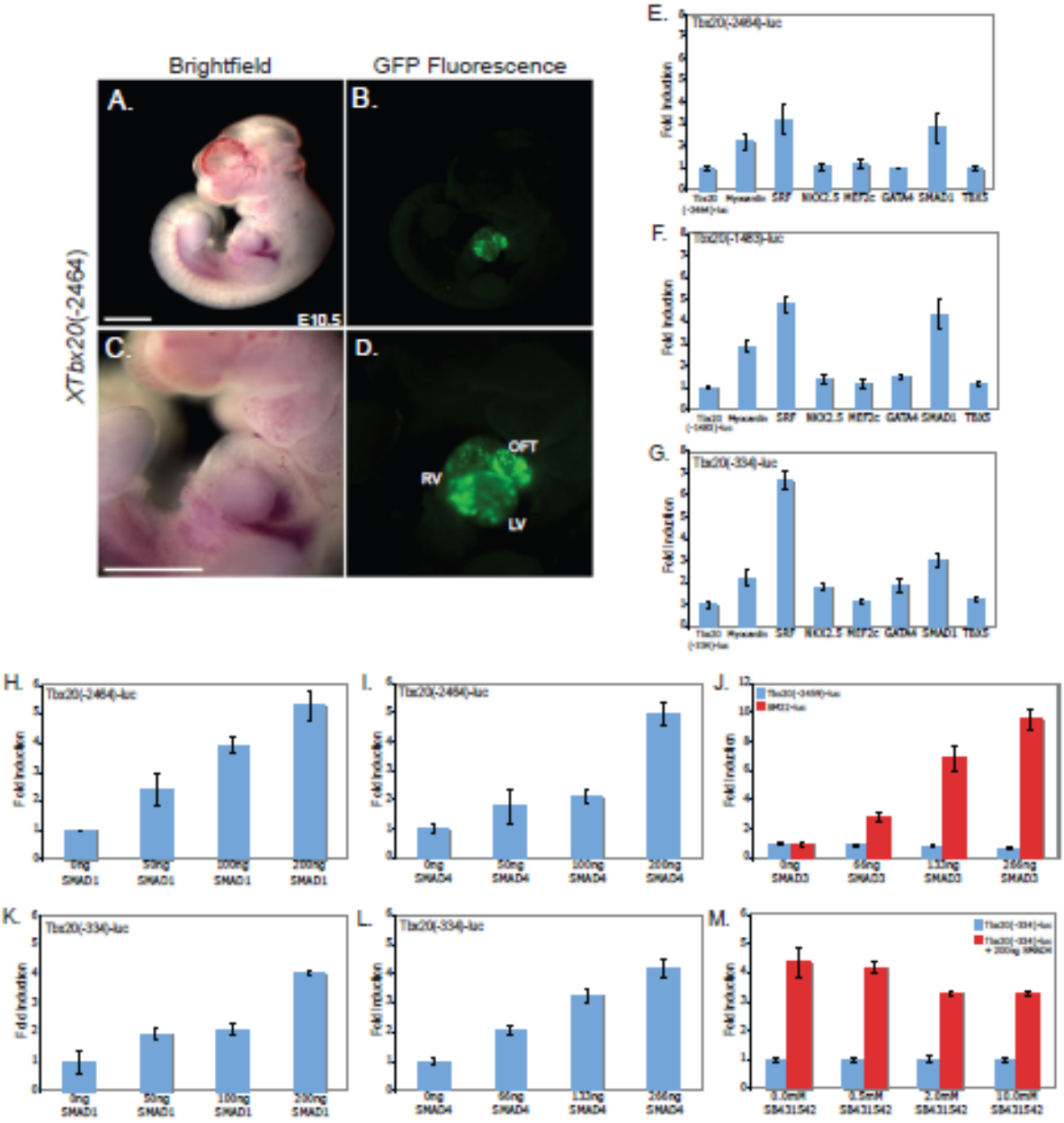
Brightfield
GFP Fluorescence
A.
B.
C.
D.
E10.5
XTbx20(-2464)
OFT
RV
LV
E.
F.
G.
H.
I.
J.
K.
L.
M.
Tbx20(-2464)-luc
Tbx20(-1483)-luc
Tbx20(-334)-luc
Fold Induction
SRF
NKX2.5
MEF2c
GATA4
SMAD1
TBX5
0ng SMAD1
50ng SMAD1
100ng SMAD1
200ng SMAD1
0ng SMAD4
50ng SMAD4
100ng SMAD4
200ng SMAD4
0ng SMAD3
66ng SMAD3
132ng SMAD3
266ng SMAD3
0.0mM SB431542
0.5mM SB431542
2.0mM SB431542
10.0mM SB431542

Figure 2.4. *XTbx20* is expressed throughout the myocardium and endocardium of the *X. laevis* heart. (A, B), *Tbx20* is expressed in both the anterior and posterior regions of the *X. laevis* stage 46 heart. Serial sections show that *Tbx20* expression overlaps with that of the myocardial marker tropomyosin (C, D) and with phospho-SMAD1/5/8 expression in the endocardium (E, F) by immunohistochemistry. (C-F), Anti-tropomyosin (Tm) staining is labeled in green, anti-pSMAD1/5/8 is labeled in red, and all nuclei are labeled with DAPI in blue. *TA-truncus arteriosus, OFT-outflow tract, LA-left atrium, V-ventricle*

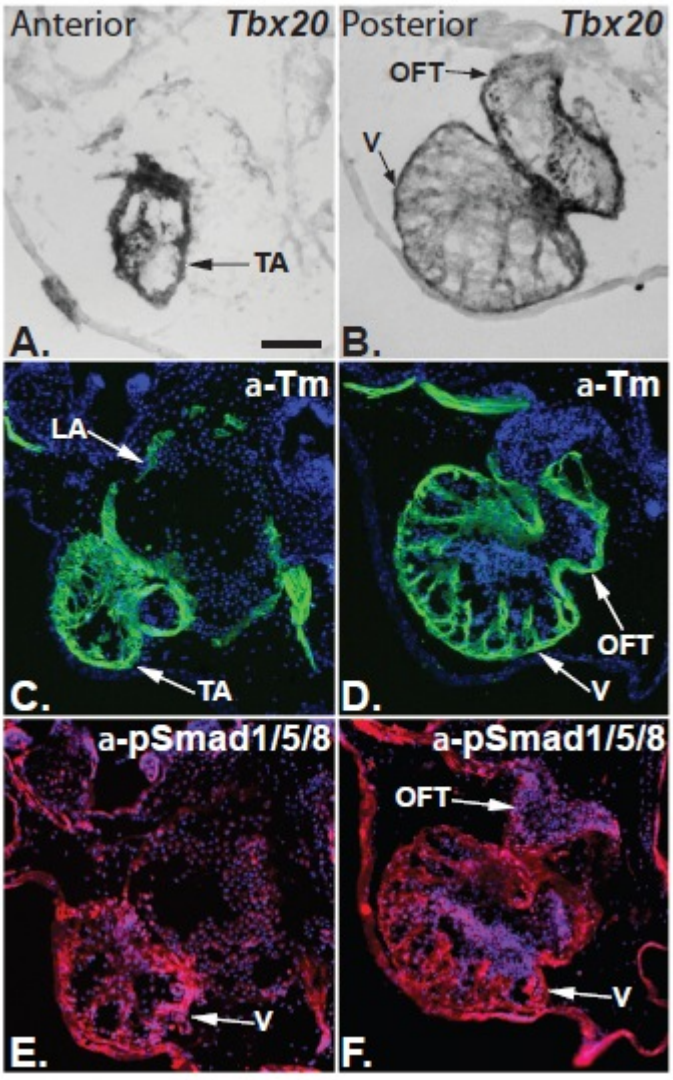

Figure 2.5. SMAD1 activation is required for cardiac specific expression of *Tbx20* in *X. Laevis*. (A-F), Transverse sections through the heart of stage 40 anterior explants show loss of nuclear phospho-SMAD1/5/8 in the myocardium of dorsomorphin-treated explants (D-E, D'-E') compared to DMSO-treated controls (A-C, A'-C') by immunohistochemistry. In the merged image, anti-phospho-SMAD1/5/8 (pSMAD1/5/8) staining is labeled in red, anti-myosin heavy chain (MHC) is labeled in green, and all nuclei are labeled with DAPI in blue. (G-L), In situ hybridizations for *Tbx20* performed on stage 40 anterior and cardiac explants show complete loss of *Tbx20* expression in the heart (H, L) but not the hindbrain (J) of dorsomorphin-treated anterior and cardiac explants compared to DMSO-treated controls (G, I, K). (M-P), Whole-mount antibody staining of stage 40 anterior explants show normal expression of the myocardial marker MHC in dorsomorphin-treated explants (N, P) compared to DMSO-treated controls (M, O). *Dorso, dorsomorphin.* Scale bars: 20 μm in (A-F'); 1 mm in (G-P).

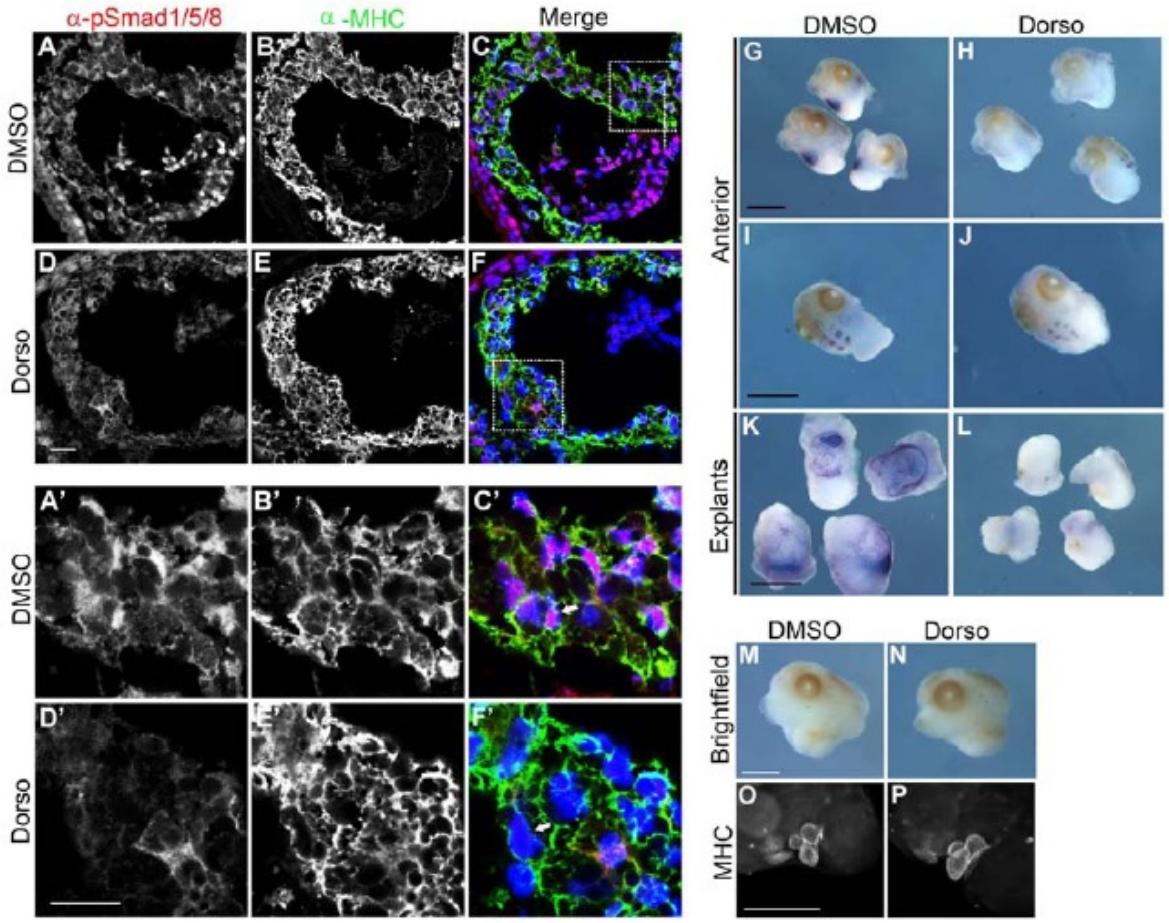
α-pSmad1/5/8
α -MHC
Merge
DMSO
Dorso
A
B
C
D
E
F
A'
B'
C'
D'
E'
F'
DMSO
Dorso
Anterior
Explants
G
H
I
J
K
L
DMSO
Dorso
Brightfield
MHC
M
N
O
P

Figure 2.6. SMAD1 binds to seven regions within the 334bp *Tbx20* regulatory element in vitro and occupies a combination of canonical and non-canonical SMAD1 binding sites in vivo. (A), Double stranded, 5' carboxyfluorescein-labeled, 30bp oligos designed for 2x coverage of the 334bp *Tbx20* cardiac regulatory element for use in fluorescence polarization assays. (B), Graphical representation of dissociation constants (Kd) for each oligo analyzed in fluorescence polarization studies. Bold type indicates oligos bound by SMAD1. (C), Schematic representation of the location of seven putative SMAD1 binding sites located within the 334bp cardiac regulatory element including the regions to be amplified by two separate sets of ChIP PCR primers. (D), Position weight matrix generated by MEME software from the sequence analysis of oligos 19, 13, 9, 6, and 2 reveals a novel non-canonical SMAD1 binding site within the 334bp cardiac regulatory element. (E), Phospho-SMAD1 occupies a combination of canonical and non-canonical SMAD1 binding sites within the 334bp cardiac regulatory element. ChIP assay was performed on stage 41 *X. tropicalis* tadpoles with a phospho-SMAD1/5/8 antibody and precipitated DNA was probed with primers against either a combination of canonical and non-canonical SMAD1 sites (Amplicon 1) or a single non-canonical SMAD1 site (Amplicon 2). For comparison, ChIP assay was performed on stage 9 *X. laevis* embryos with a β-catenin antibody, and precipitated DNA was probed with primers against *Xnr6*. Fold enrichment is the signal relative to background (no antibody control).

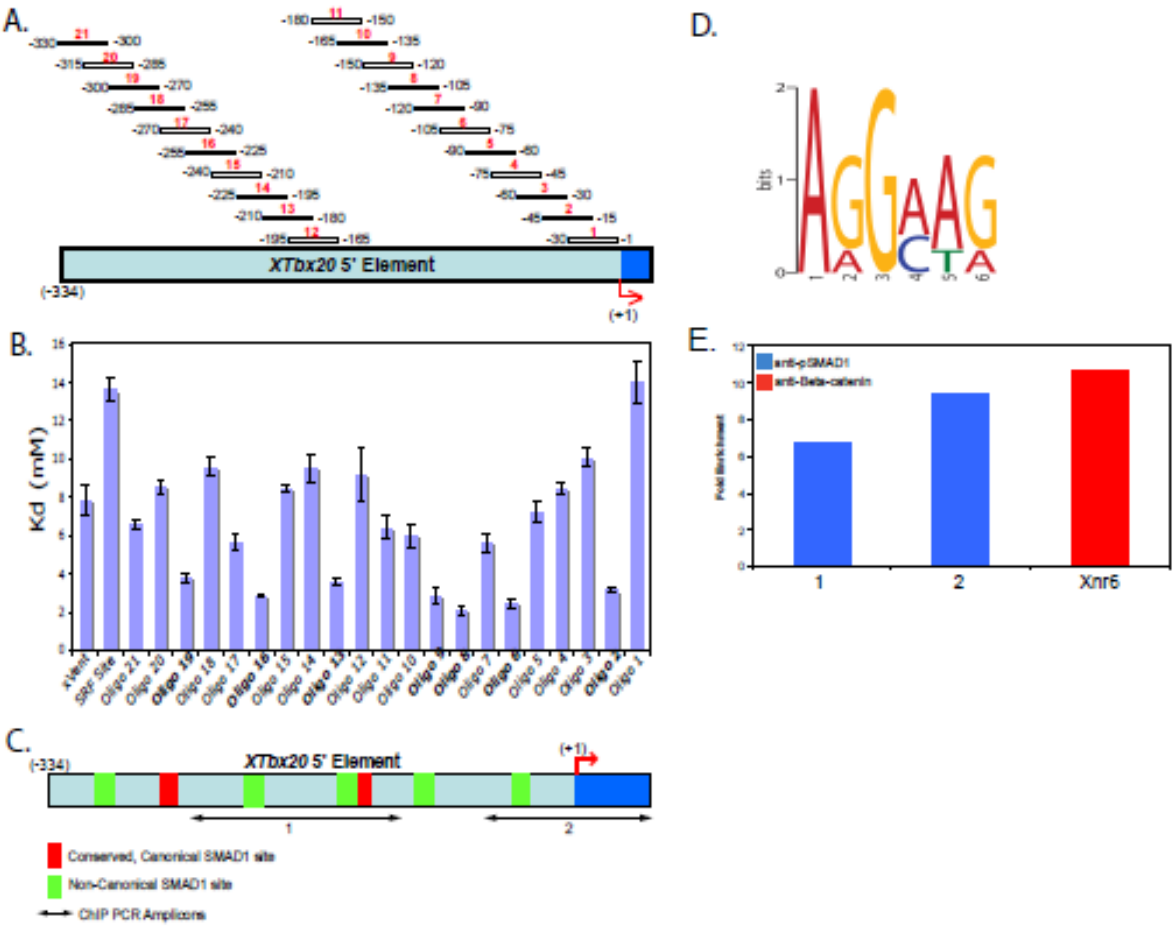
A.
XTbx20 5' Element
(-334)
(+1)
B.
Kd (nM)
C.
XTbx20 5' Element
(-334)
(+1)
Conserved, Canonical SMAD1 site
Non-Canonical SMAD1 site
ChIP PCR Amplicons
D.
bits
E.
anti-pSMAD1
anti-Beta-catenin
1
2
Xnr6

Figure 2.7. SMAD1 activation is mediated through non-canonical SMAD1 binding sites. *Tbx20* reporter constructs with mutation of the two consensus SMAD 1 binding sites alone or in combination, in the context of the *Tbx20* (-2464)-EGFP or –luc reporter constructs (A, B), and the *Tbx20*(-334)-EGFP or –luc constructs (C, D), leads to a decrease but not loss of activation in response to SAMD1. Deletion of the 334bp regulatory element was from the 2464bp reporters *Tbx20*(-2464:-334)-luc and *Tbx20*(-2464:-334)-EGFP, led to a substantial decrease in reposen to SAMD1. Fold induction reflects changes in induction relative to induction of the reporter alone, and error bars represent standard of three replicates.

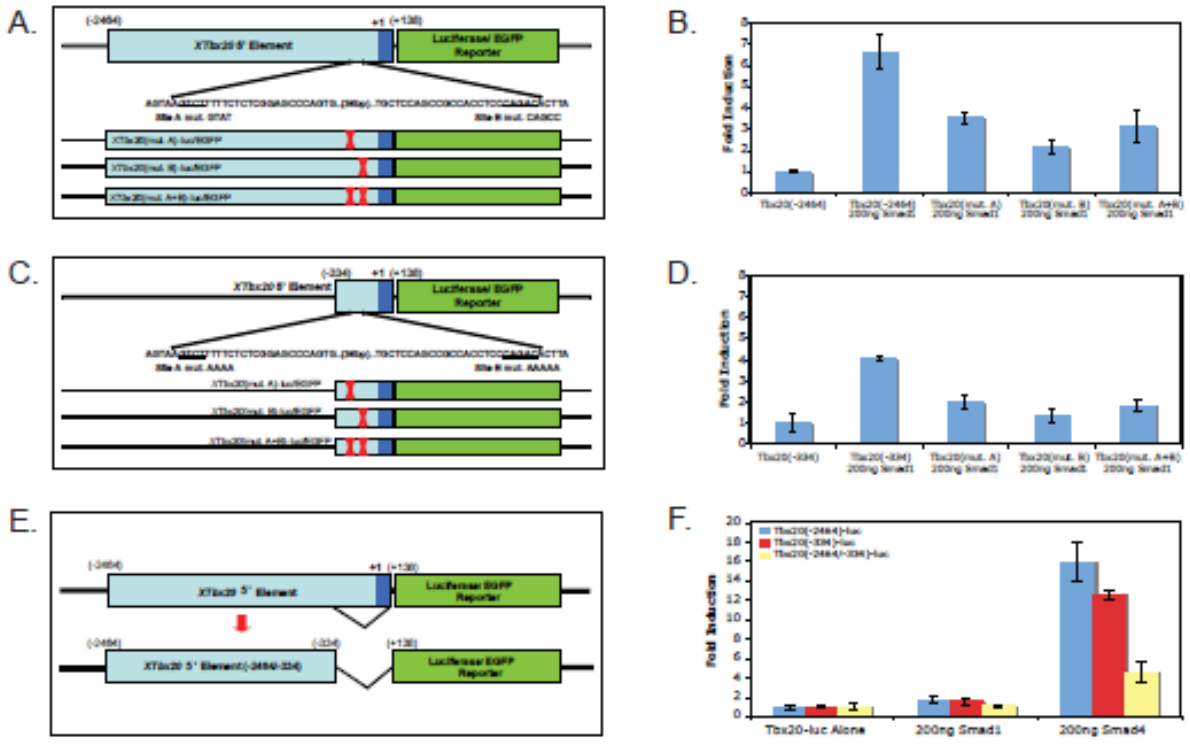

Figure 2.8. The *Xenopus Tbx20* 334bp cardiac regulatory element is expressed in a cardiac-specific manner in zebrafish. (A,B), In situ hybridization depicts expression of *Tbx20* in wild-type zebrafish embryos and *alk8*^{sk42} (Marques and Yelon, 2009) mutant siblings at the 10-somite stage; dorsal views, anterior to the top. *Tbx20* expression is reduced in both the anterior lateral plate mesoderm, including the bilateral cardiac primordia, and the midline mesenchyme of zygotic *alk8* mutants. (C-E), Lateral views of a live zebrafish embryo at 48 hpf, following injection with the *XTbx20*(-334) transgene. Injected embryos express EGFP in the myocardium.

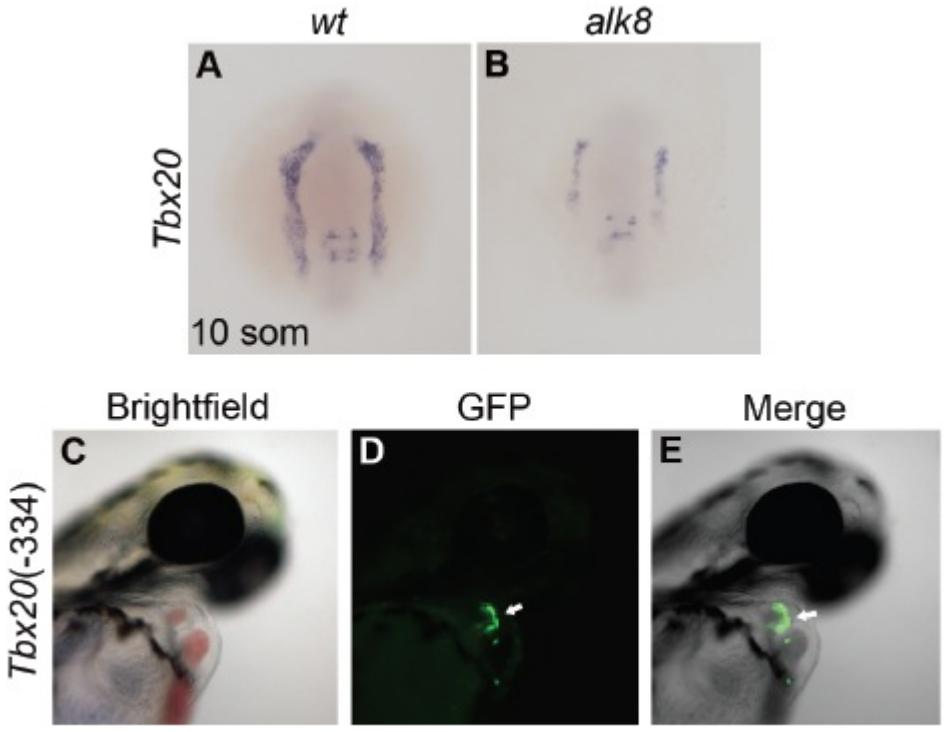

Figure S2.1. The *Tbx20*-EGFP reporter directs EGFP expression reproducibly in the heart and cement gland of transgenic siblings. (A,B), Ventral view of the anterior end of stage 46 non-transgenic (left) and transgenic siblings (right) generated from one batch of injections of the *Tbx20*(-2464)-EGFP reporter demonstrate consistent and reproducible EGFP expression within the heart and cement gland of transgenic embryos. Brightfield views of living embryos (A) and corresponding EGFP fluorescence (B) are shown.

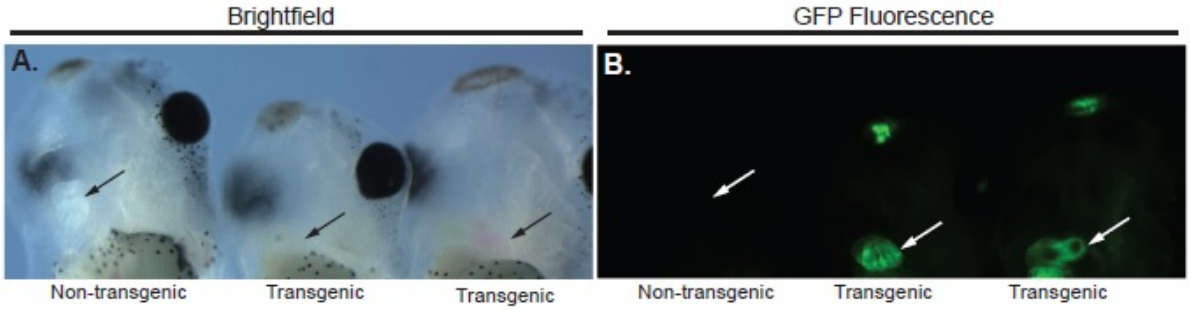

Figure S2.2. Further deletion of the *Tbx20*(-334)-EGFP reporter leads to a decrease in activity in response to SMAD4 and an increase in non-specific Tbx20 expression. (A,B), *Tbx20*(-251)-luciferase reporter (A) and *Tbx20*(-81)-luciferase reporter (B) and corresponding SMAD4 transcriptional assays. Fold induction reflects changes in induction relative to induction of the reporter alone, and error bars represent standard of three replicates. (C-F), *Tbx20*(-251)-EGFP (C, D) or *Tbx20*(-81)-EGFP (E, F) reporter constructs were introduced into *X. laevis* transgenic embryos. Transgenic embryos are located at the right of each image, while non-transgenic siblings are at the left. Brightfield views of living stage 46 embryos (C,E) and EGFP expression of corresponding embryos (D,F) are shown. *non-Tg, non-transgenic, Tg, transgenic*

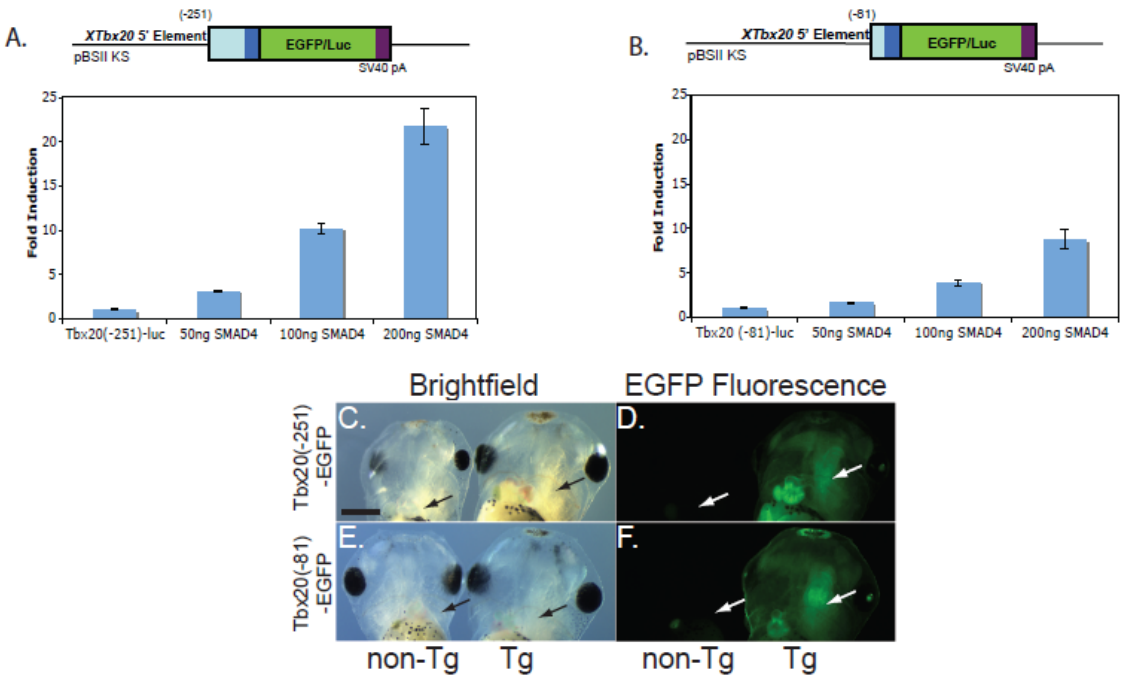

Figure S2.3. SMAD1 inhibition during cardiac chamber differentiation does not affect expression of the cardiac markers tropomyosin and Tbx5. (A,B), In situ hybridization for *Tbx5* on stage 40 DMSO (A) and dorsomorphin-treated (B) anterior explants show normal expression of *Tbx5* in the heart and cardinal vein after SMAD1 inhibition. (C-F), Whole mount antibody staining for tropomyosin of a stage 40 DMSO (C,E) or dorsomorphin-treated (D,F) anterior explant. Ventral view reveals no change in expression of tropomyosin in the heart after treatment with dorsomorphin. *Dorso, dorsomorphin*. Scale bars: 1 mm.

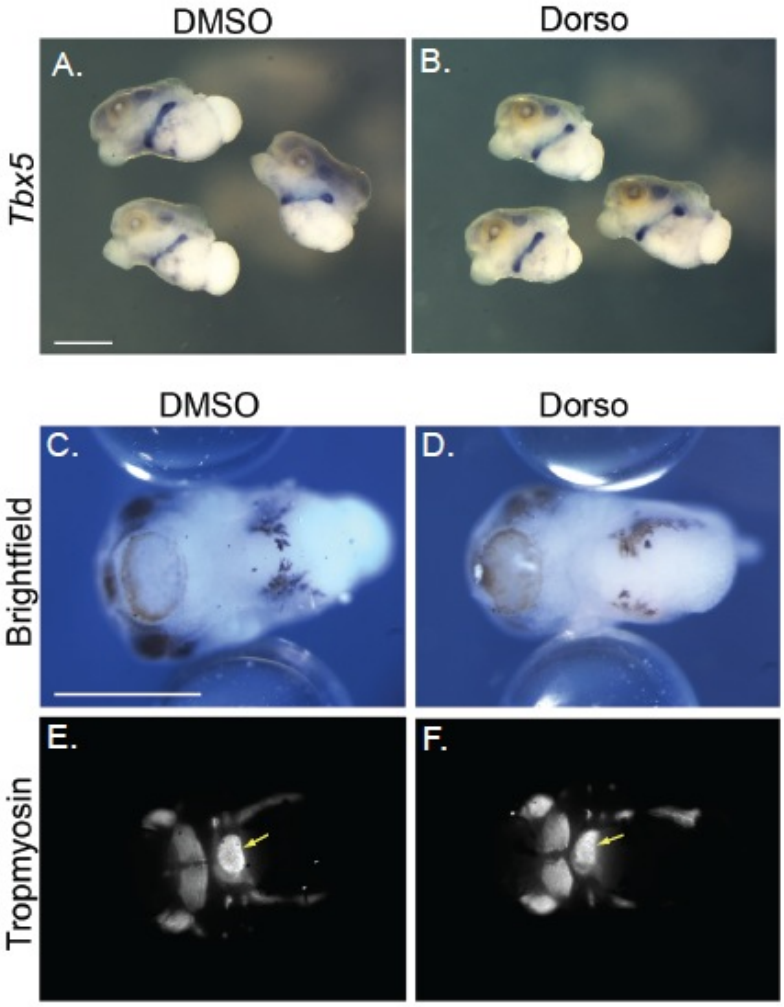

Table S2.1. **ChIP Primer Sequences.**

ChIP Primer	Primer Sequence
Xnr6 Inner/Forward	5'- GGT AGA TGA AAG GCT GAC AGG TGT G -3'
Xnr6 Inner/Reverse	5'- GGC TGT TGA AAA CTG AAA TGA AGC -3'
SMAD1 sites/Forward	5'- TTT CTC TCG GAG CCC AGT GA -3'
SMAD1 sites/Reverse	5'- GCT GAT AAG TGT CTG GGA GG -3'
Non-canonical SMAD1 site/Forward	5'- ATA GGA TCT GTG TGG CCA TG-3'
Non-canonical SMAD1 site/Reverse	5'- CTG ACA GTG GCC AGG AGA TT-3'

Table S2.2. Dissociation constants (K_d), standard deviation and nucleotide sequence for each oligo analyzed in fluorescence polarization studies (*indicates oligos bound by SMAD1).

OLIGO	Kd (mM)	Std. Dev.	Oligo Sequence
xVent	7.829	0.7465	AGAGAGAATGTTTAGCATAACAATAGC
SRF site	13.59	0.6407	AGCTTCTTTACACAGGATGTCCATATTAGGACATCTGCGTCAGCAA
Oligo 21	6.535	0.2181	CTATTTGATCAGCAAACGAGATGGATTACA
Oligo 20	8.512	0.3635	ACGAGATGGATTACAGATGAGCATCCTTAG
Oligo 19*	3.758	0.2244	GATGAGCATCCTTAGATTACTCTAAAAGCC
Oligo 18	9.539	0.4817	ATTACTCCTAAAAGCCCCGCCCTTCTCTTAT
Oligo 17	5.631	0.4146	CCGCCCTTCTCTTATGTCACGTGTGCTTTT
Oligo 16*	2.848	0.08203	GTCACGTGTGCTTTTTTTTAGTAAGTCTTT
Oligo 15	8.428	0.1427	TTTTAGTAAGTCTTTTTCTCTCGGAGCCCA
Oligo 14	9.473	0.7696	TTCTCTCGGAGCCCAGTGAGAAAAAGAAGT
Oligo 13*	3.56	0.19	GTGAGAAAAAGAAGTAGCTCGGCTGATCCT
Oligo 12	9.128	1.409	AGCTCGGCTGATCCTATCTGGCCCTGCTCC
Oligo 11	6.382	0.6181	ATCTGGCCCTGCTCCATCCCTGCTGCCCTT
Oligo 10	5.97	0.598	ATCCCTGCTGCCCTTCATTCATTGCCTGTG
Oligo 9*	2.836	0.3847	CATTCATTGCCTGTGCTCCAGCCGCCACCT
Oligo 8*	2.078	0.2239	CTCCAGCCGCCACCTCCCAGACACTTATCA
Oligo 7	5.566	0.4806	CCCAGACACTTATCAGCTGTATCAGGCAGA
Oligo 6*	2.402	0.1846	GCTGTATCAGGCAGATGTGACGCTGCAGGG
Oligo 5	7.201	0.5312	TGTGACGCTGCAGGGCTCCAATTGGCCAGG
Oligo 4	8.436	0.3279	CTCCAATTGGCCAGGAGAGAGATAGGATCT
Oligo 3	10.03	0.4913	AGAGAGATAGGATCTGTGTGGCCATGAAAT
Oligo 2*	3.106	0.1021	GTGTGGCCATGAAATTAAGGAAGCAGAGGC
Oligo 1	14.03	1.1	TAAGGAAGCAGAGGCTGAGAATGGGAACAG

REFERENCES

Ahn, D. G., Ruvinsky, I., Oates, A. C., Silver, L. M. and Ho, R. K. (2000) 'tbx20, a new vertebrate T-box gene expressed in the cranial motor neurons and developing cardiovascular structures in zebrafish', *Mech Dev* 95(1-2): 253-8.

Bauer, H., Lele, Z., Rauch, G. J., Geisler, R. and Hammerschmidt, M. (2001) 'The type I serine/threonine kinase receptor Alk8/Lost-a-fin is required for Bmp2b/7 signal transduction during dorsoventral patterning of the zebrafish embryo', *Development* 128(6): 849-58.

Blythe, S. A., Reid, C. D., Kessler, D. S. and Klein, P. S. (2009) 'Chromatin immunoprecipitation in early Xenopus laevis embryos', *Dev Dyn* 238(6): 1422-32.

Brown, D. D., Binder, O., Pagratis, M., Parr, B. A. and Conlon, F. L. (2003) 'Developmental expression of the Xenopus laevis Tbx20 orthologue', *Dev Genes Evol* 212(12): 604-7.

Caban, A. J., Hama, A. T., Lee, J. W. and Sagen, J. (2004) 'Enhanced antinociception by nicotinic receptor agonist epibatidine and adrenal medullary transplants in the spinal subarachnoid space', *Neuropharmacology* 47(1): 106-16.

Callis, T. E., Cao, D. and Wang, D. Z. (2005) 'Bone morphogenetic protein signaling modulates myocardin transactivation of cardiac genes', *Circ Res* 97(10): 992-1000.

Carson, C. T., Kinzler, E. R. and Parr, B. A. (2000) 'Tbx12, a novel T-box gene, is expressed during early stages of heart and retinal development', *Mech Dev* 96(1): 137-40.

Chang, P. S., Li, L., McAnally, J. and Olson, E. N. (2001) 'Muscle specificity encoded by specific serum response factor-binding sites', *J Biol Chem* 276(20): 17206-12.

Euler-Taimor, G. and Heger, J. (2006) 'The complex pattern of SMAD signaling in the cardiovascular system', *Cardiovasc Res* 69(1): 15-25.

Feng, X. H., Lin, X. and Derynck, R. (2000) 'Smad2, Smad3 and Smad4 cooperate with Sp1 to induce p15(Ink4B) transcription in response to TGF-beta', *EMBO J* 19(19): 5178-93.

Fisher, S., Grice, E. A., Vinton, R. M., Bessling, S. L., Urasaki, A., Kawakami, K. and McCallion, A. S. (2006) 'Evaluating the biological relevance of putative enhancers using Tol2 transposon-mediated transgenesis in zebrafish', *Nat Protoc* 1(3): 1297-305.

Fukuda, T., Kohda, M., Kanomata, K., Nojima, J., Nakamura, A., Kamizono, J., Noguchi, Y., Iwakiri, K., Kondo, T., Kurose, J. et al. (2009) 'Constitutively activated ALK2 and increased SMAD1/5 cooperatively induce bone morphogenetic protein signaling in fibrodysplasia ossificans progressiva', *J Biol Chem* 284(11): 7149-56.

Goetz, S. C., Brown, D. D. and Conlon, F. L. (2006) 'TBX5 is required for embryonic cardiac cell cycle progression', *Development* 133(13): 2575-84.

Griffin, K. J., Stoller, J., Gibson, M., Chen, S., Yelon, D., Stainier, D. Y. and Kimelman, D. (2000) 'A conserved role for H15-related T-box transcription factors in zebrafish and Drosophila heart formation', *Dev Biol* 218(2): 235-47.

Hammer, S., Toenjes, M., Lange, M., Fischer, J. J., Dunkel, I., Mebus, S., Grimm, C. H., Hetzer, R., Berger, F. and Sperling, S. (2008) 'Characterization of TBX20 in human hearts and its regulation by TFAP2', *J Cell Biochem* 104(3): 1022-33.

Hao, J., Daleo, M. A., Murphy, C. K., Yu, P. B., Ho, J. N., Hu, J., Peterson, R. T., Hatzopoulos, A. K. and Hong, C. C. (2008) 'Dorsomorphin, a selective small molecule inhibitor of BMP signaling, promotes cardiomyogenesis in embryonic stem cells', *PLoS One* 3(8): e2904.

Henningfeld, K. A., Rastegar, S., Adler, G. and Knochel, W. (2000) 'Smad1 and Smad4 are components of the bone morphogenetic protein-4 (BMP-4)-induced transcription complex of the Xvent-2B promoter', *J Biol Chem* 275(29): 21827-35.

Iio, A., Koide, M., Hidaka, K. and Morisaki, T. (2001) 'Expression pattern of novel chick T-box gene, Tbx20', *Dev Genes Evol* 211(11): 559-62.

Kirk, E. P., Sunde, M., Costa, M. W., Rankin, S. A., Wolstein, O., Castro, M. L., Butler, T. L., Hyun, C., Guo, G., Otway, R. et al. (2007) 'Mutations in cardiac T-box factor gene TBX20 are associated with diverse cardiac pathologies, including defects of septation and valvulogenesis and cardiomyopathy', *Am J Hum Genet* 81(2): 280-91.

Kraus, F., Haenig, B. and Kispert, A. (2001) 'Cloning and expression analysis of the mouse T-box gene tbx20', *Mech Dev* 100(1): 87-91.

Kretzschmar, M. and Massague, J. (1998) 'SMADs: mediators and regulators of TGF-beta signaling', *Curr Opin Genet Dev* 8(1): 103-11.

Kroll, K. L. and Amaya, E. (1996) 'Transgenic *Xenopus* embryos from sperm nuclear transplantations reveal FGF signalling requirements during gastrulation', *Development* 122: 3173-3183.

Langdon, Y. G., Goetz, S. C., Berg, A. E., Swanik, J. T. and Conlon, F. L. (2007) 'SHP-2 is required for the maintenance of cardiac progenitors', *Development* 134(22): 4119-30.

Li, L., Miano, J. M., Cserjesi, P. and Olson, E. N. (1996) 'SM22 alpha, a marker of adult smooth muscle, is expressed in multiple myogenic lineages during embryogenesis', *Circ Res* 78(2): 188-95.

Liberatore, C. M., Searcy-Schrick, R. D., Vincent, E. B. and Yutzey, K. E. (2002) 'Nkx-2.5 gene induction in mice is mediated by a Smad consensus regulatory region', *Dev Biol* 244(2): 243-56.

Lien, C. L., McAnally, J., Richardson, J. A. and Olson, E. N. (2002) 'Cardiac-specific activity of an Nkx2-5 enhancer requires an evolutionarily conserved Smad binding site', *Dev Biol* 244(2): 257-66.

Liu, C., Shen, A., Li, X., Jiao, W., Zhang, X. and Li, Z. (2008) 'T-box transcription factor TBX20 mutations in Chinese patients with congenital heart disease', *Eur J Med Genet* 51(6): 580-7.

Liu, F., Hata, A., Baker, J. C., Doody, J., Carcamo, J., Harland, R. M. and Massague, J. (1996) 'A human Mad protein acting as a BMP-regulated transcriptional activator [see comments]', *Nature* 381(6583): 620-3.

Massague, J., Seoane, J. and Wotton, D. (2005) 'Smad transcription factors', *Genes Dev* 19(23): 2783-810.

Mintzer, K. A., Lee, M. A., Runke, G., Trout, J., Whitman, M. and Mullins, M. C. (2001) 'Lost-a-fin encodes a type I BMP receptor, Alk8, acting maternally and zygotically in dorsoventral pattern formation', *Development* 128(6): 859-69.

Nieuwkoop, P. D. and Faber, J. (1967) *Normal Table of Xenopus laevis (Daudin)*, Amsterdam: North Holland.

Oh, J., Wang, Z., Wang, D. Z., Lien, C. L., Xing, W. and Olson, E. N. (2004) 'Target gene-specific modulation of myocardin activity by GATA transcription factors', *Mol Cell Biol* 24(19): 8519-28.

Qian, L., Mohapatra, B., Akasaka, T., Liu, J., Ocorr, K., Towbin, J. A. and Bodmer, R. (2008) 'Transcription factor neuromancer/TBX20 is required for cardiac function in Drosophila with implications for human heart disease', *Proc Natl Acad Sci U S A* 105(50): 19833-8.

Qiu, P., Feng, X. H. and Li, L. (2003) 'Interaction of Smad3 and SRF-associated complex mediates TGF-beta1 signals to regulate SM22 transcription during myofibroblast differentiation', *J Mol Cell Cardiol* 35(12): 1407-20.

Schlange, T., Andree, B., Arnold, H. H. and Brand, T. (2000) 'BMP2 is required for early heart development during a distinct time period', *Mech Dev* 91(1-2): 259-70.

Schultheiss, T. M., Burch, J. B. and Lassar, A. B. (1997) 'A role for bone morphogenetic proteins in the induction of cardiac myogenesis', *Genes Dev* 11(4): 451-462.

Schwartz, R. J. and Olson, E. N. (1999) 'Building the heart piece by piece: modularity of cis-elements regulating Nkx2-5 transcription', *Development* 126(19): 4187-92.

Showell, C., Christine, K. S., Mandel, E. M. and Conlon, F. L. (2006) 'Developmental expression patterns of Tbx1, Tbx2, Tbx5, and Tbx20 in Xenopus tropicalis', *Dev Dyn* 235(6): 1623-30.

Singh, R., Horsthuis, T., Farin, H. F., Grieskamp, T., Norden, J., Petry, M., Wakker, V., Moorman, A. F., Christoffels, V. M. and Kispert, A. (2009) 'Tbx20 Interacts With Smads to Confine Tbx2 Expression to the Atrioventricular Canal', *Circ Res*.

Wang, D., Chang, P. S., Wang, Z., Sutherland, L., Richardson, J. A., Small, E., Krieg, P. A. and Olson, E. N. (2001) 'Activation of cardiac gene expression by myocardin, a transcriptional cofactor for serum response factor', *Cell* 105(7): 851-62.

Yu, P. B., Hong, C. C., Sachidanandan, C., Babitt, J. L., Deng, D. Y., Hoyng, S. A., Lin, H. Y., Bloch, K. D. and Peterson, R. T. (2008) 'Dorsomorphin inhibits BMP signals required for embryogenesis and iron metabolism', *Nat Chem Biol* 4(1): 33-41.

Chapter 3

The T-box transcription factor Tbx20 recruits a unique TLE-HDAC2-Tbx18 co-repressor complex

Preface

This work is in review at the *Journal of Proteome Research*. The project was conceived by myself, Frank Conlon, and Ileana Cristea. The mass spectrometry analyses and data processing was done in collaboration with postdoctoral fellow Todd Greco and Ileanna Cristea. Graduate student Leslie Kennedy performed the Tbx18:Tbx20 co-immunoprecipitation. All other experiments were performed by myself. The manuscript was written by myself with contributions by Todd Greco; the manuscript was finalized by Frank Conlon and Ileanna Cristea.

Erin Kaltenbrun, Todd M. Greco, Leslie M. Kennedy, Tuo Li, Ileana M. Cristea, and Frank L. Conlon. (2013) The T-box transcription factor Tbx20 recruits a unique TLE-HDAC2-Tbx18 co-repressor complex. *Journal of Proteome Research* [in review].

ABSTRACT

The cardiac transcription factor Tbx20 has a critical role in the proper morphogenetic development of the vertebrate heart and has been implicated in human congenital heart disease. Although it is established that Tbx20 exerts its function in the embryonic heart through positive and negative regulation of distinct gene programs, it is unclear how Tbx20 mediates proper transcriptional regulation of its target genes. Here, using a combinatorial directed proteomics/bioinformatics approach, we present the first characterization of Tbx20 transcriptional complexes. We have systematically investigated Tbx20 protein-protein interactions by integrating a targeted proteomic analysis with gene ontology classifications and functional protein networks. The resulting proteomic data set demonstrates that Tbx20 is associated with a transcription repression network composed of TLE/Groucho co-repressors, members of the Nucleosome Remodeling and Deacetylase (NuRD) complex, the chromatin remodeling ATPases RUVBL1-RUVBL2, and the T-box repressor Tbx18. We have extended these studies by establishing that the Tbx20 interaction with TLE co-repressors occurs via an eh1 binding motif, and demonstrated that this binding event is required for proper assembly of the repression network. Importantly, we went on to validate the TLE interaction in vivo, providing the first demonstration of endogenous Tbx20 interactions in embryonic heart tissue. Together, these studies led us to propose that Tbx20 associates with a unique TLE-dependent chromatin remodeling network to prevent inappropriate gene activation within the embryonic heart.

INTRODUCTION

The development and maturation of a functional heart is a complex process that involves distinct but overlapping phases of specification, proliferation, migration, differentiation, and morphogenesis. Disturbances in any of these processes can lead to a number of congenital heart defects. Currently, congenital heart defects affect nearly 1% of all newborns and are a significant cause of infant death (Reller et al., 2008; van der Linde et al., 2011). Recent studies have demonstrated that human patients with dilated cardiomyopathy, atrial septal defects, or mitral valve disease carry mutations in the transcription factor *Tbx20,* while upregulation of *Tbx20* gene expression has been reported in patients with tetralogy of Fallot (Kirk et al., 2007; Hammer et al., 2008; Liu et al., 2008; Qian et al., 2008). *Tbx20* is a member of the T-box family of transcription factors, all of which share a well-conserved DNA binding domain known as the T-box and have diverse roles in embryonic development. *Tbx20* has been identified in many organisms, including *Drosophila*, zebrafish, *Xenopus*, and mouse, and in all species examined *Tbx20* transcripts are strongly expressed throughout the developing heart (Ahn et al., 2000; Griffin et al., 2000; Meins et al., 2000; Iio et al., 2001; Brown et al., 2003; Conlon and Yutzey, 2010; Kaltenbrun et al., 2011). Results from genetic analysis and protein depletion studies are consistent with a role for *Tbx20* during the early stages of vertebrate heart development; hearts lacking Tbx20 show a progressive loss of cardiomyocytes, a failure of the heart to undergo looping and chamber formation, and defects in cardiomyocyte maturation (Brown et al., 2005; Cai et al., 2005; Singh et al., 2005; Stennard et al., 2005; Takeuchi et al., 2005). Collectively, these studies

suggest that the sequence, expression, and function of *Tbx20* are evolutionarily conserved from flies to human.

Similar to other T-box factors, Tbx20 is localized to the nucleus, binds DNA in a sequence-specific manner, and modulates transcription of downstream target genes (Stennard et al., 2003; Brown et al., 2005; Cai et al., 2005; Singh et al., 2005; Stennard et al., 2005; Takeuchi et al., 2005; Shen et al., 2011; Sakabe et al., 2012). Results from a number of studies have shown that Tbx20 can act to both promote and repress target gene expression in the heart; however, it is unclear how Tbx20 initiates a transcriptional repressive program within the same cells in which it also acts as a potent transcriptional activator. It has been proposed that protein co-factors may act to specify Tbx20 transcriptional activity (Sakabe et al., 2012). A model in which protein co-factors act as determinants of Tbx20 activity has several unresolved issues because few *in vivo* Tbx20 co-factors have been identified. Additionally, there is uncertainty about the precise mechanism by which binding of Tbx20 to DNA results in either activation or repression of a target gene. In vitro assays have been used to demonstrate interactions between Tbx20 and a suite of cardiac transcription factors that include Tbx5, Nkx2.5, Gata4, Gata5, and Islet1 (Stennard et al., 2003; Brown et al., 2005), although none of these interactions have been shown to occur in vivo in the embryonic heart. Indeed, the presence of DNA-binding motifs for Nkx2.5, Gata4, and Tbx5 in the promoter regions of Tbx20 target genes, in combination with evidence that these transcription factors act combinatorially to promote target gene expression suggest that cardiac transcription

factors are important co-factors for Tbx20 to activate gene expression in the developing heart (Stennard et al., 2003; Takeuchi et al., 2005; Sakabe et al., 2012). However, it is not well understood how Tbx20 functions as a transcriptional repressor as co-factors that may act as functional co-repressors have not been identified. Therefore, the precise mechanisms by which Tbx20 regulates distinct gene programs in the heart remains unclear.

To begin to address these questions, we have undertaken, to our knowledge, the first proteomic study aimed at identifying Tbx20 protein interactions. Using affinity purification mass spectrometry (AP-MS) (Miteva et al., 2013), we have systematically isolated and characterized Tbx20-EGFP transcriptional complexes. With this approach, we have identified a unique Tbx20 transcription repression network that includes the Groucho-related proteins Transducin-like Enhancer of Split 1 and 3 (TLE1/3), Metastasis-associated Protein 1 (MTA1), the histone-binding proteins RBBP4 and RBBP7, RUVB-like 1 and 2, Nucleolin, Nucleophosmin, Histone Deacetylase 2 (HDAC2), and the T-box repressor Tbx18. We provide evidence that Tbx20 recruits TLE1/3 through an evolutionarily conserved N-terminal engrailed homology 1 (eh1) binding motif and demonstrate that recruitment of a subset of this network requires binding of TLE3 to Tbx20. Finally, we find that TLE family members are expressed in mouse embryonic heart tissue, and that Tbx20 interacts with both TLE1 and TLE3 in vivo during heart development, representing the first endogenous Tbx20 interactions identified in embryonic heart tissue to date. We propose a model in which Tbx20 binds to TLE factors to assemble a chromatin remodeling and

deacetylase complex on target gene loci that may act to prevent inappropriate gene activation within the cardiac lineage.

MATERIALS AND METHODS

DNA constructs

Mouse *Tbx20a* cDNA was fused to *EGFP* and cloned into the *pMONO-neo-mcs* plasmid (Invitrogen) for expression in HEK293 cells. The *Tbx20eh1mut-EGFP* construct was generated by site-direct mutagenesis (Stratagene) of phenylalanine 18 (F18L) and serine 19 (S19I) using the primers 5'-CTCTCGAGCCAATGCCTTAATCATCGCCGCGCTTATGTC -3' and 5'-GACATAAGCGCGGCGATGATTAAGGCATTGGCTCGAGAG -3' according to manufacturer's instructions. To generate the *Tbx20-HA* construct, mouse *Tbx20a* cDNA was fused to an HA epitope and cloned into *pMONO-neo-mcs*. The *pCMV2-TLE1-Flag* construct was generously provided by Dr. Stefano Stifani (Buscarlet et al., 2009). The *pCMX-TLE3* plasmid was kindly provided by Dr. Peter Tontonoz (Villanueva et al., 2011). *Tbx18-Flag* was generously provided by Dr. Chen-Leng Cai (Nie et al., 2010).

Xenopus injections and animal cap isolation

Xenopus laevis embryos were staged according to Nieuwkoop and Faber (Nieuwkoop, 1974) and injected with 1 ng *Tbx20* or *Tbx20-EGFP* mRNA at the one-cell stage using established protocols (Smith and Slack, 1983; Goetz et al., 2006). Animal caps were excised at stage 8-9 and cultured in 1X modified Barth's saline

(MBS) until sibling embryos reached stage 13. Activin-treated caps were cultured in 8 Units/mL Activin in 1X MBS.

Isolation of Tbx20-EGFP protein complexes

pMONO-Tbx20-EGFP or *Tbx20^{eh1mut}-EGFP* plasmids were transfected into HEK293 cells using FuGENE (Roche Applied Science). Tbx20-EGFP complexes and GFP complexes were immunoaffinity purified from cells using in-house developed rabbit polyclonal anti-GFP antibodies conjugated to magnetic beads, as previously described (Cristea et al., 2005). Briefly, HEK293 cells expressing Tbx20-EGFP or GFP alone were washed with cold PBS, harvested from the plate by scraping with a plastic spatula and pelleted at 1500 rpm for 10 min at 4°C. The cell pellet was resuspended in 100 µL/1 µg 20 mM HEPES, pH 7.4, containing 1.2% polyvinylpyrrolidone and protease inhibitors and snap frozen in liquid nitrogen. Cells were lysed by cryogenic grinding using a Retsch MM 301 Mixer Mill (10 cycles x 2.5 min at 30 Hz) (Retsch, Newtown, PA) and the frozen cell powder was resuspended in optimized lysis buffer (5 mL/1 g cells) (20 mM K-HEPES pH 7.4, 0.1 M KOAc, 2 mM $MgCl_2$, 0.1% Tween-20, 1 µM $ZnCl_2$, 1 µM $CaCl_2$, 150 mM NaCl, 0.5% Triton X-100 containing protease and phosphatase inhibitors). Cell lysates were homogenized using a Polytron (Kinematica) step (2 x 15 sec) and pelleted at 8000 rpm at 4°C. Cleared lysates were rotated with 7 mg magnetic beads (M270 Epoxy Dynabeads, Invitrogen) coupled to anti-GFP antibodies for 1 hr at 4°C. The magnetic beads were then washed in lysis buffer (6 x 1 mL) (without protease and phosphatase inhibitors) and eluted from the beads in 40 µL 1x LDS Sample Buffer

(Invitrogen) at 70°C for 15 min. Eluted proteins were alkylated with 100 mM iodoacetamide for 1 hr at room temperature and subjected to mass spectrometry analysis.

Mass spectrometry analysis of Tbx20-EGFP protein complexes

Immunoisolates were analyzed by mass spectrometry as previously described (Tsai et al., 2012) with minor differences. Briefly, reduced and alkylated eluates were partially resolved by SDS-PAGE on 4-12% Bis-Tris NuPAGE gels (Invitrogen) and stained using SimplyBlue Coomassie stain (Invitrogen). Each lane was divided into 1 mm slices and binned into 8 wells of a 96-well plate. Gel slices were destained in 50 mM ammonium bicarbonate (ABC) containing 50% acetonitrile (ACN). Proteins were digested in-gel with 20 mL of 12.5 ng/mL trypsin in 50 mM ABC for 5 hrs at 37°C. Tryptic peptides were extracted in 0.5% formic acid for 4 hrs at room temperature, followed by 0.5% formic acid/50% ACN for 2 hrs at room temperature. The extracted peptides were concentrated by vacuum centrifugation to 10 µL and either desalted online (trap column, Magic C_{18} AQ, 100 mm x 2.5cm) or offline using StageTips. Desalted peptides (4 mL) were separated online by reverse phase C_{18} (Acclaim PepMap RSLC, 1.8 µm, 75 µm × 25 cm) over 90 min at 250 nL/min using a Dionex Ultimate 300 nanoRSLC and detected by an LTQ Orbitrap Velos or XL mass spectrometer (Thermofisher Scientific, San Jose, CA).

The mass spectrometer was operated in data-dependent acquisition mode with dynamic exclusion enabled. A single acquisition cycle comprised a single full-

scan mass spectrum (m/z = 350–1700) in the Orbitrap (r = 30,000 at m/z = 400), followed by collision-induced dissociation (CID) fragmentation in the linear ion trap of the top 10 (XL) or 20 (Velos) most intense precursor ions. FT full scan target value was 1E6 with a max. injection time of 300 ms. IT tandem MS target values were $5E^3$ (XL) or $1E^4$ (Velos) with a maximum injection time of 100 ms. CID fragmentation was performed at an isolation width of 2.0 Th, normalized collision energy of 30, and activation time of 30 (XL) or 10 ms (Velos).

Data processing and functional protein analyses

MS/MS spectra were extracted from Thermo RAW files and searched by Proteome Discoverer/SEQUEST (version 1.3, Thermo Fisher Scientific) against the UniProt SwissProt protein sequence database (release 2010-11) containing forward and reverse entries (20,324 sequences) from human and the mouse Tbx20a sequence plus common contaminants. SEQUEST search parameters were as follows: full enzyme specificity with 2 missed cleavages, precursor and fragment tolerances, 10 ppm and 0.5 Da, fixed modification, carbamidomethylation of cysteine, and variable modifications, oxidized methionine and phosphorylation of STY. SEQUEST peptide spectrum matches (MSF files) were loaded into Scaffold software (ver. 3.5.1, Proteome Software, Inc), subjected to an X! Tandem refinement search, and then analyzed by PeptideProphet and ProteinProphet algorithms to determine peptide and protein probabilities. The high mass accuracy option for probability scoring was enabled. The following peptide modifications were included in the X!Tandem refinement search: deamidation of NQ, and acetylation of K and

amino-terminus. Protein groups were assembled by Scaffold and filtered by a minimum of 2 unique peptides. Probability thresholds were empirically defined to achieve < 1% peptide and protein FDR as assessed by matches to the reverse database. Proteins descriptions, accession numbers, and their respective unique peptides and unweighted spectrum counts were exported to Excel for further analysis.

Specific Tbx20 protein interactions were identified by spectral counting enrichment analysis (Tsai et al., 2012) comparing the Tbx20-EGFP versus EGFP alone conditions. The following criteria were applied to each individual replicate (N=3): 1) only proteins with $\geq$ 5 spectrum counts were retained, 2) only those proteins that had a spectral count enrichment of $\geq$ 2.5-fold versus GFP alone were retained, and 3) using NCBI GO annotations, proteins assigned a “nuclear” localization ontology term were retained (Table S3.1; see Table S3.2 for proteins excluded for not being associated with a nuclear localization ontology term). The proteins that fulfilled these criteria in all three replicates were imported into Cytoscape (Smoot et al., 2011) for classification into functional subgroups according to biological processes using the plugin ClueGO (Table S3.3) (Bindea et al., 2009). Proteins within GO term clusters were analyzed in STRING using protein accessions as input (Szklarczyk et al., 2011).

Comparison of interaction protein abundance versus estimated average proteome abundance, defined here as an enrichment index, was used to identify

prominent interaction candidates from the GO-classified nuclear proteins (Tsai et al., 2012). To calculate this enrichment index, first, a protein's spectral counts was normalized within each biological replicate (N = 3) by the Tbx20 spectral count ratio of each individual replicate / average. Then, normalized spectral counts were converted to NSAF (Normalized Spectral Abundance Factor) values (Zybailov et al., 2007) and further normalized by estimated proteome abundance from the human subset of the PAX (protein abundance across organisms) database (Wang et al., 2012) (Table S3.4). Tbx20 spectral counts were excluded from this analysis. We have previously shown that calculating this enrichment index helps to point out protein complexes that are prominently associating with the bait (Tsai et al., 2012). In a separate spectral counting analysis for the eh1 motif mutant, protein interactions were normalized by the eh1mut/WT Tbx20 spectral count ratio.

Analysis of Tbx20-EGFP and Tbx20^{eh1mut}-EGFP protein complexes using mass spectrometry-based spectrum counting

Tbx20-EGFP and Tbx20^{eh1mut}-EGFP complexes were immunoisolated and analyzed by LC-MS/MS as described above. Peptide and protein identifications were filtered using the criteria described above, including the requirement of at least 5 spectrum counts per protein identified for either wild-type or mutant isolations and the requirement that all proteins identified in the wild-type isolation be at least 2.5-fold enriched over isolations from EGFP-expressing cells. To determine differences in interacting proteins between wild-type and mutant Tbx20 isolations, a spectrum counting approach was employed. Spectrum counts for each protein was normalized to the number of spectrum counts for wild-type Tbx20. The fold-change, relative to

wild-type Tbx20, in spectrum counts was used as a measure of the approximate relative abundance of interacting proteins, i.e., fold-change = normalized spectrum counts of the protein in eh1mut isolation/ spectrum counts of the protein in wild-type isolation). Interacting proteins with a fold change less than or equal to 0.5 between mutant and wild-type isolations were considered to be significantly reduced in mutant isolations (Table S3.5).

Construction of a HEK293-HDAC2-EGFP stable cell line

The *HDAC2* ORF was amplified from an *HDAC2* plasmid (gift from E. Seto, Moffitt Cancer Center), and inserted into the *pLXSN-C-EGFP-FLAG* vector to create the *HDAC2-EGFP-flag* fusion, as in (Greco et al., 2011). The Phoenix^{TM} retrovirus expression system (Orbigen, San Diego, CA) was used to transduce HEK293 cells to express the *HDAC2-EGFP-FLAG* fusion according to the manufacturer's instructions. The transduced cells were selected in 300 mg/L G418 (EMD, Gibbstown, NJ) and sorted by FACS (Vantage S.E. with TurboSort II, Becton Dickinson, Franklin Lakes, NJ) to obtain a stable cell line. The nuclear localization and deacetylation activity of the GFP-tagged HDAC2 were confirmed.

Isolation of endogenous Tbx20 from mouse embryonic hearts

Pregnant CD1 females were sacrificed on embryonic day 10.5 (E10.5) and the embryos removed. Embryonic hearts (n=25) were dissected from the embryos in cold PBS and snap-frozen in liquid nitrogen. Embryonic hearts were cryogenically lysed, and endogenous Tbx20 protein complexes were immunoaffinity purified as

described using 5 mg magnetic beads (M270 Epoxy Dynabeads, Invitrogen) conjugated to anti-Tbx20 antibodies (Santa Cruz Biotechnology). The isolated proteins were analyzed by Western blotting.

Immunofluorescence and immunoblotting

For immunofluorescence of HEK293 cells, cells were cultured in 8-well chamber slides pretreated with poly-D-lysine. For live imaging of EGFP fluorescence, cells were transfected with pMONO-Tbx20-EGFP. Forty-eight hours later, the cells were rinsed with 1X PBX and DAPI added (200 ng/mL in 1X PBS) for 30 min. Cells were imaged by confocal microscopy on a Zeiss 710.

Antibodies used for immunoblotting include mouse anti-GFP (JL8) (Clontech Living Colors Monoclonal), mouse anti-Flag (M2) (Sigma), goat anti-TLE1 (N-18) (Santa Cruz Biotechnology), rabbit anti-TLE3 (M-201) (Santa Cruz Biotechnology), mouse anti-GAPDH (Millipore), and goat anti-Tbx20 (Santa Cruz Biotechnology).

RNA extraction and RT-PCR

RNA was extracted using Trizol (Invitrogen) and purified on RNeasy columns (Qiagen). cDNA synthesis was performed from 0.5-1 μg of RNA using random primers and SuperScript II reverse transcriptase (Invitrogen). Expression levels were assessed using GoTaq Green Master Mix (Promega) and Taq polymerase on a GeneAmp PCR System (Applied Biosystems). PCR products were analyzed by 2.5% agarose gel electrophoresis.

RESULTS

Tbx20-EGFP is localized to the nucleus and transcriptionally active

Identification of critical Tbx20 protein co-factors in a high throughput manner has been hampered by a lack of antibodies against Tbx20 that are suitable for directed proteomics analyses. Additionally, there are no cell lines that recapitulate endogenous Tbx20 expression and thus could provide sufficient material for large-scale proteomics studies of Tbx20 protein complexes. Since the main goal of this set of studies was to determine the general transcriptional mechanisms by which Tbx20 functions, we generated human embryonic kidney (HEK293) cells expressing Tbx20 tagged at the C-terminus with EGFP (Figure 3.1A). HEK293 cells have been used as a cell culture model for studies on the transcriptional activity of Tbx20 (Brown et al., 2005; Cai et al., 2005), indicating that this cell line contains the necessary cohort of transcriptional co-factors required for Tbx20-mediated transcriptional regulation. In agreement with its known role in transcription, Tbx20-EGFP localizes strongly to the nucleus when expressed in HEK293 cells, as shown by live GFP fluorescence microscopy (Figure 3.1B).

To confirm that the EGFP-tagged Tbx20 is transcriptionally active, we made use of a *Xenopus* animal cap assay. A recent study demonstrated that animal caps, which consist of naïve pluripotent cells, when excised from embryos injected with *Tbx20* mRNA express the early mesoderm marker *Xbra*, but not the skeletal muscle marker *Myf5*, indicating that Tbx20 can induce cell fate changes in the early embryo (Stennard et al., 2003). To assess whether EGFP-tagged Tbx20 has the same ability

to induce gene expression changes as untagged Tbx20, we injected *Tbx20* and *Tbx20-EGFP* mRNA into one-cell stage *Xenopus laevis* embryos. By stage 8, Tbx20-EGFP protein is localized throughout the animal pole of the embryo, as shown by live GFP fluorescence microscopy (Figure 3.1C). At stage 9, animal caps were excised from *Tbx20*, *Tbx20-EGFP*, and uninjected embryos and cultured until sibling whole embryos reached stage 13. After extraction of RNA, we assessed the expression of the early mesodermal markers *chordin* and *Xbra*, and as a negative control, *Myf5*, by RT-PCR and compared levels of induction to expression of these genes within whole embryos, untreated caps, and, as a positive control, caps treated with the mesoderm-inducing factor Activin. Both EGFP-tagged Tbx20 and untagged Tbx20 induce *chordin* expression to the same degree as Activin (Figure 3.1D). Further, Tbx20 and Tbx20-EGFP induce moderate levels of *Xbra* compared to Activin-induced caps; however, there was no induction of the muscle marker *Myf5* by either version of Tbx20 or by Activin treatment. Untreated caps did not express any of the tissue-specific markers tested. These data indicate that EGFP-tagged Tbx20 is transcriptionally active and retains the ability to modulate downstream gene expression.

Directed proteomics of Tbx20-EGFP interactions reveals association with a unique transcription repression network

To systematically identify Tbx20-associated proteins, we performed immunoaffinity purifications of Tbx20-EGFP complexes from HEK293 cells using a high affinity in-house developed antibody against GFP (Cristea et al., 2005). In parallel, as controls, we performed immunoaffinity purifications from cells expressing

EGFP alone (Tables S3.1, S3.2). Immunopurified proteins were partially resolved by SDS-PAGE, digested in-gel with trypsin, and analyzed by nLC-tandem MS (MS/MS) on an LTQ Orbitrap XL or an LTQ Orbitrap Velos. Three independent biological replicates were performed (Tables S3.1, S3.2); two of these immunopurifications were performed in the presence of DNase to eliminate interactions mediated by binding of factors on adjacent DNA sequences. Raw MS/MS spectra from each experiment were analyzed by SEQUEST database searches (Proteome Discoverer) and loaded into Scaffold for further analysis. Protein identifications from all three replicates were filtered using stringent confidence parameters (see Materials and Methods). A spectrum counting approach was employed to assess enrichment of protein interactions with Tbx20-EGFP relative to EGFP alone. First, proteins were required to be reproducibly present at an abundance of at least 5 spectrum counts. From these proteins, interactions that were deemed non-specific were excluded, which were defined as proteins showing less than 2.5-fold spectrum count enrichment over proteins that interact with EGFP alone. Further, given the nuclear localization of Tbx20-EGFP, proteins lacking a nuclear gene ontology term were excluded as likely non-specific associations occurring during whole-cell lysis (Table S3.2).

To assess the Tbx20 nuclear interactome as a whole, we classified the proteins passing our spectrum count and fold enrichment criteria into functional subgroups by Cytoscape, using the ClueGO plugin (Bindea et al., 2009; Smoot et al., 2011). Specifically, proteins were assigned into gene ontology (GO) term

clusters according to biological function ontologies. When we examined Tbx20 nuclear interactions, the most prominent biological function category contained 53 proteins related to RNA processing (Figure 3.2A and Table S3.3). This is expected, as it is well established that DNA template that is being actively transcribed is often closely associated with RNA processing machinery and suggests that a portion of Tbx20 binding is closely associated with active transcription. Nuclear interactions also included 13 proteins involved in nucleosome assembly (i.e., chromatin remodeling, DNA conformation change), 16 proteins assigned to DNA repair/synthesis, and 10 proteins assigned to nuclear transport (Figure 3.2A and Table S3.3). Collectively, these putative Tbx20 interactions represent different complexes and functions of Tbx20 throughout the nucleus. Given the lack of knowledge regarding the molecular mechanisms of Tbx20-mediated transcriptional regulation, we reasoned that the specific protein functions represented within the chromatin modification/remodeling category could provide new insight on the potential roles of Tbx20 in gene regulation.

In total, 114 proteins with annotated nuclear localization passed our spectrum count and fold enrichment criteria, 97% of which occur in all three biological replicates, while the remainder passed our stringent specificity criteria in at least two of the three experiments (Table S3.1). Given that chromatin remodeling and transcription repression complexes are often large multi-protein complexes, we speculated that the specific proteins represented within the ‘chromatin remodeling’ category were likely to be interconnected. To test this hypothesis, we analyzed the 5

proteins within this functional cluster (Table 3.1 and Table S3.3) using STRING, a knowledge database of known and predicted protein-protein interactions (Szklarczyk et al., 2011), with the aim of generating a predictive Tbx20 interaction network. Surprisingly, all 5 of these proteins form a highly interconnected network containing chromatin remodeling and deacetylase functions and include the chromatin-remodeling ATPase RUVBL1, the nucleolar protein Nucleophosmin (NPM1), and core components of the Nucleosome Remodeling and Deacetylase (NuRD) complex (RBBP4, RBBP7, and HDAC2)—a major ATP-dependent chromatin remodeling complex with important roles in transcription and chromatin assembly (reviewed in (Bowen et al., 2004)). In addition, NCL, RUVBL2, and MTA1, which were also found to interact with Tbx20, were integrated into this network based upon their known or predicted functional association with components of the chromatin remodeling network (Table 3.1 and Figure 3.2B, grey lines) (Li et al., 1996; Xue et al., 1998; Ikura et al., 2000; Sardiu et al., 2008).

As this is the first demonstration that Tbx20 is associated with chromatin remodeling proteins, it was unclear how Tbx20 might be functionally linked to this chromatin modification network. There is evidence that MTA family proteins interact directly with transcription factors at target gene loci (Roche et al., 2008); however, different transcription factors have been shown to bind to different regions of individual subunits of the NuRD complex (Fujita et al., 2004; Li et al., 2009). To attempt to identify the functional link between Tbx20 and the chromatin remodeling network, we first returned to our list of nuclear-enriched proteins to search for

additional components of a chromatin modification network that may have been excluded in our original analysis due to incomplete GO annotation. Surprisingly, this search uncovered the presence of the transcriptional co-repressors Transducin-like Enhancer of split 1 and 3 (TLE1 and TLE3) and the T-box transcriptional repressor Tbx18 (Figure 3.2B and Table 3.1). TLE family members are orthologs of the *Drosophila* Groucho protein and have been previously demonstrated to bind directly to T-box factors, including Tbx18 and Tbx15, through an engrailed homology 1 (eh1) binding motif and achieve transcriptional repression by recruiting histone deacetylases (Chen et al., 1999; Farin et al., 2007).

To examine if Gro/TLE factors could serve as proximal interacting partners, linking Tbx20 to chromatin remodeling complexes, we examined the relative enrichment level of proteins within the interaction network. As previously described (Tsai et al., 2012; Miteva et al., 2013), we estimated the relative enrichment of proteins within the immunoisolates by normalizing their relative protein abundances (NSAF values) (Zybailov et al., 2007) to their proteome abundances from the PAX database (pax-db.org) (Table S3.4). This relative enrichment analysis was performed for the 114 proteins with enrichment in Tbx20 immunoisolations and "nuclear" GO subcellular localization (see Table S3.3). Respective enrichment index values were then expressed on the Gro/TLE-chromatin remodeling network. We hypothesized that proteins within the interaction network having greater enrichment indices would represent more proximal and perhaps essential Tbx20 interactions. Indeed, TLE1/3 and Tbx18 comprise a group of the most highly enriched

components of the interaction network (Figure 3.2B). This supports a critical role for these proteins in regulating Tbx20 function, suggesting they may be directly linked to Tbx20.

Tbx20 forms protein complexes with TLE1/3, Tbx18, and HDAC2

The T-box proteins Tbx15 and Tbx18 have been reported to bind directly to TLE3 via N-terminal eh1 binding motifs (Farin et al., 2007), indicating that the eh1 motif may represent a common motif used by T-box transcription factors to bind Gro/TLE family members. To determine whether Tbx20 directly recruits Groucho co-repressors via an eh1 binding motif, we next investigated the interaction between Tbx20 and TLE1/3. Tbx20 contains an N-terminal eh1 binding motif that is fully conserved in all vertebrate orthologs of Tbx20 (Figure 3.3A). To confirm an interaction between Tbx20 and TLE1/3 and determine whether these interactions require the eh1 motif, we generated a *Tbx20^{eh1mut}-EGFP* expression construct in which the eh1 motif has been ablated by site-directed mutation of phenylalanine 18 and serine 19 to an isoleucine and a leucine, respectively (*Tbx20$^{F18I;\ S19L}$-EGFP*). Reciprocal immunoisolations of TLE1 and TLE3 complexes were performed in the presence of wildtype Tbx20-EGFP or Tbx20^{eh1mut}-EGFP. Mutation of the eh1 motif significantly reduced the ability of Tbx20-EGFP to co-immunoprecipitate with either TLE1 or TLE3, suggesting that Tbx20 binds TLE1/3 directly through this motif (Figure 3.3B,C).

The finding that Tbx20 interacts with both a Gro/TLE complex and the Groucho dependent repressor Tbx18 (Farin et al., 2007) indicates that Tbx20 and Tbx18 may heterodimerize to regulate a common set of targets in a Groucho dependent manner. To further investigate the interaction between Tbx20 and Tbx18, we transfected HEK293 cells with Tbx18-Flag alone or in the presence of Tbx20-EGFP. Immunopurification with an anti-Flag antibody and western blot analysis revealed efficient co-isolation of Tbx20 (Figure 3.3D). Collectively, these data imply a role for a Tbx20-Tbx18 repressor complex during vertebrate development.

To investigate the link between the Tbx20-TLE1/3 complex and HDAC2, we generated an HEK293 cell line stably expressing HDAC2 tagged at the C-terminus with EGFP. To confirm an interaction between Tbx20 and HDAC2, we performed reciprocal isolations of HDAC2-EGFP in the presence or absence of Tbx20-HA. Tbx20 was successfully co-isolated with HDAC2-EGFP (Figure 3.3E). As a number of studies indicate that binding to Groucho co-factors results in recruitment of deacetylase machinery (Chen et al., 1999), we also performed isolations of HDAC2-EGFP in the presence of over-expressed TLE3 and Tbx20. Interestingly, excess TLE3 results in a substantial increase in the amount of Tbx20 associated with HDAC2, suggesting that TLE3 stabilizes and likely bridges an interaction between Tbx20 and HDAC2 (Figure 3.3E). We also noticed that HDAC2-EGFP co-isolated with a higher amount of TLE3 in the absence of Tbx20-HA. Therefore, an alternative explanation is that Tbx20 competes or interferes with TLE3 binding to HDAC2,

possibly forming intermediate interactions with both HDAC2 and TLE3-containing complexes.

Quantitative mass spectrometry reveals that Tbx20 recruits a Groucho-dependent repressive complex

To distinguish between these possibilities and to assess precisely which components of the chromatin modification network that we identified (see Figure 3.2B) are recruited by the Tbx20-TLE3 interaction, we used label-free quantitative mass spectrometry to quantify differences between Tbx20-EGFP and Tbx20^{eh1mut}-EGFP protein complexes. To do this, we expressed Tbx20-EGFP and Tbx20^{eh1mut}-EGFP in HEK293 cells and performed parallel isolations of EGFP-tagged Tbx20 complexes. Changes in the relative abundance of interacting chromatin remodeling factors between wild-type and mutant Tbx20 complexes were assessed using a spectrum counting approach (see Materials and Methods). To correct for the total amount of isolated Tbx20 complexes between conditions, we normalized the spectrum counts for associated proteins in mutant Tbx20 complexes by wild-type Tbx20-EGFP spectrum counts. Consistent with our previous result, we did not identify any TLE1 or TLE3 in the Tbx20^{eh1mut} mutant isolation. Further, we did not observe any Tbx18 in Tbx20^{eh1mut} mutant complexes, and association with HDAC2 and RBBP4 was significantly reduced compared to wild-type, suggesting that Tbx20 interacts with these components in a Groucho-dependent manner (Figure 3.4A,B and Table S3.5). These data suggest that TLE co-repressors play a central role in the formation of a Tbx20 transcriptional repressive complex by recruiting the co-repressor Tbx18 and core components of the NuRD complex including HDAC2.

Additionally, these results confirm that using a targeted proteomics approach, we can efficiently isolate and identify specific Tbx20 interactions that may help define the mechanisms involved in Tbx20-mediated gene regulation.

Endogenous Tbx20 interacts with TLE factors in mouse embryonic hearts

Our proteomic analysis suggests that Tbx20 is linked to a transcriptional repressive complex via direct interaction with a TLE family member. To assess the endogenous Tbx20 association with TLE family members *in vivo* at the time in embryogenesis at which Tbx20 has been shown to function, we first examined the expression of all of the TLE family members in mouse embryonic day 10.5 (E10.5) heart tissue by RT-PCR. At this stage of development, *Tbx20* is uniformly expressed throughout the four-chambered embryonic heart (Kraus et al., 2001) where it is required for proper transcriptional regulation of cardiac chamber-specific genes (Cai et al., 2005; Singh et al., 2005; Stennard et al., 2005; Takeuchi et al., 2005). All of the TLE family members are highly expressed at this time, with the exception of *TLE2*, which is expressed at relatively low levels (Figure 3.5A).

Importantly, we were able to detect an interaction between endogenous Tbx20 and both TLE1 and TLE3 in the embryonic heart, indicating that Tbx20 binds both TLE factors *in vivo* during heart development (Figure 3.5B). This finding represents the first demonstration of endogenous Tbx20 protein-protein interactions from an embryonic heart. These data further validate our proteomic approach and

demonstrate for the first time that Tbx20 assembles a TLE repressor complex in the embryonic heart at the time at which Tbx20 functions in cardiac development.

DISCUSSION

Despite the critical role of Tbx20 in cardiac development, the precise mechanisms by which Tbx20 regulates distinct gene programs in the heart are not understood. Studies in mouse knockout models of Tbx20 indicate that Tbx20 is required for proper patterning and morphogenesis of working myocardium (Cai et al., 2005; Singh et al., 2005; Stennard et al., 2005; Takeuchi et al., 2005). Thus, activating and repressive activity of Tbx20 on target genes underlies the primary cardiomyocyte lineage split into specialized chamber and non-chamber myocardium. To identify and characterize the determinants of Tbx20 transcriptional activity in the heart, it is essential to identify Tbx20 interacting proteins. Our study constitutes the first comprehensive analysis of Tbx20 protein interactions. Using an unbiased proteomics/bioinformatics approach, we identified a unique transcriptional repression network that includes Groucho co-repressors, components of the NuRD complex, and a RUVBL1-RUVBL2 chromatin remodeling complex. Collectively, our data are consistent with a model in which Tbx20 recruits a Groucho co-repressor complex with histone deacetylase activity to target genes, rendering the chromatin inaccessible for activation.

Tbx20 interacts with a Gro/TLE repressor complex

The Tbx20 homolog Midline was recently demonstrated to bind Groucho directly in an eh1-dependent manner in *Drosophila* whole embryos, and this interaction was required for proper transcriptional repression of the *wingless* gene during segmentation of the ectoderm (Formaz-Preston et al., 2012). Our studies confirm and expand upon this work by demonstrating that 1) vertebrate Tbx20 interacts with Groucho homologs, 2) vertebrate Tbx20 interacts with at least two members of the Groucho-related TLE family, TLE1 and TLE3, in human cells and in the mouse embryonic heart through the eh1 motif, and 2) Tbx20-TLE interactions directly result in the recruitment of components of the chromatin-remodeling NuRD complex including HDAC2. These data suggest that recruitment of Gro/TLE co-repressor complexes and subsequent deacetylation of target loci represent an evolutionarily conserved mechanism by which Tbx20 functions and thus, one mode by which Tbx20 promotes inactive chromatin states during development. A thorough expression analysis of TLE factors in the developing heart has not been published; although, it has been reported that *TLE1* and *TLE3* transcripts were not detectable in the mouse embryonic heart by in situ hybridization (Santisteban et al., 2010). Our data, however, suggests that most members of the mouse TLE family are expressed in the heart at stage E10.5 of embryogenesis. Further, TLE1 and TLE3 proteins co-isolate with endogenous Tbx20 at E10.5. The availability of other TLE factors in the heart, and our results showing that Tbx20 interacts with both TLE1 and TLE3, suggests that Tbx20 may interact with multiple members of this family to cooperatively regulate genes in different regions of the heart. As such, it will be

interesting to determine whether individual TLE family members have distinct temporal and spatial expression patterns in the forming heart or whether they can act redundantly on Tbx20 target genes.

Our directed proteomic analysis of Tbx20 complexes combined with a label-free spectrum counting approach indicates that binding of TLE factors by Tbx20 results in the recruitment of additional members of a unique co-repressor complex, including core components of the NuRD complex HDAC2 and RBBP4, and Tbx18. Interestingly, interactions with the remainder of the repression network were unaffected by the eh1 mutation, suggesting that they are recruited independently of the eh1 binding motif and TLE recruitment. These results suggest two possibilities. First, assembly of the entire transcription repression complex could occur in two independent steps, whereby an intact TLE co-repressor complex is recruited via the eh1 binding motif, while the remainder of the complex is recruited independently via other binding motifs within Tbx20. Interestingly, RUVBL2 (also called Reptin) was demonstrated to co-occupy the *Hesx1* promoter with TLEs and HDAC1 to silence *Hesx1* expression during mouse pituitary development (Olson et al., 2006), indicating that this protein, although still present within $Tbx20^{eh1}$ mutant complexes, may be part of an intact TLE co-repressor complex.

The second possibility is that Tbx20 is a component of both a TLE co-repressor complex that include the proteins TLE1/3, Tbx18, HDAC2, and RBBP4, and also part of a broader chromatin remodeling protein interaction network that

includes RBBP7, MTA1, RUVBL1, RUVBL2, NCL, NPM1. The precise composition of Tbx20 transcriptional complexes likely varies spatially and temporally during development such that incorporation of unique subunits might impart functional specialization of the complex within specific tissue types and at defined developmental windows. In support of this notion, RUVBL1/2 (synonyms: Reptin/Pontin) complexes have been shown to have a role in the transcriptional regulation of cardiomyocyte proliferation but only after progenitors have assembled into a linear heart tube in zebrafish embryos(Rottbauer et al., 2002). Tbx20 has a well-documented role in cardiomyocyte proliferation(Cai et al., 2005) and seems to exert opposite effects on cell proliferation in embryonic versus fetal cardiomyocytes(Chakraborty and Yutzey, 2012). Therefore, it is tempting to speculate that association of Tbx20 with a RUVBL1/2 complex in fetal cardiomyocytes underlies this switch in the activity of Tbx20 transcriptional complexes. The temporal and tissue-specific regulation of Tbx20 protein complexes will be a subject of future investigation.

Transcriptional repression by Tbx20 and Tbx18

An unexpected finding of these studies is that Tbx20 interacts with the tissue-specific transcription factor Tbx18. In the developing heart, Tbx18 expression overlaps with that of Tbx20 in a subset of cardiomyocytes within the interventricular septum and a portion of the left ventricle at a stage when the heart is undergoing chamber specialization and expansion, processes that are both dependent on proper Tbx20 function (Christoffels et al., 2009; Conlon and Yutzey, 2010;

Kaltenbrun et al., 2011; Zeng et al., 2011). Thus, interaction with Tbx18 in this subset of cardiomyocytes provides one potential mechanism through which Tbx20 may function to regulate regionally distinct gene programs in the heart. Tbx18 is also expressed in the epicardium, an epithelial monolayer that covers the myocardium and is a critical source of signals and cells for the underlying myocardium (Kraus et al., 2001). Recently, a microarray analysis of isolated epicardial cells revealed Tbx20 as an epicardium-enriched transcription factor (Huang et al., 2012), opening the possibility for a Tbx18-Tbx20 transcriptional complex within the epicardium. Tbx18 also plays a prominent role in formation of the myocardial sinus horns that make up the venous pole of the heart; however, it is not clear whether Tbx20 is co-expressed with Tbx18 within this tissue (Christoffels et al., 2006). Collectively, these studies imply a role for a Tbx20-Tbx18 repressor complex during cardiovascular development and further, demonstrates that our targeted proteomic analysis of Tbx20 complexes results in the identification of tissue-specific interactions likely to be important in the context of the developing embryo.

Tbx18 has also been shown to interact with TLE3 via an eh1 binding motif within the N-terminus of the protein (Farin et al., 2007). In this study, transcriptional assays demonstrated that Tbx18 can repress activation of the *Nppa/ANF* promoter by the cardiac transcription factors Gata4, Nkx2.5, and Tbx5. This finding was interpreted as Tbx18 abrogation of *Nppa/ANF* expression through competition with Tbx5, a second T-box protein, for T-box binding sites (TBEs) within the *Nppa/ANF* promoter. Similarly, Tbx18 is predicted to repress Tbx6-mediated activation of the

Notch ligand *Delta-like 1* (*Dll1*) in anterior somites through competition with Tbx6 (Farin et al., 2007). Collectively, these data imply a model in which Tbx18 competes with other T-box activators for occupancy of TBEs and subsequently achieves repression by recruiting a TLE co-repressor complex to the target gene. In contrast, our data strongly implies a mechanism by which Tbx20 and Tbx18 are simultaneously bound to TLE3 at their respective eh1 motifs, and that binding of Tbx20 to TLE3 is a critical event preceding its interaction with Tbx18. Therefore, it appears that Tbx18 and Tbx20 may be acting cooperatively as repressors on a common set of target genes. Our lab has previously reported that Tbx20 also interacts physically with Tbx5 (Brown et al., 2005), suggesting that heterodimerization with other T-box factors may represent an important mechanism by which Tbx20 regulates gene expression in the embryo. This model is consistent with a recent study demonstrating that cardiogenic transcription factors act on enhancers in a cooperative manner (Junion et al., 2012). In this “transcription factor collective” model, occupancy of one or more of the transcription factors on a target locus initiates the recruitment of the remainder of the transcription factors via protein-protein interactions (as opposed to a specific arrangement of sequence motifs within the target promoter).

In summary, the goal of our study was to expand upon the current knowledge of the Tbx20 transcriptional network. By combining immunoaffinity purification with targeted proteomics and functional network analysis, we have identified a Tbx20 transcription repression network with chromatin remodeling and deacetylase

functions. We also identified Tbx18 as a Tbx20 interaction, raising the question of whether Tbx20 transcriptional repression relies on cooperative activity of Tbx20 and other cardiac transcription factors, similar to what has been shown for Tbx20 transcriptional activation in the presence of the activators Gata4, Nkx2.5, and Tbx5 (Stennard et al., 2003; Takeuchi et al., 2005). Future studies will aim to delineate the biological role of these repressive interactions, particularly as they relate to regulation of the cardiogenic program.

ACKNOWLEDGEMENTS

These studies were funding by grants to F.L.C from NIH/NHLBI (RO1 DE018825 and RO1 HL089641), to I.M.C. from NIH/NIDA (DP1DA026192) and HFSPO (RGYoo79/2009-C), and by an American Heart Association Pre-Doctoral Fellowship and a UNC Dissertation Completion Fellowship awarded to E.K. We also thank Panna Tandon in the Conlon Lab for critical reading of the manuscript.

Figure 3.1. Tbx20-EGFP is nuclear-localized and transcriptionally active. (A) Schematic of EGFP-tagged (green) Tbx20 expression construct, showing the N-terminal (white), T-box (black), transactivation (blue), and repression (brown) domains. A putative Tbx5 protein-protein interaction (PPI) domain lies within the N-terminus and T-box. Numbers denote amino acid residues. (B) Tbx20-EGFP is localized to the nucleus in HEK293 cells, as confirmed by live GFP fluorescence and colocalization with DAPI. (C) *Tbx20-EGFP* mRNA was injected at the 1-cell stage into *Xenopus* embryos. Expression of *Tbx20-EGFP* in the animal pole of stage 9 *Xenopus* embryos was confirmed by live GFP fluorescence. (D) RT-PCR analysis of the mesodermal genes *chordin* and *Xbra* and the skeletal muscle gene *Myf5* in stage 13 whole embryos, stage-matched untreated animal caps, Activin-treated animal caps, *Tbx20*-injected animal caps, and *Tbx20-EGFP*-injected animal caps. The housekeeping gene *Gapdh* was used as a loading control for all RT-PCR reactions.

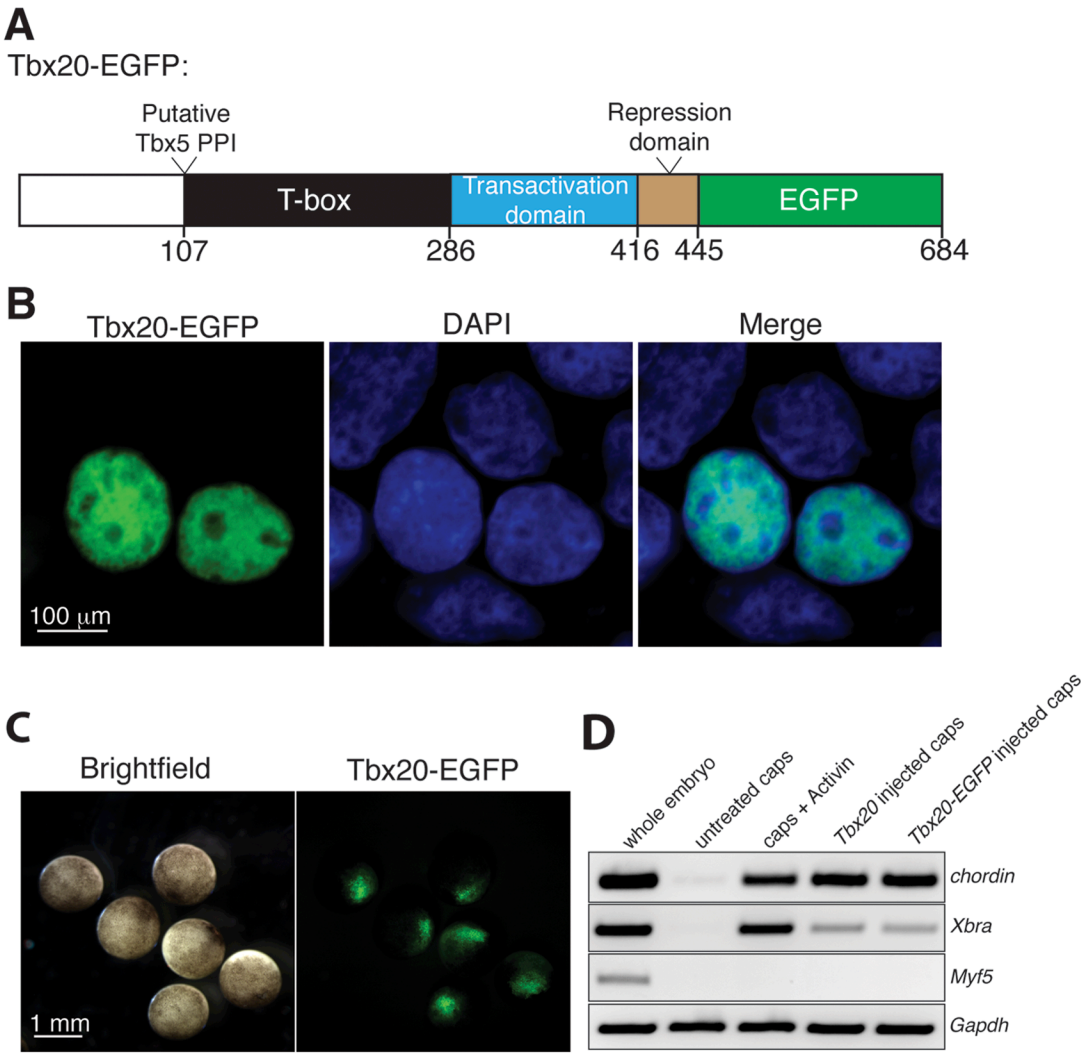
A
Tbx20-EGFP:
Putative
Tbx5 PPI
Repression
domain
T-box
Transactivation
domain
EGFP
107
286
416
445
684
B
Tbx20-EGFP
DAPI
Merge
100 μm
C
Brightfield
Tbx20-EGFP
1 mm
D
whole embryo
untreated caps
caps + Activin
Tbx20 injected caps
Tbx20-EGFP injected caps
chordin
Xbra
Myf5
Gapdh

Figure 3.2. Directed proteomics of Tbx20-EGFP protein complexes reveals association of Tbx20 with an HDAC-containing chromatin remodeling and Groucho transcriptional protein network. (A) GO enrichment analysis of Tbx20 interactions using ClueGO clustering according to biological function ontologies. (B) The Cytoscape network was assembled from automated retrieval and manual curation of protein functional associations using STRING analysis (grey lines) and literature curation (solid black lines), respectively. Potential interactions/functional associations with Tbx20 are indicated by black dashed lines. Nodes are labeled with respective gene symbols and enrichment index values (see Materials and Methods) are represented by node size and blue color intensity.

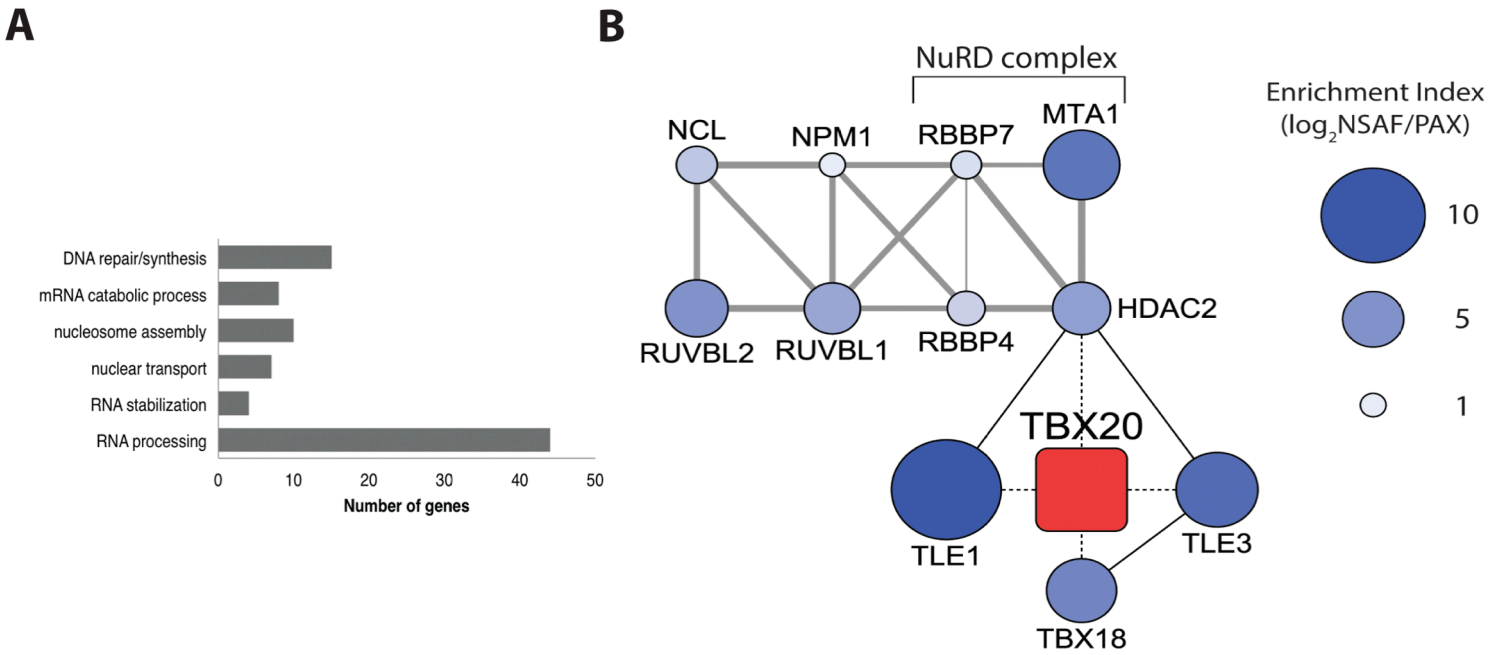
A
DNA repair/synthesis
mRNA catabolic process
nucleosome assembly
nuclear transport
RNA stabilization
RNA processing
0
10
20
30
40
50
Number of genes
B
NuRD complex
NCL
NPM1
RBBP7
MTA1
RUVBL2
RUVBL1
RBBP4
HDAC2
TBX20
TLE1
TLE3
TBX18
Enrichment Index
(log2NSAF/PAX)
10
5
1

Figure 3.3. Tbx20 interacts with TLE1/3, HDAC2, and Tbx18. (A) Protein sequence alignment of an N-terminal eh1 binding motif in Tbx20 demonstrating complete conservation of the eh1 motif across all vertebrate homologs of Tbx20. h, human; m, mouse; x, Xenopus; z, zebrafish. (B) Reciprocal immunoisolations of TLE1-Flag (FL) complexes from HEK293 cells expressing either Tbx20-EGFP or $Tbx20^{eh1mut}$ -EGFP. (C) Reciprocal immunoisolations of TLE3 complexes from HEK293 cells expressing either Tbx20-EGFP or $Tbx20^{eh1mut}$-EGFP. (D) Reciprocal immunoisolations of Tbx18-Flag (FL) complexes from HEK293 cells expressing Tbx18-Flag in the presence or absence of Tbx20-EGFP. (E) Reciprocal immunoisolations of HDAC2-GFP from HEK293 cells expressing Tbx20-HA and/or TLE3.

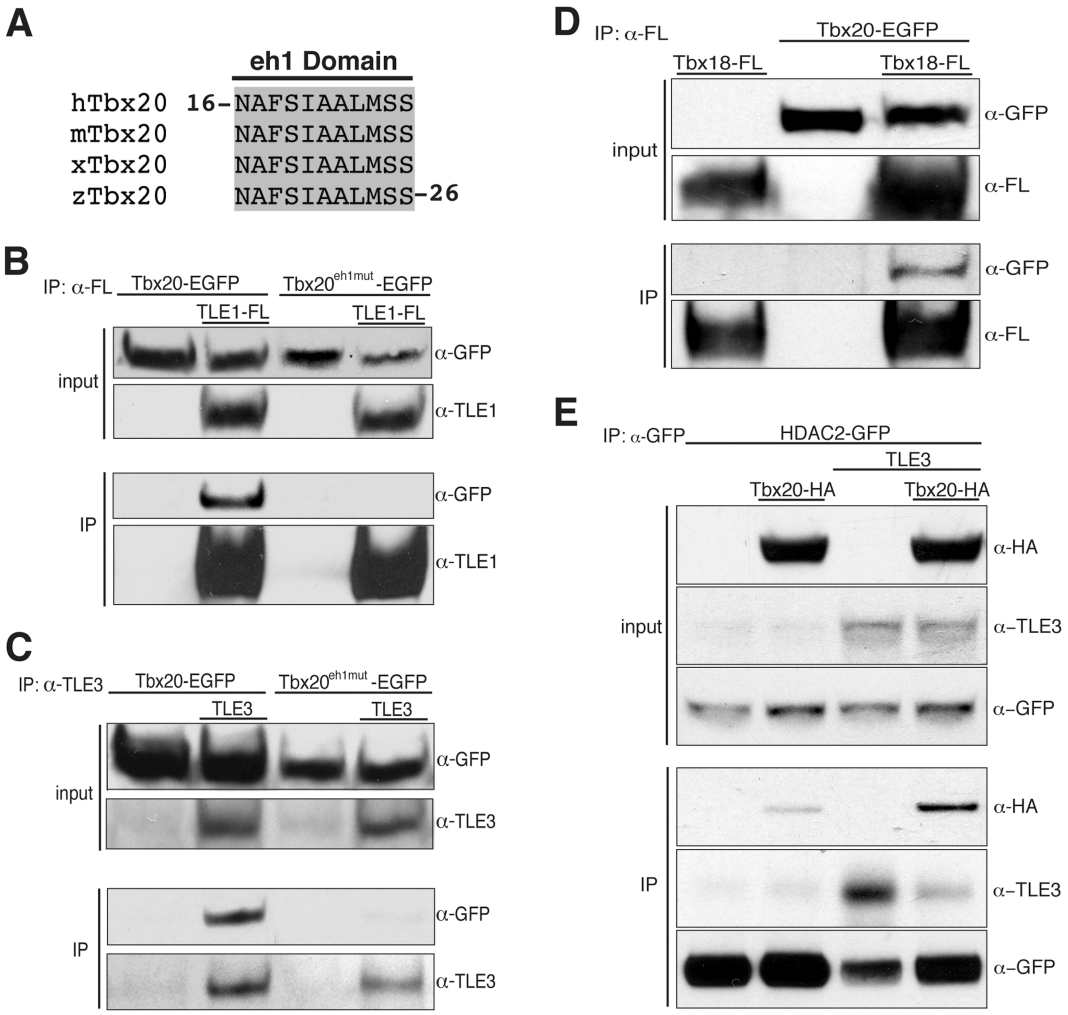
A
eh1 Domain
hTbx20 16-NAFSIAALMSS
mTbx20 NAFSIAALMSS
xTbx20 NAFSIAALMSS
zTbx20 NAFSIAALMSS-26
B
IP: α-FL
Tbx20-EGFP
Tbx20eh1mut-EGFP
TLE1-FL
TLE1-FL
input
α-GFP
α-TLE1
IP
α-GFP
α-TLE1
C
IP: α-TLE3
Tbx20-EGFP
Tbx20eh1mut-EGFP
TLE3
TLE3
input
α-GFP
α-TLE3
IP
α-GFP
α-TLE3
D
IP: α-FL
Tbx20-EGFP
Tbx18-FL
Tbx18-FL
input
α-GFP
α-FL
IP
α-GFP
α-FL
E
IP: α-GFP
HDAC2-GFP
TLE3
Tbx20-HA
Tbx20-HA
input
α-HA
α–TLE3
α–GFP
IP
α-HA
α–TLE3
α–GFP

Figure 3.4. Tbx20 assembles a Groucho-Tbx20 repression complex via the eh1 binding motif. Wild-type Tbx20-EGFP and Tbx20^{eh1mut}-EGFP were immunoaffinity purified from HEK293 cells with associated proteins and analyzed by mass spectrometry. Fold changes in spectrum counts for each interaction illustrated in (A) is shown for the isolated Tbx20^{eh1mut} mutant versus wild-type Tbx20. (B) The relative size of the circles indicates increased or decreased relative abundance of each interaction as determined by the fold-change in spectrum counts for mutant versus wild-type Tbx20 isolations.

A

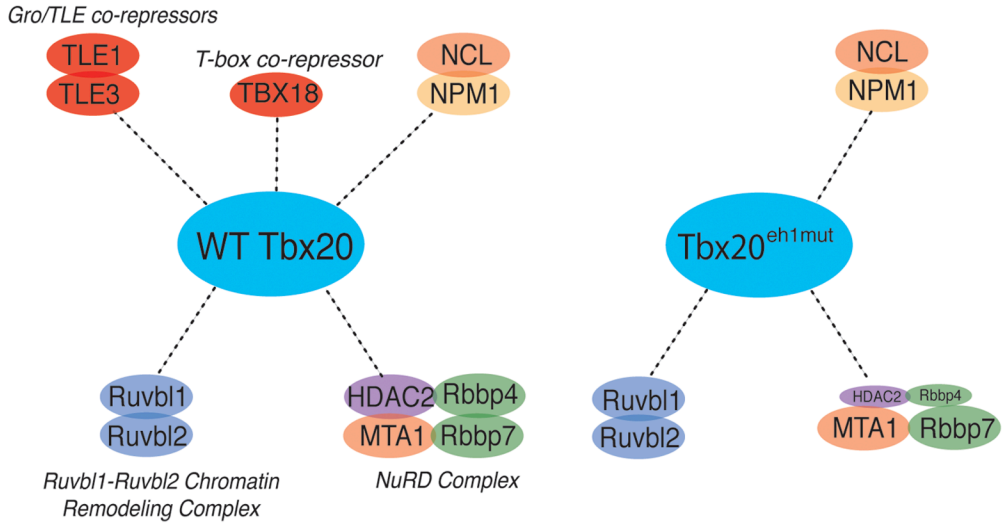

B

Tbx20 Interacting Protein	Gene Name	Fold Change (vs WT)
Transducin-like enhancer protein 1	TLE1	-
Transducin-like enhancer protein 3	TLE3	-
T-box transcription factor TBX18	TBX18	-
Histone binding protein Rbbp4	RBBP4	0.5
Histone deacetylase 2	HDAC2	0.3
Nucleolin	NCL	1.4
Nucleophosmin	NPM1	1.0
Ruvb-like 1	RUVBL1	0.8
Ruvb-like 2	RUVBL2	1.0
Metastasis-associated protein 1	MTA1	0.7
Histone binding protein Rbbp7	RBBP7	0.6

Figure 3.5. Endogenous Tbx20 interacts with TLE1/3 in mouse embryonic hearts. (A) RT-PCR analysis of *TLE* family members and cardiac-specific markers *Nkx2.5* and *Tbx20* in E10.5 heart tissue. All samples derived from embryonic hearts dissected at E10.5. (B) 25 hearts were dissected, and endogenous Tbx20 complexes were isolated with an antibody against Tbx20, analyzed by SDS-PAGE, and immunoblotted with antibodies against TLE1 and TLE3. In parallel and as a control, a mock immunoprecipitation was performed in the absence of Tbx20 antibody.

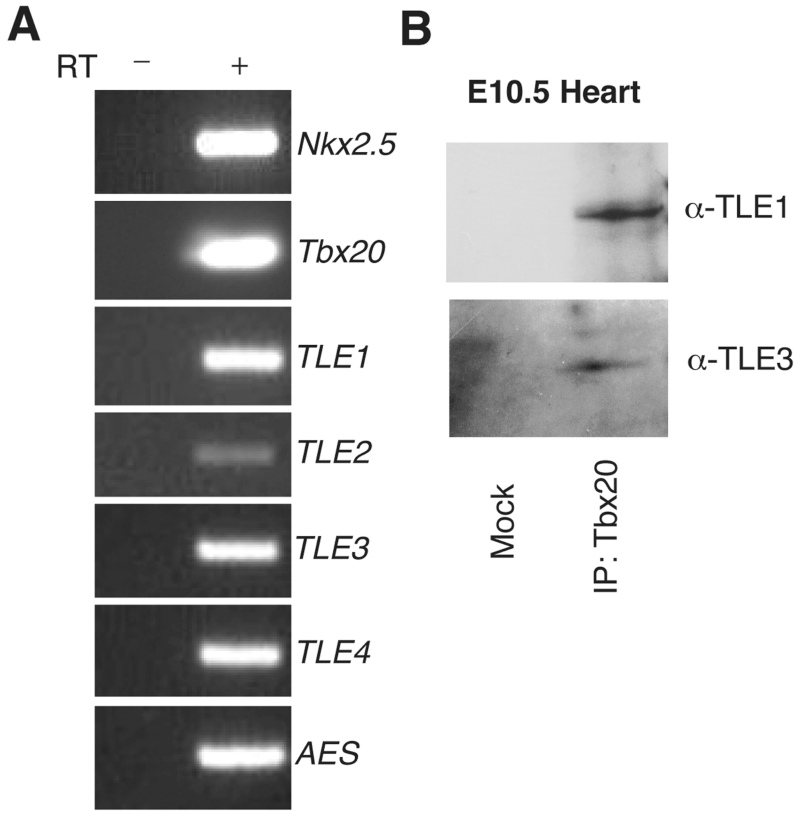

Table 3.1. Tbx20-associated proteins identified by LC-MS/MS. Numbers represent an average across three experimental replicates.

Protein description	Gene name	GFP	Tbx20-EGFP		
		Spectrum counts	Spectrum counts	Unique peptides	Percent coverage
T-Box transcription factor Tbx20	**Tbx20**	**1**	**707**	**54**	**73**
Green fluorescent protein	GFP	429	411	23	63
T-box transcription factor Tbx18	Tbx18	1	11	2	5
Transducin-like enhancer of split 1	TLE1	1	17	5	15
Transducin-like enhancer of split 3	TLE3	2	29	13	23
Histone-binding protein Rbbp4	RBBP4	3	15	7	21
Histone-binding protein Rbbp7	RBBP7	1	10	2	16
Histone deacetylase 2	HDAC2	3	11	3	14
Metastasis-associated protein MTA1	MTA1	1	7	4	7
Nucleophosmin	NPM1	7	40	10	51
Nucleolin	NCL	14	65	14	22
RuvB-like 1	RUVBL1	3	23	8	23
RuvB-like 2	RUVBL2	4	24	10	24

Table S3.1. Nuclear-enriched DNA-independent Tbx20 interactions from three independent immunoisolations. Tbx20 associations that occur in the presence of DNase, are nuclear-enriched, and meet specificity criteria (see Materials and Methods) in three independent immunoisolations.

Protein Description	Gene Name	Accession	MW (kDa)	LTQ-Orbitrap XL									LTQ-Orbitrap Velos				
				GFP	Tbx20-GFP				Tbx20-GFP (DNase-treated)				GFP	Tbx20-GFP (DNase-treated)			
				Spectrum counts	Spectrum counts	Unique peptides	Percent Coverage	Fold Enrichment	Spectrum counts	Unque peptides	Percent Coverage	Fold Enrichment	Spectrum counts	Spectrum counts	Unique peptides	Percent Coverage	Fold Enrichment
Green flourescent protein	GFP	P42212	27	**687**	**273**	18	63	0.4	**696**	35	74	1.0	**171**	**264**	17	53	1.5
T-box transcription factor TBX20	TBX20	Q9ES03	49	**1**	**556**	35	71	556.0	**1280**	88	78	1280.0	**0**	**284**	39	71	284.0
DNA-dependent protein kinase catalytic subunit	PRKDC	P78527	469	**1**	**294**	100	28	294.0	**13**	8	2	13.0	**92**	**335**	101	27	3.6
Heterogeneous nuclear ribonucleoprotein K	HNRNPK	P61978	51	**8**	**159**	19	57	19.9	**124**	18	52	15.5	**45**	**124**	18	48	2.8
Nucleolar RNA helicase 2	DDX21	Q9NR30	87	**6**	**147**	37	54	24.5	**59**	25	42	9.8	**43**	**118**	30	40	2.7
Glyceraldehyde-3-phosphate dehydrogenase	GAPDH	P04406	36	**13**	**86**	13	53	6.6	**82**	13	44	6.3	**34**	**110**	17	44	3.2
Heterogeneous nuclear ribonucleoproteins A2/B1	HNRNPA2B1	P22626	37	**3**	**93**	19	61	31.0	**79**	20	65	26.3	**40**	**124**	24	58	3.1
Heterogeneous nuclear ribonucleoprotein R	HNRNPR	O43390	71	**1**	**107**	23	39	107.0	**61**	16	34	61.0	**26**	**71**	20	33	2.7
Heterogeneous nuclear ribonucleoprotein L	HNRNPL	P14866	64	**1**	**84**	20	49	84.0	**83**	18	50	83.0	**35**	**90**	20	42	2.6
Myb-binding protein 1A	MYBBP1A	Q9BQG0	149	**1**	**149**	30	27	149.0	**52**	29	26	52.0	**26**	**157**	43	34	6.0
X-ray repair cross-complementing protein 6	XRCC6	P12956	70	**1**	**101**	22	48	101.0	**41**	19	42	41.0	**30**	**86**	21	41	2.9
Transketolase	TKT	P29401	68	**1**	**92**	16	32	92.0	**56**	14	30	56.0	**17**	**52**	15	27	3.1
Malate dehydrogenase, mitochondrial	MDH2	P40926	36	**1**	**75**	15	59	75.0	**47**	17	62	47.0	**14**	**115**	19	70	8.2
Nucleolar protein 56	NOP56	O00567	66	**1**	**73**	25	53	73.0	**57**	15	37	57.0	**27**	**73**	23	52	2.7
Transcription intermediary factor 1-beta	TRIM28	Q13263	89	**1**	**95**	17	40	95.0	**41**	14	33	41.0	**38**	**117**	20	35	3.1
Putative pre-mRNA-splicing factor ATP-dependent RNA helicase DHX15	DHX15	O43143	91	**1**	**94**	23	34	94.0	**31**	12	17	31.0	**24**	**72**	19	27	3.0
Spliceosome RNA helicase BAT1	BAT1	Q13838	49	**1**	**74**	12	31	74.0	**35**	10	32	35.0	**23**	**93**	18	45	4.0
60S ribosomal protein L4	RPL4	P36578	48	**2**	**59**	14	36	29.5	**32**	9	28	16.0	**15**	**87**	20	44	5.8
Splicing factor, proline- and glutamine-rich	SFPQ	P23246	76	**1**	**67**	15	28	67.0	**29**	12	20	29.0	**18**	**58**	15	24	3.2
Non-POU domain-containing octamer-binding protein	NONO	Q15233	54	**1**	**70**	15	42	70.0	**34**	12	36	34.0	**17**	**91**	19	46	5.4
Heat shock 70 kDa protein 4	HSPA4	P34932	94	**1**	**82**	16	27	82.0	**14**	7	12	14.0	**22**	**71**	21	36	3.2
Polypyrimidine tract-binding protein 1	PTBP1	P26599	57	**1**	**54**	11	31	54.0	**37**	12	32	37.0	**9**	**29**	12	27	3.2
T-complex protein 1 subunit delta	CCT4	P50991	58	**1**	**56**	15	38	56.0	**33**	13	35	33.0	**20**	**56**	15	36	2.8
Heterogeneous nuclear ribonucleoprotein A3	HNRNPA3	P51991	40	**1**	**52**	14	40	52.0	**30**	9	29	30.0	**18**	**77**	13	31	4.3
Putative ribosomal RNA methyltransferase NOP2	NOP2	P46087	89	**2**	**60**	20	31	30.0	**25**	14	23	12.5	**18**	**53**	20	29	2.9
Histone H1.4	HIST1H1E	P10412	22	**1**	**44**	9	26	44.0	**39**	12	39	39.0	**17**	**46**	2	32	2.7
Exportin-2	CSE1L	P55060	110	**1**	**55**	21	27	55.0	**16**	9	12	16.0	**10**	**58**	16	20	5.8
Nucleolar protein 58	NOP58	Q9Y2X3	60	**2**	**43**	14	35	21.5	**39**	15	40	19.5	**23**	**64**	19	43	2.8
Double-stranded RNA-specific adenosine deaminase	ADAR	P55265	136	**1**	**55**	14	16	55.0	**21**	9	10	21.0	**17**	**56**	18	19	3.3
Transducin-like enhancer protein 1	TLE1	Q04724	83	**1**	**11**	2	8	11.0	**36**	12	33	36.0	**1**	**5**	2	5	5.0
Transducin-like enhancer protein 3	TLE3	Q04726	83	**1**	**16**	7	12	16.0	**60**	26	41	60.0	**2**	**10**	7	16	5.0
Guanine nucleotide-binding protein subunit beta-2-like 1	GNB2L1	P63244	35	**4**	**40**	15	67	10.0	**27**	12	48	6.8	**10**	**45**	12	47	4.5
Cullin-associated NEDD8-dissociated protein 1	CAND1	Q86VP6	136	**1**	**55**	14	15	55.0	**18**	9	9	18.0	**28**	**77**	21	19	2.8
Leucine-rich PPR motif-containing protein, mitochondrial	LRPPRC	P42704	158	**1**	**38**	16	15	38.0	**22**	12	10	22.0	**22**	**79**	26	21	3.6
T-complex protein 1 subunit beta	CCT2	P78371	57	**1**	**41**	13	35	41.0	**28**	12	32	28.0	**25**	**68**	18	35	2.7
Puromycin-sensitive aminopeptidase	NPEPPS	P55786	103	**1**	**53**	21	28	53.0	**17**	10	12	17.0	**21**	**70**	20	24	3.3
Heterogeneous nuclear ribonucleoprotein G	RBMX	P38159	42	**1**	**36**	8	21	36.0	**35**	16	40	35.0	**12**	**72**	16	40	6.0
Ribosomal L1 domain-containing protein 1	RSL1D1	O76021	55	**1**	**33**	12	28	33.0	**30**	17	41	30.0	**12**	**46**	21	39	3.8
Nucleophosmin	NPM1	P06748	33	**2**	**32**	8	40	16.0	**32**	10	45	16.0	**11**	**56**	13	68	5.1
40S ribosomal protein S3	RPS3	P23396	27	**4**	**36**	13	60	9.0	**23**	12	52	5.8	**5**	**30**	15	64	6.0
T-complex protein 1 subunit epsilon	CCT5	P48643	60	**1**	**37**	15	31	37.0	**21**	12	26	21.0	**13**	**39**	14	25	3.0
Interleukin enhancer-binding factor 2	ILF2	Q12905	43	**1**	**45**	11	37	45.0	**17**	7	23	17.0	**19**	**69**	13	35	3.6
Core histone macro-H2A.1	H2AFY	O75367	40	**3**	**35**	11	40	11.7	**16**	7	25	5.3	**17**	**47**	8	33	2.8
Protein RCC2	RCC2	Q9P258	56	**1**	**29**	9	23	29.0	**18**	7	20	18.0	**1**	**31**	14	38	31.0
rRNA 2'-O-methyltransferase fibrillarin	FBL	P22087	34	**1**	**28**	10	42	28.0	**23**	8	32	23.0	**8**	**35**	12	39	4.4
60S ribosomal protein L3	RPL3	P39023	46	**1**	**35**	11	33	35.0	**10**	6	14	10.0	**12**	**54**	13	26	4.5
Apoptosis-inducing factor 1, mitochondrial	AIFM1	O95831	67	**2**	**31**	12	27	15.5	**12**	7	21	6.0	**10**	**47**	15	26	4.7
DNA mismatch repair protein Msh6	MSH6	P52701	153	**1**	**32**	10	10	32.0	**17**	8	8	17.0	**11**	**39**	23	20	3.5
General transcription factor II-I	GTF2I	P78347	112	**1**	**31**	14	21	31.0	**14**	8	11	14.0	**9**	**44**	17	22	4.9
Serine/arginine-rich splicing factor 1	SRSF1	Q07955	28	**1**	**23**	10	38	23.0	**24**	12	42	24.0	**10**	**47**	12	44	4.7
60S acidic ribosomal protein P0	RPLP0	P05388	34	**1**	**30**	10	45	30.0	**16**	7	30	16.0	**13**	**47**	13	40	3.6
40S ribosomal protein SA	RPSA	P08865	33	**1**	**24**	8	44	24.0	**21**	5	23	21.0	**11**	**37**	10	41	3.4

Table S3.1. - Continued

Protein Description	Gene Name	Accession	MW (kDa)	LTQ-Orbitrap XL									LTQ-Orbitrap Velos				
				GFP	Tbx20-GFP				Tbx20-GFP (DNase-treated)				GFP	Tbx20-GFP (DNase-treated)			
				Spectrum counts	Spectrum counts	Unique peptides	Percent Coverage	Fold Enrichment	Spectrum counts	Unque peptides	Percent Coverage	Fold Enrichment	Spectrum counts	Spectrum counts	Unique peptides	Percent Coverage	Fold Enrichment
GTP-binding nuclear protein Ran	RAN	P62826	24	1	28	7	36	28.0	12	6	30	12.0	4	37	10	38	9.3
Putative rRNA methyltransferase 3	FTSJ3	Q8IY81	97	1	22	8	11	22.0	18	9	17	18.0	12	41	16	25	3.4
Heterochromatin protein 1-binding protein 3	HP1BP3	Q5SSJ5	61	1	27	10	20	27.0	15	5	10	15.0	5	34	12	28	6.8
Splicing factor U2AF 65 kDa subunit	U2AF2	P26368	54	1	24	5	15	24.0	17	8	27	17.0	9	26	6	23	2.9
Protein KIAA1967	KIAA1967	Q8N163	103	1	29	14	26	29.0	14	6	10	14.0	12	38	16	25	3.2
Heterogeneous nuclear ribonucleoprotein F	HNRNPF	P52597	46	3	56	8	38	18.7	16	6	24	5.3	21	66	11	40	3.1
Superkiller viralicidic activity 2-like 2	SKIV2L2	P42285	118	1	23	14	18	23.0	13	5	6	13.0	13	34	14	15	2.6
Arginyl-tRNA synthetase, cytoplasmic	RARS	P54136	75	1	28	8	16	28.0	12	6	12	12.0	11	30	11	20	2.7
Proliferation-associated protein 2G4	PA2G4	Q9UQ80	44	1	25	9	27	25.0	17	10	32	17.0	4	73	14	41	18.3
Serrate RNA effector molecule homolog	SRRT	Q9BXP5	101	1	23	10	15	23.0	11	8	9	11.0	11	36	16	20	3.3
60S ribosomal protein L5	RPL5	P46777	34	2	24	9	42	12.0	12	5	23	6.0	6	31	9	33	5.2
Proliferating cell nuclear antigen	PCNA	P12004	29	1	19	8	48	19.0	18	9	32	18.0	2	27	10	47	13.5
THO complex subunit 2	THOC2	Q8NI27	183	1	27	14	10	27.0	6	3	2	6.0	3	35	15	10	11.7
Prohibitin-2	PHB2	Q99623	33	1	20	9	37	20.0	13	8	32	13.0	8	33	13	48	4.1
Heterogeneous nuclear ribonucleoprotein Q	SYNCRIP	O60506	70	1	61	8	25	61.0	22	4	17	22.0	21	53	9	29	2.5
40S ribosomal protein S3a	RPS3A	P61247	30	1	20	10	39	20.0	14	7	32	14.0	5	30	13	48	6.0
H/ACA ribonucleoprotein complex subunit 4	DKC1	O60832	58	1	13	5	13	13.0	17	9	24	17.0	4	21	11	26	5.3
Aconitate hydratase, mitochondrial	ACO2	Q99798	85	1	27	9	17	27.0	8	4	7	8.0	13	44	16	26	3.4
Probable ATP-dependent RNA helicase DDX27	DDX27	Q96GQ7	90	1	27	13	18	27.0	6	4	8	6.0	10	30	12	17	3.0
T-box transcription factor TBX18	TBX18	O95935	65	1	10	2	5	10.0	17	2	5	17.0	0	5	2	5	5.0
Serine/threonine-protein phosphatase PP1-gamma catalytic subunit	PPP1CC	P36873	37	1	21	8	30	21.0	12	6	26	12.0	4	21	3	30	5.3
RRP12-like protein	RRP12	Q5JTH9	144	1	16	9	10	16.0	7	4	5	7.0	12	51	18	17	4.3
Small ubiquitin-related modifier 2	SUMO2	P61956	11	1	24	2	23	24.0	8	2	23	8.0	5	17	2	23	3.4
Host cell factor 1	HCFC1	P51610	209	1	21	9	6	21.0	8	4	3	8.0	8	35	14	10	4.4
Complement component 1 Q subcomponent-binding protein, mitochondrial	C1QBP	Q07021	31	1	16	6	32	16.0	15	5	32	15.0	3	34	9	39	11.3
THO complex subunit 4	THOC4	Q86V81	27	1	16	6	36	16.0	11	5	34	11.0	8	23	9	36	2.9
KH domain-containing, RNA-binding, signal transduction-associated protein 1	KHDRBS1	Q07666	48	1	19	6	23	19.0	10	4	20	10.0	2	17	8	23	8.5
Probable ATP-dependent RNA helicase DDX23	DDX23	Q9BUQ8	96	1	22	11	14	22.0	8	4	5	8.0	3	18	8	11	6.0
Eukaryotic initiation factor 4A-III	EIF4A3	P38919	47	1	15	6	18	15.0	16	6	21	16.0	19	68	19	38	3.6
Ribosomal RNA processing protein 1 homolog B	RRP1B	Q14684	84	1	20	9	16	20.0	7	3	6	7.0	4	18	8	16	4.5
Histone-binding protein RBBP4	RBBP4	Q09028	48	2	17	7	23	8.5	9	4	14	4.5	3	19	9	26	6.3
RNA-binding protein Raly	RALY	Q9UKM9	32	1	16	8	24	16.0	10	4	17	10.0	7	23	12	35	3.3
Nucleolar transcription factor 1	UBTF	P17480	89	1	18	9	15	18.0	6	3	5	6.0	6	15	8	12	2.5
U4/U6.U5 tri-snRNP-associated protein 1	SART1	O43290	90	1	17	10	17	17.0	8	4	7	8.0	7	27	13	24	3.9
Ribosome biogenesis protein BOP1	BOP1	Q14137	84	1	20	10	18	20.0	8	4	9	8.0	6	16	8	15	2.7
ELAV-like protein 1	ELAVL1	Q15717	36	1	21	9	38	21.0	7	4	21	7.0	10	34	14	49	3.4
Pre-mRNA-processing factor 6	PRPF6	O94906	107	1	16	7	9	16.0	11	5	6	11.0	5	29	18	22	5.8
NF-kappa-B-repressing factor	NKRF	O15226	78	1	22	11	20	22.0	6	3	5	6.0	4	18	11	17	4.5
Prohibitin	PHB	P35232	30	1	12	7	39	12.0	10	5	23	10.0	5	30	13	49	6.0
Histone H1x	H1FX	Q92522	22	1	13	6	31	13.0	10	4	26	10.0	2	26	8	41	13.0
Poly(rC)-binding protein 2	PCBP2	Q15366	39	1	19	4	23	19.0	19	4	25	19.0	9	44	8	31	4.9
Inosine-5'-monophosphate dehydrogenase 2	IMPDH2	P12268	56	1	20	8	17	20.0	6	3	6	6.0	3	52	13	25	17.3
Calreticulin	CALR	P27797	48	1	15	6	19	15.0	8	4	14	8.0	10	56	13	38	5.6
Transportin-1	TNPO1	Q92973	102	1	16	6	8	16.0	6	4	6	6.0	7	21	9	12	3.0
Spermatid perinuclear RNA-binding protein	STRBP	Q96SI9	74	1	34	5	12	34.0	9	1	5	9.0	10	26	2	8	2.6
Protein arginine N-methyltransferase 5	PRMT5	O14744	73	1	15	5	11	15.0	6	3	7	6.0	5	19	7	16	3.8
CCAAT/enhancer-binding protein zeta	CEBPZ	Q03701	121	1	14	7	8	14.0	8	5	6	8.0	12	31	12	12	2.6
ATP-dependent DNA helicase Q1	RECQL	P46063	73	1	16	5	7	16.0	6	2	3	6.0	5	15	7	14	3.0
Nucleolar complex protein 3 homolog	NOC3L	Q8WTT2	93	1	8	3	5	8.0	12	6	11	12.0	4	23	10	15	5.8

Table S3.1. - Continued

Protein Description	Gene Name	Accession	MW (kDa)	LTQ-Orbitrap XL									LTQ-Orbitrap Velos				
				GFP	Tbx20-GFP				Tbx20-GFP (DNase-treated)				GFP	Tbx20-GFP (DNase-treated)			
				Spectrum counts	Spectrum counts	Unique peptides	Percent Coverage	Fold Enrichment	Spectrum counts	Unque peptides	Percent Coverage	Fold Enrichment	Spectrum counts	Spectrum counts	Unique peptides	Percent Coverage	Fold Enrichment
RuvB-like 2	RUVBL2	Q9Y230	51	**1**	**12**	6	17	12.0	**7**	4	9	7.0	**6**	**53**	20	47	8.8
RuvB-like 1	RUVBL1	Q9Y265	50	**1**	**9**	5	15	9.0	**8**	4	11	8.0	**5**	**51**	15	42	10.2
Septin-2	SEPT2	Q15019	41	**1**	**11**	6	26	11.0	**8**	4	16	8.0	**4**	**11**	5	22	2.8
Heterogeneous nuclear ribonucleoprotein A0	HNRNPA0	Q13151	31	**1**	**10**	3	17	10.0	**7**	3	16	7.0	**5**	**13**	5	20	2.6
Nucleolar and coiled-body phosphoprotein 1	NOLC1	Q14978	74	**1**	**6**	4	4	6.0	**9**	2	11	9.0	**3**	**9**	4	6	3.0
TAR DNA-binding protein 43	TARDBP	Q13148	45	**1**	**8**	4	15	8.0	**9**	4	15	9.0	**2**	**18**	5	14	9.0
Proteasome subunit alpha type-1	PSMA1	P25786	30	**1**	**10**	5	20	10.0	**6**	3	14	6.0	**1**	**13**	9	30	13.0
Core histone macro-H2A.2	H2AFY2	Q9P0M6	40	**1**	**7**	1	6	7.0	**6**	2	11	6.0	**5**	**24**	11	33	4.8
14-3-3 protein theta	YWHAQ	P27348	28	**1**	**11**	3	20	11.0	**10**	3	26	10.0	**8**	**46**	7	38	5.8
Probable ATP-dependent RNA helicase DDX47	DDX47	Q9H0S4	51	**1**	**6**	3	9	6.0	**6**	3	8	6.0	**4**	**14**	9	27	3.5
Histone H1.2	HIST1H1C	P16403	21	**1**	**43**	3	25	43.0	**40**	3	43	40.0	**16**	**50**	10	31	3.1
Histone deacetylase 2	HDAC2	Q92769	55	**1**	**13**	1	11	13.0	**11**	2	13	11.0	**4**	**10**	7	19	2.5
Nucleolin	NCL	P19338	77	**1**	**112**	18	27	112.0	**29**	11	19	29.0	**26**	**53**	13	19	2.0
Histone-binding protein RBBP7	RBBP7	Q16576	48	**0**	**13**	3	19	13.0	**4**	1	8	4.0	**2**	**14**	3	20	7.0
Metastasis-associated protein 1	MTA1	Q13330	81	**0**	**8**	6	12	8.0	**2**	1	2	2.0	**2**	**10**	5	8	5.0

Table S3.2. Proteins excluded from nuclear-enriched DNA-independent Tbx20 interactions identified in three independent isolations. Tbx20 associations that pass specificity criteria (see Materials and Methods), but are lost in the presence of DNase and/or do not have a known nuclear localization.

Protein Description	Gene Name	Accession	MW (kDa)	LTQ-Orbitrap XL			LTQ-Orbitrap Velos	
				GFP (spectrum counts)	Tbx20-GFP (spectrum counts)	Tbx20-GFP (spectrum counts)	GFP (spectrum counts)	Tbx20-GFP (spectrum counts)
Actin, cytoplasmic 2	ACTG1	P63261	42	48	279	223		
Heat shock protein HSP 90-beta	HSP90AB1	P08238	83	15	241	151		
Tubulin alpha-1B chain	TUBA1B	P68363	50	18	235	169		
Tubulin beta-2C chain	TUBB2C	P68371	50	10	247	149	109	297
Heat shock cognate 71 kDa protein	HSPA8	P11142	71	18	240	199		
Elongation factor 2	EEF2	P13639	95	9	232	104		
Alpha-enolase	ENO1	P06733	47	10	198	103		
Ubiquitin-like modifier-activating enzyme 1	UBA1	P22314	118	2	213	97	65	168
Fatty acid synthase	FASN	P49327	273	2	266	21		
60 kDa heat shock protein, mitochondrial	HSPD1	P10809	61	2	138	118	37	158
Elongation factor 1-alpha 1	EEF1A1	P68104	50	19	143	86		
Heat shock protein HSP 90-alpha	HSP90AA1	P07900	85	1	214	121		
ATP synthase subunit alpha, mitochondrial	ATP5A1	P25705	60	3	85	74	32	100
Tubulin beta chain	TUBB	P07437	50	13	285	200		
Stress-70 protein, mitochondrial	HSPA9	P38646	74	2	98	64	33	167
Clathrin heavy chain 1	CLTC	Q00610	192	2	122	23		
L-lactate dehydrogenase A chain	LDHA	P00338	37	6	75	46	12	57
Endoplasmin	HSP90B1	P14625	92	4	104	53	83	211
L-lactate dehydrogenase B chain	LDHB	P07195	37	7	88	54	20	114
ATP synthase subunit beta, mitochondrial	ATP5B	P06576	57	1	65	51	33	158
ADP/ATP translocase 2	SLC25A5	P05141	33	11	66		10	64
C-1-tetrahydrofolate synthase, cytoplasmic	MTHFD1	P11586	102	1	82	24	19	114
D-3-phosphoglycerate dehydrogenase	PHGDH	O43175	57	1	72	42	24	70
Creatine kinase B-type	CKB	P12277	43	1	84	24	10	88
T-complex protein 1 subunit theta	CCT8	P50990	60	1	58	37	29	108
T-complex protein 1 subunit zeta	CCT6A	P40227	58	1	58	33		
T-complex protein 1 subunit alpha	TCP1	P17987	60	1	60	36		
T-complex protein 1 subunit eta	CCT7	Q99832	59	2	56	37		
Eukaryotic initiation factor 4A-I	EIF4A1	P60842	46	1	60	24	30	106
T-complex protein 1 subunit gamma	CCT3	P49368	61	1	58	23	22	63
Phosphoglycerate kinase 1	PGK1	P00558	45	1	54	35	13	127
Polyadenylate-binding protein 1	PABPC1	P11940	71	1	52	23		
Neutral alpha-glucosidase AB	GANAB	Q14697	107	1	46	28		
Heat shock protein 75 kDa, mitochondrial	TRAP1	Q12931	80	1	47	30	16	103
60S ribosomal protein L6	RPL6	Q02878	33	1	49	19	10	47
40S ribosomal protein S4, X isoform	RPS4X	P62701	30	5	36	27	11	32
Leucyl-tRNA synthetase, cytoplasmic	LARS	Q9P2J5	134	1	46	20	33	91
Aspartate aminotransferase, mitochondrial	GOT2	P00505	48	1	44	16	9	44
Fructose-bisphosphate aldolase A	ALDOA	P04075	39	1	39	12	17	78
60S ribosomal protein L7	RPL7	P18124	29	1	31	23	8	32
Triosephosphate isomerase	TPI1	P60174	27	1	34	24	7	87
Adenosylhomocysteinase	AHCY	P23526	48	3	35	15	8	51
14-3-3 protein epsilon	YWHAE	P62258	29	1	38	19	13	73
Serine hydroxymethyltransferase, mitochondrial	SHMT2	P34897	56	1	40	11	11	56
60S ribosomal protein L8	RPL8	P62917	28	3	26	18	3	23
Proline-, glutamic acid- and leucine-rich protein 1	PELP1	Q8IZL8	120	1	33	9		
Delta-1-pyrroline-5-carboxylate synthase	ALDH18A1	P54886	87	1	30	10	10	51
ATP-dependent RNA helicase DDX18	DDX18	Q9NVP1	75	1	26	15		
Voltage-dependent anion-selective channel protein 2	VDAC2	P45880	32	1	25	15	8	33
Elongation factor Tu, mitochondrial	TUFM	P49411	50	1	28	12	9	83
Sodium/potassium-transporting ATPase subunit alpha-	ATP1A1	P05023	113	1	33	9		
ATP-dependent RNA helicase DDX1	DDX1	Q92499	82	1	32	7		
Citrate synthase, mitochondrial	CS	O75390	52	1	29	11	6	28
60S ribosomal protein L7a	RPL7A	P62424	30	1	26	12	7	41
Elongation factor 1-gamma	EEF1G	P26641	50	1	28	10	14	57
Eukaryotic translation initiation factor 3 subunit B	EIF3B	P55884	92	1	26	11		

Table S3.2. - Continued

Protein Description	Gene Name	Accession	MW (kDa)	LTQ-Orbitrap XL			LTQ-Orbitrap Velos	
				GFP (spectrum counts)	Tbx20-GFP (spectrum counts)	Tbx20-GFP (spectrum counts)	GFP (spectrum counts)	Tbx20-GFP (spectrum counts)
Actin, alpha cardiac muscle 1	ACTC1	P68032	42	27	123	124	81	220
Bifunctional aminoacyl-tRNA synthetase	EPRS	P07814	171	1	21	13	25	82
Desmoplakin	DSP	P15924	332	6	21			
Ornithine aminotransferase, mitochondrial	OAT	P04181	49	1	21	15	3	21
26S proteasome non-ATPase regulatory subunit 1	PSMD1	Q99460	106	1	22	11		
Calnexin	CANX	P27824	68	1	27	9	15	48
Valyl-tRNA synthetase	VARS	P26640	140	1	20	12	14	46
Methionyl-tRNA synthetase, cytoplasmic	MARS	P56192	101	1	25	6	17	42
Eukaryotic translation initiation factor 3 subunit L	EIF3L	Q9Y262	67	1	19	12	5	21
Acetyl-CoA acetyltransferase, mitochondrial	ACAT1	P24752	45	1	16	15	6	55
60S ribosomal protein L18	RPL18	Q07020	22	3	16	9	6	25
Voltage-dependent anion-selective channel protein 1	VDAC1	P21796	31	4	19		7	37
Glycyl-tRNA synthetase	GARS	P41250	83	1	21	9	6	26
Eukaryotic translation initiation factor 3 subunit C	EIF3C	Q99613	105	1	22	8	10	25
26S proteasome non-ATPase regulatory subunit 3	PSMD3	O43242	61	1	16	11		
Protein disulfide-isomerase A3	PDIA3	P30101	57	1	14	13	20	103
Succinate dehydrogenase [ubiquinone] flavoprotein subunit, mitochondrial	SDHA	P31040	73	1	22	7	4	20
Histidine-rich glycoprotein	HRG	P04196	60	5	19		3	11
Cytochrome b-c1 complex subunit 2, mitochondrial	UQCRC2	P22695	48	1	16	11	3	56
26S proteasome non-ATPase regulatory subunit 2	PSMD2	Q13200	100	1	19	10		
Inositol-3-phosphate synthase 1	ISYNA1	Q9NPH2	61	1	19	10	2	10
Glutamate dehydrogenase 1, mitochondrial	GLUD1	P00367	61	1	9	15	5	53
Peroxiredoxin-2	PRDX2	P32119	22	6	18			
Mitochondrial 2-oxoglutarate/malate carrier protein	SLC25A11	Q02978	34	2	11	13	3	21
40S ribosomal protein S8	RPS8	P62241	24	2	17	6	7	36
Phosphoribosylformylglycinamidine synthase	PFAS	O15067	145	1	19	7		
Purine nucleoside phosphorylase	PNP	P00491	32	1	16	8	3	32
Electron transfer flavoprotein subunit alpha, mitochondrial	ETFA	P13804	35	1	11	14	3	33
Inorganic pyrophosphatase	PPA1	Q15181	33	1	15	7	2	28
Asparaginyl-tRNA synthetase, cytoplasmic	NARS	O43776	63	1	16	6	9	29
Malate dehydrogenase, cytoplasmic	MDH1	P40925	36	1	17	7	4	25
Annexin A2	ANXA2	P07355	39	1	9	13		
Tubulin alpha-1C chain	TUBA1C	Q9BQE3	50	16	204	152		
Transaldolase	TALDO1	P37837	38	1	12	10	1	16
Tubulin alpha-1A chain	TUBA1A	Q71U36	50	18	192	152		
Phosphate carrier protein, mitochondrial	SLC25A3	Q00325	40	1	11	8	5	19
Dihydrolipoyl dehydrogenase, mitochondrial	DLD	P09622	54	1	13	7	5	37
ATP synthase subunit gamma, mitochondrial	ATP5C1	P36542	33	1	14	7	3	7
60S ribosomal protein L13	RPL13	P26373	24	2	9	9		
Phosphoglycerate mutase 1	PGAM1	P18669	29	1	8	9	3	30
Protein disulfide-isomerase A4	PDIA4	P13667	73	2	10	6	47	139
Eukaryotic translation initiation factor 2 subunit 3	EIF2S3	P41091	51	1	7	6	5	21
Ubiquitin carboxyl-terminal hydrolase 5	USP5	P45974	96	1	9	6	8	21
CTP synthase 1	CTPS	P17812	67	1	9	6	6	21
ADP/ATP translocase 3	SLC25A6	P12236	33	9	47		10	44
ATP-binding cassette sub-family E member 1	ABCE1	P61221	67	1	9	6	3	11
F-actin-capping protein subunit alpha-1	CAPZA1	P52907	33	1	8	7	5	13
14-3-3 protein zeta/delta	YWHAZ	P63104	28	1	15	8		
Polyadenylate-binding protein 4	PABPC4	Q13310	71	1	29	8		
14-3-3 protein beta/alpha	YWHAB	P31946	28	1	7	7	9	46
Cytoplasmic dynein 1 heavy chain 1	DYNC1H1	Q14204	532	1	54			
Structural maintenance of chromosomes flexible hinge domain-containing protein 1	SMCHD1	A6NHR9	226	1	37			
Profilin-1	PFN1	P07737	15	3	33		14	36
Sarcoplasmic/endoplasmic reticulum calcium ATPase 2	ATP2A2	P16615	115	1	33			
WD repeat-containing protein 36	WDR36	Q8NI36	105	1	25			
Threonyl-tRNA synthetase, cytoplasmic	TARS	P26639	83	1	25		14	35
Putative ATP-dependent RNA helicase DHX30	DHX30	Q7L2E3	134	1	18			
Tyrosine-protein kinase BAZ1B	BAZ1B	Q9UIG0	171	2	24			
Plastin-3	PLS3	P13797	71	1	23			
GMP synthase [glutamine-hydrolyzing]	GMPS	P49915	77	1	19		3	16
Dolichyl-diphosphooligosaccharide--protein glycosyltransferase subunit 1	RPN1	P04843	69	2	22			
Pre-mRNA 3'-end-processing factor FIP1	FIP1L1	Q6UN15	67	1	22			
NADH-ubiquinone oxidoreductase 75 kDa subunit, mitochondrial	NDUFS1	P28331	79	1	19		10	40
Bifunctional purine biosynthesis protein PURH	ATIC	P31939	65	1	19		11	30
Myosin-10	MYH10	P35580	229	1	17			

Table S3.2. - Continued

Protein Description	Gene Name	Accession	MW (kDa)	LTQ-Orbitrap XL			LTQ-Orbitrap Velos	
				GFP (spectrum counts)	Tbx20-GFP (spectrum counts)	Tbx20-GFP (spectrum counts)	GFP (spectrum counts)	Tbx20-GFP (spectrum counts)
Rab GDP dissociation inhibitor beta	GDI2	P50395	51	1	15		11	37
6-phosphogluconate dehydrogenase, decarboxylating	PGD	P52209	53	1	16		7	31
Multifunctional protein ADE2	PAICS	P22234	47	1	17		4	35
Trifunctional enzyme subunit beta, mitochondrial	HADHB	P55084	51	1	14		5	29
Putative helicase MOV-10	MOV10	Q9HCE1	114	1	16			
Translational activator GCN1	GCN1L1	Q92616	293	2	8			
Coatomer subunit alpha	COPA	P53621	138	1	12			
60S ribosomal protein L15	RPL15	P61313	24	1	14		7	20
Talin-1	TLN1	Q9Y490	270	1	16			
Alanyl-tRNA synthetase, cytoplasmic	AARS	P49588	107	2	10		12	60
Phenylalanyl-tRNA synthetase beta chain	FARSB	Q9NSD9	66	1	9		3	20
NAD-dependent malic enzyme, mitochondrial	ME2	P23368	65	1	11		5	14
Phosphoserine aminotransferase	PSAT1	Q9Y617	40	1	13		5	24
Dolichyl-diphosphooligosaccharide--protein glycosyltransferase 48 kDa subunit	DDOST	P39656	51	1	10			
Glutaminyl-tRNA synthetase	QARS	P47897	88	1	12			
Eukaryotic translation initiation factor 3 subunit D	EIF3D	O15371	64	1	10			
Coatomer subunit gamma-2	COPG2	Q9UBF2	98	1	14			
Glycogen phosphorylase, liver form	PYGL	P06737	97	1	14		5	17
Protein KRI1 homolog	KRI1	Q8N9T8	83	1	11		2	15
Annexin A5	ANXA5	P08758	36	1	11		4	24
4-trimethylaminobutyraldehyde dehydrogenase	ALDH9A1	P49189	54	1	7		2	17
Asparagine synthetase [glutamine-hydrolyzing]	ASNS	P08243	64	1	12			
Carbonyl reductase [NADPH] 1	CBR1	P16152	30	1	13		3	10
Calcium homeostasis endoplasmic reticulum protein	CHERP	Q8IWX8	104	1	9			
60S ribosomal protein L13a	RPL13A	P40429	24	2	11		7	17
Dynamin-2	DNM2	P50570	98	1	10			
Lactotransferrin	LTF	P02788	78	1	13			
Voltage-dependent anion-selective channel protein 3	VDAC3	Q9Y277	31	1	8		3	24
Probable E3 ubiquitin-protein ligase TRIP12	TRIP12	Q14669	220	1	10			
Protein disulfide-isomerase	P4HB	P07237	57	1	9		14	48
Lon protease homolog, mitochondrial	LONP1	P36776	106	1	10		10	58
Obg-like ATPase 1	OLA1	Q9NTK5	45	1	10		2	14
AP-1 complex subunit beta-1	AP1B1	Q10567	105	1	10			
Glutathione reductase, mitochondrial	GSR	P00390	56	1	11		1	15
3-ketoacyl-CoA thiolase, mitochondrial	ACAA2	P42765	42	1	12		5	22
Probable ATP-dependent RNA helicase DDX10	DDX10	Q13206	101	1	9			
ATPase family AAA domain-containing protein 3C	ATAD3C	Q5T2N8	46	1	8			
Coatomer subunit beta'	COPB2	P35606	102	1	10			
Tricarboxylate transport protein, mitochondrial	SLC25A1	P53007	34	1	9		2	13
Vinculin	VCL	P18206	124	1	8		7	21
Interferon-induced, double-stranded RNA-activated protein kinase	EIF2AK2	P19525	62	1	11			
Phosphatidylethanolamine-binding protein 1	PEBP1	P30086	21	1	12		2	19
Programmed cell death 6-interacting protein	PDCD6IP	Q8WUM4	96	1	8			
Isoleucyl-tRNA synthetase, mitochondrial	IARS2	Q9NSE4	114	1	8		6	20
Ribose-phosphate pyrophosphokinase 1	PRPS1	P60891	35	1	7		1	13
Protein disulfide-isomerase A6	PDIA6	Q15084	48	1	7		16	55
Serpin H1	SERPINH1	P50454	46	1	8		11	30
Heat shock protein 105 kDa	HSPH1	Q92598	97	1	21			
Hypoxanthine-guanine phosphoribosyltransferase	HPRT1	P00492	25	1	9		2	24
Annexin A6	ANXA6	P08133	76	1	9		5	18
Probable ubiquitin carboxyl-terminal hydrolase FAF-X	USP9X	Q93008	290	1	9			
Mitochondrial carrier homolog 2	MTCH2	Q9Y6C9	33	1	6		2	9
S-adenosylmethionine synthase isoform type-2	MAT2A	P31153	44	1	6		1	15
Actin-related protein 2	ACTR2	P61160	45	1	9		4	13
Glucose-6-phosphate 1-dehydrogenase	G6PD	P11413	59	1	9		6	17
Very long-chain specific acyl-CoA dehydrogenase, mitochondrial	ACADVL	P49748	70	1	8			
Serine/threonine-protein kinase PRP4 homolog	PRPF4B	Q13523	117	1	8		6	15
Pyruvate dehydrogenase E1 component subunit alpha, somatic form, mitochondrial	PDHA1	P08559	43	1	8		3	19
Interferon-induced protein with tetratricopeptide repeats 3	IFIT3	O14879	56	1	8			
Calpain-1 catalytic subunit	CAPN1	P07384	82	1	6			
Dihydropyrimidinase-related protein 2	DPYSL2	Q16555	62	1	9			
Ig alpha-1 chain C region	IGHA1	P01876	38	1	10			
Cytochrome b-c1 complex subunit 1, mitochondrial	UQCRC1	P31930	53	1	6		2	17
ATP-dependent RNA helicase DHX8	DHX8	Q14562	139	1	6			
Tubulin--tyrosine ligase-like protein 12	TTLL12	Q14166	74	1	7		4	13

Table S3.2. - Continued

Protein Description	Gene Name	Accession	MW (kDa)	LTQ-Orbitrap XL			LTQ-Orbitrap Velos	
				GFP (spectrum counts)	Tbx20-GFP (spectrum counts)	Tbx20-GFP (spectrum counts)	GFP (spectrum counts)	Tbx20-GFP (spectrum counts)
Serine/threonine-protein phosphatase 1 regulatory subunit 10	PPP1R10	Q96QC0	99	1	6		0	12
Monofunctional C1-tetrahydrofolate synthase, mitochondrial	MTHFD1L	Q6UB35	106	1	6		6	14
Cytoskeleton-associated protein 5	CKAP5	Q14008	226	1	7			
Alpha-centractin	ACTR1A	P61163	43	1	9		3	11
Eukaryotic translation initiation factor 2 subunit 1	EIF2S1	P05198	36	1	6		1	15
Ubiquitin thioesterase OTUB1	OTUB1	Q96FW1	31	1	6		2	15
WD repeat-containing protein 46	WDR46	O15213	68	1	6			
Ubiquitin-like protein ISG15	ISG15	P05161	18	1	6			
Isochorismatase domain-containing protein 1	ISOC1	Q96CN7	32	1	6		1	8
Peroxiredoxin-6	PRDX6	P30041	25	1	7			
TRM1-like protein	TRM1L	Q7Z2T5	82	1	7			
Intron-binding protein aquarius	AQR	O60306	171	1	8			
WD repeat-containing protein 1	WDR1	O75083	66	1	8			
Methylmalonyl-CoA mutase, mitochondrial	MUT	P22033	83	1	7		3	12
Tryptophanyl-tRNA synthetase, cytoplasmic	WARS	P23381	53	1	8		3	25
BTB/POZ domain-containing protein KCTD12	KCTD12	Q96CX2	36	1	7		0	13
Galectin-3-binding protein	LGALS3BP	Q08380	65	1	7		1	17
14-3-3 protein gamma	YWHAG	P61981	28	1	9		5	35
ERO1-like protein alpha	ERO1L	Q96HE7	54	1	6		1	5
Alcohol dehydrogenase [NADP+]	AKR1A1	P14550	37	1	6		1	12
Transcription elongation factor B polypeptide 3	TCEB3	Q14241	90	1	7			
Glyoxalase domain-containing protein 4	GLOD4	Q9HC38	35	1	7		1	10
Interferon-induced protein with tetratricopeptide repeats 1	IFIT1	P09914	55	1	7			
Keratin, type II cytoskeletal 78	KRT78	Q8N1N4	57	1	7			
Rab GDP dissociation inhibitor alpha	GDI1	P31150	51	1	9		5	32
NADH dehydrogenase [ubiquinone] 1 alpha subcomplex subunit 9, mitochondrial	NDUFA9	Q16795	43	1	6		1	9
Phosphoglucomutase-1	PGM1	P36871	61	1	6		2	8
Isocitrate dehydrogenase [NAD] subunit alpha, mitochondrial	IDH3A	P50213	40	1	6		3	18
Septin-9	SEPT9	Q9UHD8	65	1	6			
AFG3-like protein 2	AFG3L2	Q9Y4W6	89	1	6			
Vimentin	VIM	P08670	54	59	158			
Putative RNA-binding protein Luc7-like 2	LUC7L2	Q9Y383	47	6	15		1	23
60S ribosomal protein L31	RPL31	P62899	14	3	8		2	9
60S ribosomal protein L27a	RPL27A	P46776	17	3	8		2	5
UPF0027 protein C22orf28	C22orf28	Q9Y310	55	1		8	7	27
Ig alpha-1 chain V-IV region Len		P01625	13	1		6		
Dihydrolipoyllysine-residue acetyltransferase component of pyruvate dehydrogenase complex, mitochondrial	DLAT	P10515	69	1		6	4	20
Rho GDP-dissociation inhibitor 1	ARHGDIA	P52565	23	1		8	4	17
Electron transfer flavoprotein subunit beta	ETFB	P38117	28	1		7	0	21
Aspartyl-tRNA synthetase, cytoplasmic	DARS	P14868	57				10	34
Thioredoxin-dependent peroxide reductase, mitochondrial	PRDX3	P30048	28				4	20
Peptidyl-prolyl cis-trans isomerase B	PPIB	P23284	24				8	21
Glutathione S-transferase P	GSTP1	P09211	23				3	25
Tubulin beta-2A chain	TUBB2A	Q13885	50				84	238
60S ribosomal protein L10a	RPL10A	P62906	25				4	22
60S ribosomal protein L10	RPL10	P27635	25				5	23
Fumarate hydratase, mitochondrial	FH	P07954	55				0	28
NAD(P) transhydrogenase, mitochondrial	NNT	Q13423	114				6	23
Pyruvate dehydrogenase E1 component subunit beta, mitochondrial	PDHB	P11177	39				3	24
60S ribosomal protein L19	RPL19	P84098	23				5	20
60S ribosomal protein L21	RPL21	P46778	19				4	18
3-hydroxyacyl-CoA dehydrogenase type-2	HSD17B10	Q99714	27				3	23
Kinesin-1 heavy chain	KIF5B	P33176	110				7	20
Ras-related protein Rab-5C	RAB5C	P51148	23				3	15
Glutathione S-transferase omega-1	GSTO1	P78417	28				1	20
Eukaryotic peptide chain release factor subunit 1	ETF1	P62495	49				1	20
60S ribosomal protein L12	RPL12	P30050	18				4	11
Succinyl-CoA:3-ketoacid-coenzyme A transferase 1, mitochondrial	OXCT1	P55809	56				2	24
Protein transport protein Sec23A	SEC23A	Q15436	86				7	18
Enoyl-CoA hydratase, mitochondrial	ECHS1	P30084	31				1	20
Peroxiredoxin-4	PRDX4	Q13162	31				7	24
Sideroflexin-1	SFXN1	Q9H9B4	36				1	17
Fructose-bisphosphate aldolase C	ALDOC	P09972	39				3	21
60S ribosomal protein L24	RPL24	P83731	18				3	11
Cytochrome c oxidase subunit 2	MT-CO2	P00403	26				2	15
NADH-cytochrome b5 reductase 3	CYB5R3	P00387	34				4	15
WD repeat-containing protein 18	WDR18	Q9BV38	47				1	22
60S ribosomal protein L18a	RPL18A	Q02543	21				3	9
Guanine nucleotide-binding protein G(I)/G(S)/G(T) subunit beta-1	GNB1	P62873	37				2	16
NADPH:adrenodoxin oxidoreductase, mitochondrial	FDXR	P22570	54				0	18
Inorganic pyrophosphatase 2, mitochondrial	PPA2	Q9H2U2	38				1	13
Tubulin beta-6 chain	TUBB6	Q9BUF5	50				42	133
Lactoylglutathione lyase	GLO1	Q04760	21				2	12

Table S3.2. - Continued

Protein Description	Gene Name	Accession	MW (kDa)	LTQ-Orbitrap XL			LTQ-Orbitrap Velos	
				GFP (spectrum counts)	Tbx20-GFP (spectrum counts)	Tbx20-GFP (spectrum counts)	GFP (spectrum counts)	Tbx20-GFP (spectrum counts)
Hsc70-interacting protein	ST13	P50502	41				2	12
Isocitrate dehydrogenase [NADP] cytoplasmic	IDH1	O75874	47				2	13
F-actin-capping protein subunit beta	CAPZB	P47756	31				2	14
Probable alanyl-tRNA synthetase, mitochondrial	AARS2	Q5JTZ9	107				2	14
Cytochrome c1, heme protein, mitochondrial	CYC1	P08574	35				1	13
Copine-3	CPNE3	O75131	60				3	12
Neutral amino acid transporter B(0)	SLC1A5	Q15758	57				4	15
Spermidine synthase	SRM	P19623	34				1	15
Isocitrate dehydrogenase [NAD] subunit beta, mitochondrial	IDH3B	O43837	42				1	15
60S ribosomal protein L22	RPL22	P35268	15				4	10
Protein-L-isoaspartate(D-aspartate) O-methyltransferase	PCMT1	P22061	25				3	12
Ribonuclease inhibitor	RNH1	P13489	50				2	14
Adenylate kinase 2, mitochondrial	AK2	P54819	26				0	11
Eukaryotic translation initiation factor 3 subunit F	EIF3F	O00303	38				4	11
Serpin B6	SERPINB6	P35237	43				3	9
Serine/threonine-protein phosphatase PGAM5, mitochondrial	PGAM5	Q96HS1	32				2	10
Vesicle-associated membrane protein-associated protein A	VAPA	Q9P0L0	28				2	11
40S ribosomal protein S23	RPS23	P62266	16				3	10
Adenylosuccinate lyase	ADSL	P30566	55				2	9
Phenylalanyl-tRNA synthetase alpha chain	FARSA	Q9Y285	58				1	7
Medium-chain specific acyl-CoA dehydrogenase, mitochondrial	ACADM	P11310	47				1	11
Biliverdin reductase A	BLVRA	P53004	33				1	10
NADH dehydrogenase [ubiquinone] iron-sulfur protein 3, mitochondrial	NDUFS3	O75489	30				1	10
Eukaryotic translation initiation factor 3 subunit I	EIF3I	Q13347	37				3	11
Echinoderm microtubule-associated protein-like 4	EML4	Q9HC35	109				4	9
DnaJ homolog subfamily B member 11	DNAJB11	Q9UBS4	41				3	12
Seryl-tRNA synthetase, cytoplasmic	SARS	P49591	59				1	9
ATP synthase subunit O, mitochondrial	ATP5O	P48047	23				2	6
Polyribonucleotide nucleotidyltransferase 1, mitochondrial	PNPT1	Q8TCS8	86				3	8
NADH dehydrogenase [ubiquinone] iron-sulfur protein 2, mitochondrial	NDUFS2	O75306	53				2	12
Cytosolic acyl coenzyme A thioester hydrolase	ACOT7	O00154	42				2	11
Elongation factor 1-delta	EEF1D	P29692	31				1	8
14-3-3 protein eta	YWHAH	Q04917	28				3	27
Leucine-rich repeat-containing protein 47	LRRC47	Q8N1G4	63				3	10
Mitochondrial import receptor subunit TOM40 homolog	TOMM40	O96008	38				2	7
Microtubule-associated protein 4	MAP4	P27816	121				2	5
Nicotinamide phosphoribosyltransferase	NAMPT	P43490	56				2	10
Phosphoenolpyruvate carboxykinase [GTP], mitochondrial	PCK2	Q16822	71				2	10
Coronin-1C	CORO1C	Q9ULV4	53				3	7
Aspartate aminotransferase, cytoplasmic	GOT1	P17174	46				1	10
Adenylyl cyclase-associated protein 1	CAP1	Q01518	52				2	14
Mitochondrial import inner membrane translocase subunit TIM44	TIMM44	O43615	51				1	9
39S ribosomal protein L38, mitochondrial	MRPL38	Q96DV4	45				2	7
ATP synthase subunit b, mitochondrial	ATP5F1	P24539	29				2	6
Vacuolar protein sorting-associated protein 26A	VPS26A	O75436	38				1	8
Catalase	CAT	P04040	60				1	6
Multiple myeloma tumor-associated protein 2	MMTAG2	Q9BU76	29				3	10
ADP-sugar pyrophosphatase	NUDT5	Q9UKK9	24				1	8
Apolipoprotein A-I-binding protein	APOA1BP	Q8NCW5	32				1	10
Calcyclin-binding protein	CACYBP	Q9HB71	26				2	10
Mitochondrial-processing peptidase subunit alpha	PMPCA	Q10713	58				2	8
60S ribosomal protein L28	RPL28	P46779	16				1	5
Transforming protein RhoA	RHOA	P61586	22				1	6
Sterol-4-alpha-carboxylate 3-dehydrogenase, decarboxylating	NSDHL	Q15738	42				2	9
Histidyl-tRNA synthetase, cytoplasmic	HARS	P12081	57				2	6
Ras-related protein Rap-1b	RAP1B	P61224	21				2	5
V-type proton ATPase subunit B, brain isoform	ATP6V1B2	P21281	57				2	8
Cathepsin D	CTSD	P07339	45				2	6
Leucine-rich repeat-containing protein 59	LRRC59	Q96AG4	35				1	12
Eukaryotic translation initiation factor 3 subunit H	EIF3H	O15372	40				2	9
Isocitrate dehydrogenase [NADP], mitochondrial	IDH2	P48735	51				1	10
28S ribosomal protein S22, mitochondrial	MRPS22	P82650	41				1	8
UPF0465 protein C5orf33	C5orf33	Q4G0N4	49				0	10
Pyrroline-5-carboxylate reductase 1, mitochondrial	PYCR1	P32322	33				0	8

Table S3.2. - Continued

Protein Description	Gene Name	Accession	MW (kDa)	LTQ-Orbitrap XL			LTQ-Orbitrap Velos	
				GFP (spectrum counts)	Tbx20-GFP (spectrum counts)	Tbx20-GFP (spectrum counts)	GFP (spectrum counts)	Tbx20-GFP (spectrum counts)
39S ribosomal protein L37, mitochondrial	MRPL37	Q9BZE1	48				0	12
3,2-trans-enoyl-CoA isomerase, mitochondrial	DCI	P42126	33				0	9
Trans-2,3-enoyl-CoA reductase	TECR	Q9NZ01	36				2	5
Kinesin-like protein KIF2A	KIF2A	O00139	80				2	6
Thyroid receptor-interacting protein 13	TRIP13	Q15645	49				2	8
Abhydrolase domain-containing protein 10, mitochondrial	ABHD10	Q9NUJ1	34				0	8
Putative ATP-dependent Clp protease proteolytic subunit, mitochondrial	CLPP	Q16740	30				0	11
Dedicator of cytokinesis protein 7	DOCK7	Q96N67	243				2	6
60S ribosomal protein L37a	RPL37A	P61513	10				2	6
Estradiol 17-beta-dehydrogenase 12	HSD17B12	Q53GQ0	34				1	7
NADH dehydrogenase [ubiquinone] flavoprotein 1, mitochondrial	NDUFV1	P49821	51				2	8
Succinate-semialdehyde dehydrogenase, mitochondrial	ALDH5A1	P51649	57				1	9
60S ribosomal protein L35a	RPL35A	P18077	13				2	6
Tubulin-specific chaperone D	TBCD	Q9BTW9	133				1	6
N-alpha-acetyltransferase 25, NatB auxiliary subunit	NAA25	Q14CX7	112				1	11
Fatty aldehyde dehydrogenase	ALDH3A2	P51648	55				2	7
Succinyl-CoA ligase [GDP-forming] subunit beta, mitochondrial	SUCLG2	Q96I99	47				1	7
Glutaredoxin-3	GLRX3	O76003	37				1	7
Succinyl-CoA ligase [GDP-forming] subunit alpha, mitochondrial	SUCLG1	P53597	36				0	8
Elongation factor 1-beta	EEF1B2	P24534	25				0	9
Mitochondrial-processing peptidase subunit beta	PMPCB	O75439	54				2	5
Elongation factor G, mitochondrial	GFM1	Q96RP9	83				1	10
Thioredoxin-like protein 1	TXNL1	O43396	32				1	6
Methylcrotonoyl-CoA carboxylase beta chain, mitochondrial	MCCC2	Q9HCC0	61				1	9
Amidophosphoribosyltransferase	PPAT	Q06203	57				1	7
AP-1 complex subunit gamma-1	AP1G1	O43747	91				2	5
Carbonic anhydrase 2	CA2	P00918	29				1	8
Aflatoxin B1 aldehyde reductase member 2	AKR7A2	O43488	40				1	6
Short/branched chain specific acyl-CoA dehydrogenase, mitochondrial	ACADSB	P45954	47				0	9
Endoplasmic reticulum resident protein 44	ERP44	Q9BS26	47				2	8
ATP synthase subunit f, mitochondrial	ATP5J2	P56134	11				2	5
Glyoxylate reductase/hydroxypyruvate reductase	GRHPR	Q9UBQ7	36				2	5
Xaa-Pro dipeptidase	PEPD	P12955	55				2	6
Serine/threonine-protein phosphatase 2A 55 kDa regulatory subunit B alpha isoform	PPP2R2A	P63151	52				1	5
Sec1 family domain-containing protein 1	SCFD1	Q8WVM8	72				2	6
Succinate dehydrogenase [ubiquinone] iron-sulfur subunit, mitochondrial	SDHB	P21912	32				1	10
Creatine kinase U-type, mitochondrial	CKMT1A	P12532	47				1	10
Cat eye syndrome critical region protein 5	CECR5	Q9BXW7	46				0	7
Ferrochelatase, mitochondrial	FECH	P22830	48				0	8
39S ribosomal protein L15, mitochondrial	MRPL15	Q9P015	33				0	6
Kynurenine--oxoglutarate transaminase 3	CCBL2	Q6YP21	51				0	8
Ras-related protein Rab-35	RAB35	Q15286	23				0	5
28S ribosomal protein S27, mitochondrial	MRPS27	Q92552	48				2	5
Zinc finger CCHC domain-containing protein 8	ZCCHC8	Q6NZY4	79				2	5
Erlin-2	ERLIN2	O94905	38				2	5
2-oxoglutarate dehydrogenase, mitochondrial	OGDH	Q02218	116				1	8
DnaJ homolog subfamily C member 9	DNAJC9	Q8WXX5	30				1	8
Eukaryotic translation initiation factor 2 subunit 2	EIF2S2	P20042	38				1	6
3-hydroxyisobutyryl-CoA hydrolase, mitochondrial	HIBCH	Q6NVY1	43				1	8
Endoplasmic reticulum resident protein 29	ERP29	P30040	29				0	5
Galactokinase	GALK1	P51570	42				0	8
Pyrroline-5-carboxylate reductase 2	PYCR2	Q96C36	34				0	5
39S ribosomal protein L4, mitochondrial	MRPL4	Q9BYD3	35				2	7
Platelet-activating factor acetylhydrolase IB subunit beta	PAFAH1B2	P68402	26				1	8
Zinc finger MYM-type protein 4	ZMYM4	Q5VZL5	173				2	5
Ribosomal RNA-processing protein 7 homolog A	RRP7A	Q9Y3A4	32				1	6
NEDD8-activating enzyme E1 regulatory subunit	NAE1	Q13564	60				1	6
Complement C4-A	C4A	P0C0L4	193				1	5
CDK5 regulatory subunit-associated protein 3	CDK5RAP3	Q96JB5	57				1	7
28S ribosomal protein S7, mitochondrial	MRPS7	Q9Y2R9	28				0	5
Coproporphyrinogen-III oxidase, mitochondrial	CPOX	P36551	50				0	7
3-hydroxyisobutyrate dehydrogenase, mitochondrial	HIBADH	P31937	35				0	9
Reticulocalbin-1	RCN1	Q15293	39				0	5
Protein NipSnap homolog 1	NIPSNAP1	Q9BPW8	33				1	6
Thioredoxin domain-containing protein 5	TXNDC5	Q8NBS9	48				1	6
28S ribosomal protein S34, mitochondrial	MRPS34	P82930	26				1	5
Protein FAM98B	FAM98B	Q52LJ0	37				1	5
Glucosidase 2 subunit beta	PRKCSH	P14314	59				1	7
Protein phosphatase methylesterase 1	PPME1	Q9Y570	42				1	5
Basigin	BSG	P35613	42				0	5

Table S3.2. - Continued

Protein Description	Gene Name	Accession	MW (kDa)	LTQ-Orbitrap XL			LTQ-Orbitrap Velos	
				GFP (spectrum counts)	Tbx20-GFP (spectrum counts)	Tbx20-GFP (spectrum counts)	GFP (spectrum counts)	Tbx20-GFP (spectrum counts)
Pre-B-cell leukemia transcription factor 2	PBX2	P40425	46				0	5
Isovaleryl-CoA dehydrogenase, mitochondrial	IVD	P26440	46				0	6
Phosphoglucomutase-2	PGM2	Q96G03	68				1	7
60S ribosomal protein L29	RPL29	P47914	18				1	8
Phosphoribosyl pyrophosphate synthase-associated protein 2	PRPSAP2	O60256	41				1	6
28S ribosomal protein S9, mitochondrial	MRPS9	P82933	46				1	7
Platelet-activating factor acetylhydrolase IB subunit gamma	PAFAH1B3	Q15102	26				1	6
Serine/threonine-protein kinase MST4	MST4	Q9P289	47				1	5
NADH dehydrogenase [ubiquinone] 1 alpha subcomplex subunit 10, mitochondrial	NDUFA10	O95299	41				1	8
Eukaryotic translation initiation factor 3 subunit M	EIF3M	Q7L2H7	43				0	6
Tubulin beta-4 chain	TUBB4	P04350	50				94	235
2',3'-cyclic-nucleotide 3'-phosphodiesterase	CNP	P09543	48				1	5
Cytoplasmic dynein 1 light intermediate chain 1	DYNC1LI1	Q9Y6G9	57				1	5
ADP/ATP translocase 1	SLC25A4	P12235	33				4	38
Calcium-binding mitochondrial carrier protein Aralar1	SLC25A12	O75746	75				2	11
Glycerol kinase	GK	P32189	61				1	6
Alcohol dehydrogenase class-3	ADH5	P11766	40				0	6
Signal recognition particle receptor subunit beta	SRPRB	Q9Y5M8	30				0	6
Protein NipSnap homolog 2	GBAS	O75323	34				0	5
Protein FAM49B	FAM49B	Q9NUQ9	37				0	7
V-set and immunoglobulin domain-containing protein 8	VSIG8	Q5VU13	44				1	8
Branched-chain-amino-acid aminotransferase, mitochondrial	BCAT2	O15382	44				0	7
Monocarboxylate transporter 1	SLC16A1	P53985	54				1	5
GTP:AMP phosphotransferase, mitochondrial	AK3	Q9UIJ7	26				1	5
39S ribosomal protein L39, mitochondrial	MRPL39	Q9NYK5	39				1	5
39S ribosomal protein L9, mitochondrial	MRPL9	Q9BYD2	30				0	5
PDZ and LIM domain protein 1	PDLIM1	O00151	36				0	5
tRNA pseudouridine synthase A, mitochondrial	PUS1	Q9Y606	47				0	5
L-aminoadipate-semialdehyde dehydrogenase-phosphopantetheinyl transferase	AASDHPPT	Q9NRN7	36				0	5
Glutathione synthetase	GSS	P48637	52				0	5
Exocyst complex component 4	EXOC4	Q96A65	111				1	6
Ras-related protein Rab-5B	RAB5B	P61020	24				1	8
Phosphoribosyl pyrophosphate synthase-associated protein 1	PRPSAP1	Q14558	39				0	5
39S ribosomal protein L45, mitochondrial	MRPL45	Q9BRJ2	35				0	5
Calpain small subunit 1	CAPNS1	P04632	28				1	5
28S ribosomal protein S18b, mitochondrial	MRPS18B	Q9Y676	29				0	5
Selenide, water dikinase 1	SEPHS1	P49903	43				0	5
Sorting nexin-2	SNX2	O60749	58				0	6
Hsp90 co-chaperone Cdc37	CDC37	Q16543	44				0	6
39S ribosomal protein L44, mitochondrial	MRPL44	Q9H9J2	38				0	5
N(G),N(G)-dimethylarginine dimethylaminohydrolase 1	DDAH1	O94760	31				0	5
28S ribosomal protein S31, mitochondrial	MRPS31	Q92665	45				0	5
Pyridoxal phosphate phosphatase	PDXP	Q96GD0	32				0	5
Sorbitol dehydrogenase	SORD	Q00796	38				0	5
Complement C3	C3	P01024	187				0	9
Omega-amidase NIT2	NIT2	Q9NQR4	31				0	5
28S ribosomal protein S35, mitochondrial	MRPS35	P82673	37				0	6
Cell division protein kinase 5	CDK5	Q00535	33				0	9
Vesicle-associated membrane protein-associated protein B/C	VAPB	O95292	27				0	6
Spermatogenesis-associated protein 5	SPATA5	Q8NB90	98				2	5
Histone H1t	HIST1H1T	P22492	22				3	11

Table S3.3. GO analysis of nuclear-enriched interactions by biological functions.

	Functional Group				
	RNA processing	nuclear transport	nucleosome assembly	nuclear-transcribed mRNA catabolic process, nonsense-mediated decay	DNA repair
Gene Name	ADAR	CALR	H1FX	EIF4A3	DDB1
	BOP1	DDX39B	H2AFY	HSPA4	DKC1
	DDX23	EIF4A3	H2AFY2	RPL3	MSH6
	DDX39B	KHDRBS1	HDAC2	RPL4	NONO
	DDX47	LRPPRC	HIST1H1C	RPL5	NPM1
	DDX54	RAN	HIST1H1E	RPLP0	PCNA
	DHX15	RPSA	HP1BP3	RPS3	PRKDC
	DKC1	SRSF1	NPM1	RPS3A	RECQL
	EIF4A3	THOC2	RBBP4	RPSA	RPS3
	ELAVL1	U2AF2	RBBP7	TARDBP	RUVBL1
	FBL		RECQL		RUVBL2
	FTSJ3		RUVBL1		SFPQ
	HNRNPA0		RUVBL2		SMC3
	HNRNPA2B1				TRIM28
	HNRNPA3				XRCC5
	HNRNPF				XRCC6
	HNRNPK				
	HNRNPL				
	HNRNPR				
	KHDRBS1				
	KIAA1967				
	NOLC1				
	NONO				
	NOP2				
	NOP56				
	NOP58				
	PA2G4				
	PCBP2				
	PRMT5				
	PRPF6				
	PSMA1				
	PTBP1				
	RALY				
	RARS				
	RBMX				
	RPL3				
	RPL4				
	RPL5				
	RPLP0				
	RPS3				
	RPS3A				
	RPSA				
	RRP1B				
	SART1				
	SFPQ				
	SKIV2L2				
	SRRT				
	SRSF1				
	SYNCRIP				
	TARDBP				
	THOC2				
	TNPO1				
	U2AF2				

Table S3.4. Enrichment analysis of nuclear-enriched Tbx20 associations.

Protein Description	Gene	UniProt Accession	Length	Tbx20-GFP 1	Tbx20-GFP 2	Tbx20-GFP 3	Tbx20-GFP 1	Tbx20-GFP 2	Tbx20-GFP 3	Avg Spectrum Counts	NSpC	NSAF	PAX, ppm	NSAF-PAX	nNASF-PAX	log2nNASF-PAX
T-box transcription factor TBX20	TBX20	Q9ES03	445	556	284	1280	707	707	707	707						
Transducin-like enhancer protein 1	TLE1	Q04724	770	11	5	36	14	20	12	15	0.020	0.002	0.2	8390.9	1556.7	10.6
Probable ATP-dependent RNA helicase DDX27	DDX27	Q96GQ7	796	27	30	6	34	3	75	37	0.047	0.004	0.7	5288.3	981.1	9.9
Putative ribosomal RNA methyltransferase NOP2	NOP2	P46087	812	60	53	25	76	14	132	74	0.091	0.007	3.3	2074.3	384.8	8.6
Small ubiquitin-related modifier 2	SUMO2	P61956	95	24	17	8	31	4	42	26	0.271	0.020	11.1	1839.5	341.3	8.4
Myb-binding protein 1A	MYBBP1A	Q9BQG0	1328	149	157	52	189	29	391	203	0.153	0.012	10.6	1086.3	201.5	7.7
Heterogeneous nuclear ribonucleoprotein G	RBMX	P38159	391	36	72	35	46	19	179	81	0.208	0.016	15.8	993.1	184.2	7.5
Transducin-like enhancer protein 3	TLE3	Q04726	772	16	10	60	20	33	25	26	0.034	0.003	2.7	930.4	172.6	7.4
NF-kappa-B-repressing factor	NKRF	O15226	690	22	18	6	28	3	45	25	0.037	0.003	3.3	834.1	154.7	7.3
Probable ATP-dependent RNA helicase DDX47	DDX47	Q9H0S4	455	6	14	6	8	3	35	15	0.034	0.003	3.3	772.8	143.4	7.2
Spliceosome RNA helicase BAT1	BAT1	Q13838	428	74	93	35	94	19	231	115	0.269	0.020	28.8	702.6	130.4	7.0
Nucleolar complex protein 3 homolog	NOC3L	Q8WTT2	800	8	23	12	10	7	57	25	0.031	0.002	3.7	624.8	115.9	6.9
Putative rRNA methyltransferase 3	FTSJ3	Q8IY81	847	22	41	18	28	10	102	47	0.055	0.004	6.7	624.0	115.8	6.9
Metastasis-associated protein 1	MTA1	Q13330	715	8	10	2	10	1	25	12	0.017	0.001	2.1	602.0	111.7	6.8
RRP12-like protein	RRP12	Q5JTH9	1297	16	51	7	20	4	127	50	0.039	0.003	6.0	486.9	90.3	6.5
THO complex subunit 2	THOC2	Q8NI27	1593	27	35	6	34	3	87	42	0.026	0.002	4.6	426.6	79.1	6.3
RNA-binding protein Raly	RALY	Q9UKM9	306	16	23	10	20	6	57	28	0.091	0.007	16.7	408.4	75.8	6.2
Double-stranded RNA-specific adenosine deaminase	ADAR	P55265	1226	55	56	21	70	12	139	74	0.060	0.005	11.3	400.4	74.3	6.2
T-box transcription factor TBX18	TBX18	O95935	607	10	5	17	13	9	12	12	0.019	0.001	3.9	362.8	67.3	6.1
Probable ATP-dependent RNA helicase DDX23	DDX23	Q9BUQ8	820	22	18	8	28	4	45	26	0.031	0.002	6.6	356.6	66.1	6.0
Eukaryotic initiation factor 4A-III	EIF4A3	P38919	411	15	68	16	19	9	169	66	0.160	0.012	34.0	354.3	65.7	6.0
U4/U6.U5 tri-snRNP-associated protein 1	SART1	O43290	800	17	27	8	22	4	67	31	0.039	0.003	8.5	345.9	64.2	6.0
Ribosome biogenesis protein BOP1	BOP1	Q14137	746	20	16	8	25	4	40	23	0.031	0.002	6.8	344.9	64.0	6.0
Nucleolar protein 56	NOP56	O00567	594	73	73	57	93	31	182	102	0.172	0.013	40.9	316.3	58.7	5.9
CCAAT/enhancer-binding protein zeta	CEBPZ	Q03701	1054	14	31	8	18	4	77	33	0.031	0.002	7.9	299.7	55.6	5.8
Pre-mRNA-processing factor 6	PRPF6	O94906	941	16	29	11	20	6	72	33	0.035	0.003	8.9	297.3	55.2	5.8
Apoptosis-inducing factor 1, mitochondrial	AIFM1	O95831	613	31	47	12	39	7	117	54	0.089	0.007	22.8	292.9	54.3	5.8
Nucleolar protein 58	NOP58	Q9Y2X3	529	43	64	39	55	22	159	78	0.148	0.011	40.2	278.1	51.6	5.7
DNA mismatch repair protein Msh6	MSH6	P52701	1360	32	39	17	41	9	97	49	0.036	0.003	10.2	266.4	49.4	5.6
Spermatid perinuclear RNA-binding protein	STRBP	Q96SI9	672	34	26	9	43	5	65	38	0.056	0.004	16.3	258.9	48.0	5.6
Putative pre-mRNA-splicing factor ATP-dependent RNA helicase DHX15	DHX15	O43143	795	94	72	31	119	17	179	105	0.132	0.010	42.4	235.3	43.7	5.4
Puromycin-sensitive aminopeptidase	NPEPPS	P55786	919	53	70	17	67	9	174	84	0.091	0.007	32.1	213.7	39.6	5.3
Nucleolar RNA helicase 2	DDX21	Q9NR30	783	147	118	59	187	33	294	171	0.218	0.016	77.4	212.6	39.4	5.3
RuvB-like 2	RUVBL2	Q9Y230	463	12	53	7	15	4	132	50	0.109	0.008	40.4	202.8	37.6	5.2
Heterogeneous nuclear ribonucleoprotein A3	HNRNPA3	P51991	378	52	77	30	66	17	192	91	0.242	0.018	92.6	196.8	36.5	5.2
Superkiller viralicidic activity 2-like 2	SKIV2L2	P42285	1042	23	34	13	29	7	85	40	0.039	0.003	19.1	152.7	28.3	4.8
Protein KIAA1967	KIAA1967	Q8N163	923	29	38	14	37	8	95	46	0.050	0.004	26.3	144.0	26.7	4.7
Interleukin enhancer-binding factor 2	ILF2	Q12905	390	45	69	17	57	9	172	79	0.204	0.015	108.0	142.1	26.4	4.7
Heterogeneous nuclear ribonucleoprotein R	HNRNPR	O43390	633	107	71	61	136	34	177	115	0.182	0.014	97.2	141.4	26.2	4.7
Histone H1x	H1FX	Q92522	213	13	26	10	17	6	65	29	0.136	0.010	73.2	139.7	25.9	4.7
Histone deacetylase 2	HDAC2	Q92769	488	13	10	11	17	6	25	16	0.032	0.002	17.7	138.1	25.6	4.7
Ribosomal L1 domain-containing protein 1	RSL1D1	O76021	490	33	46	30	42	17	114	58	0.118	0.009	65.4	135.6	25.2	4.7
Host cell factor 1	HCFC1	P51610	2035	21	35	8	27	4	87	39	0.019	0.001	11.1	131.4	24.4	4.6
Exportin-2	CSE1L	P55060	971	55	58	16	70	9	144	74	0.077	0.006	46.8	123.3	22.9	4.5
RuvB-like 1	RUVBL1	Q9Y265	456	9	51	8	11	4	127	48	0.104	0.008	64.7	121.5	22.5	4.5
Serrate RNA effector molecule homolog	SRRT	Q9BXP5	876	23	36	11	29	6	90	42	0.048	0.004	29.9	119.8	22.2	4.5
Cullin-associated NEDD8-dissociated protein 1	CAND1	Q86VP6	1230	55	77	18	70	10	192	90	0.074	0.006	46.8	118.5	22.0	4.5
Ribosomal RNA processing protein 1 homolog B	RRP1B	Q14684	758	20	18	7	25	4	45	25	0.033	0.002	21.2	115.8	21.5	4.4
Poly(rC)-binding protein 2	PCBP2	Q15366	365	19	44	19	24	10	109	48	0.132	0.010	87.7	113.1	21.0	4.4
DNA-dependent protein kinase catalytic subunit	PRKDC	P78527	4128	294	335	13	374	7	834	405	0.098	0.007	65.6	112.7	20.9	4.4
Arginyl-tRNA synthetase, cytoplasmic	RARS	P54136	660	28	30	12	36	7	75	39	0.059	0.004	40.4	110.1	20.4	4.4
rRNA 2'-O-methyltransferase fibrillarin	FBL	P22087	321	28	35	23	36	13	87	45	0.141	0.011	97.4	108.8	20.2	4.3
Heterochromatin protein 1-binding protein 3	HP1BP3	Q5SSJ5	553	27	34	15	34	8	85	42	0.077	0.006	58.1	99.4	18.4	4.2
Protein arginine N-methyltransferase 5	PRMT5	O14744	637	15	19	6	19	3	47	23	0.036	0.003	28.0	98.1	18.2	4.2
TAR DNA-binding protein 43	TARDBP	Q13148	414	8	18	9	10	5	45	20	0.048	0.004	37.2	97.7	18.1	4.2
H/ACA ribonucleoprotein complex subunit 4	DKC1	O60832	514	13	21	17	17	9	52	26	0.051	0.004	40.9	93.4	17.3	4.1
ATP-dependent DNA helicase Q1	RECQL	P46063	649	16	15	6	20	3	37	20	0.031	0.002	26.0	90.8	16.8	4.1
Serine/arginine-rich splicing factor 1	SRSF1	Q07955	248	23	47	24	29	13	117	53	0.214	0.016	188.0	85.9	15.9	4.0

Table S3.4. - Continued

Protein Description	Gene	UniProt Accession	Length	Tbx20-GFP 1	Tbx20-GFP 2	Tbx20-GFP 3	Tbx20-GFP 1	Tbx20-GFP 2	Tbx20-GFP 3	Avg Spectrum Counts	NSpC	NSAF	PAX, ppm	NSAF-PAX	nNASF-PAX	log2nNASF-PAX
Nucleolar and coiled-body phosphoprotein 1	NOLC1	Q14978	699	6	9	9	8	5	22	12	0.017	0.001	14.7	85.5	15.9	4.0
Heterogeneous nuclear ribonucleoprotein Q	SYNCRIP	O60506	623	61	53	22	78	12	132	74	0.119	0.009	107.0	83.5	15.5	4.0
Heat shock 70 kDa protein 4	HSPA4	P34932	840	82	71	14	104	8	177	96	0.115	0.009	104.0	83.0	15.4	3.9
Proliferation-associated protein 2G4	PA2G4	Q9UQ80	394	25	73	17	32	9	182	74	0.188	0.014	172.0	82.6	15.3	3.9
Heterogeneous nuclear ribonucleoproteins A2/B1	HNRNPA2B1	P22626	353	93	124	79	118	44	309	157	0.444	0.033	442.0	75.7	14.0	3.8
Transportin-1	TNPO1	Q92973	898	16	21	6	20	3	52	25	0.028	0.002	28.1	75.6	14.0	3.8
Serine/threonine-protein phosphatase PP1-gamma catalytic subunit	PPP1CC	P36873	323	21	21	12	27	7	52	29	0.088	0.007	93.9	70.9	13.1	3.7
ELAV-like protein 1	ELAVL1	Q15717	326	21	34	7	27	4	85	38	0.118	0.009	126.0	70.4	13.1	3.7
Core histone macro-H2A.1	H2AFY	O75367	372	35	47	16	44	9	117	57	0.153	0.011	164.0	70.1	13.0	3.7
Protein RCC2	RCC2	Q9P258	522	29	31	18	37	10	77	41	0.079	0.006	85.4	69.8	13.0	3.7
General transcription factor II-I	GTF2I	P78347	998	31	44	14	39	8	109	52	0.052	0.004	56.7	69.5	12.9	3.7
Heterogeneous nuclear ribonucleoprotein F	HNRNPF	P52597	415	56	66	16	71	9	164	81	0.196	0.015	215.0	68.8	12.8	3.7
Non-POU domain-containing octamer-binding protein	NONO	Q15233	471	70	91	34	89	19	226	111	0.236	0.018	260.0	68.5	12.7	3.7
Septin-2	SEPT2	Q15019	361	11	11	8	14	4	27	15	0.042	0.003	46.5	68.5	12.7	3.7
Nucleolar transcription factor 1	UBTF	P17480	764	18	15	6	23	3	37	21	0.028	0.002	32.1	65.1	12.1	3.6
Leucine-rich PPR motif-containing protein, mitochondrial	LRPPRC	P42704	1394	38	79	22	48	12	197	86	0.061	0.005	73.4	63.1	11.7	3.5
Transcription intermediary factor 1-beta	TRIM28	Q13263	835	95	117	41	121	23	291	145	0.173	0.013	211.0	62.0	11.5	3.5
Heterogeneous nuclear ribonucleoprotein K	HNRNPK	P61978	463	159	124	124	202	68	309	193	0.417	0.031	552.0	56.9	10.6	3.4
Aconitate hydratase, mitochondrial	ACO2	Q99798	780	27	44	8	34	4	109	49	0.063	0.005	86.6	55.1	10.2	3.4
Inosine-5'-monophosphate dehydrogenase 2	IMPDH2	P12268	514	20	52	6	25	3	129	53	0.103	0.008	144.0	53.7	10.0	3.3
Prohibitin	PHB	P35232	272	12	30	10	15	6	75	32	0.117	0.009	176.0	50.1	9.3	3.2
Splicing factor, proline- and glutamine-rich	SFPQ	P23246	707	67	58	29	85	16	144	82	0.116	0.009	181.0	48.2	8.9	3.2
Proteasome subunit alpha type-1	PSMA1	P25786	263	10	13	6	13	3	32	16	0.061	0.005	105.0	44.0	8.2	3.0
T-complex protein 1 subunit delta	CCT4	P50991	539	56	56	33	71	18	139	76	0.141	0.011	249.0	42.8	7.9	3.0
X-ray repair cross-complementing protein 6	XRCC6	P12956	609	101	86	41	128	23	214	122	0.200	0.015	358.0	42.1	7.8	3.0
Heterogeneous nuclear ribonucleoprotein L	HNRNPL	P14866	589	84	90	83	107	46	224	126	0.213	0.016	396.0	40.6	7.5	2.9
Prohibitin-2	PHB2	Q99623	299	20	33	13	25	7	82	38	0.128	0.010	249.0	38.7	7.2	2.8
40S ribosomal protein S3	RPS3	P23396	243	36	30	23	46	13	75	44	0.183	0.014	365.0	37.7	7.0	2.8
40S ribosomal protein S3a	RPS3A	P61247	264	20	30	14	25	8	75	36	0.136	0.010	275.0	37.3	6.9	2.8
Histone H1.4	HIST1H1E	P10412	219	44	46	39	56	22	114	64	0.292	0.022	591.0	37.2	6.9	2.8
60S ribosomal protein L5	RPL5	P46777	297	24	31	12	31	7	77	38	0.128	0.010	263.0	36.7	6.8	2.8
Nucleolin	NCL	P19338	710	112	53	29	142	16	132	97	0.136	0.010	283.0	36.3	6.7	2.8
14-3-3 protein theta	YWHAQ	P27348	245	11	46	10	14	6	114	45	0.182	0.014	379.0	36.2	6.7	2.7
Histone H1.2	HIST1H1C	P16403	213	43	50	40	55	22	124	67	0.315	0.024	666.0	35.6	6.6	2.7
Splicing factor U2AF 65 kDa subunit	U2AF2	P26368	475	24	26	17	31	9	65	35	0.073	0.006	158.0	35.0	6.5	2.7
GTP-binding nuclear protein Ran	RAN	P62826	216	28	37	12	36	7	92	45	0.207	0.016	448.0	34.9	6.5	2.7
T-complex protein 1 subunit beta	CCT2	P78371	535	41	68	28	52	15	169	79	0.148	0.011	324.0	34.3	6.4	2.7
Proliferating cell nuclear antigen	PCNA	P12004	261	19	27	18	24	10	67	34	0.129	0.010	293.0	33.3	6.2	2.6
Transketolase	TKT	P29401	623	92	52	56	117	31	129	92	0.148	0.011	340.0	32.9	6.1	2.6
60S ribosomal protein L3	RPL3	P39023	403	35	54	10	44	6	134	61	0.152	0.011	359.0	32.0	5.9	2.6
60S acidic ribosomal protein P0	RPLP0	P05388	317	30	47	16	38	9	117	55	0.172	0.013	426.0	30.5	5.7	2.5
Malate dehydrogenase, mitochondrial	MDH2	P40926	338	75	115	47	95	26	286	136	0.402	0.030	1023.0	29.6	5.5	2.5
40S ribosomal protein SA	RPSA	P08865	295	24	37	21	31	12	92	45	0.152	0.011	388.0	29.4	5.5	2.4
Histone-binding protein RBBP4	RBBP4	Q09028	425	17	19	9	22	5	47	25	0.058	0.004	155.0	28.2	5.2	2.4
THO complex subunit 4	THOC4	Q86V81	257	16	23	11	20	6	57	28	0.108	0.008	299.0	27.3	5.1	2.3
60S ribosomal protein L4	RPL4	P36578	427	59	87	32	75	18	216	103	0.241	0.018	690.0	26.4	4.9	2.3
T-complex protein 1 subunit epsilon	CCT5	P48643	541	37	39	21	47	12	97	52	0.096	0.007	295.0	24.5	4.5	2.2
Heterogeneous nuclear ribonucleoprotein A0	HNRNPA0	Q13151	305	10	13	7	13	4	32	16	0.053	0.004	171.0	23.6	4.4	2.1
Core histone macro-H2A.2	H2AFY2	Q9P0M6	372	7	24	6	9	3	60	24	0.064	0.005	207.0	23.5	4.4	2.1
Guanine nucleotide-binding protein subunit beta-2-like 1	GNB2L1	P63244	317	40	45	27	51	15	112	59	0.187	0.014	720.0	19.6	3.6	1.9
Polypyrimidine tract-binding protein 1	PTBP1	P26599	531	54	29	37	69	20	72	54	0.101	0.008	399.0	19.1	3.5	1.8
Histone-binding protein RBBP7	RBBP7	Q16576	425	13	14	4	17	2	35	18	0.042	0.003	197.0	16.1	3.0	1.6
KH domain-containing, RNA-binding, signal transduction-associated protein 1	KHDRBS1	Q07666	443	19	17	10	24	6	42	24	0.054	0.004	280.0	14.6	2.7	1.4
Nucleophosmin	NPM1	P06748	294	32	56	32	41	18	139	66	0.224	0.017	1523.0	11.1	2.1	1.0
Complement component 1 Q subcomponent-binding protein, mitochondrial	C1QBP	Q07021	282	16	34	15	20	8	85	38	0.134	0.010	1106.0	9.1	1.7	0.8
Calreticulin	CALR	P27797	417	15	56	8	19	4	139	54	0.130	0.010	1504.0	6.5	1.2	0.3
Glyceraldehyde-3-phosphate dehydrogenase	GAPDH	P04406	335	86	110	82	109	45	274	143	0.426	0.032	5958.0	5.4	1.0	0.0

Table S3.5. Label-free quantitative mass spectrometric analyses of nuclear-enriched Tbx20- and Tbx20^{eh1mut}-associated proteins.

Protein Description	Gene Name	Accession	MW (kDa)	GFP	Tbx20-EGFP	Tbx20eh1mut-EGFP		eh1mut counts/ WT counts
				Spectrum counts	Spectrum counts	Spectrum counts	Normalized spectrum counts	
Transducin-like enhancer protein 1	TLE1	Q04724	83	1	5	0	0	0.0
Transducin-like enhancer protein 3	TLE3	Q04726	83	2	10	0	0	0.0
Serine/arginine-rich splicing factor 1	SRSF1	Q07955	28	10	47	8	12	0.2
T-box transcription factor TBX18	TBX18	O95935	65	0	5	0	0	0.0
Spermatid perinuclear RNA-binding protein	STRBP	Q96SI9	74	10	26	8	12	0.4
Histone-binding protein RBBP4	RBBP4	Q09028	48	3	19	7	10	0.5
Histone deacetylase 2	HDAC2	Q92769	55	4	10	2	3	0.3
Green flourescent protein	GFP	P42212	27	171	264	134	194	0.7
T-box transcription factor TBX20	TBX20	Q9ES03	49	0	284	196	284	1.0
DNA-dependent protein kinase catalytic subunit	PRKDC	P78527	469	92	335	210	304	0.9
Heterogeneous nuclear ribonucleoprotein K	HNRNPK	P61978	51	45	124	73	106	0.9
Nucleolar RNA helicase 2	DDX21	Q9NR30	87	43	118	62	90	0.8
Glyceraldehyde-3-phosphate dehydrogenase	GAPDH	P04406	36	34	110	104	151	1.4
Heterogeneous nuclear ribonucleoproteins A2/B1	HNRNPA2B1	P22626	37	40	124	97	141	1.1
Heterogeneous nuclear ribonucleoprotein R	HNRNPR	O43390	71	26	71	44	64	0.9
Heterogeneous nuclear ribonucleoprotein L	HNRNPL	P14866	64	35	90	54	78	0.9
Myb-binding protein 1A	MYBBP1A	Q9BQG0	149	26	157	84	122	0.8
X-ray repair cross-complementing protein 6	XRCC6	P12956	70	30	86	59	85	1.0
Transketolase	TKT	P29401	68	17	52	44	64	1.2
Malate dehydrogenase, mitochondrial	MDH2	P40926	36	14	115	83	120	1.0
Nucleolar protein 56	NOP56	O00567	66	27	73	45	65	0.9
Transcription intermediary factor 1-beta	TRIM28	Q13263	89	38	117	67	97	0.8
Putative pre-mRNA-splicing factor ATP-dependent RNA helicase DHX15	DHX15	O43143	91	24	72	35	51	0.7
Spliceosome RNA helicase BAT1	BAT1	Q13838	49	23	93	57	83	0.9
60S ribosomal protein L4	RPL4	P36578	48	15	87	49	71	0.8
Splicing factor, proline- and glutamine-rich	SFPQ	P23246	76	18	58	40	58	1.0
Non-POU domain-containing octamer-binding protein	NONO	Q15233	54	17	91	64	93	1.0
Heat shock 70 kDa protein 4	HSPA4	P34932	94	22	71	36	52	0.7
Polypyrimidine tract-binding protein 1	PTBP1	P26599	57	9	29	20	29	1.0
T-complex protein 1 subunit delta	CCT4	P50991	58	20	56	30	43	0.8
Heterogeneous nuclear ribonucleoprotein A3	HNRNPA3	P51991	40	18	77	51	74	1.0
Putative ribosomal RNA methyltransferase NOP2	NOP2	P46087	89	18	53	21	30	0.6
Histone H1.4	HIST1H1E	P10412	22	17	46	41	59	1.3
Exportin-2	CSE1L	P55060	110	10	58	30	43	0.7
Nucleolar protein 58	NOP58	Q9Y2X3	60	23	64	36	52	0.8
Double-stranded RNA-specific adenosine deaminase	ADAR	P55265	136	17	56	25	36	0.6
Guanine nucleotide-binding protein subunit beta-2-like 1	GNB2L1	P63244	35	10	45	41	59	1.3
Cullin-associated NEDD8-dissociated protein 1	CAND1	Q86VP6	136	28	77	52	75	1.0
Leucine-rich PPR motif-containing protein, mitochondrial	LRPPRC	P42704	158	22	79	51	74	0.9
T-complex protein 1 subunit beta	CCT2	P78371	57	25	68	44	64	0.9
Puromycin-sensitive aminopeptidase	NPEPPS	P55786	103	21	70	46	67	1.0
Heterogeneous nuclear ribonucleoprotein G	RBMX	P38159	42	12	72	56	81	1.1
Ribosomal L1 domain-containing protein 1	RSL1D1	O76021	55	12	46	21	30	0.7
Nucleophosmin	NPM1	P06748	33	11	56	37	54	1.0
40S ribosomal protein S3	RPS3	P23396	27	5	30	42	61	2.0
T-complex protein 1 subunit epsilon	CCT5	P48643	60	13	39	22	32	0.8
Interleukin enhancer-binding factor 2	ILF2	Q12905	43	19	69	52	75	1.1
Core histone macro-H2A.1	H2AFY	O75367	40	17	47	34	49	1.0
Protein RCC2	RCC2	Q9P258	56	1	31	17	25	0.8
rRNA 2'-O-methyltransferase fibrillarin	FBL	P22087	34	8	35	25	36	1.0
60S ribosomal protein L3	RPL3	P39023	46	12	54	38	55	1.0
Apoptosis-inducing factor 1, mitochondrial	AIFM1	O95831	67	10	47	36	52	1.1
DNA mismatch repair protein Msh6	MSH6	P52701	153	11	39	25	36	0.9
General transcription factor II-I	GTF2I	P78347	112	9	44	22	32	0.7
60S acidic ribosomal protein P0	RPLP0	P05388	34	13	47	32	46	1.0
40S ribosomal protein SA	RPSA	P08865	33	11	37	36	52	1.4
GTP-binding nuclear protein Ran	RAN	P62826	24	4	37	20	29	0.8
Putative rRNA methyltransferase 3	FTSJ3	Q8IY81	97	12	41	24	35	0.8
Heterochromatin protein 1-binding protein 3	HP1BP3	Q5SSJ5	61	5	34	17	25	0.7
Splicing factor U2AF 65 kDa subunit	U2AF2	P26368	54	9	26	15	22	0.8
Protein KIAA1967	KIAA1967	Q8N163	103	12	38	15	22	0.6
Heterogeneous nuclear ribonucleoprotein F	HNRNPF	P52597	46	21	66	40	58	0.9

Table S3.5. - Continued

Protein Description	Gene Name	Accession	MW (kDa)	GFP	Tbx20-EGFP	Tbx20eh1mut-EGFP		eh1mut counts/ WT counts
				Spectrum counts	Spectrum counts	Spectrum counts	Normalized spectrum counts	
Arginyl-tRNA synthetase, cytoplasmic	RARS	P54136	75	**11**	**30**	16	**23**	0.8
Proliferation-associated protein 2G4	PA2G4	Q9UQ80	44	**4**	**73**	46	**67**	0.9
Serrate RNA effector molecule homolog	SRRT	Q9BXP5	101	**11**	**36**	21	**30**	0.8
60S ribosomal protein L5	RPL5	P46777	34	**6**	**31**	26	**38**	1.2
Proliferating cell nuclear antigen	PCNA	P12004	29	**2**	**27**	20	**29**	1.1
THO complex subunit 2	THOC2	Q8NI27	183	**3**	**35**	15	**22**	0.6
Prohibitin-2	PHB2	Q99623	33	**8**	**33**	28	**41**	1.2
Heterogeneous nuclear ribonucleoprotein Q	SYNCRIP	O60506	70	**21**	**53**	36	**52**	1.0
40S ribosomal protein S3a	RPS3A	P61247	30	**5**	**30**	22	**32**	1.1
H/ACA ribonucleoprotein complex subunit 4	DKC1	O60832	58	**4**	**21**	10	**14**	0.7
Aconitate hydratase, mitochondrial	ACO2	Q99798	85	**13**	**44**	22	**32**	0.7
Probable ATP-dependent RNA helicase DDX27	DDX27	Q96GQ7	90	**10**	**30**	18	**26**	0.9
Serine/threonine-protein phosphatase PP1-gamma catalytic subunit	PPP1CC	P36873	37	**4**	**21**	18	**26**	1.2
RRP12-like protein	RRP12	Q5JTH9	144	**12**	**51**	34	**49**	1.0
Small ubiquitin-related modifier 2	SUMO2	P61956	11	**5**	**17**	15	**22**	1.3
Host cell factor 1	HCFC1	P51610	209	**8**	**35**	20	**29**	0.8
Complement component 1 Q subcomponent-binding protein, mitochondrial	C1QBP	Q07021	31	**3**	**34**	18	**26**	0.8
THO complex subunit 4	THOC4	Q86V81	27	**8**	**23**	14	**20**	0.9
KH domain-containing, RNA-binding, signal transduction-associated protein 1	KHDRBS1	Q07666	48	**2**	**17**	9	**13**	0.8
Probable ATP-dependent RNA helicase DDX23	DDX23	Q9BUQ8	96	**3**	**18**	15	**22**	1.2
Eukaryotic initiation factor 4A-III	EIF4A3	P38919	47	**19**	**68**	33	**48**	0.7
Ribosomal RNA processing protein 1 homolog B	RRP1B	Q14684	84	**4**	**18**	10	**14**	0.8
RNA-binding protein Raly	RALY	Q9UKM9	32	**7**	**23**	14	**20**	0.9
Nucleolar transcription factor 1	UBTF	P17480	89	**6**	**15**	17	**25**	1.6
U4/U6.U5 tri-snRNP-associated protein 1	SART1	O43290	90	**7**	**27**	11	**16**	0.6
Ribosome biogenesis protein BOP1	BOP1	Q14137	84	**6**	**16**	8	**12**	0.7
ELAV-like protein 1	ELAVL1	Q15717	36	**10**	**34**	24	**35**	1.0
Pre-mRNA-processing factor 6	PRPF6	O94906	107	**5**	**29**	12	**17**	0.6
NF-kappa-B-repressing factor	NKRF	O15226	78	**4**	**18**	16	**23**	1.3
Prohibitin	PHB	P35232	30	**5**	**30**	28	**41**	1.4
Histone H1x	H1FX	Q92522	22	**2**	**26**	15	**22**	0.8
Poly(rC)-binding protein 2	PCBP2	Q15366	39	**9**	**44**	33	**48**	1.1
Inosine-5'-monophosphate dehydrogenase 2	IMPDH2	P12268	56	**3**	**52**	27	**39**	0.8
Calreticulin	CALR	P27797	48	**10**	**56**	36	**52**	0.9
Transportin-1	TNPO1	Q92973	102	**7**	**21**	14	**20**	1.0
Protein arginine N-methyltransferase 5	PRMT5	O14744	73	**5**	**19**	10	**14**	0.8
CCAAT/enhancer-binding protein zeta	CEBPZ	Q03701	121	**12**	**31**	12	**17**	0.6
ATP-dependent DNA helicase Q1	RECQL	P46063	73	**5**	**15**	6	**9**	0.6
Nucleolar complex protein 3 homolog	NOC3L	Q8WTT2	93	**4**	**23**	11	**16**	0.7
RuvB-like 2	RUVBL2	Q9Y230	51	**6**	**53**	35	**51**	1.0
RuvB-like 1	RUVBL1	Q9Y265	50	**5**	**51**	29	**42**	0.8
Septin-2	SEPT2	Q15019	41	**4**	**11**	9	**13**	1.2
Heterogeneous nuclear ribonucleoprotein A0	HNRNPA0	Q13151	31	**5**	**13**	6	**9**	0.7
Nucleolar and coiled-body phosphoprotein 1	NOLC1	Q14978	74	**3**	**9**	4	**6**	0.6
TAR DNA-binding protein 43	TARDBP	Q13148	45	**2**	**18**	10	**14**	0.8
Proteasome subunit alpha type-1	PSMA1	P25786	30	**1**	**13**	16	**23**	1.8
Core histone macro-H2A.2	H2AFY2	Q9P0M6	40	**5**	**24**	11	**16**	0.7
14-3-3 protein theta	YWHAQ	P27348	28	**8**	**46**	29	**42**	0.9
Probable ATP-dependent RNA helicase DDX47	DDX47	Q9H0S4	51	**4**	**14**	9	**13**	0.9
Histone H1.2	HIST1H1C	P16403	21	**16**	**50**	49	**71**	1.4
Nucleolin	NCL	P19338	77	**26**	**53**	50	**72**	1.4
Histone-binding protein RBBP7	RBBP7	Q16576	48	**2**	**14**	6	**9**	0.6
Metastasis-associated protein 1	MTA1	Q13330	81	**2**	**10**	5	**7**	0.7

REFERENCES

Ahn, D. G., Ruvinsky, I., Oates, A. C., Silver, L. M. and Ho, R. K. (2000) 'tbx20, a new vertebrate T-box gene expressed in the cranial motor neurons and developing cardiovascular structures in zebrafish', *Mechanisms of development* 95(1-2): 253-8.

Bindea, G., Mlecnik, B., Hackl, H., Charoentong, P., Tosolini, M., Kirilovsky, A., Fridman, W. H., Pages, F., Trajanoski, Z. and Galon, J. (2009) 'ClueGO: a Cytoscape plug-in to decipher functionally grouped gene ontology and pathway annotation networks', *Bioinformatics* 25(8): 1091-3.

Bowen, N. J., Fujita, N., Kajita, M. and Wade, P. A. (2004) 'Mi-2/NuRD: multiple complexes for many purposes', *Biochimica et biophysica acta* 1677(1-3): 52-7.

Brown, D. D., Binder, O., Pagratis, M., Parr, B. A. and Conlon, F. L. (2003) 'Developmental expression of the Xenopus laevis Tbx20 orthologue', *Development genes and evolution* 212(12): 604-7.

Brown, D. D., Martz, S. N., Binder, O., Goetz, S. C., Price, B. M., Smith, J. C. and Conlon, F. L. (2005) 'Tbx5 and Tbx20 act synergistically to control vertebrate heart morphogenesis', *Development* 132(3): 553-63.

Buscarlet, M., Hermann, R., Lo, R., Tang, Y., Joachim, K. and Stifani, S. (2009) 'Cofactor-activated phosphorylation is required for inhibition of cortical neuron differentiation by Groucho/TLE1', *PloS one* 4(12): e8107.

Cai, C. L., Zhou, W., Yang, L., Bu, L., Qyang, Y., Zhang, X., Li, X., Rosenfeld, M. G., Chen, J. and Evans, S. (2005) 'T-box genes coordinate regional rates of proliferation and regional specification during cardiogenesis', *Development* 132(10): 2475-87.

Chakraborty, S. and Yutzey, K. E. (2012) 'Tbx20 regulation of cardiac cell proliferation and lineage specialization during embryonic and fetal development in vivo', *Developmental biology* 363(1): 234-46.

Chen, G., Fernandez, J., Mische, S. and Courey, A. J. (1999) 'A functional interaction between the histone deacetylase Rpd3 and the corepressor groucho in Drosophila development', *Genes & development* 13(17): 2218-30.

Christoffels, V. M., Grieskamp, T., Norden, J., Mommersteeg, M. T., Rudat, C. and Kispert, A. (2009) 'Tbx18 and the fate of epicardial progenitors', *Nature* 458(7240): E8-9; discussion E9-10.

Christoffels, V. M., Mommersteeg, M. T., Trowe, M. O., Prall, O. W., de Gier-de Vries, C., Soufan, A. T., Bussen, M., Schuster-Gossler, K., Harvey, R. P., Moorman, A. F. et al. (2006) 'Formation of the venous pole of the heart from an Nkx2-5-negative precursor population requires Tbx18', *Circulation research* 98(12): 1555-63.

Conlon, F. L. and Yutzey, K. E. (2010) T-Box Factors. in N. Rosenthal and R. P. Harvey (eds.) *Heart Development and Regeneration*, vol. Volume 2: Elsevier.

Cristea, I. M., Williams, R., Chait, B. T. and Rout, M. P. (2005) 'Fluorescent proteins as proteomic probes', *Molecular & cellular proteomics : MCP* 4(12): 1933-41.

Farin, H. F., Bussen, M., Schmidt, M. K., Singh, M. K., Schuster-Gossler, K. and Kispert, A. (2007) 'Transcriptional repression by the T-box proteins Tbx18 and Tbx15 depends on Groucho corepressors', *The Journal of biological chemistry* 282(35): 25748-59.

Formaz-Preston, A., Ryu, J. R., Svendsen, P. C. and Brook, W. J. (2012) 'The Tbx20 homolog Midline represses wingless in conjunction with Groucho during the maintenance of segment polarity', *Developmental biology* 369(2): 319-29.

Fujita, N., Jaye, D. L., Geigerman, C., Akyildiz, A., Mooney, M. R., Boss, J. M. and Wade, P. A. (2004) 'MTA3 and the Mi-2/NuRD complex regulate cell fate during B lymphocyte differentiation', *Cell* 119(1): 75-86.

Goetz, S. C., Brown, D. D. and Conlon, F. L. (2006) 'TBX5 is required for embryonic cardiac cell cycle progression', *Development* 133(13): 2575-84.

Greco, T. M., Yu, F., Guise, A. J. and Cristea, I. M. (2011) 'Nuclear import of histone deacetylase 5 by requisite nuclear localization signal phosphorylation', *Molecular & cellular proteomics : MCP* 10(2): M110 004317.

Griffin, K. J., Stoller, J., Gibson, M., Chen, S., Yelon, D., Stainier, D. Y. and Kimelman, D. (2000) 'A conserved role for H15-related T-box transcription factors in zebrafish and Drosophila heart formation', *Developmental biology* 218(2): 235-47.

Hammer, S., Toenjes, M., Lange, M., Fischer, J. J., Dunkel, I., Mebus, S., Grimm, C. H., Hetzer, R., Berger, F. and Sperling, S. (2008) 'Characterization of TBX20 in human hearts and its regulation by TFAP2', *Journal of cellular biochemistry* 104(3): 1022-33.

Huang, G. N., Thatcher, J. E., McAnally, J., Kong, Y., Qi, X., Tan, W., DiMaio, J. M., Amatruda, J. F., Gerard, R. D., Hill, J. A. et al. (2012) 'C/EBP transcription factors mediate epicardial activation during heart development and injury', *Science* 338(6114): 1599-603.

Iio, A., Koide, M., Hidaka, K. and Morisaki, T. (2001) 'Expression pattern of novel chick T-box gene, Tbx20', *Development genes and evolution* 211(11): 559-62.

Ikura, T., Ogryzko, V. V., Grigoriev, M., Groisman, R., Wang, J., Horikoshi, M., Scully, R., Qin, J. and Nakatani, Y. (2000) 'Involvement of the TIP60 histone acetylase complex in DNA repair and apoptosis', *Cell* 102(4): 463-73.

Junion, G., Spivakov, M., Girardot, C., Braun, M., Gustafson, E. H., Birney, E. and Furlong, E. E. (2012) 'A transcription factor collective defines cardiac cell fate and reflects lineage history', *Cell* 148(3): 473-86.

Kaltenbrun, E., Tandon, P., Amin, N. M., Waldron, L., Showell, C. and Conlon, F. L. (2011) 'Xenopus: An emerging model for studying congenital heart disease', *Birth defects research. Part A, Clinical and molecular teratology* 91(6): 495-510.

Kirk, E. P., Sunde, M., Costa, M. W., Rankin, S. A., Wolstein, O., Castro, M. L., Butler, T. L., Hyun, C., Guo, G., Otway, R. et al. (2007) 'Mutations in cardiac T-box factor gene TBX20 are associated with diverse cardiac pathologies, including defects of septation and valvulogenesis and cardiomyopathy', *American journal of human genetics* 81(2): 280-91.

Kraus, F., Haenig, B. and Kispert, A. (2001) 'Cloning and expression analysis of the mouse T-box gene Tbx18', *Mechanisms of development* 100(1): 83-6.

Li, R., Zhang, H., Yu, W., Chen, Y., Gui, B., Liang, J., Wang, Y., Sun, L., Yang, X., Zhang, Y. et al. (2009) 'ZIP: a novel transcription repressor, represses EGFR oncogene and suppresses breast carcinogenesis', *The EMBO journal* 28(18): 2763-76.

Li, Y. P., Busch, R. K., Valdez, B. C. and Busch, H. (1996) 'C23 interacts with B23, a putative nucleolar-localization-signal-binding protein', *European journal of biochemistry / FEBS* 237(1): 153-8.

Liu, C., Shen, A., Li, X., Jiao, W., Zhang, X. and Li, Z. (2008) 'T-box transcription factor TBX20 mutations in Chinese patients with congenital heart disease', *European journal of medical genetics* 51(6): 580-7.

Meins, M., Henderson, D. J., Bhattacharya, S. S. and Sowden, J. C. (2000) 'Characterization of the human TBX20 gene, a new member of the T-Box gene family closely related to the Drosophila H15 gene', *Genomics* 67(3): 317-32.

Miteva, Y. V., Budayeva, H. G. and Cristea, I. M. (2013) 'Proteomics-based methods for discovery, quantification, and validation of protein-protein interactions', *Analytical chemistry* 85(2): 749-68.

Nie, X., Sun, J., Gordon, R. E., Cai, C. L. and Xu, P. X. (2010) 'SIX1 acts synergistically with TBX18 in mediating ureteral smooth muscle formation', *Development* 137(5): 755-65.

Nieuwkoop, P. D. a. F., J. (1974) *Normal table of Xenopus laevis (Daudin).* , Amsterdam, The Netherlands: North Holland.

Olson, L. E., Tollkuhn, J., Scafoglio, C., Krones, A., Zhang, J., Ohgi, K. A., Wu, W., Taketo, M. M., Kemler, R., Grosschedl, R. et al. (2006) 'Homeodomain-mediated beta-catenin-dependent switching events dictate cell-lineage determination', *Cell* 125(3): 593-605.

Qian, L., Mohapatra, B., Akasaka, T., Liu, J., Ocorr, K., Towbin, J. A. and Bodmer, R. (2008) 'Transcription factor neuromancer/TBX20 is required for cardiac function in Drosophila with implications for human heart disease', *Proceedings of the National Academy of Sciences of the United States of America* 105(50): 19833-8.

Reller, M. D., Strickland, M. J., Riehle-Colarusso, T., Mahle, W. T. and Correa, A. (2008) 'Prevalence of congenital heart defects in metropolitan Atlanta, 1998-2005', *The Journal of pediatrics* 153(6): 807-13.

Roche, A. E., Bassett, B. J., Samant, S. A., Hong, W., Blobel, G. A. and Svensson, E. C. (2008) 'The zinc finger and C-terminal domains of MTA proteins are required for FOG-2-mediated transcriptional repression via the NuRD complex', *Journal of molecular and cellular cardiology* 44(2): 352-60.

Rottbauer, W., Saurin, A. J., Lickert, H., Shen, X., Burns, C. G., Wo, Z. G., Kemler, R., Kingston, R., Wu, C. and Fishman, M. (2002) 'Reptin and pontin antagonistically regulate heart growth in zebrafish embryos', *Cell* 111(5): 661-72.

Sakabe, N. J., Aneas, I., Shen, T., Shokri, L., Park, S. Y., Bulyk, M. L., Evans, S. M. and Nobrega, M. A. (2012) 'Dual transcriptional activator and repressor roles of TBX20 regulate adult cardiac structure and function', *Human molecular genetics* 21(10): 2194-204.

Santisteban, P., Recacha, P., Metzger, D. E. and Zaret, K. S. (2010) 'Dynamic expression of Groucho-related genes Grg1 and Grg3 in foregut endoderm and antagonism of differentiation', *Developmental dynamics : an official publication of the American Association of Anatomists* 239(3): 980-6.

Sardiu, M. E., Cai, Y., Jin, J., Swanson, S. K., Conaway, R. C., Conaway, J. W., Florens, L. and Washburn, M. P. (2008) 'Probabilistic assembly of human protein interaction networks from label-free quantitative proteomics', *Proceedings of the National Academy of Sciences of the United States of America* 105(5): 1454-9.

Shen, T., Aneas, I., Sakabe, N., Dirschinger, R. J., Wang, G., Smemo, S., Westlund, J. M., Cheng, H., Dalton, N., Gu, Y. et al. (2011) 'Tbx20 regulates a genetic program essential to adult mouse cardiomyocyte function', *The Journal of clinical investigation* 121(12): 4640-54.

Singh, M. K., Christoffels, V. M., Dias, J. M., Trowe, M. O., Petry, M., Schuster-Gossler, K., Burger, A., Ericson, J. and Kispert, A. (2005) 'Tbx20 is essential for cardiac chamber differentiation and repression of Tbx2', *Development* 132(12): 2697-707.

Smith, J. C. and Slack, J. M. (1983) 'Dorsalization and neural induction: properties of the organizer in Xenopus laevis', *Journal of embryology and experimental morphology* 78: 299-317.

Smoot, M. E., Ono, K., Ruscheinski, J., Wang, P. L. and Ideker, T. (2011) 'Cytoscape 2.8: new features for data integration and network visualization', *Bioinformatics* 27(3): 431-2.

Stennard, F. A., Costa, M. W., Elliott, D. A., Rankin, S., Haast, S. J., Lai, D., McDonald, L. P., Niederreither, K., Dolle, P., Bruneau, B. G. et al. (2003) 'Cardiac T-box factor Tbx20 directly interacts with Nkx2-5, GATA4, and GATA5 in regulation of gene expression in the developing heart', *Developmental biology* 262(2): 206-24.

Stennard, F. A., Costa, M. W., Lai, D., Biben, C., Furtado, M. B., Solloway, M. J., McCulley, D. J., Leimena, C., Preis, J. I., Dunwoodie, S. L. et al. (2005) 'Murine T-box transcription factor Tbx20 acts as a repressor during heart development, and is essential for adult heart integrity, function and adaptation', *Development* 132(10): 2451-62.

Szklarczyk, D., Franceschini, A., Kuhn, M., Simonovic, M., Roth, A., Minguez, P., Doerks, T., Stark, M., Muller, J., Bork, P. et al. (2011) 'The STRING database in 2011: functional interaction networks of proteins, globally integrated and scored', *Nucleic acids research* 39(Database issue): D561-8.

Takeuchi, J. K., Mileikovskaia, M., Koshiba-Takeuchi, K., Heidt, A. B., Mori, A. D., Arruda, E. P., Gertsenstein, M., Georges, R., Davidson, L., Mo, R. et al. (2005) 'Tbx20 dose-dependently regulates transcription factor networks required for mouse heart and motoneuron development', *Development* 132(10): 2463-74.

Tsai, Y. C., Greco, T. M., Boonmee, A., Miteva, Y. and Cristea, I. M. (2012) 'Functional proteomics establishes the interaction of SIRT7 with chromatin remodeling complexes and expands its role in regulation of RNA polymerase I transcription', *Molecular & cellular proteomics : MCP* 11(5): 60-76.

van der Linde, D., Konings, E. E., Slager, M. A., Witsenburg, M., Helbing, W. A., Takkenberg, J. J. and Roos-Hesselink, J. W. (2011) 'Birth prevalence of congenital heart disease worldwide: a systematic review and meta-analysis', *Journal of the American College of Cardiology* 58(21): 2241-7.

Villanueva, C. J., Waki, H., Godio, C., Nielsen, R., Chou, W. L., Vargas, L., Wroblewski, K., Schmedt, C., Chao, L. C., Boyadjian, R. et al. (2011) 'TLE3 is a

dual-function transcriptional coregulator of adipogenesis', *Cell metabolism* 13(4): 413-27.

Wang, M., Weiss, M., Simonovic, M., Haertinger, G., Schrimpf, S. P., Hengartner, M. O. and von Mering, C. (2012) 'PaxDb, a database of protein abundance averages across all three domains of life', *Molecular & cellular proteomics : MCP* 11(8): 492-500.

Xue, Y., Wong, J., Moreno, G. T., Young, M. K., Cote, J. and Wang, W. (1998) 'NURD, a novel complex with both ATP-dependent chromatin-remodeling and histone deacetylase activities', *Molecular cell* 2(6): 851-61.

Zeng, B., Ren, X. F., Cao, F., Zhou, X. Y. and Zhang, J. (2011) 'Developmental patterns and characteristics of epicardial cell markers Tbx18 and Wt1 in murine embryonic heart', *Journal of biomedical science* 18: 67.

Zybailov, B. L., Florens, L. and Washburn, M. P. (2007) 'Quantitative shotgun proteomics using a protease with broad specificity and normalized spectral abundance factors', *Molecular bioSystems* 3(5): 354-60.

Chapter 4

A novel method to detect cardiac-specific Tbx20 protein-protein interactions reveals association with a broad chromatin-remodeling network

ABSTRACT

Previous work demonstrated that Tbx20 associates with a transcription repression network in human cells (Chapter 3). To extend these studies and investigate the cardiac-specific components of Tbx20 transcription complexes, we have developed a novel approach to isolate endogenous Tbx20 protein complexes from mouse ESC-derived cardiomyocytes. Specifically, we have developed an Avitag-tagged Tbx20 knock-in cell line that allows for a high throughput mass spectrometry approach to identify cardiac-specific Tbx20 protein interactions. Here, we demonstrate the feasibility of this approach by presenting evidence of efficient Tbx20 isolation from ESC-derived cardiac progenitors. We go on to show that Tbx20 co-isolates with known binding partners, Gata4 and TLE3, in these cells. In addition, we observed association with a broad network of chromatin-remodeling proteins, including components of the NuRD, SWI/SNF, and INO80 complexes. These studies represent the first comprehensive analysis of Tbx20 protein complexes from cardiac cells and greatly enhance our understanding of the Tbx20 transcription network during heart development.

INTRODUCTION

Transition from a pluripotent cell into a functional cardiomyocyte requires the activity of a number of critical cardiogenic transcription factors. Tbx20 interacts with a suite of other transcription factors within the developing heart to drive cardiac gene expression (Stennard et al., 2003; Takeuchi et al., 2005), and a number of studies also demonstrate a role for Tbx20 in transcriptional repression during cardiac development (Cai et al., 2005; Singh et al., 2005; Sakabe et al., 2012). Therefore, the activities of Tbx20 appear to be context dependent and ultimately controlled by co-activators and co-repressors. We have previously observed that Tbx20 interacts with a network of co-repressors in human cells including members of the NuRD and INO80 chromatin remodeling complexes (Chapter 3), implying that Tbx20 may interact with chromatin remodelers to regulate gene expression in the developing heart. However, it is unclear which components of this network may represent cardiac-specific interactions. Additionally, protein-protein interactions that occur in a tissue-specific and/or temporal manner during cardiomyocyte development were likely to be excluded from our previous analysis due to the difficulties in isolating endogenous Tbx20 from its native cell type.

Therefore, to gain insight into the Tbx20 cardiac transcription network and to understand how Tbx20 acts as a repressor within the context of the developing heart, we sought to identify Tbx20 interaction partners from ESC-derived cardiac progenitor cells. To allow us to isolate endogenous Tbx20, we generated mouse

ESCs in which the Avitag (Schatz, 1993) is inserted into the endogenous Tbx20 locus and that stably express the *E. coli.* biotin ligase BirA. Subsequent directed differentiation of *Tbx20^{Avi}; BirA* ESCs into cardiomyocytes allows for BirA-mediated biotinylation of the Avitag at the time and place where Tbx20 is endogenously expressed over the course of cardiomyocyte differentiation. Tbx20 protein complexes were then isolated using a streptavidin purification approach (de Boer et al., 2003) and subjected to mass spectrometry analysis to identify interaction partners. Utilizing the biotin/avidin system for protein purification has a number of crucial benefits for this set of studies. First, it completely obviates the need for a high-affinity antibody, which for many transcription factors including Tbx20 simply do not exist. Second, the interaction of biotin with avidin is one of the highest affinity interactions known in nature (Savage et al., 1992). Finally, BirA specifically conjugates biotin to the 15 amino acid Avitag sequence (Cronan and Reed, 2000; Cull and Schatz, 2000), a synthetic sequence that is not reproduced in any mammalian genome allowing for highly specific tagging and subsequent isolation of the target protein.

In this study, we demonstrate that using the biotin/avidin system in combination with directed cardiac differentiation of mouse ESCs we are able to efficiently isolate endogenous Tbx20 protein from cardiac progenitor cells. Using this system we are able to detect an interaction with the cardiac transcription factor Gata4, a known binding partner of Tbx20 that is specifically expressed in the developing heart. We also detect an association with TLE3, an interaction we have

previously shown to take place in the mouse embryonic heart and in human cells (Chapter 3). In addition, we identified a number of chromatin-associated proteins not yet shown to interact with Tbx20, including several proteins in the INO80, SWI/SNF, and NuRD chromatin remodeling complexes. Collectively, these studies provide the first demonstrate that Tbx20 associates with a broad chromatin remodeling network to modify gene expression in cardiac progenitor cells.

MATERIALS AND METHODS

DNA Constructs

The *pLenti-BirA* plasmid was obtained from Addgene (Addgene plasmid 29649; principal investigator Eric Campeau) and modified to contain a polyadenylation signal for expression in mammalian cells. In collaboration with the UNC gene therapy core facility, the *pLenti-BirA* plasmid was packaged and purified into a concentrated lentivirus.

Generation of *Tbx20^{Avi}; BirA* cell line and differentiation

To generate a targeting construct to introduce the Avitag into the mouse *Tbx20* locus, the *Avitag* sequence followed by a *loxP*-flanked *neo* cassette was inserted into the stop codon of exon 8 of a *Tbx20a* genomic fragment derived from a 129 Sv genomic BAC library. The targeting construct was linearized and electroporated into ES cells of E14TG2a.4 origin. Targeted ES cells were placed under 250 µg/mL G418 selection for 7-10 days to test for neomycin resistance. G418-resistant ES cell clones (n=384) were screened for homologous recombination

in the *Tbx20* locus by southern blot analysis (Southern, 1975). Three ES cell clones were correctly targeted, and one of these clones was subsequently used to derive the *Tbx20*$^{Avi/+}$*; BirA* cell line. Briefly, *Tbx20*$^{Avi/+}$ ES cells were grown to approximately 40% confluence, then transduced with 5 MOI *Lenti-BirA* for 8 hrs. Twenty-four hours following transduction, cells were placed under 200 µg/mL hygromycin selection for 4-5 days. Hygro-resistant *Tbx20*$^{Avi/+}$ cells were subsequently used for cardiomyocyte differentiations.

Tbx20$^{Avi/+}$*; BirA* ES cells were maintained on gelatin-coated dishes in a feeder-free culture system and differentiated according to the Keller protocol (Kattman et al., 2011). ES cells were differentiated in serum-free (SF) media as described previously (Gadue et al., 2006). Briefly, ES cells were trypsinized and cultured at 75,000 cells/mL on uncoated petri dishes in SF medium without additional growth factors for 48 hrs. Two-day-old aggregated embryoid bodies (EBs) were dissociated and the cells reaggregated for 48 hrs in SF medium containing 5 ng/mL human Activin A, 0.1 ng/mL human BMP4, and 5 ng/mL human VEGF (all growth factors purchased from R&D Systems). Four-day-old EBs were dissociated and 2 x 10^6 cells were seeded into individual gelatin-coated wells of a 6-well dish in StemPro-34 SF medium (Invitrogen) supplemented with 2 mM L-glutamine, 1 mM ascorbic acid, 5 ng/mL human VEGF, 20 ng/mL human bFGF, and 50 ng/mL human FGF10 (R&D Systems). Cardiomyocyte monolayers were maintained in this media for 4-5 additional days with cells typically beginning to beat 2 days after seeding onto gelatin (total of 7-8 days of differentiation).

Immunofluorescence and immunoblotting

For immunofluorescence of cardiomyocytes, four-day-old ES cell-derived embryoid bodies were dissociated and seeded into 8-well chamber slides precoated with 0.1% gelatin. Induced cardiomyocytes were fixed on day 7 of differentiation in 4% paraformaldehyde for 20 min at room temperature, washed 3 times in 1X PBS, permeabilized in 0.1% Triton X-100 in 1X PBS for 10 min, and blocked in 10% fetal bovine serum (FBS) in 1X PBS containing 0.1% Tween 20 for 30 min. Anti-myosin heavy chain (Abcam) was applied overnight, followed by 3 washes in 1X PBS, and incubation with goat anti-mouse Alexa 546 (Invitrogen) for 1 hr. Cells were incubated in DAPI (200 ng/mL in ethanol) for 30 min and visualized by confocal microscopy on a Zeiss 710. Antibodies used for immunoblotting include mouse anti-GAPDH (Millipore) and chick anti-BirA (Abcam).

RNA extraction and RT-PCR

RNA was extracted using Trizol (Invitrogen) and purified on RNeasy columns (Qiagen). cDNA synthesis was performed from 0.5-1 μg of RNA using random primers and SuperScript II reverse transcriptase (Invitrogen). Expression levels were assessed using GoTaq Green Master Mix (Promega) and Taq polymerase on a GeneAmp PCR System (Applied Biosystems). PCR products were analyzed by 2.5% agarose gel electrophoresis.

Isolation of Tbx20-Avitag complexes from cardiac progenitor cells

Day 4 *Tbx20^{Avi}; BirA* EBs and, as a control, Day 4 *Tbx20^{Avi}* EBs were collected and washed with cold PBS. The EBs were pelleted at 1500 rpm for 10 min at 4°C. The cell pellet was resuspended in 100 µL/1 µg 20 mM HEPES, pH 7.4, containing 1.2% polyvinylpyrrolidone and protease inhibitors and snap frozen in liquid nitrogen. Cells were lysed by cryogenic grinding using a Retsch MM 301 Mixer Mill (10 cycles x 2.5 min at 30 Hz) (Retsch, Newtown, PA) and the frozen cell powder was resuspended in optimized lysis buffer (5 mL/1 g cells) (20 mM K-HEPES pH 7.4, 0.1 M KOAc, 2 mM $MgCl_2$, 0.1% Tween-20, 1 µM $ZnCl_2$, 1 µM $CaCl_2$, 200 mM NaCl, 0.5% Triton X-100 containing protease and phosphatase inhibitors) followed by a 10 min rotation at 4° to improve extraction. Cell lysates were homogenized using a Polytron (Kinematica) step (2 x 15 sec), followed by DNase treatment (10 U/mL lysate) for 30 min at room temperature. DNase-treated lysates were pelleted at 3000 rpm at 4°C. Cleared lysates were rotated with 6 mg magnetic beads coupled to streptavidin (M270 Streptavidin Dynabeads, Invitrogen) for 4 hrs at 4°C. The magnetic beads were then washed in lysis buffer (6 x 1 mL) (without protease and phosphatase inhibitors) and eluted from the beads in 80 mM sodium acetate, 95% formamide, pH 9.0 at 95°C for 15 min. LDS Sample Buffer (Invitrogen) and reducing agent (Invitrogen) (final 1X concentration of both) were added to eluates and eluted proteins were alkylated with 100 mM iodoacetamide for 1 hr at room temperature and subjected to mass spectrometry analysis.

Mass spectrometry analysis of Tbx20 protein complexes

Immunoisolates were analyzed by mass spectrometry as previously described (Chapter 3).

RESULTS

Generation of a *Tbx20^{Avitag}* knock-in mouse ESC line

To allow for immunoaffinity purification of endogenous Tbx20 protein complexes, we introduced a short synthetic sequence known as the Avitag into the endogenous *Tbx20* locus through homologous recombination in mouse ESCs. The Avitag was introduced into the carboxy terminus of the *Tbx20a* isoform (Figure 4.1A) and a *Tbx20$^{Avi/+}$* ESC clone was obtained (Figure 4.1B). Tbx20 protein tagged with the Avitag can be biotinylated through recognition of the Avitag sequence by the *E. coli* biotin ligase BirA, allowing for immobilization of Tbx20 immunocomplexes on streptavidin-coupled beads. To accomplish this, we generated a lentivirus that ubiquitously expresses BirA under the control of the PGK promoter. We then transduced *Tbx20$^{Avi/+}$* ESCs with the BirA lentivirus and placed the cells under hygromycin selection to eliminate any cells that did not integrate the *BirA* construct (Figure 4.2A). To obtain cardiac progenitor cells expressing tagged Tbx20 and BirA, we differentiated hygromycin-resistant *Tbx20$^{Avi/+}$* cells using a serum-free differentiation method developed by Kattman et al. that reproducibly generates cultures containing >60% cardiomyocytes (Kattman et al., 2011) (Figure 4.2A). Hygromycin-resistant *Tbx20$^{Avi/+}$* cells stably express *BirA* through Day 4 of the differentiation protocol (Figure 4.2B).

Molecular analysis of *Tbx20*$^{Avi/+}$*; BirA* cell populations at each day of differentiation revealed gene expression patterns consistent with normal cardiac development (Figure 4.2C). Expression of *Mesp1*, which is closely associated with specification of cardiac mesoderm (Bondue et al., 2011), peaks at day 3 of differentiation and is quickly downregulated. Markers of cardiac progenitors including *Gata4/5* (Kelley et al., 1993; Laverriere et al., 1994), *Tbx5* (Horb and Thomsen, 1999), *Nkx2.5* (Bodmer et al., 1990), and *Isl1* (Cai et al., 2003) are expressed starting at day 3 and continue to be expressed for the duration of the culture. Terminal differentiation of cardiomyocytes is marked by the onset of expression of *cardiac Troponin T (cTnT)* (Toyota and Shimada, 1981) at day 5, indicating efficient development of a cardiogenic population of cells. Further, rapid downregulation of the beta isoform of *actin* (*β-actin*) (Garrels and Gibson, 1976), which is expressed in non-muscle or non-contractile cells, coincides with the upregulation in *cTnT* expression, indicating a transition into terminally differentiated cardiomyocytes at this stage. *Tbx20-Avitag* transcripts recapitulate endogenous *Tbx20a* expression and are at the highest levels in cardiac progenitors at day 4 and in differentiated cardiomyocytes at day 7. This is consistent with a role for Tbx20 in early cardiac development and in the later stages of cardiomyocyte morphogenesis and specialization (Kraus et al., 2001; Brown et al., 2005; Cai et al., 2005; Singh et al., 2005; Stennard et al., 2005; Takeuchi et al., 2005). Additionally, *Tbx20*$^{Avi/+}$*; BirA* cells routinely immunostain positive for the cardiomyocyte muscle protein Myosin Heavy Chain (MHC) and contract by day 6 of differentiation (Figure 4.2D and data not

shown). Collectively, these results demonstrate a novel approach to isolating Tbx20 protein-protein interactions and will be a powerful tool for studying the tissue-specific functions of Tbx20 in the context of cardiomyocyte development.

The Avitag-BirA system successfully isolates known Tbx20 protein-protein interactions

To determine if the Avitag-BirA system can be used to isolate endogenous Tbx20 from cardiac progenitor cells and to identify cardiac-specific factors that associate with Tbx20, we isolated Tbx20 complexes from Day 4 *Tbx20^{Avi}; BirA* EBs. As a negative control, we performed streptavidin purifications on *Tbx20^{Avi}* EBs. In the absence of BirA, Tbx20 is not biotinylated or able to bind streptavidin; therefore, this serves as a control for the specificity of the Tbx20 isolation and allows us to identify (and subsequently exclude from our analyses) endogenously biotinylated proteins that non-specifically bind the beads. Immunocomplexes from *Tbx20^{Avi}; BirA* EBs (Avi-BirA) and *Tbx20^{Avi}* EBs (Avi) were sequenced by mass spectrometry. Using this technique, Tbx20 was successfully isolated from Avi-BirA EBs (Figure 4.3A, B and Table 4.1). In addition, we identified the factors Gata4 and TLE3, proteins previously shown to complex with Tbx20 in the context of heart development ((Stennard et al., 2003) and Chapter 3), as Tbx20-associated proteins in ESC-derived cardiac progenitors (Table 4.1). Interestingly, we never detect a Tbx20-TLE3 association in Day 7 ESC-derived cardiomyocytes, indicating that there is a temporal requirement for this interaction specifically within cardiac progenitors that have not yet undergone terminal differentiation (data not shown).

Tbx20 interacts with a chromatin remodeling network in cardiac progenitors

We have previously demonstrated that Tbx20 interacts with chromatin remodeling proteins in human cells (Chapter 3). Therefore, to characterize the composition of the cardiac-specific Tbx20 chromatin remodeling network, we looked for components of chromatin remodeling complexes with known roles in cardiac development (see Introduction). This preliminary search revealed association of Tbx20 with a number of chromatin remodeling proteins. This network includes several proteins within the INO80 complex (Ruvbl1, Ruvbl2, Actl6a), the NuRD complex (Rbbp4/RbAp48, Rbbp7/RbAp46, Hdac1, Gatad2a/p66α, Gatad2b/p66β), and the SWI/SNF complex (Smarcc1/BAF155, Smarcd1/BAF60A, Actl6a/BAF53) (Table 4.1). We previously identified interactions with the INO80 complex and members of the NuRD complex (see Chapter 3); this data provides further evidence of those interactions and implies that association with chromatin remodelers is critical for Tbx20-mediated regulation of cardiac differentiation.

DISCUSSION

We have previously characterized the Tbx20 transcriptional proteome in human cells and found that Tbx20 interacts with a number of chromatin remodelers. To expand upon this work and to begin to characterize the cardiac-specific components of the Tbx20 transcription network, we have developed a novel approach to isolate endogenous Tbx20 protein complexes from mouse ESC-derived cardiomyocytes. This system allows for highly effective immunoaffinity purification of Tbx20 complexes at various stages of cardiomyocyte differentiation, providing us

with the ability to compare the Tbx20 transcription network at different stages of cardiomyocyte development. As evidence that the Avitag-BirA approach is a sensitive and reliable method to detect Tbx20 protein-protein interactions, we detected two known cardiac-specific Tbx20 associations. The first, Gata4, is a cardiac transcription factor that has been demonstrated to directly interact with Tbx20 in vitro, and to synergize with Tbx20 to activate cardiac gene expression (Stennard et al., 2003; Takeuchi et al., 2005); however, the present study represents the first demonstration of a physical interaction between Gata4 and Tbx20 in cardiac cells. The second, TLE3, we have previously demonstrated to interact with Tbx20 in HEK 293 cells and in mouse embryonic hearts (Chapter 3). In this study, we identified a Tbx20-TLE3 interaction in cells that have not yet transitioned to terminally differentiated cardiomyocytes. Further, we never detect this interaction in Day 7 ESC-derived cardiomyocytes (data not shown) indicating that there is a temporal requirement for a Tbx20-TLE co-repressor complex in cardiac progenitors. Further investigation will be needed to examine the precise role this complex plays in cardiac differentiation.

Using the Avitag-BirA technology, we provide the first demonstration of a cardiac-specific Tbx20 chromatin remodeling network. Our mass spectrometry analysis indicates that Tbx20 interacts with a number of different chromatin remodeling complexes in cardiac progenitors. This network includes the INO80 complex components Ruvbl1 and Ruvbl2, both of which we detected in our previous proteomic analyses and which have documented roles in cardiac growth in zebrafish

(Chapter 3 and (Rottbauer et al., 2002). Tbx20 is required for proliferation in the developing heart (Cai et al., 2005; Shelton and Yutzey, 2007; Chakraborty and Yutzey, 2012); therefore, it will be interesting to determine if the function of Tbx20 in maintaining proper proliferation is dependent upon interaction with the INO80 complex in the developing heart.

Our previous proteomic studies identified components of the NuRD complex in complex with Tbx20. Our preliminary studies in cardiac progenitor cells provide independent confirmation of this data, and expand upon those studies by demonstrating interaction with additional components of the NuRD complex. The cardiac Tbx20-NuRD complex includes the MBD-binding proteins Gatad2a/p66α and Gatad2b/p66β, the histone-binding proteins Rbbp4 and Rbbp7, and Hdac1. Interestingly, in human cells we found Tbx20 associated with Hdac2; however, in cardiac cells, Tbx20 is associated with Hdac1. This could be due to functional redundancy between Hdac1 and Hdac2, as myocardium deletion of both genes, but not of each gene individually, results in defects in myocardial growth and morphogenesis (Montgomery et al., 2007). Additionally, Hdac1 and Hdac2 redundantly regulate a number of gene targets in the heart and have both been shown to occupy the *Tnni2* promoter in neonatal rat cardiomyocytes, indicating that Hdac1 and -2 regulate a common set of genes in the heart (Montgomery et al., 2007).

We also observed the core catalytic subunit of NuRD, Chd4/Mi-2β, and MTA2 in the Avitag-BirA isolation; however, these interactions were not enriched over the Avitag isolations (data not shown). As the analysis presented here represents a single Tbx20 immunoisolation, additional independent immunoisolations are needed to determine if Chd4 and MTA2 are bona fide Tbx20 associations. Interestingly, we do not observe MBD subunits in either the human (Chapter 3) or cardiac Tbx20-NuRD complexes we have identified. As MBD proteins are implicated in targeting the NuRD complex to genomic locations through their association with methylated DNA, it is likely that targeting of the Tbx20-NuRD complex relies solely on Tbx20 binding to target promoters and subsequent recruitment of the NuRD complex. Collectively, these data present the first evidence that Tbx20 associates with the NuRD complex in cardiac cells, implying that Tbx20 is involved in chromatin remodeling and histone deacetylation of target genes.

Tbx20 also interacts with members of the SWI/SNF remodeling complex in cardiac progenitor cells. The specific SWI/SNF subunits we identified, BAF155, BAF60a, and BAF53, represent components that are common to both SWI/SNF ATP-dependent chromatin remodeling complexes PBAF and BAF. BAF complexes have a well-documented role in chromatin activation through interaction with cardiac transcription factors on cardiac promoters (Lickert et al., 2004; Takeuchi et al., 2011); SWI/SNF complexes also function to transcriptionally repress genes in the heart through recruitment of HDACs (Hang et al., 2010). *Tbx20* interacts genetically with *Brg1* (Takeuchi et al., 2011), a component of BAF complexes, during cardiac

development; however, a physical interaction between Tbx20 and SWI/SNF components was not demonstrated prior to this study. Further studies will aim to delineate the precise role a Tbx20-BAF complex plays in regulating Tbx20 target genes in the developing heart.

In conclusion, we have demonstrated that Tbx20 interacts with a broad network of chromatin remodeling proteins in cardiac progenitor cells (Figure 4.4), interactions that are predicted to result in both transcriptional activation and repression of gene expression. This work implicates Tbx20 as an important dual transcriptional activator and repressor in the developing myocardium. These results further underscore the complexity of the Tbx20 transcription network, and suggest that disease-causing mutations in Tbx20 may lead to disruption of interaction networks critical for proper Tbx20-mediated transcriptional regulation.

ACKNOWLEDGMENTS

I would like to thank Leslie Kennedy for her assistance in the identification of a *Tbx20*^{Avi} ESC recombinant by southern blot. Additionally, I would like to thank an undergraduate student, Evan Farina, for his assistance with the RT-PCR analysis of the ESC-derived cardiomyocytes. Finally, all proteomic analyses were performed in collaboration with Ileana Cristea's group at Princeton University. Postdoctoral fellow Todd Greco in the Cristea lab in particular was critical to the success of the mass spectrometry analyses.

Figure 4.1. Generation of *Tbx20*^{Avitag} allele. (A) The *Avitag* targeting construct was introduced into the stop codon of exon 8 and contains two arms of *Tbx20* homology, the *Avitag* sequence, and a *PGK-Neomycin* cassette flanked by *loxP* sites for positive selection of targeted ES cell clones. HindIII restriction sites are indicated and were used to screen by southern blot for recombinants. (B) Southern blot showing successful integration of the *Avitag* into one allele of the *Tbx20* locus.

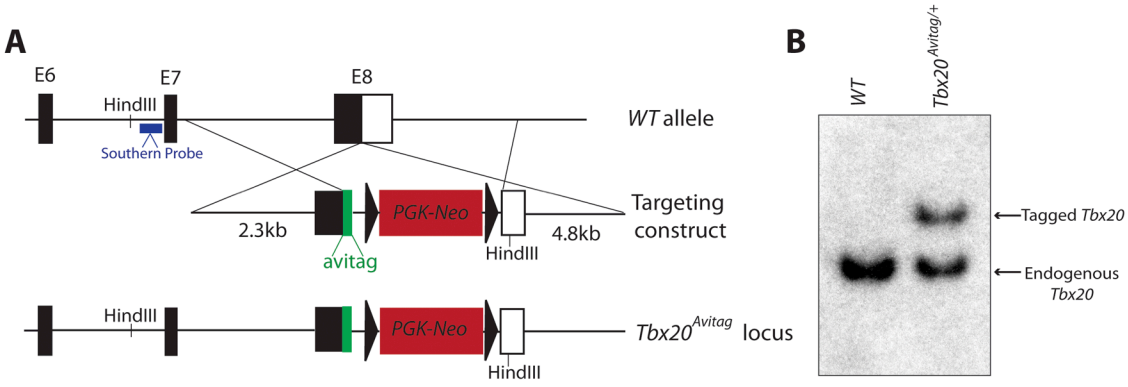

Figure 4.2. Directed cardiac differentiation of *Tbx20^{Avi}; BirA* ESCs recapitulates normal cardiogenesis. (A) Experimental design for generating *Tbx20^{Avi}; BirA* cardiomyocytes. *Tbx20$^{Avi/+}$* ES cells were transduced with a BirA lentivirus and placed under selection to remove cells that failed to integrate the BirA construct. *Tbx20$^{Avi/+}$; BirA* ES cells were induced to form embryoid bodies (EBs) and were cultured in conditions to generate induced cardiomyocytes (iCMs) by day 5 of differentiation. (B) Western blot showing stable levels of BirA protein after BirA transduction and 4 days of differentiation. (C) RT-PCR analysis of genes that sequentially mark non-contractile or non-muscle cells (yellow), specified cardiac mesoderm (red), cardiac progenitors (green), and differentiated cardiomyocytes (blue) across stages of cardiac differentiation of ESCs. Note that expression levels of *Tbx20-Avitag* recapitulate that of untagged *Tbx20a*. All samples are derived from cells taken at indicated stage of differentiation. *Rps29* was used as a loading control for RT-PCR reactions. (D) Induced cardiomyocytes stain positive for MHC, as shown by immunoflourescence of day 7 cardiomyocytes with anti-MHC antibody and DAPI co-stain.

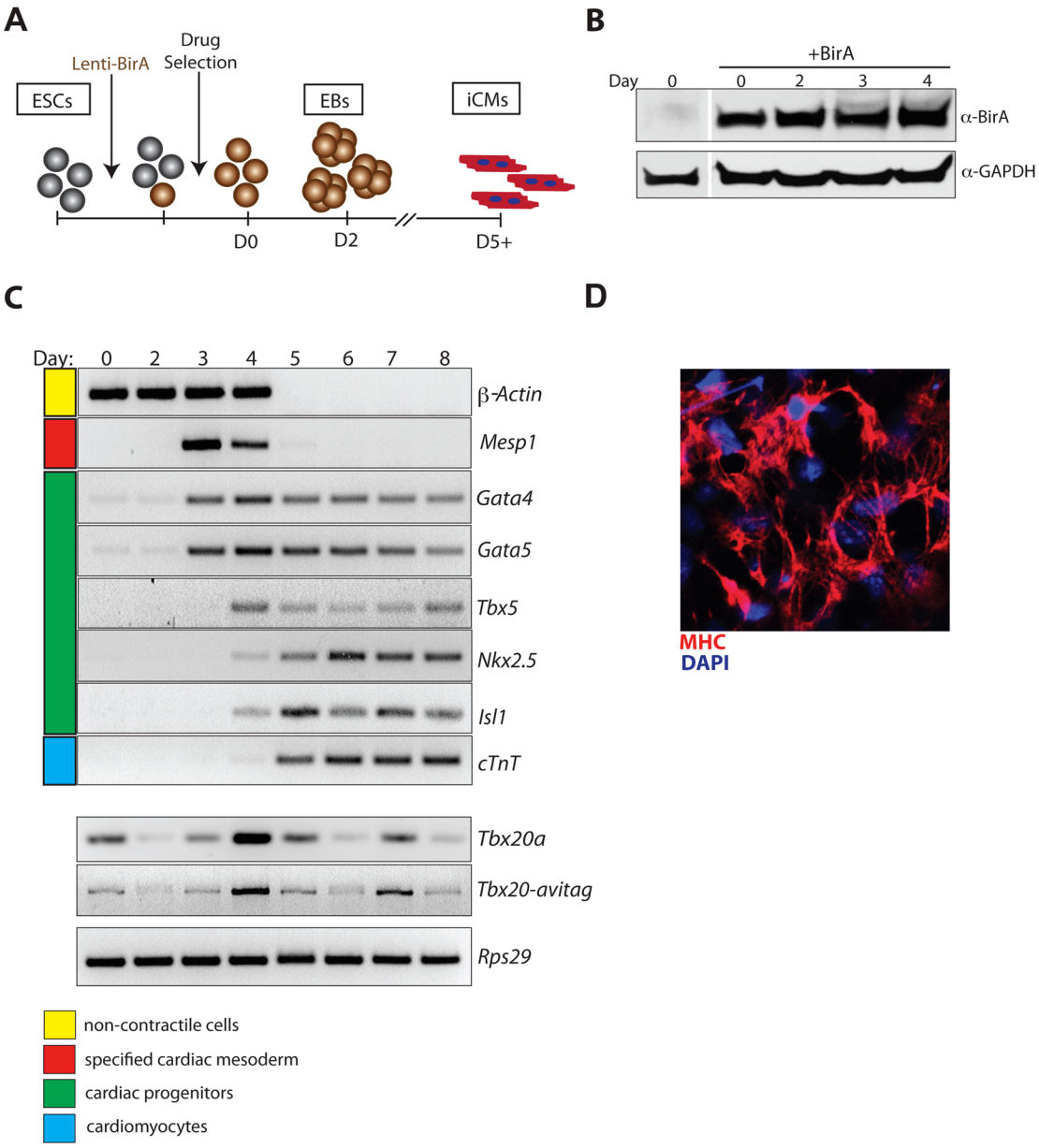
A
Lenti-BirA
Drug Selection
ESCs
EBs
iCMs
D0
D2
D5+
B
+BirA
Day 0 0 2 3 4
α-BirA
α-GAPDH
C
Day: 0 2 3 4 5 6 7 8
β-Actin
Mesp1
Gata4
Gata5
Tbx5
Nkx2.5
Isl1
cTnT
Tbx20a
Tbx20-avitag
Rps29
non-contractile cells
specified cardiac mesoderm
cardiac progenitors
cardiomyocytes
D
MHC
DAPI

Figure 4.3. Endogenous Tbx20 is isolated from *Tbx20^{Avi}; BirA* cardiac progenitor cells. (A) Endogenous Tbx20 was immunoprecipitated from Day 4 *Tbx20^{Avi}; BirA* or *Tbx20^{Avi}* EBs on streptavidin-conjugated beads and analyzed by western blot analysis with a streptavidin-HRP conjugate. (B) Identification of Tbx20 peptide by LC-MS/MS analysis.

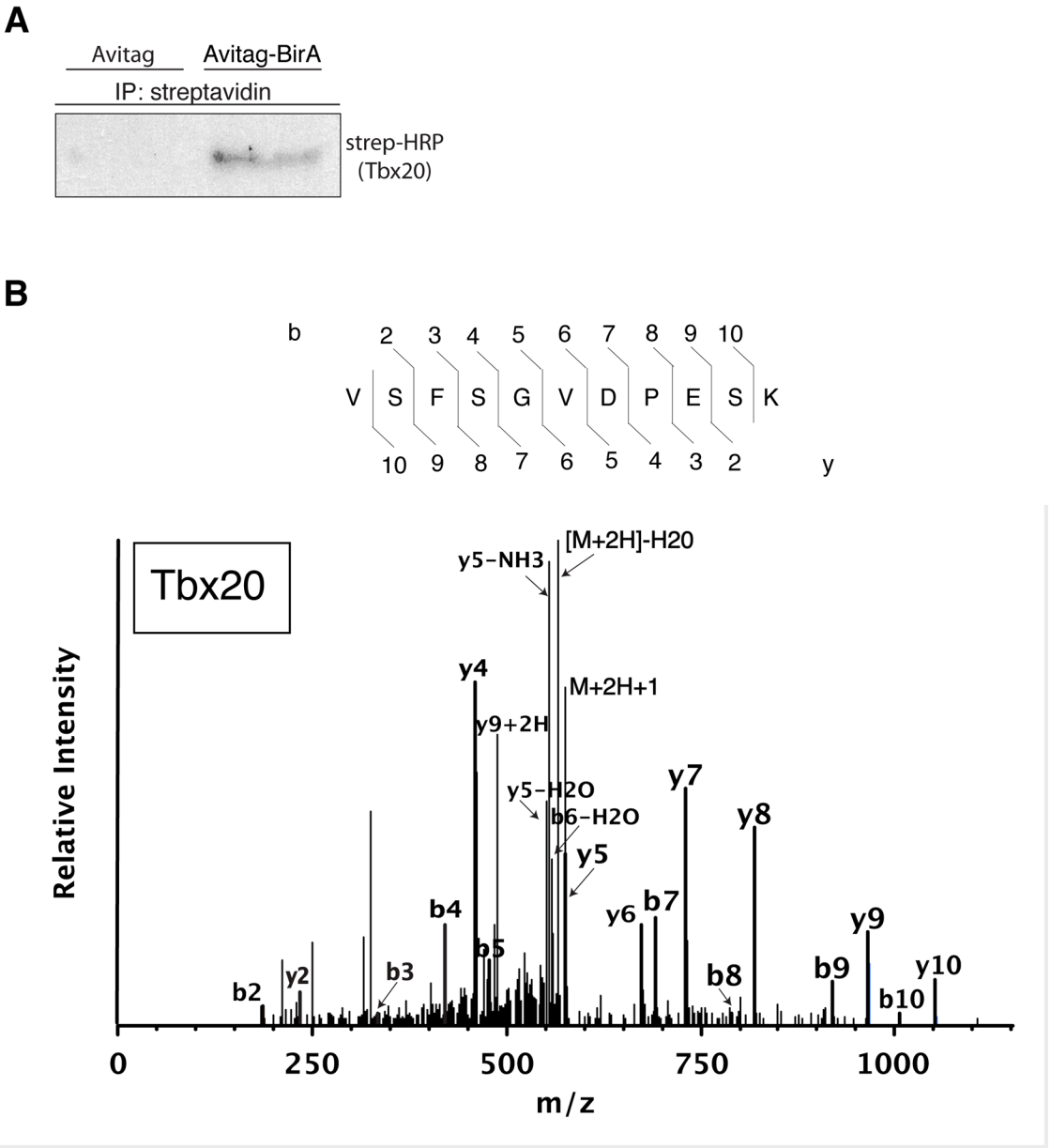

Figure 4.4. Model of the cardiac Tbx20 chromatin remodeling network. The chromatin remodeling interaction network was assembled from automated retrieval of protein functional associations using STRING analysis. Black lines represent evidence of physical binding. Blue lines represent interactions inferred by functional associations. Nodes are labeled with respective gene symbols.

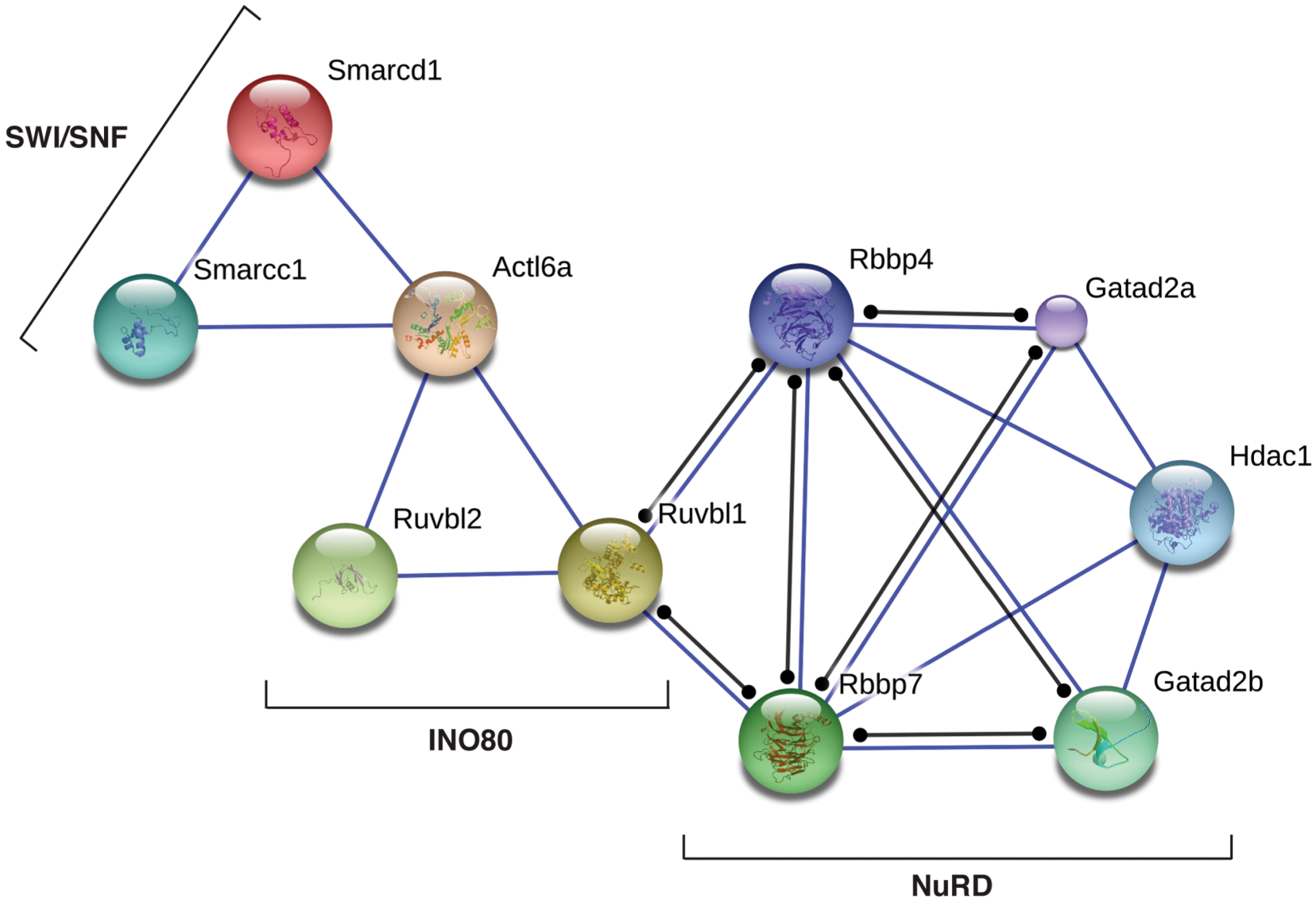
SWI/SNF
Smarcd1
Smarcc1
Actl6a
Ruvbl2
Ruvbl1
INO80
Rbbp4
Gatad2a
Hdac1
Rbbp7
Gatad2b
NuRD

Table 4.1. Tbx20 interacting proteins in cardiac progenitor cells (N=1).

Protein description	Gene name	Avitag	Avitag-BirA
		Spectrum counts	Spectrum counts
T-Box transcription factor Tbx20	**Tbx20**	**4**	**14**
GATA binding protein 4	**Gata4**	**0**	**9**
Transducin-like enhancer of split 3	**Tle3**	**0**	**3**
INO80 complex (3):		**19**	**91**
RuvB-like 1	Ruvbl1	12	34
RuvB-like 2	Ruvbl2	0	37
Actin-like protein 6A	Actl6a	7	20
NuRD complex (5):		**25**	**50**
Histone-binding protein Rbbp4	Rbbp4	11	13
Histone-binding protein Rbbp7	Rbbp7	6	9
Histone deacetylase 1	Hdac1	7	13
Transcriptional repressor p66 alpha	Gatad2a	0	7
Transcriptional repressor p66 beta	Gatad2b	1	8
SWI/SNF complex (3):		**18**	**35**
SWI/SNF complex subunit SMARCC1	Smarcc1	8	10
SWI/SNF-related matrix-associated actin-dependent regulator of chromatin subfamily D member 1	Smarcd1	3	5
Actin-like protein 6A	Actl6a	7	20

REFERENCES

Bodmer, R., Jan, L. Y. and Jan, Y. N. (1990) 'A new homeobox-containing gene, msh-2, is transiently expressed early during mesoderm formation of Drosophila', *Development* 110(3): 661-9.

Bondue, A., Tannler, S., Chiapparo, G., Chabab, S., Ramialison, M., Paulissen, C., Beck, B., Harvey, R. and Blanpain, C. (2011) 'Defining the earliest step of cardiovascular progenitor specification during embryonic stem cell differentiation', *The Journal of cell biology* 192(5): 751-65.

Brown, D. D., Martz, S. N., Binder, O., Goetz, S. C., Price, B. M., Smith, J. C. and Conlon, F. L. (2005) 'Tbx5 and Tbx20 act synergistically to control vertebrate heart morphogenesis', *Development* 132(3): 553-63.

Cai, C. L., Liang, X., Shi, Y., Chu, P. H., Pfaff, S. L., Chen, J. and Evans, S. (2003) 'Isl1 identifies a cardiac progenitor population that proliferates prior to differentiation and contributes a majority of cells to the heart', *Developmental cell* 5(6): 877-89.

Cai, C. L., Zhou, W., Yang, L., Bu, L., Qyang, Y., Zhang, X., Li, X., Rosenfeld, M. G., Chen, J. and Evans, S. (2005) 'T-box genes coordinate regional rates of proliferation and regional specification during cardiogenesis', *Development* 132(10): 2475-87.

Chakraborty, S. and Yutzey, K. E. (2012) 'Tbx20 regulation of cardiac cell proliferation and lineage specialization during embryonic and fetal development in vivo', *Developmental biology* 363(1): 234-46.

Cronan, J. E., Jr. and Reed, K. E. (2000) 'Biotinylation of proteins in vivo: a useful posttranslational modification for protein analysis', *Methods in enzymology* 326: 440-58.

Cull, M. G. and Schatz, P. J. (2000) 'Biotinylation of proteins in vivo and in vitro using small peptide tags', *Methods in enzymology* 326: 430-40.

de Boer, E., Rodriguez, P., Bonte, E., Krijgsveld, J., Katsantoni, E., Heck, A., Grosveld, F. and Strouboulis, J. (2003) 'Efficient biotinylation and single-step purification of tagged transcription factors in mammalian cells and transgenic mice', *Proceedings of the National Academy of Sciences of the United States of America* 100(13): 7480-5.

Gadue, P., Huber, T. L., Paddison, P. J. and Keller, G. M. (2006) 'Wnt and TGF-beta signaling are required for the induction of an in vitro model of primitive streak formation using embryonic stem cells', *Proceedings of the National Academy of Sciences of the United States of America* 103(45): 16806-11.

Garrels, J. I. and Gibson, W. (1976) 'Identification and characterization of multiple forms of actin', *Cell* 9(4 PT 2): 793-805.

Hang, C. T., Yang, J., Han, P., Cheng, H. L., Shang, C., Ashley, E., Zhou, B. and Chang, C. P. (2010) 'Chromatin regulation by Brg1 underlies heart muscle development and disease', *Nature* 466(7302): 62-7.

Horb, M. E. and Thomsen, G. H. (1999) 'Tbx5 is essential for heart development', *Development* 126(8): 1739-51.

Kattman, S. J., Witty, A. D., Gagliardi, M., Dubois, N. C., Niapour, M., Hotta, A., Ellis, J. and Keller, G. (2011) 'Stage-specific optimization of activin/nodal and BMP signaling promotes cardiac differentiation of mouse and human pluripotent stem cell lines', *Cell stem cell* 8(2): 228-40.

Kelley, C., Blumberg, H., Zon, L. I. and Evans, T. (1993) 'GATA-4 is a novel transcription factor expressed in endocardium of the developing heart', *Development* 118(3): 817-27.

Kraus, F., Haenig, B. and Kispert, A. (2001) 'Cloning and expression analysis of the mouse T-box gene tbx20', *Mechanisms of development* 100(1): 87-91.

Laverriere, A. C., MacNeill, C., Mueller, C., Poelmann, R. E., Burch, J. B. and Evans, T. (1994) 'GATA-4/5/6, a subfamily of three transcription factors transcribed in developing heart and gut', *The Journal of biological chemistry* 269(37): 23177-84.

Lickert, H., Takeuchi, J. K., Von Both, I., Walls, J. R., McAuliffe, F., Adamson, S. L., Henkelman, R. M., Wrana, J. L., Rossant, J. and Bruneau, B. G. (2004) 'Baf60c is essential for function of BAF chromatin remodelling complexes in heart development', *Nature* 432(7013): 107-12.

Montgomery, R. L., Davis, C. A., Potthoff, M. J., Haberland, M., Fielitz, J., Qi, X., Hill, J. A., Richardson, J. A. and Olson, E. N. (2007) 'Histone deacetylases 1 and 2 redundantly regulate cardiac morphogenesis, growth, and contractility', *Genes & development* 21(14): 1790-802.

Rottbauer, W., Saurin, A. J., Lickert, H., Shen, X., Burns, C. G., Wo, Z. G., Kemler, R., Kingston, R., Wu, C. and Fishman, M. (2002) 'Reptin and pontin antagonistically regulate heart growth in zebrafish embryos', *Cell* 111(5): 661-72.

Sakabe, N. J., Aneas, I., Shen, T., Shokri, L., Park, S. Y., Bulyk, M. L., Evans, S. M. and Nobrega, M. A. (2012) 'Dual transcriptional activator and repressor roles of TBX20 regulate adult cardiac structure and function', *Human molecular genetics* 21(10): 2194-204.

Savage, M. D., Mattson, G., Desai, S., Nielander, G. W., Morgensen, S. and Conklin, E. J. (1992) *Avidin-Biotin Chemistry: A Handbook*: Pierce Chemical Company, Rockford, IL.
Schatz, P. J. (1993) 'Use of peptide libraries to map the substrate specificity of a peptide-modifying enzyme: a 13 residue consensus peptide specifies biotinylation in Escherichia coli', *Bio/technology* 11(10): 1138-43.

Shelton, E. L. and Yutzey, K. E. (2007) 'Tbx20 regulation of endocardial cushion cell proliferation and extracellular matrix gene expression', *Developmental biology* 302(2): 376-88.

Singh, M. K., Christoffels, V. M., Dias, J. M., Trowe, M. O., Petry, M., Schuster-Gossler, K., Burger, A., Ericson, J. and Kispert, A. (2005) 'Tbx20 is essential for cardiac chamber differentiation and repression of Tbx2', *Development* 132(12): 2697-707.

Southern, E. M. (1975) 'Detection of specific sequences among DNA fragments separated by gel electrophoresis', *Journal of molecular biology* 98(3): 503-17.

Stennard, F. A., Costa, M. W., Elliott, D. A., Rankin, S., Haast, S. J., Lai, D., McDonald, L. P., Niederreither, K., Dolle, P., Bruneau, B. G. et al. (2003) 'Cardiac T-box factor Tbx20 directly interacts with Nkx2-5, GATA4, and GATA5 in regulation of gene expression in the developing heart', *Developmental biology* 262(2): 206-24.

Stennard, F. A., Costa, M. W., Lai, D., Biben, C., Furtado, M. B., Solloway, M. J., McCulley, D. J., Leimena, C., Preis, J. I., Dunwoodie, S. L. et al. (2005) 'Murine T-box transcription factor Tbx20 acts as a repressor during heart development, and is essential for adult heart integrity, function and adaptation', *Development* 132(10): 2451-62.

Takeuchi, J. K., Lou, X., Alexander, J. M., Sugizaki, H., Delgado-Olguin, P., Holloway, A. K., Mori, A. D., Wylie, J. N., Munson, C., Zhu, Y. et al. (2011) 'Chromatin remodelling complex dosage modulates transcription factor function in heart development', *Nature communications* 2: 187.

Takeuchi, J. K., Mileikovskaia, M., Koshiba-Takeuchi, K., Heidt, A. B., Mori, A. D., Arruda, E. P., Gertsenstein, M., Georges, R., Davidson, L., Mo, R. et al. (2005) 'Tbx20 dose-dependently regulates transcription factor networks required for mouse heart and motoneuron development', *Development* 132(10): 2463-74.

Toyota, N. and Shimada, Y. (1981) 'Differentiation of troponin in cardiac and skeletal muscles in chicken embryos as studied by immunofluorescence microscopy', *The Journal of cell biology* 91(2 Pt 1): 497-504.

Chapter 5

Discussion and Future Directions

The formation of the 4-chambered vertebrate heart arises from a series of complex processes during embryonic development that includes the specification and differentiation of the different cardiac cell types within the heart, proliferation, and morphological movements of the early heart fields (Harvey, 2002; Buckingham et al., 2005; Evans et al., 2010). These processes are directed through the activity of a number of critical cardiogenic transcription factors that act combinatorially to promote proper heart growth and specialization (Sepulveda et al., 1998; Morin et al., 2000; Hiroi et al., 2001; Stennard et al., 2003; Vincentz et al., 2008; Junion et al., 2012). One of these factors, Tbx20, is critical for heart development; however, there are huge deficiencies in our understanding of how Tbx20 activity is regulated during cardiogenesis. This dissertation comprises a set of studies that investigates the Tbx20 transcription network. *Tbx20* cardiac expression during chamber maturation in the embryo is directly regulated by BMP signaling. In an effort to identify the mechanisms by which Tbx20 regulates downstream gene targets during heart development, we employed two proteomic screens to characterize the composition of Tbx20 transcription complexes. From these screens, we observed that Tbx20

recruits multiple transcriptional co-repressors and chromatin remodeling complexes, thus laying the foundation for a much expanded Tbx20 transcription network that encompasses multiple mechanisms of activation and repression.

Tbx20 cardiac expression is regulated by BMP signaling

In Chapter 2, we identify a *Xenopus* Tbx20 cardiac enhancer that acts downstream of BMP signaling in the embryonic heart. Interestingly, this enhancer is critical for the maintenance of Tbx20 expression in the heart at a time when the cardiac chambers are undergoing specialization and expansion, processes that are arrested in the absence of Tbx20 function (Cai et al., 2005; Singh et al., 2005). This finding implicates the BMP pathway as a critical source of signaling for proper chamber maturation, and furthermore, suggests that the initiation of Tbx20 expression in cardiac progenitor cells occurs independently of the BMP-responsive cardiac enhancer we identified. Consistent with this set of studies, Zhang et al. (Zhang et al., 2011) observed that *Tbx20* is a downstream target of BMP10 during ventricular wall development and maturation in the mouse. Additionally, the investigators observed that the effect of *BMP10* overexpression on *Tbx20* expression was limited to ventricular cardiomyocytes; *Tbx20* expression in the atria and atrioventricular cushions was unaffected by changes in BMP10 levels in the heart. An earlier report in chicken embryo explants demonstrated that *Tbx20* expression in the endocardial cushions is up-regulated by BMP2 (Shelton and Yutzey, 2007). Collectively, these studies suggest that signaling through the BMP arm of the TGFα superfamily represents a key signaling pathway in the regulation of

Tbx20 expression in the heart. The precise tissue and temporal specificity of *Tbx20* expression may be regulated by the differential expression of various BMP ligands within the developing heart and their ability to bind distinct *Tbx20* regulatory elements. As such, it will be interesting to identify the endogenous ligand, perhaps a BMP ligand, that lies upstream of *Tbx20* activation within cardiac progenitor cells.

A role for Groucho/TLE in cardiac development

Chapter 3 details the identification of a Tbx20 transcription repression network in HEK 293 cells that includes an intact TLE-HDAC co-repressor complex. Tbx20 binds TLE1/3 through an N-terminal eh1 binding motif; binding of Tbx20 to TLE results in recruitment of HDAC2 to the protein complex. We additionally verified that Tbx20 forms a complex with TLE factors in vivo in the developing heart, and in ESC-derived cardiac progenitors. These studies imply that Groucho/TLE factors have a role in transcriptional repression in the embryonic heart by interacting with Tbx20. The eh1 binding motif has been identified in a number of other T-box factors (Copley, 2005), some of which have important roles in cardiovascular development including *Tbx2*, *Tbx3*, and *Tbx18* (Harrelson et al., 2004; Hoogaars et al., 2004; Christoffels et al., 2006). Therefore, Tbx20-mediated recruitment of a TLE co-repressor complex may represent a more global mechanism of repression utilized by T-box factors during heart development.

The *Drosophila Groucho* gene was originally named for the bunches of bristles above the eyes that result from a viable mutation within the *Enhancer of split*

complex, a chromosomal region that gives rise to 13 separate transcripts including members of the bHLH family of transcription factors (also known as Hairy-related proteins) (Lindsley and Grell, 1968; Knust et al., 1992). Hairy-related proteins play critical roles during neurogenesis by repressing target genes when bound to Groucho (Paroush et al., 1994; Fisher et al., 1996). Groucho was subsequently demonstrated to act as a transcriptional co-repressor when bound to other subsets of DNA binding factors including Runt domain proteins Engrailed and Dorsal (Dubnicoff et al., 1997; Jimenez et al., 1997). Therefore, Groucho proteins are recruited to target promoters by binding to sequence specific transcription factors.

The four vertebrate homologues of *Drosophila Gro* are termed *transducin-like enhancer of split* (*TLE*) *1-4* due to homology with the β subunit of transducin, a heterotrimeric G protein (Stifani et al., 1992). A fifth member of the TLE family encodes the closely related Amino Enhancer of split (Aes) (Miyasaka et al., 1993). Aes is highly similar to the amino terminal domains of other TLE proteins but lacks the C-terminal WD-40 repeats that mediate interaction with DNA-binding proteins (Miyasaka et al., 1993). Aes does harbor the Q-domain, a multimerization motif that facilitates interactions with other Groucho members (Miyasaka et al., 1993; Pinto and Lobe, 1996; Chen and Courey, 2000). Aes proteins can antagonize TLE-mediated repression in a dominant negative manner by binding to Gro/TLE through the Q domain (Muhr et al., 2001; Swingler et al., 2004). Binding of Aes proteins to Gro/TLE also blunts repressive function of Gro proteins, as Aes does not interact with HDACs (Brantjes et al., 2001). *TLE1-4* are expressed broadly throughout

mouse development; however, individual TLE proteins are expressed in combinatorial as well as complementary patterns during cell differentiation suggesting non-redundant functions (Stifani et al., 1992; Yao et al., 1998; Gasperowicz and Otto, 2005). Further studies support this and demonstrate that TLE proteins having distinct functions during development, TLE1 is involved in myogenesis, hematopoiesis, neurogenesis, and eye development (Imai et al., 1998; Yao et al., 2000; Gao et al., 2001; Zhu et al., 2002; Swingler et al., 2004); TLE2 in osteogenesis (Thirunavukkarasu et al., 1998); TLE3 in placental and adipose development (Nakayama et al., 1997; Villanueva et al., 2011); and TLE4 in B cell development and left-right asymmetry (Eberhard et al., 2000; Linderson et al., 2004; Bajoghli et al., 2007).

Of the TLE family members, TLE4 in the only TLE protein previously linked to heart development (Bajoghli et al., 2005; Bajoghli et al., 2007). Misexpression of *Aes* to block Groucho co-repressor function in medaka embryos results in an alteration in heart tube orientation (Bajoghli et al., 2005; Bajoghli et al., 2007). Interestingly, *TLE4* misexpression also leads to cardiac laterality defects (Bajoghli et al., 2007). *Nkx2.5* is expressed normally in these embryos, indicating that heart looping defects are not secondary to a disruption in cardiac specification. *Aes*- and *TLE4*- injected embryos also display displacements of other visceral organs in including the spleen, gallbladder and gut indicating a general disruption of embryonic left-right patterning rather than a cardiac-specific defect (Bajoghli et al., 2007). Indeed, the first visible symmetry break in the embryo occurs when the symmetrical heart tube undergoes a

rightward looping (Mercola, 1999). In the medaka fish, *TLE4* appears to affect left-right patterning of the embryo by both regulating *Brachyury* expression within the dorsal forerunner cells that give rise to Kupffer's vesicle and by regulating the asymmetric activities of the *Nodal* and *Lefty* genes later in embryogenesis (Bajoghli et al., 2007). A cell autonomous role for Groucho proteins within cardiac cells of the developing heart has not yet been established.

Evidence suggests that Gro/TLE proteins mediate transcriptional repression through a number of mechanisms. It has long been known that both *Drosophila* and mammalian Gro/TLE proteins interact with class I histone deacetylases (Chen et al., 1999; Brantjes et al., 2001). Additional studies in *Drosophila* demonstrate that histone deacetylase activity is required for efficient repression by Gro, and mutations in *Gro* and *Rpd3* have synergistic effects on embryonic development (Chen et al., 1999). Further, inhibition of histone deacetylase activity by trichostatin A (TSA) treatment results in a loss of Gro-mediated transcriptional repression by the homeodomain protein NK-3 (Choi et al., 1999). A recent study demonstrates that Gro colocalizes with Rpd3 on a target gene, and this colocalization is associated with deacetylation of lysines in the histone tails of H3 and H4 (Winkler et al., 2010). A decrease in acetylation levels leads to increased nucleosome density and therefore transcriptional repression (Winkler et al., 2010). Interestingly, in all of these studies, histone deacetylase inhibition, either by TSA treatment or RNAi knockdown of *Rpd3* in *Drosophila* cells, does not result in a complete loss of Gro-mediated repression indicating that Gro may utilize histone deacetylase-independent

mechanisms of silencing (Chen et al., 1999; Choi et al., 1999; Winkler et al., 2010). Further, *Rpd3* mutants display relatively mild defects in embryogenesis, again suggesting that Gro proteins do not function solely through recruitment of histone deacetylases (Mannervik and Levine, 1999).

One line of evidence indicates that Groucho proteins oligomerize along areas of the genome to promote a silent chromatin structure (Chen et al., 1998; Sekiya and Zaret, 2007; Martinez and Arnosti, 2008; Winkler et al., 2010). A role for Groucho oligomerization was first implicated by the observation that native Gro forms a tetramer in solution; point mutations that block tetramerization of Gro also block repression by Gro in cultured *Drosophila* cells (Chen et al., 1998). Recent studies have shown that Gro contacts a large region of chromatin consisting of several kilobases suggesting that Gro oligomers may modify chromatin over extensive regions (Sekiya and Zaret, 2007; Martinez and Arnosti, 2008). Further, the formation of higher order Gro/TLE oligomers that blanket a genomic region seems to result in a condensation of the chromatin, which functions to impair activator recruitment (Sekiya and Zaret, 2007). Collectively, these studies support a model of Groucho repression in which 1) Groucho/TLE is recruited to a target gene through interaction with a sequence-specific transcription factor, 2) Gro/TLE recruits a histone deacetylase complex, which deacetylates local histone tails leading to a more closed chromatin configuration, and 3) Gro/TLE simultaneously recruits additional Gro/TLE subunits to form higher order Gro complexes across the genomic region, resulting in further condensing the chromatin and blocking activator access to the template.

T-box factors are critical drivers of distinct subprograms during cardiac development (Bruneau et al., 2001; Harrelson et al., 2004; Brown et al., 2005; Christoffels et al., 2006; Mesbah et al., 2008; Wiese et al., 2009; Scambler, 2010); however, there are still large gaps in our understanding of the precise mechanisms by which T-box proteins mediate transcriptional activation or repression. In particular, very little is known about how T-box factors act as repressors due to a lack of knowledge regarding T-box protein associations with known co-repressors and a dearth of direct transcriptional targets. Our studies have identified a role for a Groucho/TLE-Hdac complex in Tbx20-mediated transcriptional repression. Repression by the T-box factor Tbx18 also relies on binding to Groucho proteins (Farin et al., 2007). Interestingly, we identified Tbx18 as part of a TLE-recruited repression complex. The biological relevance of a Tbx20-Tbx18 repressor complex is unclear due to limited regions of coexpression; however, this finding testifies to the potential of T-box factors to form Groucho repression complexes. Heterodimerization with other T-box factors may serve to increase target site specificity.

The T-box factors Tbx2 and Tbx3 act as transcriptional repressors and contain a highly conserved eh1 domain (Lingbeek et al., 2002; Copley, 2005; Yarosh et al., 2008), implying the potential to form Groucho repression complexes. Additionally, Tbx3 interacts with Hdac1, 2, 3, and 5 in primary breast cancer cells, and Tbx3 repressive function in these cells requires HDAC activity (Yarosh et al., 2008). Class I Hdacs have a well-established role in heart development and function indicating that histone deacetylation is crucial for proper transcriptional control of

heart development (Montgomery et al., 2007; Montgomery et al., 2008; Trivedi et al., 2008; Trivedi et al., 2010). These studies strongly imply that formation of TLE-HDAC complexes may represent a significant repression mechanism for T-box factors in the developing heart. Additional studies are needed to examine the roles of individual TLE family members in heart development to determine if there is functional redundancy among TLE proteins in the heart, or if there are distinct requirements for individual TLEs within specific cardiac regions.

Tbx20 is part of a broad chromatin remodeling network in the heart

Our studies demonstrate for the first time that Tbx20 interacts with components of multiple chromatin remodeling complexes in cardiac cells. The chromatin remodeling network includes the INO80 complex, NuRD complex, and the SWI/SNF complex. As previously described, the INO80 complex has been implicated in heart development in one report, which showed that it is required for the regulation of cardiac growth in zebrafish (Rottbauer et al., 2002). This is first report of an interaction between a cardiac transcription factor and components of the INO80, providing a plausible mechanism for targeting INO80 activity in the developing heart. The similarity in the proliferation phenotypes resulting from *Tbx20* gain-of-function mutations and the activating mutation in *Reptin* (*Ruvbl2*) suggest that a Tbx20-INO80 complex regulates embryonic cardiomyocyte proliferation in the forming heart (Rottbauer et al., 2002; Chakraborty and Yutzey, 2012).

SWI/SNF complexes have a well-established role in heart development (Lickert et al., 2004; Wang et al., 2004; Stankunas et al., 2008; Takeuchi and Bruneau, 2009; Hang et al., 2010; Takeuchi et al., 2011). SWI/SNF complexes are thought to potentiate transcription factor activation of cardiac genes through nucleosome mobilization that permits the binding of factors to DNA template. A genetic interaction between *Tbx20* and BAF complex member *Brg1* has previously been demonstrated (Takeuchi et al., 2011); however, this is the first demonstration of a physical interaction between Tbx20 and members of the SWI/SNF. Other cardiac transcription factors including Tbx5, Nkx2.5, and Gata4 have been shown to physically interact with Brg1 (Takeuchi et al., 2011). Interestingly, we also identified Gata4 as a Tbx20-associated protein in ESC-derived cardiac progenitors, providing further evidence of protein complexes that contain a complement of cardiac transcription factors and SWI/SNF components. These studies provide further support for a model of heart-specific chromatin activation through interactions of cardiac transcription factors with BAF complexes.

An exciting and novel finding of this work was the demonstration of a Tbx20-NuRD association in human cells and ESC-derived cardiac progenitors. The NuRD complex is associated with histone deacetylase activity and functions as a transcriptional repressor (Xue et al., 1998). The defining components of the NuRD complex, as determined by multiple independent purifications, include an Mi-2 chromatin remodeling subunit, an Mbd3 subunit, and an Mta subunit (Tong et al., 1998; Wade et al., 1998; Xue et al., 1998; Zhang et al., 1998). Mta subunits (Mta1,

2, or 3) are mutually exclusive and contribute to functional diversity of the NuRD complex (Yao and Yang, 2003; Fujita et al., 2004). Mbd3 protein, although highly homologous to the mCpG-binding protein Mbd2, does not appear to bind mCpG directly indicating that another factor is required for localization of the NuRD complex to DNA template (Saito and Ishikawa, 2002). NuRD also contains a core histone deacetylase complex that traditionally includes Hdac1, Hdac2, Rbbp4 (RbAp46), and Rbbp7 (RbAp48) (Tong et al., 1998; Wade et al., 1998; Xue et al., 1998; Zhang et al., 1998). The chromatin remodeling activity of Mi-2 may allow the deacetylases access to the histone tails. The Gatad2a (p66α) and Gatad2b (p66β) proteins are also associated with NuRD. We have demonstrated that Tbx20 interacts with many components of the mammalian NuRD complex in ESC-derived cardiac progenitor cells.

The role of the NuRD complex in embryonic development has been assessed by looking at the requirement for NuRD components during early development. *Drosophila* Mi-2 is critical for HOX gene repression during embryo patterning (Kehle et al., 1998). A requirement for NuRD in early cell fate decisions was demonstrated by the observation that ablation of *Mbd3* in the mouse is embryonic lethal at E5.5 (Hendrich et al., 2001). Subsequent studies demonstrate a requirement for Mbd3 for proper differentiation of ES cells to a variety of cell fates, indicating that the NuRD complex creates an epigenetic state in ES cells that allows for commitment to certain lineages (Kaji et al., 2006). *Gatad2a* null mice live substantially longer than the *Mbd3* null mice but die at around E10.5 with a range of developmental defects that

includes a severe delay in development (Marino and Nusse, 2007). The early requirement for the NuRD complex in embryonic development has prevented the identification of a role for the NuRD complex specifically within the developing heart. As such, it would be interesting to investigate the phenotypes that arise from conditional deletion of NuRD components specifically within the heart. Nonetheless, we have demonstrated that Tbx20 recruits the NuRD complex in ESC-derived cardiac progenitor cells implicating the NuRD complex in transcriptional control of cardiac differentiation and/or proliferation.

Taken together, these studies implicate Tbx20 as a critical dual activator and repressor of target gene expression during heart development and demonstrate that Tbx20 interacts with a number of repressor and chromatin remodeling complexes to ensure proper transcriptional regulation of target genes. Additionally, our data indicate that proper control of Tbx20 target gene expression occurs through selective association with distinct transcription complexes. It will be of great interest to determine the relationship between individual Tbx20 target genes and the unique transcription complexes we have identified.

Future Directions

It is clear from a number of studies that Tbx20 acts to direct multiple critical processes throughout cardiogenesis, including fetal cardiomyocyte proliferation, cardiac chamber maturation, and adult cardiomyocyte function (Brown et al., 2005; Cai et al., 2005; Shen et al., 2011; Chakraborty and Yutzey, 2012). We speculate

then that Tbx20 transcriptional activity is mediated through temporal interactions with unique transcription complexes during cardiomyocyte development. Our studies have thus far established association of Tbx20 with a number of repression and chromatin remodeling complexes, one of which- a TLE repressor complex- is assembled in cardiac progenitor cells and not differentiated cardiomyocytes, providing one example of a Tbx20 transcription complex that is temporally regulated during cardiomyocyte differentiation. It will be interesting to define the temporal core components of the other Tbx20 transcription complexes we have identified over the course of cardiomyocyte differentiation and to investigate the requirements for those interactions during distinct developmental windows. Together, these investigations will define the components of Tbx20 transcription complexes more fully during cardiac development and delineate the effects of assembling distinct transcription complexes on Tbx20 function in cardiomyocytes.

In addition to defining the role of various Tbx20 transcription complexes in heart development, it will be critical to link the activity of these complexes to Tbx20 target gene expression in the embryo. Very few direct targets of Tbx20 in the embryo have been identified, and this hinders our understanding of the precise gene programs regulated by Tbx20 during heart development. The identification of Tbx20 target genes has been hampered by a lack of ChIP-grade antibodies against Tbx20. However, we have presented the generation of a novel mouse ESC line that has been genetically modified to have a *Tbx20* allele tagged with the Avitag. This cell line, in addition to being highly amenable to systems based proteomics approaches,

will also allow us to perform chromatin immunoprecipitation followed by high throughput sequencing of Tbx20-DNA complexes over the course of cardiomyocyte differentiation. To complement this work, it would be interesting to determine the overlap between Tbx20 target genes and the target sites of distinct transcription complexes known to associate with Tbx20. Taken together, these studies will allow us to generate a genomic-proteomic profile of Tbx20 during cardiomyocyte differentiation.

The T-box family of transcription factors is an evolutionary ancient family of proteins that have expanded from the founding T-box member, Brachyury (Naiche et al., 2005). The expansion of the T-box family coincided with the divergence of T-box factor functions such that *T-box* genes now regulate multiple developmental processes in a wide range of tissues and organs. Early approaches to understand how T-box genes function demonstrated that most T-box proteins act as transcriptional activators (Kispert et al., 1995; Conlon et al., 1996; Zhang and King, 1996); however, recent work by our laboratory and others have since confirmed that T-box proteins function as both activators and repressors (Lingbeek et al., 2002; Cai et al., 2005; Singh et al., 2005; Stennard et al., 2005; Farin et al., 2007). Studies on the function of T-box proteins during development are consistent with a general role for the T-box family in cell specification and differentiation (Naiche et al., 2005). The mechanisms by which these closely related genes exert different effects during embryogenesis is not well understood; however, the unique function of each T-box factor is likely dictated by the stage of development, the tissue-restricted gene

expression of each factor, and the specific target genes of each factor. The common evolutionary history of T-box genes and their similar functions during embryogenesis suggests that T-box factors likely employ similar mechanisms of gene regulation. Therefore, the Tbx20 chromatin remodeling network we have identified may represent a core interaction network that is crucial to the function of all T-box factors. Future investigations will seek to reveal the proteomic profiles of other T-box factors to determine if the findings outlined here represent a global T-box interaction network. Additionally, it will be interesting to determine if chromatin remodeling is an evolutionarily conserved mechanism of T-box gene regulation by examining T-box protein interactions in invertebrates like *Drosophila* and *Caenorhabditis elegans*, which have 8 and 20 T-box members, respectively (Pflugfelder et al., 1992; Kispert et al., 1994; Agulnik et al., 1995; Plageman and Yutzey, 2005).

In conclusion, these studies have provided important insight into the mechanisms by which Tbx20 acts to regulate transcription within the vertebrate heart. In addition, it represents the first unbiased assessment of Tbx20 protein-protein interactions, which has contributed greatly to our understanding of the Tbx20 transcription network. Many of our findings, most notably that of a Tbx20-TLE-HDAC repressor complex, likely represent global mechanisms of transcriptional regulation used by other cardiac transcription factors, particularly other cardiac T-box factors. Our current understanding of the precise components of the gene programs regulated by cardiac transcription factors is limited due to a paucity of information regarding the direct embryonic gene targets of cardiac transcription factors;

however, it is likely that many cardiac transcription factors regulate common sets of genes. *ANF* is an example of a cardiac gene that is regulated by many individual cardiac transcription factors (Durocher et al., 1996; Lee et al., 1998; Morin et al., 2000; Small and Krieg, 2003; Plageman and Yutzey, 2004). As such, it is likely that cardiac transcription factors employ many of the same protein complexes to regulate downstream transcription. For instance, multiple T-box factors employ a TLE repressor complex (Farin et al., 2007), and several cardiac transcription factors are known to interact with the SWI/SNF complex (Takeuchi et al., 2011). Therefore, the Tbx20 protein-protein interactions we have identified here likely represent complexes that are critical for the activity of a number of transcription factors in the heart on diverse sets of target genes. However, it is important to note that mutation or misregulation of one cardiac transcription is sufficient to lead to congenital heart disease indicating that each factor also has a unique requirement during heart development. Therefore, it will be critical to repeat the studies outlined in this thesis for all members of the cardiac transcription factor collective to gain a comprehensive understanding of the players involved in embryonic heart patterning and congenital heart disease. Finally, Tbx20 has recently been shown to contribute to heart function and disease in adults (Shen et al., 2011) indicating that our findings are likely to extend to the role of Tbx20 in regulating genetic programs postnatally and in the adult heart.

Most importantly, the identification of novel determinants of Tbx20 activity through the comprehensive proteomics studies outlined in this thesis will yield

additional candidate genes associated with human congenital heart disease and lead to a greater understanding of how Tbx20 contributes to congenital heart disease. As previously mentioned, future studies seeking to identify the embryonic gene targets and the protein interactome for each individual cardiac transcription factor will lead to an even more comprehensive list of potential risk factors for congenital heart disease. Why is this so critical, and how will these findings improve our treatment of congenital heart defects in human patients? Currently, congenital heart malformations are treated primarily through surgical repair of the malformed region. As such, early detection of these malformations in the newborn is critical to avoid mortality, morbidity, and handicap. Despite this, heart disease goes unrecognized in newborn babies in more than half of those with congenital cardiac malformations due to the fact that many infants with heart defects are asymptomatic at birth (Richmond and Wren, 2001). Some of the most dangerous diagnoses, such as left ventricular outflow tract obstructions, become symptomatic only once they are established on a rapidly deteriorating course that can lead to death in mere hours (Abu-Harb et al., 1994). In the age of genomics, it is now possible to detect genetic risk factors early in pregnancy, well before physical signs of disease arise, leading to a more detailed assessment of fetal heart health. Therefore, the challenge presented to us is, in many ways, a problem of numbers. We simply do not know many of the players involved in the transcriptional control of heart patterning. My thesis work seeks to address this deficiency and has revealed previously unknown components of the cardiac transcription network that are likely to be important in heart development, function, and disease. In the future, the identification of additional risk

factors for congenital heart disease must be one of critical importance for both a better understanding of the biology of heart development, as well as for the improvement in our ability to detect disruptions in this process.

REFERENCES

Abu-Harb, M., Wyllie, J., Hey, E., Richmond, S. and Wren, C. (1994) 'Presentation of obstructive left heart malformations in infancy', *Archives of disease in childhood. Fetal and neonatal edition* 71(3): F179-83.

Agulnik, S. I., Bollag, R. J. and Silver, L. M. (1995) 'Conservation of the T-box gene family from Mus musculus to Caenorhabditis elegans', *Genomics* 25(1): 214-9.

Bajoghli, B., Aghaallaei, N. and Czerny, T. (2005) 'Groucho corepressor proteins regulate otic vesicle outgrowth', *Developmental dynamics : an official publication of the American Association of Anatomists* 233(3): 760-71.

Bajoghli, B., Aghaallaei, N., Soroldoni, D. and Czerny, T. (2007) 'The roles of Groucho/Tle in left-right asymmetry and Kupffer's vesicle organogenesis', *Developmental biology* 303(1): 347-61.

Brantjes, H., Roose, J., van De Wetering, M. and Clevers, H. (2001) 'All Tcf HMG box transcription factors interact with Groucho-related co-repressors', *Nucleic acids research* 29(7): 1410-9.

Brown, D. D., Martz, S. N., Binder, O., Goetz, S. C., Price, B. M., Smith, J. C. and Conlon, F. L. (2005) 'Tbx5 and Tbx20 act synergistically to control vertebrate heart morphogenesis', *Development* 132(3): 553-63.

Bruneau, B. G., Nemer, G., Schmitt, J. P., Charron, F., Robitaille, L., Caron, S., Conner, D. A., Gessler, M., Nemer, M., Seidman, C. E. et al. (2001) 'A murine model of Holt-Oram syndrome defines roles of the T-box transcription factor Tbx5 in cardiogenesis and disease', *Cell* 106(6): 709-21.

Buckingham, M., Meilhac, S. and Zaffran, S. (2005) 'Building the mammalian heart from two sources of myocardial cells', *Nature reviews. Genetics* 6(11): 826-35.

Cai, C. L., Zhou, W., Yang, L., Bu, L., Qyang, Y., Zhang, X., Li, X., Rosenfeld, M. G., Chen, J. and Evans, S. (2005) 'T-box genes coordinate regional rates of proliferation and regional specification during cardiogenesis', *Development* 132(10): 2475-87.

Chakraborty, S. and Yutzey, K. E. (2012) 'Tbx20 regulation of cardiac cell proliferation and lineage specialization during embryonic and fetal development in vivo', *Developmental biology* 363(1): 234-46.

Chen, G. and Courey, A. J. (2000) 'Groucho/TLE family proteins and transcriptional repression', *Gene* 249(1-2): 1-16.

Chen, G., Fernandez, J., Mische, S. and Courey, A. J. (1999) 'A functional interaction between the histone deacetylase Rpd3 and the corepressor groucho in Drosophila development', *Genes & development* 13(17): 2218-30.

Chen, G., Nguyen, P. H. and Courey, A. J. (1998) 'A role for Groucho tetramerization in transcriptional repression', *Molecular and cellular biology* 18(12): 7259-68.

Choi, C. Y., Kim, Y. H., Kwon, H. J. and Kim, Y. (1999) 'The homeodomain protein NK-3 recruits Groucho and a histone deacetylase complex to repress transcription', *The Journal of biological chemistry* 274(47): 33194-7.

Christoffels, V. M., Mommersteeg, M. T., Trowe, M. O., Prall, O. W., de Gier-de Vries, C., Soufan, A. T., Bussen, M., Schuster-Gossler, K., Harvey, R. P., Moorman, A. F. et al. (2006) 'Formation of the venous pole of the heart from an Nkx2-5-negative precursor population requires Tbx18', *Circulation research* 98(12): 1555-63.

Conlon, F. L., Sedgwick, S. G., Weston, K. M. and Smith, J. C. (1996) 'Inhibition of Xbra transcription activation causes defects in mesodermal patterning and reveals autoregulation of Xbra in dorsal mesoderm', *Development* 122(8): 2427-35.

Copley, R. R. (2005) 'The EH1 motif in metazoan transcription factors', *BMC genomics* 6: 169.

Dubnicoff, T., Valentine, S. A., Chen, G., Shi, T., Lengyel, J. A., Paroush, Z. and Courey, A. J. (1997) 'Conversion of dorsal from an activator to a repressor by the global corepressor Groucho', *Genes & development* 11(22): 2952-7.

Durocher, D., Chen, C. Y., Ardati, A., Schwartz, R. J. and Nemer, M. (1996) 'The atrial natriuretic factor promoter is a downstream target for Nkx-2.5 in the myocardium', *Molecular and cellular biology* 16(9): 4648-55.

Eberhard, D., Jimenez, G., Heavey, B. and Busslinger, M. (2000) 'Transcriptional repression by Pax5 (BSAP) through interaction with corepressors of the Groucho family', *The EMBO journal* 19(10): 2292-303.

Evans, S. M., Yelon, D., Conlon, F. L. and Kirby, M. L. (2010) 'Myocardial lineage development', *Circulation research* 107(12): 1428-44.

Farin, H. F., Bussen, M., Schmidt, M. K., Singh, M. K., Schuster-Gossler, K. and Kispert, A. (2007) 'Transcriptional repression by the T-box proteins Tbx18 and Tbx15 depends on Groucho corepressors', *The Journal of biological chemistry* 282(35): 25748-59.

Fisher, A. L., Ohsako, S. and Caudy, M. (1996) 'The WRPW motif of the hairy-related basic helix-loop-helix repressor proteins acts as a 4-amino-acid transcription repression and protein-protein interaction domain', *Molecular and cellular biology* 16(6): 2670-7.

Fujita, N., Jaye, D. L., Geigerman, C., Akyildiz, A., Mooney, M. R., Boss, J. M. and Wade, P. A. (2004) 'MTA3 and the Mi-2/NuRD complex regulate cell fate during B lymphocyte differentiation', *Cell* 119(1): 75-86.

Gao, X., Chandra, T., Gratton, M. O., Quelo, I., Prud'homme, J., Stifani, S. and St-Arnaud, R. (2001) 'HES6 acts as a transcriptional repressor in myoblasts and can induce the myogenic differentiation program', *The Journal of cell biology* 154(6): 1161-71.

Gasperowicz, M. and Otto, F. (2005) 'Mammalian Groucho homologs: redundancy or specificity?', *Journal of cellular biochemistry* 95(4): 670-87.

Hang, C. T., Yang, J., Han, P., Cheng, H. L., Shang, C., Ashley, E., Zhou, B. and Chang, C. P. (2010) 'Chromatin regulation by Brg1 underlies heart muscle development and disease', *Nature* 466(7302): 62-7.

Harrelson, Z., Kelly, R. G., Goldin, S. N., Gibson-Brown, J. J., Bollag, R. J., Silver, L. M. and Papaioannou, V. E. (2004) 'Tbx2 is essential for patterning the atrioventricular canal and for morphogenesis of the outflow tract during heart development', *Development* 131(20): 5041-52.

Harvey, R. P. (2002) 'Patterning the vertebrate heart', *Nature reviews. Genetics* 3(7): 544-56.

Hendrich, B., Guy, J., Ramsahoye, B., Wilson, V. A. and Bird, A. (2001) 'Closely related proteins MBD2 and MBD3 play distinctive but interacting roles in mouse development', *Genes & development* 15(6): 710-23.

Hiroi, Y., Kudoh, S., Monzen, K., Ikeda, Y., Yazaki, Y., Nagai, R. and Komuro, I. (2001) 'Tbx5 associates with Nkx2-5 and synergistically promotes cardiomyocyte differentiation', *Nature genetics* 28(3): 276-80.

Hoogaars, W. M., Tessari, A., Moorman, A. F., de Boer, P. A., Hagoort, J., Soufan, A. T., Campione, M. and Christoffels, V. M. (2004) 'The transcriptional repressor Tbx3 delineates the developing central conduction system of the heart', *Cardiovascular research* 62(3): 489-99.

Imai, Y., Kurokawa, M., Tanaka, K., Friedman, A. D., Ogawa, S., Mitani, K., Yazaki, Y. and Hirai, H. (1998) 'TLE, the human homolog of groucho, interacts with AML1 and acts as a

repressor of AML1-induced transactivation', *Biochemical and biophysical research communications* 252(3): 582-9.

Jimenez, G., Paroush, Z. and Ish-Horowicz, D. (1997) 'Groucho acts as a corepressor for a subset of negative regulators, including Hairy and Engrailed', *Genes & development* 11(22): 3072-82.

Junion, G., Spivakov, M., Girardot, C., Braun, M., Gustafson, E. H., Birney, E. and Furlong, E. E. (2012) 'A transcription factor collective defines cardiac cell fate and reflects lineage history', *Cell* 148(3): 473-86.

Kaji, K., Caballero, I. M., MacLeod, R., Nichols, J., Wilson, V. A. and Hendrich, B. (2006) 'The NuRD component Mbd3 is required for pluripotency of embryonic stem cells', *Nature cell biology* 8(3): 285-92.

Kehle, J., Beuchle, D., Treuheit, S., Christen, B., Kennison, J. A., Bienz, M. and Muller, J. (1998) 'dMi-2, a hunchback-interacting protein that functions in polycomb repression', *Science* 282(5395): 1897-900.

Kispert, A., Herrmann, B. G., Leptin, M. and Reuter, R. (1994) 'Homologs of the mouse Brachyury gene are involved in the specification of posterior terminal structures in Drosophila, Tribolium, and Locusta', *Genes & development* 8(18): 2137-50.

Kispert, A., Koschorz, B. and Herrmann, B. G. (1995) 'The T protein encoded by Brachyury is a tissue-specific transcription factor', *The EMBO journal* 14(19): 4763-72.

Knust, E., Schrons, H., Grawe, F. and Campos-Ortega, J. A. (1992) 'Seven genes of the Enhancer of split complex of Drosophila melanogaster encode helix-loop-helix proteins', *Genetics* 132(2): 505-18.

Lee, Y., Shioi, T., Kasahara, H., Jobe, S. M., Wiese, R. J., Markham, B. E. and Izumo, S. (1998) 'The cardiac tissue-restricted homeobox protein Csx/Nkx2.5 physically associates with the zinc finger protein GATA4 and cooperatively activates atrial natriuretic factor gene expression', *Molecular and cellular biology* 18(6): 3120-9.

Lickert, H., Takeuchi, J. K., Von Both, I., Walls, J. R., McAuliffe, F., Adamson, S. L., Henkelman, R. M., Wrana, J. L., Rossant, J. and Bruneau, B. G. (2004) 'Baf60c is essential for function of BAF chromatin remodelling complexes in heart development', *Nature* 432(7013): 107-12.

Linderson, Y., Eberhard, D., Malin, S., Johansson, A., Busslinger, M. and Pettersson, S. (2004) 'Corecruitment of the Grg4 repressor by PU.1 is critical for Pax5-mediated repression of B-cell-specific genes', *EMBO reports* 5(3): 291-6.

Lindsley, D. L. and Grell, E. H. (1968) 'Genetic Variations of Drosophila melanogaster', *Carnegie Institution of Washington Publication* 627.

Lingbeek, M. E., Jacobs, J. J. and van Lohuizen, M. (2002) 'The T-box repressors TBX2 and TBX3 specifically regulate the tumor suppressor gene p14ARF via a variant T-site in the initiator', *The Journal of biological chemistry* 277(29): 26120-7.

Mannervik, M. and Levine, M. (1999) 'The Rpd3 histone deacetylase is required for segmentation of the Drosophila embryo', *Proceedings of the National Academy of Sciences of the United States of America* 96(12): 6797-801.

Marino, S. and Nusse, R. (2007) 'Mutants in the mouse NuRD/Mi2 component P66alpha are embryonic lethal', *PloS one* 2(6): e519.

Martinez, C. A. and Arnosti, D. N. (2008) 'Spreading of a corepressor linked to action of long-range repressor hairy', *Molecular and cellular biology* 28(8): 2792-802.

Mercola, M. (1999) 'Embryological basis for cardiac left-right asymmetry', *Seminars in cell & developmental biology* 10(1): 109-16.

Mesbah, K., Harrelson, Z., Theveniau-Ruissy, M., Papaioannou, V. E. and Kelly, R. G. (2008) 'Tbx3 is required for outflow tract development', *Circulation research* 103(7): 743-50.

Miyasaka, H., Choudhury, B. K., Hou, E. W. and Li, S. S. (1993) 'Molecular cloning and expression of mouse and human cDNA encoding AES and ESG proteins with strong similarity to Drosophila enhancer of split groucho protein', *European journal of biochemistry / FEBS* 216(1): 343-52.

Montgomery, R. L., Davis, C. A., Potthoff, M. J., Haberland, M., Fielitz, J., Qi, X., Hill, J. A., Richardson, J. A. and Olson, E. N. (2007) 'Histone deacetylases 1 and 2 redundantly regulate cardiac morphogenesis, growth, and contractility', *Genes & development* 21(14): 1790-802.

Montgomery, R. L., Potthoff, M. J., Haberland, M., Qi, X., Matsuzaki, S., Humphries, K. M., Richardson, J. A., Bassel-Duby, R. and Olson, E. N. (2008) 'Maintenance of cardiac energy metabolism by histone deacetylase 3 in mice', *The Journal of clinical investigation* 118(11): 3588-97.

Morin, S., Charron, F., Robitaille, L. and Nemer, M. (2000) 'GATA-dependent recruitment of MEF2 proteins to target promoters', *The EMBO journal* 19(9): 2046-55.

Muhr, J., Andersson, E., Persson, M., Jessell, T. M. and Ericson, J. (2001) 'Groucho-mediated transcriptional repression establishes progenitor cell pattern and neuronal fate in the ventral neural tube', *Cell* 104(6): 861-73.

Naiche, L. A., Harrelson, Z., Kelly, R. G. and Papaioannou, V. E. (2005) 'T-box genes in vertebrate development', *Annual review of genetics* 39: 219-39.

Nakayama, H., Liu, Y., Stifani, S. and Cross, J. C. (1997) 'Developmental restriction of Mash-2 expression in trophoblast correlates with potential activation of the notch-2 pathway', *Developmental genetics* 21(1): 21-30.
Paroush, Z., Finley, R. L., Jr., Kidd, T., Wainwright, S. M., Ingham, P. W., Brent, R. and Ish-Horowicz, D. (1994) 'Groucho is required for Drosophila neurogenesis, segmentation, and sex determination and interacts directly with hairy-related bHLH proteins', *Cell* 79(5): 805-15.

Pflugfelder, G. O., Roth, H. and Poeck, B. (1992) 'A homology domain shared between Drosophila optomotor-blind and mouse Brachyury is involved in DNA binding', *Biochemical and biophysical research communications* 186(2): 918-25.

Pinto, M. and Lobe, C. G. (1996) 'Products of the grg (Groucho-related gene) family can dimerize through the amino-terminal Q domain', *The Journal of biological chemistry* 271(51): 33026-31.

Plageman, T. F., Jr. and Yutzey, K. E. (2004) 'Differential expression and function of Tbx5 and Tbx20 in cardiac development', *The Journal of biological chemistry* 279(18): 19026-34.

Plageman, T. F., Jr. and Yutzey, K. E. (2005) 'T-box genes and heart development: putting the "T" in heart', *Developmental dynamics : an official publication of the American Association of Anatomists* 232(1): 11-20.

Richmond, S. and Wren, C. (2001) 'Early diagnosis of congenital heart disease', *Seminars in neonatology : SN* 6(1): 27-35.

Rottbauer, W., Saurin, A. J., Lickert, H., Shen, X., Burns, C. G., Wo, Z. G., Kemler, R., Kingston, R., Wu, C. and Fishman, M. (2002) 'Reptin and pontin antagonistically regulate heart growth in zebrafish embryos', *Cell* 111(5): 661-72.

Saito, M. and Ishikawa, F. (2002) 'The mCpG-binding domain of human MBD3 does not bind to mCpG but interacts with NuRD/Mi2 components HDAC1 and MTA2', *The Journal of biological chemistry* 277(38): 35434-9.

Scambler, P. J. (2010) '22q11 deletion syndrome: a role for TBX1 in pharyngeal and cardiovascular development', *Pediatric cardiology* 31(3): 378-90.

Sekiya, T. and Zaret, K. S. (2007) 'Repression by Groucho/TLE/Grg proteins: genomic site recruitment generates compacted chromatin in vitro and impairs activator binding in vivo', *Molecular cell* 28(2): 291-303.

Sepulveda, J. L., Belaguli, N., Nigam, V., Chen, C. Y., Nemer, M. and Schwartz, R. J. (1998) 'GATA-4 and Nkx-2.5 coactivate Nkx-2 DNA binding targets: role for regulating early cardiac gene expression', *Molecular and cellular biology* 18(6): 3405-15.

Shelton, E. L. and Yutzey, K. E. (2007) 'Tbx20 regulation of endocardial cushion cell proliferation and extracellular matrix gene expression', *Developmental biology* 302(2): 376-88.
Shen, T., Aneas, I., Sakabe, N., Dirschinger, R. J., Wang, G., Smemo, S., Westlund, J. M., Cheng, H., Dalton, N., Gu, Y. et al. (2011) 'Tbx20 regulates a genetic program essential to adult mouse cardiomyocyte function', *The Journal of clinical investigation* 121(12): 4640-54.

Singh, M. K., Christoffels, V. M., Dias, J. M., Trowe, M. O., Petry, M., Schuster-Gossler, K., Burger, A., Ericson, J. and Kispert, A. (2005) 'Tbx20 is essential for cardiac chamber differentiation and repression of Tbx2', *Development* 132(12): 2697-707.

Small, E. M. and Krieg, P. A. (2003) 'Transgenic analysis of the atrialnatriuretic factor (ANF) promoter: Nkx2-5 and GATA-4 binding sites are required for atrial specific expression of ANF', *Developmental biology* 261(1): 116-31.

Stankunas, K., Hang, C. T., Tsun, Z. Y., Chen, H., Lee, N. V., Wu, J. I., Shang, C., Bayle, J. H., Shou, W., Iruela-Arispe, M. L. et al. (2008) 'Endocardial Brg1 represses ADAMTS1 to maintain the microenvironment for myocardial morphogenesis', *Developmental cell* 14(2): 298-311.

Stennard, F. A., Costa, M. W., Elliott, D. A., Rankin, S., Haast, S. J., Lai, D., McDonald, L. P., Niederreither, K., Dolle, P., Bruneau, B. G. et al. (2003) 'Cardiac T-box factor Tbx20 directly interacts with Nkx2-5, GATA4, and GATA5 in regulation of gene expression in the developing heart', *Developmental biology* 262(2): 206-24.

Stennard, F. A., Costa, M. W., Lai, D., Biben, C., Furtado, M. B., Solloway, M. J., McCulley, D. J., Leimena, C., Preis, J. I., Dunwoodie, S. L. et al. (2005) 'Murine T-box transcription factor Tbx20 acts as a repressor during heart development, and is essential for adult heart integrity, function and adaptation', *Development* 132(10): 2451-62.

Stifani, S., Blaumueller, C. M., Redhead, N. J., Hill, R. E. and Artavanis-Tsakonas, S. (1992) 'Human homologs of a Drosophila Enhancer of split gene product define a novel family of nuclear proteins', *Nature genetics* 2(4): 343.

Swingler, T. E., Bess, K. L., Yao, J., Stifani, S. and Jayaraman, P. S. (2004) 'The proline-rich homeodomain protein recruits members of the Groucho/Transducin-like enhancer of split protein family to co-repress transcription in hematopoietic cells', *The Journal of biological chemistry* 279(33): 34938-47.

Takeuchi, J. K. and Bruneau, B. G. (2009) 'Directed transdifferentiation of mouse mesoderm to heart tissue by defined factors', *Nature* 459(7247): 708-11.

Takeuchi, J. K., Lou, X., Alexander, J. M., Sugizaki, H., Delgado-Olguin, P., Holloway, A. K., Mori, A. D., Wylie, J. N., Munson, C., Zhu, Y. et al. (2011) 'Chromatin remodelling complex

dosage modulates transcription factor function in heart development', *Nature communications* 2: 187.

Thirunavukkarasu, K., Mahajan, M., McLarren, K. W., Stifani, S. and Karsenty, G. (1998) 'Two domains unique to osteoblast-specific transcription factor Osf2/Cbfa1 contribute to its transactivation function and its inability to heterodimerize with Cbfbeta', *Molecular and cellular biology* 18(7): 4197-208.

Tong, J. K., Hassig, C. A., Schnitzler, G. R., Kingston, R. E. and Schreiber, S. L. (1998) 'Chromatin deacetylation by an ATP-dependent nucleosome remodelling complex', *Nature* 395(6705): 917-21.

Trivedi, C. M., Lu, M. M., Wang, Q. and Epstein, J. A. (2008) 'Transgenic overexpression of Hdac3 in the heart produces increased postnatal cardiac myocyte proliferation but does not induce hypertrophy', *The Journal of biological chemistry* 283(39): 26484-9.

Trivedi, C. M., Zhu, W., Wang, Q., Jia, C., Kee, H. J., Li, L., Hannenhalli, S. and Epstein, J. A. (2010) 'Hopx and Hdac2 interact to modulate Gata4 acetylation and embryonic cardiac myocyte proliferation', *Developmental cell* 19(3): 450-9.

Villanueva, C. J., Waki, H., Godio, C., Nielsen, R., Chou, W. L., Vargas, L., Wroblewski, K., Schmedt, C., Chao, L. C., Boyadjian, R. et al. (2011) 'TLE3 is a dual-function transcriptional coregulator of adipogenesis', *Cell metabolism* 13(4): 413-27.

Vincentz, J. W., Barnes, R. M., Firulli, B. A., Conway, S. J. and Firulli, A. B. (2008) 'Cooperative interaction of Nkx2.5 and Mef2c transcription factors during heart development', *Developmental dynamics : an official publication of the American Association of Anatomists* 237(12): 3809-19.

Wade, P. A., Jones, P. L., Vermaak, D. and Wolffe, A. P. (1998) 'A multiple subunit Mi-2 histone deacetylase from Xenopus laevis cofractionates with an associated Snf2 superfamily ATPase', *Current biology : CB* 8(14): 843-6.

Wang, Z., Zhai, W., Richardson, J. A., Olson, E. N., Meneses, J. J., Firpo, M. T., Kang, C., Skarnes, W. C. and Tjian, R. (2004) 'Polybromo protein BAF180 functions in mammalian cardiac chamber maturation', *Genes & development* 18(24): 3106-16.

Wiese, C., Grieskamp, T., Airik, R., Mommersteeg, M. T., Gardiwal, A., de Gier-de Vries, C., Schuster-Gossler, K., Moorman, A. F., Kispert, A. and Christoffels, V. M. (2009) 'Formation of the sinus node head and differentiation of sinus node myocardium are independently regulated by Tbx18 and Tbx3', *Circulation research* 104(3): 388-97.

Winkler, C. J., Ponce, A. and Courey, A. J. (2010) 'Groucho-mediated repression may result from a histone deacetylase-dependent increase in nucleosome density', *PloS one* 5(4): e10166.

Xue, Y., Wong, J., Moreno, G. T., Young, M. K., Cote, J. and Wang, W. (1998) 'NURD, a novel complex with both ATP-dependent chromatin-remodeling and histone deacetylase activities', *Molecular cell* 2(6): 851-61.
Yao, J., Liu, Y., Husain, J., Lo, R., Palaparti, A., Henderson, J. and Stifani, S. (1998) 'Combinatorial expression patterns of individual TLE proteins during cell determination and differentiation suggest non-redundant functions for mammalian homologs of Drosophila Groucho', *Development, growth & differentiation* 40(2): 133-46.

Yao, J., Liu, Y., Lo, R., Tretjakoff, I., Peterson, A. and Stifani, S. (2000) 'Disrupted development of the cerebral hemispheres in transgenic mice expressing the mammalian Groucho homologue transducin-like-enhancer of split 1 in postmitotic neurons', *Mechanisms of development* 93(1-2): 105-15.

Yao, Y. L. and Yang, W. M. (2003) 'The metastasis-associated proteins 1 and 2 form distinct protein complexes with histone deacetylase activity', *The Journal of biological chemistry* 278(43): 42560-8.

Yarosh, W., Barrientos, T., Esmailpour, T., Lin, L., Carpenter, P. M., Osann, K., Anton-Culver, H. and Huang, T. (2008) 'TBX3 is overexpressed in breast cancer and represses p14 ARF by interacting with histone deacetylases', *Cancer research* 68(3): 693-9.

Zhang, J. and King, M. L. (1996) 'Xenopus VegT RNA is localized to the vegetal cortex during oogenesis and encodes a novel T-box transcription factor involved in mesodermal patterning', *Development* 122(12): 4119-29.

Zhang, W., Chen, H., Wang, Y., Yong, W., Zhu, W., Liu, Y., Wagner, G. R., Payne, R. M., Field, L. J., Xin, H. et al. (2011) 'Tbx20 transcription factor is a downstream mediator for bone morphogenetic protein-10 in regulating cardiac ventricular wall development and function', *The Journal of biological chemistry* 286(42): 36820-9.

Zhang, Y., LeRoy, G., Seelig, H. P., Lane, W. S. and Reinberg, D. (1998) 'The dermatomyositis-specific autoantigen Mi2 is a component of a complex containing histone deacetylase and nucleosome remodeling activities', *Cell* 95(2): 279-89.

Zhu, C. C., Dyer, M. A., Uchikawa, M., Kondoh, H., Lagutin, O. V. and Oliver, G. (2002) 'Six3-mediated auto repression and eye development requires its interaction with members of the Groucho-related family of co-repressors', *Development* 129(12): 2835-49.

Appendix 1

Xenopus: An emerging model for studying congenital heart disease

Preface

This work was published as a review article in the journal *Birth Defects Research A: Clinical and Molecular Teratology.* It was written primarily by myself and postdoctoral fellow Panna Tandon, with minor contributions by postdoctoral fellow Nirav Amin, graduate student Lauren Waldron, and postdoctoral fellow Chris Showell. The manuscript was finalized by Frank Conlon and Chris Showell.

K**altenbrun E.,Tandon P., Amin N.M., Waldon L. Showell C., and Conlon F.L.** Xenopus: An emerging model for studing congenital heart disease (2011) *Birth Defects Res A Clin Mol Teratol.* Jun;91(6):495-510.

ABSTRACT

Congenital heart defects affect nearly 1% of all newborns and are a significant cause of infant death. Clinical studies have identified a number of congenital heart syndromes associated with mutations in genes that are involved in the complex process of cardiogenesis. The African clawed frog, *Xenopus*, has been instrumental

in studies of vertebrate heart development and provides a valuable tool to investigate the molecular mechanisms underlying human congenital heart diseases. In this review, we discuss the methodologies that make *Xenopus* an ideal model system to investigate heart development and disease. We also outline congenital heart conditions linked to cardiac genes that have been well-studied in *Xenopus* and describe some emerging technologies that will further aid in the study of these complex syndromes.

INTRODUCTION

Xenopus as a Model System for Human Congenital Heart Disease

It is becoming increasingly clear that many forms of human disease are associated with defects in genes required for early steps in embryonic development. The African clawed frog, *Xenopus* shares surprising similarities with humans both genetically and anatomically. Thus, the molecular and cellular pathways through which these genes function can be elucidated using *Xenopus* to model vertebrate heart development and disease. *Xenopus* has numerous advantages as a model system in which to identify and characterize cellular and developmental processes. Unlike the mouse, the *Xenopus* embryo develops externally, and its early patterning and morphogenesis have been extensively studied. The *Xenopus* embryo is relatively large and is amenable to surgical manipulations, allowing defined regions to be excised and cultured in simple salt solutions in which the developmental and downstream transcriptional effects of exogenous growth factors can be determined. These classical approaches are complemented by molecular techniques that allow

the overexpression or knockdown of specific gene products in the early embryo (Harvey and Melton, 1988; Heasman et al., 2000). In addition, transgenesis techniques are well established and technologies are continually being optimized (Chesneau et al., 2008). Moreover, recent sequence annotation and assembly of the *Xenopus tropicalis* genome has demonstrated that it has long regions in which genes exhibit remarkably similar synteny relationships to those found in the human genome (Showell and Conlon, 2007; Hellsten et al., 2010). Specifically, regarding human congenital heart disease (CHD), *Xenopus* has unique advantages for studying cardiovascular development (Warkman and Krieg, 2006; Bartlett and Weeks, 2008; Evans et al., 2010). First, early *Xenopus* development can proceed in the absence of a functional circulation system, allowing defects to be extensively analyzed in living embryos. Second, *Xenopus* has a pulmonary system and a two-chambered atrium. Third, *Xenopus* has a well-established fate map that is not confounded by extensive cell mixing (Dale and Slack, 1987; Moody, 1987). Only three hours after fertilization, it is possible to identify the blastomeres that will give rise to the adult heart. Collectively, this unique set of attributes places *Xenopus* as an ideal model system for studying congenital heart defects and in this review we will describe the experimental tools available to researchers, together with the existing *Xenopus* models of human CHDs (Table A1.1).

METHODS FOR STUDYING HEART DEVELOPMENT AND DISEASE IN *XENOPUS*

Protein Depletion and Overexpression

The advent of effective antisense techniques has enabled researchers to associate developmental processes with the genes that control them. The most extensively used of these techniques are the use of morpholino oligonucleotides (MOs), which inhibit the function of specific genes by preventing translation or splicing of messenger RNA (mRNA). This technique has resulted in the publication of many studies of heart development in *Xenopus* that have advanced our understanding of this process in vertebrates (Brown et al., 2005; Garriock et al., 2005a; Small et al., 2005; Zhang et al., 2005; Inui et al., 2006; Kumano et al., 2006; Brown et al., 2007; Hilton et al., 2007; Bartlett and Weeks, 2008; Christine and Conlon, 2008; Movassagh and Philpott, 2008; Nagao et al., 2008). MO antisense oligonucleotides are neutrally charged synthetic nucleic acid analogs that are stable, soluble, and bind to RNA with high affinity (Heasman et al., 2000; Moulton, 2007). In addition, they are resistant to nuclease degradation and have limited interaction with proteins (Summerton, 2007; Eisen and Smith, 2008; Bill et al., 2009). MOs are designed to reduce gene function in two ways. First, the MO can be designed to target sequences in the 5′ untranslated region close to the translation initiation codon of the gene to sterically block the attachment of the ribosomal machinery and inhibit protein translation (Heasman et al., 2000). Alternatively, MOs can be designed to target the splice junctions in the pre-mRNA strand, resulting in the incorporation of intron-encoded amino acids and, in many cases, early termination of translation via premature stop codons or by a shift in the reading frame of the subsequent sequence (Morcos, 2007).

Strategies other than MOs have been employed to inhibit gene function. These include antisense RNA injection (Harland and Weintraub, 1985; Melton, 1985; Dagle and Weeks, 2001), RNA interference in which the RNA is targeted for degradation by the binding of small inhibitory RNA molecules and recruitment of the RNA-induced silencing complex (Zhou and others, 2002; Summerton, 2007), DNA with chemically modified phosphate linkages that employs cellular RNase H to cleave the target RNA strand (Summerton, 2007), and peptide nucleic acid nucleotides which sterically block RNA translation in a similar way to MOs (Harland and Weintraub, 1985; Melton, 1985; Dagle and Weeks, 2001; Zhou et al., 2002; Summerton, 2007). However, due to few off-target effects, their binding success and their commercial availability, MOs have become a favored tool for studying gene function in vertebrate models (Knudsen and Nielsen, 1996; Summerton, 2007).

Protein overexpression can be as valuable a technique as protein depletion to determine the role of a particular gene in development. The microinjection of capped mRNA into the *Xenopus* embryo has commonly been used to study heart development in the context of globally increased function of the protein under investigation, the effects of lateral- and lineage-specific overexpression, and to study isoform-specific phenotypes (Campione et al., 1999; Kitaguchi et al., 2000; Stennard et al., 2003; Goetz et al., 2006). Overexpression of truncated or mutated proteins can also be utilized to reproduce and investigate phenotypes caused by mutations identified in human patients with CHD (Ataliotis et al., 2005; Bartlett et al., 2007). Furthermore, protein function can

be manipulated in a spatio-temporal manner by injecting hormone-inducible constructs with timed dexamethasone application (Kitaguchi et al., 2000; Afouda et al., 2008).

Xenopus Explants for Cardiogenic Assays

The *Xenopus* embryo is particularly amenable to tissue explant assays due to its unique ability to heal after microsurgery. In addition, *Xenopus* embryonic tissue can survive in the absence of added nutrients (due to the yolk contained in embryonic cells) allowing culture of tissue explants in a simple saline solution. The first use of *Xenopus* explants in a cardiogenic assay was performed by Horst Grunz in 1992 (Grunz, 1992) who demonstrated that the isolated blastopore lip, fated to give rise to notochord and somites but not the heart, gives rise to differentiated cardiac tissue when cultured in the presence of the growth factor-blocking compound suramin. This demonstrated the importance of growth factor signaling in negatively regulating the induction of cardiac cell fate in the dorsal marginal zone (DMZ), which restricts cardiac cell fate to two bilateral groups of cells in the dorsoanterior mesoderm of the gastrula. Similar experiments by Schneider and Mercola have shown that Wnt signaling can antagonize cardiac specification in DMZ explants. When an arc of dorsal marginal zone mesoderm containing the heart progenitors is excised from the equatorial region of the gastrula and cultured in isolation it gives rise to differentiated, beating cardiac tissue. However, overexpression of *wnt3A* and *wnt8* in these DMZ explants by injection of plasmid DNA into dorsal blastomeres results in a downregulation of cardiac marker expression, suggesting that inhibition of endogenous Wnt signaling might be

required for proper heart induction (Schneider and Mercola, 2001). Indeed, when the Wnt inhibitors *dickkopf1* or *crescent* are expressed ectopically in non-cardiogenic ventral marginal zone (VMZ) explants, cardiac terminal differentiation can be induced. This results in the striking observation of beating cardiac tissue within the cultured explants (Schneider and Mercola, 2001). A role has also been identified for *wnt11*, encoding a non-canonical Wnt antagonist, in the induction of heart formation by the observation that it is sufficient to induce expression of cardiac markers and differentiation of contractile cardiac tissue in VMZ explants (Pandur et al., 2002). As WNT11 both inhibits β-catenin through the canonical pathway and activates JNKAs WNT11 also inhibits β-catenin through the canonical pathway, Pandur *et al.* injected mRNA encoding a dominant negative LEF-1 and observed that disruption of β-catenin signaling alone fails to induce a contractile phenotype in VMZ explants. s. This result indicates that heart induction may require both 1) low levels of Wnt/**β**-catenin activity and, 2) activation of non-canonical Wnt/JNK signaling through WNT11 activation of the non-canonical Wnt signaling cascade through WNT11 is required for cardiac differentiation in this assay (Pandur et al., 2002). Alternately, it could reflect activity differences between TCF and LEF factors in β-catenin inhibition as another group demonstrated that injection of a dominant negative TCF3 was indeed sufficient to induce cardiogenesis in *Xenopus* animal caps.

Explants have also been used to investigate factors required for induction of cardiogenesis via a loss-of-function approach. For example, MO knockdown of *hex* (a transcription factor induced by antagonists of the canonical Wnt pathway) in DMZ

explants resulted in loss of cardiac markers, indicating that heart induction by Wnt antagonists relies upon activation of *hex* (Foley and Mercola, 2005).

The *Xenopus* animal cap also serves as a useful tissue for cardiogenic assays and can be used to examine the ability of various molecules to affect cardiac gene expression and differentiation. The animal cap consists of prospective ectoderm at the animal pole of a blastula embryo and is fated to become epidermal and neural tissues. Because the ectodermal cells of the animal pole are pluripotent, they can be induced to give rise to alternate cell lineages, including mesodermal derivatives such as the heart. Logan and Mohun demonstrated that cardiac muscle is induced in animal caps treated with high concentrations of the mesoderm-inducing factor activin (Logan and Mohun, 1993). A more recent protocol involving the dissociation and reaggregation of animal caps in the presence of activin results in beating animal cap explants that can form ectopic hearts in *Xenopus* adults following transplantation into the hosts at embryonic stages (Ariizumi et al., 2003). As with DMZ and VMZ explants, animal caps have been used to advance our understanding of the role of WNT signaling during cardiogenesis. Activin-induced expression of GATA factors in animal caps is abolished upon injection of an inducible form of β-catenin, suggesting that Wnt signaling may act to repress *gata* gene expression to restrict cardiogenesis (Afouda et al., 2008). In addition, inhibition of *gata4* and *gata6* by MO injection in animal cap explants results in decreased *wnt11* expression, whereas injection of inducible versions of *Gata4* and *Gata6* results in upregulation of *wnt11* expression, placing GATA factors in a regulatory pathway that links canonical

and non-canonical Wnt signaling during cardiogenesis (Pandur et al., 2002; Afouda et al., 2008).

Finally, prospective cardiac tissue itself can be explanted from the embryo and used for cardiogenic assays in the absence of the rest of the embryo. This technique is particularly useful when it is necessary to bypass an early embryonic requirement for a gene to assess its later role in the developing heart. In short, tissue posterior to the cement gland including the heart field can be excised starting at stage 22 when the cardiac precursor populations form a ridge of tissue on top of underlying endoderm. In isolation, these explants will go on to form beating hearts in culture (Raffin et al., 2000; Langdon et al., 2007). Using this assay, a recent study identified a role for SHP-2, a protein tyrosine phosphatase that is disrupted in human CHD, in the maintenance of cardiac progenitors (Langdon et al., 2007).

Xenopus Transgenesis

The development of transgenesis in *Xenopus* has allowed investigators to introduce heritable genetic modifications into the frog genome, propelling *Xenopus* forward as both a genetic and developmental model. Transgenic procedures in *Xenopus* have primarily been used for promoter/enhancer analyses and for expressing transgenes in a tissue-specific manner with defined promoters. Early experiments involving microinjection of circular or linear DNA demonstrated that integration into the genome occurred in a significant number of injected embryos (Rusconi and Schaffner, 1981; Etkin and Roberts, 1983; Andres et al., 1984; Bendig

and Williams, 1984; Etkin et al., 1984). The first characterization of transgenic frogs produced by this method showed that the resulting animals were mosaic and that the copy number was highly variable, even within cells from the same animal (Etkin and Pearman, 1987). It was not until the development of the Restriction Enzyme Mediated Integration (REMI) strategy that the problem of mosaicism was overcome (Kroll and Amaya, 1996b). Using this method, sperm nuclei are incubated with linearized DNA and a restriction enzyme along with egg extracts which promote DNA decondensation. The modified sperm nuclei are then injected into unfertilized eggs, where the foreign DNA is believed to integrate randomly into the genomic DNA during the DNA repair process prior to the first cell division (Amaya and Kroll, 1999; Smith et al., 2006).

Other methods of transgenesis that utilize different core insertion techniques have been used with varying success. Transposable elements such as *Sleeping Beauty* or the *Tol2* transposon have been used as an alternative to REMI to facilitate transgene integration in *Xenopus* (Kawakami et al., 2000; Kawakami et al., 2004; Parinov et al., 2004; Choo et al., 2006; Hamlet et al., 2006; Sinzelle et al., 2006; Yergeau and Mead, 2007; Yergeau et al., 2009). The more commonly used transposon *Tol2* is an active and autonomous transposable element that can integrate into one or multiple sites in the genome and has been used successfully in zebrafish for insertional mutagenesis, although this method of transgenesis in *Xenopus* has not been as efficient as expected. Other groups have optimized the use of integrase-mediated transgenesis utilizing the bacteriophage ΦC31 and the

more frequently used *I-SceI* meganuclease (Allen and Weeks, 2005; Allen and Weeks, 2009). The *I-SceI* meganuclease, originally isolated from *Saccharomyces cerevisiae,* is used to digest transgene DNA containing *I-SceI* 18-bp recognition sites and this reaction mixture is injected into unfertilized eggs where it integrates randomly into the host genome. Copy number of integrated transgenes is relatively low, ranging from one to four, compared to the REMI method which typically results in the integration of transgene concatemers (two to six copies) at four to eight sites in the genome (Kroll and Amaya, 1996a). (Jacquier and Dujon, 1985; Ogino et al., 2006; Pan et al., 2006).

The developmental regulation of several cardiac genes has been characterized with *Xenopus* transgenesis, leading to a clearer picture of the complex gene regulatory networks that guide heart development. This commonly involves *in vivo* analysis of *cis*-regulatory regions that drive cardiac expression in the heart and is accomplished by inserting the promoter of interest upstream of a reporter transgene, such as green fluorescent protein (GFP), to follow transgene expression in the live embryo. This approach has been used to identify cardiac-specific regulatory elements for *atrial natriuretic factor* (*anf*), *cardiac α-Actin*, *myosin Light Chain 2* (*mlc2*), *myosin light chain 1v* (*mlc1v*), *nkx2-5*, *alpha myosin heavy chain* (*α-mhc*), and *tbx20* (Sparrow et al., 2000; Latinkić et al., 2002; Small and Krieg, 2003; Latinkić et al., 2004; Garriock et al., 2005b; Smith et al., 2005; Mandel et al., 2010). Additional studies examining the mechanisms of regulating these cardiac elements have revealed much about the signaling pathways that act on cardiac genes during

development. Importantly, many of these regulatory elements are evolutionarily conserved as they are sufficient for cardiac-specific expression in other vertebrates including mice.

One of the benefits of transgenesis is the ability to tightly control the spatial and temporal expression of a transgene during development with tissue-specific promoters. Several cardiac promoters that drive expression throughout the developing heart have been used with great success to misexpress a gene of interest specifically in the heart-forming region. Using transgenic embryos expressing *bmp4* under the control of the *mlc2* promoter, Breckenridge *et al.* demonstrated that ectopic expression throughout the developing heart results in randomization of the direction of cardiac looping, indicating that asymmetric BMP4 signaling is required for proper cardiac looping (Breckenridge et al., 2001).

CONGENITAL HEART DISEASE

Atrial Septal Defects: *Nkx2.5* and *Gata4*

Atrial Septal Defects (ASD) are relatively common and account for 10% of all human congenital heart defects (Hoffman and Kaplan, 2002). ASD refers to a failure of the atrial septum to fully separate the right and left atrial chambers after birth and is often accompanied by other forms of CHD including cardiac conduction system abnormalities. The cardiac transcription factor *Nkx2.5* is mutated in a number of patients with non-syndromic ASD, suggesting a critical function for this gene in the septogenesis process (Schott et al., 1998; Benson et al., 1999).

Nkx2.5 encodes a homeodomain protein that is highly conserved from *Drosophila* to human. *Nkx2.5* is expressed early in development, and in combination with other cardiac transcription factors, helps define the cardiogenic field in which it plays an essential role in the specification of cardiac progenitors from the cardiogenic mesoderm. Cardiac expression of *Nkx2.5* persists into adulthood, however, a complete understanding of the role NKX2.5 plays during the later stages of heart formation has been complicated by the fact that targeted disruption of murine *Nkx2.5* results in embryonic lethality at E9-E10, prior to heart looping (Lyons, 1995). Interestingly, a recent study in *Xenopus* demonstrated that injection of two truncated forms of *Xenopus laevis* NKX2.5, corresponding to two human NKX2.5 point mutations identified in patients with cardiac defects including ASD and atrioventricular conduction delays, results in atrial septal and conduction system defects (Schott et al., 1998; Bartlett et al., 2007). Significantly, this study focused on the effects of injecting mutant forms of *nkx2.5*on internal changes to the hearts of stage 46 embryos when the *Xenopus* heart is fully looped with chambers, septae, valves, and a functional conduction system (Bartlett et al., 2007). The results suggest that early expression of mutant *nkx2.5* in the frog can lead to a late phenotype that includes cardiac defects consistent with those seen in human disease.

NKX2.5 has also been shown to physically interact with the cardiac zinc finger transcription factor GATA4, an additional gene mutated in in patients with ASD

(Durocher et al., 1997; Lee et al., 1998; Sepulveda et al., 1998; Pehlivan et al., 1999; Garg et al., 2003). The NKX2.5-GATA4 interaction synergistically activates cardiac promoters during the cardiogenic program, suggesting that deficiencies in either member of this transcriptional complex can result in ASDs (Durocher et al., 1997; Lee et al., 1998; Sepulveda et al., 1998). Studies utilizing the embryonic carcinoma P19 cell line have shown *Gata4* to be essential for cardiac differentiation. However, *Gata4* null mice can generate differentiated cardiac myocytes that express contractile proteins but are deficient in ventral morphogenesis, resulting in a failure of cardiomyocytes to form a linear heart tube at the ventral midline (cardia bifida) (Grepin et al., 1995; Grepin et al., 1997; Kuo et al., 1997; Molkentin et al., 1997). Recent studies in *Xenopus* complement the mouse work and demonstrate with MOs that *gata4* is dispensable for cardiac specification but essential for proper heart morphogenesis downstream of the induction of the myocardium (Haworth et al., 2008). Interestingly, when GATA4, GATA5, and GATA6 are all depleted from *Xenopus* embryos, *myosin heavy chain* expression is completely lost from most morphant embryos, suggesting that there is GATA factor redundancy in the regulation of myocardial differentiation, providing a possible explanation for the persistent presence of differentiated cardiomyocytes in *Gata4*$^{-/-}$ mice (Peterkin et al., 2007).

DiGeorge Syndrome: *Tbx1*

DiGeorge syndrome (DGS) is a congenital disorder that has many overlapping characteristics with velo-cardio-facial syndrome and conotruncal anomaly face syndrome due to shared deletions within chromosome band *22q11.2*

(Yamagishi and Srivastava, 2003; Baldini, 2004). For this reason, these syndromes are collectively known as *22q11* deletion syndrome (*del22q11DS*). Approximately 80% of neonates displaying *del22q11DS* have congenital heart defects that include Tetralogy of Fallot, persistent truncus arterious, and cardio-facial abnormalities (Epstein, 2001; Yamagishi and Srivastava, 2003; Baldini, 2004; Di Felice and Zummo, 2009; Momma, 2010; Starr, 2010).

DGS is one of the most prevalent chromosomal microdeletion genetic disorders. The region of chromosome *22q11.2* that is deleted in DGS encompasses 1.5 to 3 Mb and includes 24-30 genes (Epstein, 2001; Yamagishi and Srivastava, 2003; Baldini, 2004). A heterozygous mouse genetic model in which the orthologous chromosomal region affected in DGS is deleted displays similar phenotypes as those in human patients (Lindsay et al., 1999; Lindsay and Baldini, 2001). The deleted region frequently includes the locus encoding the T-box transcription factor *Tbx1*. In a genetic analysis screen, five patients were identified who exhibited DGS phenotypes and had *Tbx1* mutations but not chromosomal microdeletions, suggesting that *Tbx1* may be contributing to the DGS phenotype in these individuals (Yagi et al., 2003). DGS abnormalities have been correlated with disrupted pharyngeal and neural crest patterning during development. Subsequently, *Tbx1* was shown to be expressed in the pharyngeal arches, and mouse genetic models have demonstrated that *Tbx1* haplo-insufficiency disrupts the development of the fourth pharyngeal arch arteries, possibly in conjunction with FGF8 signaling (Chapman et al., 1996; Lindsay et al., 2001b; Merscher et al., 2001; Kochilas et al.,

2002; Sauka-Spengler et al., 2002; Vitelli et al., 2002; Kochilas et al., 2003; Baldini, 2004; Ataliotis et al., 2005; Showell et al., 2006). In addition, *Tbx1* plays a role in growth and septation of the outflow tract (OFT). Conditionally ablating *Tbx1* in the *Nkx2.5* domain of the secondary heart field results in mild pharyngeal defects and a severe defect in aorto-pulmonary septation of the OFT that is associated with neural crest migration defects and reduced proliferation of cells in the secondary heart field (Waldo et al., 2001; Xu et al., 2004). FGF signaling may be involved in the latter event as there is a reduction in *Fgf10* expression in the secondary heart field in *Tbx1*-null mice. Further, *Fgf10* is a direct transcriptional target of *Tbx1 in vitro* (Waldo et al., 2001; Xu et al., 2004). Interestingly, the defect in OFT septation suggests a dose-dependent role for *Tbx1* because this phenotype can be partially rescued upon reestablishing *Tbx1* expression (Jerome and Papaioannou, 2001; Lindsay et al., 2001a; Xu et al., 2004).

Tbx1 has been identified in many vertebrates including *Xenopus laevis* and *Xenopus tropicalis*. In these model systems, the expression domains of *tbx1* replicate those seen in other vertebrates, namely the pharyngeal arches, otic vesicle, and mesenchyme surrounding the OFT (Chapman et al., 1996; Sauka-Spengler et al., 2002; Kochilas et al., 2003; Ataliotis et al., 2005; Showell et al., 2006). A dominant interfering mutant of *tbx1* injected into *Xenopus* embryos results in very similar phenotypes to those of mice deficient in *Tbx1*, including pharyngeal defects, unlooped heart, pericardial edema, and a reduction in anterior structures. These defects can be rescued by co-injecting wild-type *tbx1* mRNA. To lineage trace

the fate of TBX1-deficient cells, Ataliotis *et al.* co-injected *β-galactosidase* mRNA and the dominant interfering mutant *tbx1* mRNA into *Xenopus* embryos and identified a requirement for TBX1 in cells that contribute to pharyngeal mesoderm (Ataliotis et al., 2005). Additionally, recent advances in *Xenopus* transgenesis have enabled researchers to analyze cardiac and craniofacial phenotypes in embryos with reduced functions of specific genes, effectively generating models of CHD such as DGS. Using the active promoter of *mlc1v* to drive GFP, craniofacial and cardiac muscle formation was followed in *Xenopus* embryos injected with the dominant interfering mutant of *tbx1*, enabling real-time visualization of cardiac structural defects in developing embryos (Smith et al., 2005).

Holt-Oram Syndrome: *Tbx5*

Holt-Oram Syndrome (HOS), also known as heart-hand syndrome, is a congenital autosomal dominant disorder that primarily affects the heart and upper limbs (Holt and Oram, 1960). HOS is the most common heart-hand syndrome, affecting nearly 1 in 100,000 total births (Basson et al., 1994). Approximately 75% of patients with HOS experience cardiac defects, most commonly ASD, ventricular septal defects (VSD), and/or defects in the cardiac conduction system (Basson et al., 1994; Benson et al., 1996; Newbury-Ecob et al., 1996; Cross et al., 2000; McDermott et al., 2005). Atypical phenotypes have also been discovered and characterized, and phenotypic expression is variable even within families (Newbury-Ecob et al., 1996; Sletten and Pierpont, 1996; Brassington et al., 2003; Lehner et al., 2003; McDermott et al., 2005; Garavelli et al., 2008). HOS is often caused by mutations in the coding region of the T-box transcription factor *Tbx5* on chromosome

12q.24.1 (Basson et al., 1997; Li et al., 1997; Basson et al., 1999). More than 70% of patients with HOS have a mutation in the *Tbx5* coding exons, and 85% of these mutations are *de novo* (McDermott et al., 2005). Most HOS mutations are predicted to result in haploinsufficiency of *Tbx5* (Li et al., 1997; Basson et al., 1999).

Mice lacking *Tbx5* do not survive past E10.5 due to arrested cardiac development caused by impaired cardiac differentiation (Bruneau et al., 2001). Heterozygous *Tbx5*$^{del/+}$ mice display subtle defects in the paw and wrist, enlarged hearts with ASD, cardiac conduction defects, and a variety of additional complex cardiac defects reminiscent of patients with HOS. The expression of several cardiac genes is reduced in mice lacking *Tbx5*. Two of these genes, *ANF* and *Cx40,* are also reduced in mice expressing 50% of the normal TBX5 levels (Moskowitz et al., 2004). Similar heart and limb defects are observed in the orthologous *Tbx5* zebrafish mutant *heartstrings*, suggesting that both the expression domain and protein function of *Tbx5* are conserved among vertebrates (Garrity et al., 2002). In *Xenopus, tbx5* is first expressed in the migrating heart primordia and eye anlage of the late neurula embryo. Its expression is maintained in the primitive heart tube, although its expression becomes more graded after looping of the heart, with higher expression in the ventricle than the atria (Horb and Thomsen, 1999; Showell et al., 2006). Consistent with work in other organisms, *Tbx5* was demonstrated to be critical for proper heart morphogenesis in *Xenopus* (Horb and Thomsen, 1999; Brown et al., 2005). Overexpression of a dominant negative hormone-inducible form of TBX5 blocks heart tube formation, whereas knockdown of *tbx5* expression by MO results

in reduced cardiac cell number and an unlooped heart tube (Horb and Thomsen, 1999; Brown et al., 2005). The decrease in cardiac cell number in the *tbx5* morphant embryos was demonstrated to result from a proliferation defect caused by a delay or arrest in the G1/S phase of the cell cycle, implicating a role for TBX5 in cardiac cell cycle control (Goetz et al., 2006). These results from *Xenopus* as well as those from human studies (Hatcher et al., 2001), suggest that HOS defects may in part arise from a decrease in cell cycle progression and cardiac cell proliferation in *Tbx5*-expressing regions. In addition, work in a number of model systems has demonstrated a conserved role for *Tbx5* in the regulation of cardiac-specific gene expression (Liberatore et al., 2000; Bruneau et al., 2001; Hatcher et al., 2001; Hiroi et al., 2001; Garrity et al., 2002; Plageman and Yutzey, 2004; Brown et al., 2005).

Spectrum of Congenital Heart Defects: *Tbx20*

Tbx20 is a member of the T-box family of transcription factors and is one of the first genes to be expressed in the cardiac lineage along with *Nkx2.5*, *Gata4*, and *Tbx5*. In all species examined, expression of *Tbx20* is maintained throughout the primary heart field, in both myocardium and endocardium, as development proceeds and persists in the adult heart. Kirk *et al.* were the first group to identify mutations in human *Tbx20* in patients with familial CHD (Kirk et al., 2007). The two mutations identified are both in the T-box DNA binding domain and segregate with a spectrum of cardiac pathologies including ASD, VSD, valve disease, pulmonary hypertension, and cardiomyopathy. Loss-of-function mutations were the first to be identified. However, several other groups have since identified new *Tbx20* mutations with both loss- and gain-of-function that are associated with CHD (Posch et al.; Liu et al.,

2008; Qian et al., 2008). In addition, upregulation of *Tbx20* expression has been noted in patients with Tetralogy of Fallot (Hammer et al., 2008). The wide range of defects associated with mutant or misregulated *Tbx20* may be the result of the expression of *Tbx20* in both myocardium and endocardium, where endocardial cushions give rise to valves and the interventricular septum.

Although the early expression of *Tbx20* in cardiogenic mesoderm suggests a role in the specification, migration, and/or differentiation of cardiac progenitors, a requirement for TBX20 is not evident until the early stages of heart morphogenesis, as shown by studies in fish and frogs (Szeto et al., 2002; Brown et al., 2005). Upon MO knockdown of *Tbx20* in zebrafish and *Xenopus* embryos, morphant embryos display unlooped heart tubes and pericardial edema, but express markers of cardiac specification and differentiation, indicating an essential role for TBX20 in cardiac morphogenesis. In addition, TBX20-depleted *Xenopus* hearts have reduced cardiomyocyte cell numbers and fail to properly form chambers (Brown et al., 2005). Likewise, mice lacking *Tbx20* undergo normal cardiac specification and differentiation, but development is arrested in the primary linear heart tube stage, and chamber differentiation is not initiated (Cai et al., 2005; Singh et al., 2005; Stennard et al., 2005; Takeuchi et al., 2005). There also appears to be a proliferation defect in *Tbx20* null hearts that is thought to be mediated by a loss of repression of *Tbx2*, thereby allowing aberrant repression of the cell cycle gene *N-Myc* in chamber myocardium (Cai et al., 2005; Singh et al., 2005). The misregulation of *Tbx2* in

Tbx20 mutant hearts may partially explain the loss of cardiomyocytes seen in *Xenopus* and mouse *Tbx20* mutants.

The frequent occurrence of cardiac defects resulting from perturbations in the complex regulatory network guiding the cardiomyogenic program highlights the importance of understanding the interactions that occur between members of this network. *Xenopus* embryos co-injected with MOs against *tbx20* and *tbx5* display a more severe cardiac phenotype than single mutants, indicating that TBX20 and TBX5 cooperate to regulate cardiac morphogenesis (Brown et al., 2005). TBX20 physically interacts with the cardiac transcription factors NKX2.5, GATA4, GATA5, and TBX5 and, in transcription assays, TBX20 synergistically activates cardiac promoters in the presence of NKX2.5, GATA4, and ISLET1 (Stennard et al., 2003; Brown et al., 2005; Takeuchi et al., 2005). Surprisingly, in transient transcription assays, the shorter TBX20b isoform, which is terminated shortly after the T-box domain, is more effective at activating reporter gene expression than the longer TBX20a that is the predominant isoform expressed in the heart during development (Stennard et al., 2003). To determine which TBX20 isoform promotes changes in morphogenesis and gene expression *in vivo*, *Tbx20a* and *Tbx20b* mRNAs were injected into *Xenopus* embryos . Overexpression of *Tbx20a*, but not *Tbx20b*, results in multiple developmental defects, including shortening of the anterior/posterior axis and secondary axis formation (Stennard and others, 2003). *Tbx20* mRNAs were also injected into explanted *Xenopus* animal pole caps resulting in an upregulation of the early mesoderm marker *Xbra* and the cardiac marker *Nkx2.5* in the *Tbx20a*-injected,

but not *Tbx20b*-injected, caps (Stennard and others, 2003). These studies suggest that the C-terminal domain of TBX20a is essential for TBX20 activity in the embryo and highlight the utility of *Xenopus* embryo assays for investigating the biological relevance of *in vitro* findings.

Noonan Syndrome: *Shp-2*

Noonan syndrome is one of the most common forms of CHD. The disorder leads to several cardiac developmental abnormalities including ASD, VSD, pulmonary stenosis, and hypertrophic cardiomyopathy (Noonan, 1968; Noonan, 1994). Noonan syndrome was shown to be associated with mis-sense mutations in *SHP-2* in approximately half of affected individuals (Tartaglia et al., 2001; Kosaki et al., 2002; Maheshwari et al., 2002; Tartaglia et al., 2002). *Shp-2* mis-sense mutations are associated with a gain-of-function and are thought to result in prolonged downstream activation of several growth factors including epidermal growth factors (EGFs), fibroblast growth factors (FGFs), and platelet-derived growth factor (Feng et al., 1994; Van Vactor et al., 1998; Feng, 1999; Qu, 2000; Zhang et al., 2000; Tartaglia et al., 2001). Interestingly, patients with acute myelogenous leukemia (AML), acute lymphoblastic leukemia (ALL), and juvenile myelomonocytic leukemia (JMML) carry a second, mostly mutually exclusive, somatically introduced subset of mis-sense mutations in *Shp-2*, strongly suggesting a genotype-phenotype relationship between *Shp-2* mis-sense mutations and disease (Musante et al., 2003; Tartaglia et al., 2003; Bentires-Alj et al., 2004; Loh et al., 2004; Kratz et al., 2005). However, the cellular and biochemical basis for the role of SHP-2 in Noonan syndrome, AML, ALL, and JMML is unknown.

Shp-2 is a widely expressed non-receptor tyrosine phosphatase comprised of two tandemly arranged SH2 domains and a protein tyrosine phosphatase (PTP) domain. *Shp-2*, also known as *Sh-Ptp2*, *Ptpn11*, *Ptp1d*, and *Ptp2c*, is the vertebrate homologue of the Drosophila gene *corkscrew* (*csw*). The sequence, expression pattern, and function of *Shp-2* are highly conserved throughout evolution. For example, *Xenopus* and human orthologues display 94% sequence identity, and as in fly and mouse, *Xenopus shp-2* is believed to be ubiquitously expressed (Tang et al., 1995; Langdon et al., 2007). Moreover, several animal models have suggested a critical role for *Shp-2* in vertebrate development. For example, mice expressing an internal deletion of the amino-terminal (N-SH2) domain of *Shp-2* die at late gastrulation and display several mesodermal abnormalities including heart and vascular defects (Saxton et al., 1997; Saxton and Pawson, 1999; Yang et al., 2006). In addition *Shp-2* mutant cells derived from homozygous mutant embryos show that *Shp-2* is required for full and sustained activation of the MAPK pathway in response to FGF, thus demonstrating that SHP-2 functions downstream of the FGF/MAPK pathway *in vivo* (Saxton et al., 1997; Saxton and Pawson, 1999). Consistent with these findings, studies in *Xenopus* have shown that a dominant negative form of *Xenopus Shp-2* can completely block mesoderm formation in response to both MAPK and FGF (Tang et al., 1995). Furthermore, *in vitro* and tissue culture studies have shown that *csw/Shp-2* interacts directly with the FGF inhibitor SPROUTY, leading to SPROUTY phosphorylation and inactivation (Hanafusa et al., 2004; Jarvis et al., 2006).

In the mouse and chick, SHP-2 is required in the EGF pathway for formation of cardiac valves. However, because approximately one-third of patients with Noonan-associated heart defects appear to undergo normal valvulogenesis (Chen et al., 2000; Krenz et al., 2005), it remains unclear if SHP-2 is required downstream of other receptor tyrosine kinase receptors for other aspects of heart development. To address whether SHP-2 functions in cardiac pathways in addition to EGF and valvulogenesis and to bypass the early embryonic requirements for SHP-2, Langdon et al. (2007) used a *Xenopus* cardiac explant assay and chemical SHP-2 inhibitors to demonstrate that SHP-2 is required for the survival of actively proliferating cardiac progenitor populations but not those that have exited the cell cycle. It was further demonstrated that SHP-2 is directly phosphorylated on specific residues *in vivo* in response to FGF signaling, that SHP-2 co-immunoprecipitates with the FGF receptor adaptor, and that a constitutively active Noonan-associated *Shp-2* mutation can rescue cardiac defects induced by FGF inhibition. Collectively, these studies imply that SHP-2 functions in the FGF/MAPK pathway to maintain survival of proliferating populations of cardiac progenitor cells. However, it remains to be determined why mis-sense mutations in *Shp-2* lead to a tissue-specific effect in animals and humans.

Heterotaxy and Cardiac Looping Defects: *Zic3*

Heterotaxy (*situs ambiguus*) is a spectrum disorder in which the position of thoracic and abdominal organs is abnormal. Heterotaxy malformations are thought to arise from defective left-right patterning during embryonic development.

Establishing laterality in the embryo is a complex process involving a multitude of spatio-temporal signaling events (Mercola, 1999; Boorman and Shimeld, 2002). Initially, cells in the left-right coordinator (posterior notochord in mammals, gastrocoel roof plate in *Xenopus*, and Kupffer's vesicle in zebrafish) adjacent to the organizing node develop specialized motile cilia that generate a leftward fluid flow and an asymmetrical morphogen gradient (Tabin and Vogan, 2003; Blum et al., 2009; Sutherland and Ware, 2009). The subsequent lateralized expression of nodal, a member of the transforming growth factor β (TGFβ) family, is then thought to be involved in specifying left-right asymmetry via the notch signaling pathway (Krebs et al., 2003; Raya et al., 2003). *Pitx2*, a paired homeobox transcription factor, also plays a crucial role in organ symmetry, particularly in heart looping, downstream of nodal signaling (Ryan et al., 1998).

One of the first major morphological symmetry-breaking events in vertebrates occurs when the relatively symmetrical heart tube undergoes a rightward (dextral) bend, after which a complex process of looping and septation results in the mature multi-chambered heart (Mercola, 1999; Manner, 2000; Boorman and Shimeld, 2002; Manner, 2009). Cardiac looping defects are commonly observed in cases of heterotaxy, and these defects account for approximately 3% of all CHDs. Other common heart phenotypes seen in heterotaxic patients include ASD, VSD, transposition of the great arteries, double outlet right ventricle, single ventricle, and aortic arch defects (Bowers et al., 1996; Lin et al., 2000; Belmont et al., 2004; Sutherland and Ware, 2009). Numerous cases of familial clustering of heterotaxy

have been identified, suggesting autosomal inheritance of the disorder. However, X-linked inheritance has also been shown, involving mutations in the conserved zinc-finger transcription factor gene, *Zic3* (Gebbia et al., 1997; Ware et al., 2004). Heart defects and altered nodal expression are observed in *Zic3* mutant mice (Purandare et al., 2002). In *Xenopus* embryos, *zic3* is expressed in the mesoderm of the gastrulating embryo in a left-right (L-R) symmetrical fashion, however, unilateral right-sided overexpression of *zic3* is sufficient to disturb the L-R axis, resulting in abnormal heart and gut looping and affecting the lateral expression of *pitx2* and *nodal related 1 (Xnrl)* (Kitaguchi and others, 2000). *Xenopus zic3* is therefore considered to have a conserved early role in transducing signals from the left-right organizer and establishing asymmetry (Kitaguchi et al., 2000; Kitaguchi et al., 2002).

The amphibian model system has historically been used to study left-right patterning since the early 1900s by Spemann and colleagues. Subsequently, the *Xenopus* model was established, and has proven ideally suited to study the role of left-right laterality, using well-accepted techniques such as lineage tracing and fate mapping, in the process of heart development (Gormley and Nascone-Yoder, 2003; Blum et al., 2009). One of the first events in *Xenopus* embryonic development is cleavage at the one-cell stage to form two blastomeres, the descendents of which will contribute almost exclusively to either the left or the right side of the embryo. This feature enables researchers to independently alter signaling events or gene expression unilaterally to determine their effect on asymmetry and to conduct left-right lineage tracing experiments, particularly of the heart region (Branford et al.,

2000; Kitaguchi et al., 2000; Kitaguchi et al., 2002; Dagle et al., 2003; Chen et al., 2004; Ramsdell et al., 2006; Toyoizumi et al., 2006; Jahr et al., 2008). Recent work in *Xenopus* has demonstrated that cell lineages in the heart display a high degree of asymmetry, and that defects in left-right patterning alter cardiomyocyte allocation and differentiation in the heart, leading to cardiac malformations (Chen et al., 2004; Ramsdell et al., 2006). The *Xenopus* model is therefore an optimal organism to study the fate of cardiac cell populations and to determine how specific genes such as *Zic3* may be involved in establishing laterality in the heart and their roles in heterotaxic phenotypes.

Axenfeld-Reiger Syndrome: *Pitx2* and *FoxC1*

Axenfeld-Rieger syndrome (ARS) is a complex autosomal dominant disorder primarily characterized by anomalies of the anterior segment of the eye, face, teeth, and umbilical stump. Congenital heart defects, including ASD, pseudotruncus arteriosus, and mitral valve and intraventricular septal defects have also been reported in a number of patients with ARS (Cunningham et al., 1998; Mammi et al., 1998; Davies et al., 1999; Bekir and Gungor, 2000; Baruch and Erickson, 2001; Grosso et al., 2002; Maclean et al., 2005; Calcagni et al., 2006; Aysenur Pac et al., 2008; Weisschuh et al., 2008; Antevil et al., 2009; Akkus and Argin, 2010). Linkage analyses have identified four different loci in humans, *4q25*, *6p25*, *13q14*, and *16q24*, each of which has been independently associated with ARS. Further analyses of *4q25* and *6p25* in patients with ARS have uncovered mutations in two genes, *Pitx2* and *Foxc1,* respectively (Amendt et al., 2000; Hjalt and Semina, 2005; Maclean et al., 2005).

Pitx2 is a highly conserved homeodomain transcription factor that is expressed asymmetrically in the left lateral plate mesoderm in chick, zebrafish, *Xenopus*, and mouse embryos (Ryan et al., 1998; Campione et al., 1999). At heart-forming stages, *pitx2* expression continues to be restricted to the left half of the heart tube in *Xenopus* embryos. In mouse, *Pitx2* is expressed in the left side of the heart tube and in the left ventricle, OFT, and atrium during heart looping (Ryan et al., 1998). The defects observed in *Pitx2* null and hypomorphic mice, such as altered looping of the heart, absence of atrial septation, and dysmorphic ventricular septation, recapitulate the defects observed in human ARS patients with *Pitx2* dysfunction (Gage et al., 1999; Lin et al., 1999; Lu et al., 1999).

The use of *Xenopus* has been instrumental in understanding the dual role of *Pitx2* in heart development, firstly in directing the looping of the heart tube and secondly in controlling the morphogenesis of the cardiac chambers. Misexpression of *pitx2* by injection of its mRNA on the right side of the *Xenopus* embryo results in a reversal of heart looping, showing the conserved role of *pitx2* in directing this event. The restricted expression of *pitx2* is likely to be downstream of the TGFβ signaling family, as bilateral injections of mRNA encoding nodal or activin results in bilateral expression of the gene (Campione et al., 1999). Further, injection of a dominant negative form of the activin type II receptor into *Xenopus* embryos alters *pitx2* expression levels and subsequent heart looping. These findings are supported by similar experiments in chick (Ryan et al., 1998). Of the three isoforms of *Pitx2* present during development, experiments in *Xenopus*, zebrafish, and mouse

demonstrate that *Pitx2*c is the isoform that is specifically expressed in heart (Essner et al., 2000; Schweickert et al., 2000). The injection of modified antisense oligonucleotides that mediate degradation of *pitx2*c mRNA in *Xenopus* embryos results in cardiac defects that are very similar to phenotypes observed in *Pitx2* mutant mice, including abnormal atrial septation, extracellular matrix restriction, abnormal positioning of the atrial and ventricular chambers, and restriction of ventricular development. These tadpoles also exhibit dramatic straightening of the OFT, followed by a rightward migration (Dagle et al., 2003). This study demonstrates the conservation of *pitx2* function in *Xenopus* cardiac development and its relationship to ARS. It has recently been shown that *Pitx2* patterns the second heart field and is required to specify the left versus right atrium (Liu et al., 2002; Ai et al., 2006; Galli et al., 2008). It will be interesting to determine if *Xenopus* can be exploited as a useful model for testing the effects of various ARS-derived mutations on *Pitx2* function during second heart field development and for further identifying the mechanisms by which *Pitx2* functions.

Foxc1 is a member of the forkhead family of transcription factors and is expressed in endothelial and mesenchymal cells of the developing heart as well as in endocardial cushions derived from cardiac neural crest cells (Iida et al., 1997; Winnier et al., 1999; Kume et al., 2001; Seo et al., 2006). *Foxc1* transcripts have also been detected in the second heart field and in the proepicardium (Seo and Kume, 2006). In the newly formed heart, *Foxc1* is expressed in the atrial septum, the venous, aortic and pulmonary valves, and the mitral and tricuspid valves (Swiderski

et al., 1999). Consistent with its widespread expression in the heart, FOXC1 plays a critical role in heart valve formation and atrial septation as suggested by the cardiac defects noted in mice mutant for *Foxc1.* Specifically, *Foxc1* homozygous mutants display interruption or coarctation of the aortic arch, VSD, and pulmonary and aortic valve dysplasia (Winnier et al., 1999). Mice lacking both *Foxc1* and the closely related Fox transcription factor *Foxc2* have even more severe cardiac abnormalities consisting of hypoplasia or lack of the OFT and right ventricle as well as the inflow tract, and dysplasia of the OFT and atrioventricular cushions. These mice also have an abnormally formed epicardium, reduced cell proliferation, and increased apoptosis of neural crest cells (Winnier et al., 1999; Kume et al., 2001; Seo and Kume, 2006).

Foxc1 has been identified in *Xenopus* and is present in cardiac lineages (Koster et al., 1998; Gessert and Kuhl, 2009). Depletion of *foxc1* during early *Xenopus* development results in downregulation of adhesion molecules involved in mesoderm development and increased apoptosis, correlating with the phenotypes observed in the mouse mutants (Cha et al., 2007). It remains to be determined if reduction of FOXC1 levels in *Xenopus* has similar effects on cardiac morphology to those observed in mouse knockouts and patients with ARS. However, the early phenotypes of FOXC1 depletion during *Xenopus* development provide a model in which to investigate the phenotypic changes that result from *Foxc1* disruption.

CHARGE Syndrome: *Chd7*

CHARGE syndrome (Coloboma, Heart defects, choanal Atresia, Retarded growth and development, Genital abnormalities, and Ear anomalies) is a complex disease associated with a number of cardiac abnormalities including Tetralogy of Fallot, atrioventricular canal defects, and aortic arch anomalies (Davenport et al., 1986). The majority of individuals with CHARGE syndrome have mutations in the coding region of *chromodomain helicase DNA binding protein 7* (*Chd7)* (Vissers et al., 2004; Aramaki et al., 2006; Jongmans et al., 2006; Lalani et al., 2006; Delahaye et al., 2007; Wincent et al., 2008; Kaliakatsos et al., 2010; Wessels et al., 2010).

Chd7 expression has been characterized in the chick and mouse, where it has been found to be expressed mainly in the neural ectoderm and branchial arches (Bosman et al., 2005; Aramaki et al., 2007; Hurd et al., 2007). Mutant *Chd7* mice display defects in neural stem cell proliferation, olfaction, and some cardiac defects, including formation of the interventricular septum (Bosman et al., 2005; Adams et al., 2007; Hurd et al., 2007; Layman et al., 2009). It has been proposed that the multiple phenotypes in CHARGE syndrome are caused by defects in neural crest cell (NCC) migration (Siebert et al., 1985). Recently, *Chd7* was found to be expressed in *Xenopus* NCCs as well as in human NC-like cells. MO knockdown of *chd7* in *Xenopus* perturbs the migration of NCCs to the pharyngeal arches. This phenotype is partially rescued by injecting human *Chd7* mRNA, suggesting that the molecular function of CHD7 is well-conserved. In addition, overexpression of human *Chd7* with a substitution of a conserved lysine residue in its ATPase domain results in a

dominant-negative effect (Bajpai et al., 2010). This dominant negative effect recapitulates the major features of CHARGE syndrome described above, including abnormal positioning of the truncus arteriosus and OFT. Analysis of markers associated with NCCs reveal that *chd7* is not required for the induction or survival of NCCs, but for their specification. The expression of *sox9*, *twist*, and *slug*, genes that mark multipotent, migrating NCCs, is severely perturbed in *chd7* downregulated embryos (Sauka-Spengler and Bronner-Fraser, 2008; Bajpai et al., 2010). These studies in *Xenopus* have provided a powerful *in vivo* model in which to study the role of NCCs in heart development and the CHDs that result from improper NCC migration and specification. More recently, the chromatin remodeling factors CHD8 and BRG1 have been shown to physically interact with CHD7 (Bajpai et al., 2010; Batsukh et al., 2010) and *Brg1* was demonstrated to play a role in regulating cardiac growth and differentiation (Hang et al., 2010). The roles of *Chd8* and *Brg1* in a *Xenopus* model of CHARGE syndrome could aid in the understanding of this complex syndrome.

FUTURE DIRECTIONS AND EMERGING TECHNOLOGIES IN *XENOPUS*

Investigating a Role for the Epicardium in Congenital Heart Disease

The epicardium is a mesothelial sheet of cells surrounding the myocardium of the developing looped heart in many vertebrate organisms (Ho and Shimada, 1978; Viragh and Challice, 1981; Hirakow, 1992; Manner et al., 2001; Jahr et al., 2008; Pombal et al., 2008; Serluca, 2008). The epicardial structure arises from the pro-epicardial organ (PEO), which is situated on the sinus venosus. These mesothelial cells cluster and bridge over towards the ventricular surface of the heart and migrate

onto the myocardial surface as an epithelial-like sheet. Subsequently, subsets of epicardial cells undergo epithelial-mesenchymal transition (EMT) and migrate into the sub-epicardial space and myocardium where they differentiate into various cell populations including fibroblasts and smooth muscle cells of the coronary vasculature (Manner et al., 2001; Lie-Venema et al., 2007; Winter and Gittenberger-de Groot, 2007). The epicardium is thought to play a mitogenic role in cardiomyocyte growth and has been shown to be important for cardiac repair in adult zebrafish (Lepilina et al., 2006). Recently, adult human epicardium-derived cells (EPDCs) were demonstrated to have a paracrine role in improving mammalian cardiac function when co-transfected with cardiomyocytes into an infarcted murine heart (Winter et al., 2007; Winter et al., 2009). Thus, the epicardium may have the potential to stimulate cardiac repair and regeneration, given the right conditions.

Various congenital heart diseases display abnormalities that may arise from improper epicardium formation or differentiation of EPDCs. In avian embryos in which either the pro-epicardial organ is ablated or the epithelial-mesenchymal transition of EPDCs is disrupted, defects are seen in the compact layer of the myocardium, while the inner curvature of the heart is wider and often displays a double outlet right ventricle, indicative of a heart looping defect (Gittenberger-de Groot et al., 2000; Lie-Venema et al., 2005; Manner et al., 2005). Ventricular non-compaction is also seen when genes involved in epicardium formation, e.g., *Wt1* and *RXRα*, are knocked out in the mouse (Moore et al., 1998; Merki et al., 2005). In addition to their roles in regulating the development of the compact ventricular and

atrial myocardia, EPDCs are involved in the development of cardiac structures associated with the conduction system. The annulus fibrosus, which plays an important insulating role in the cardiac conduction system, is derived from the epicardium, and EPDCs also influence the formation of the peripheral Purkinje fiber network from ventricular cardiomyocytes (Eralp et al., 2006; Zhou et al., 2010). Electrophysiological cardiac defects, such as Wolff-Parkinson-White syndrome and Mahaim tachycardia, may therefore have an origin in improper epicardium or EPDC formation.

EPDCs also contribute cells to the atrioventricular cushions and valves, and disrupting epicardium formation can lead to aberrant valve formation (Gittenberger-de Groot et al., 1998; Gittenberger-de Groot et al., 2000; Perez-Pomares et al., 2002; Manner et al., 2005). It is conceivable that disorders in which the valve leaflet has not fully delaminated - for example, Ebstein's anomaly (tricuspid valve leaflet) - might result from defects in epicardial patterning or signaling (Attenhofer Jost et al., 2005; Lie-Venema et al., 2007). Ventricular non-compaction may also be indicative of an epicardial defect as shown by mouse knockout models of genes involved in epicardium formation, e.g., *Wt1* and *RXRα*, or in PEO ablation studies in chick (Moore et al., 1998; Manner et al., 2005; Merki et al., 2005; Sucov et al., 2009). Interestingly, the *Fog-2* knockout mouse, which has an epicardial defect phenotype, displays many of the anomalies described above - including tricuspid atresia, thin myocardium, double outlet right ventricles, and VSD (Svensson et al., 2000; Tevosian et al., 2000; Clark et al., 2006).

To date, little is known about how the epicardium develops and functions in *Xenopus* embryos. Scanning electron microscopy has demonstrated the presence of the PEO on the right side of the septum transversum in *Xenopus* embryos, similar to other vertebrates (Jahr et al., 2008). Furthermore, genes characteristic of the vertebrate PEO and epicardium are conserved in *Xenopus* (Jahr et al., 2008). The *Xenopus* model lends itself to studying the epicardium and potential defects in valve formation and conduction systems due to the ease of manipulating gene function and the established techniques of tissue explanting, antisense MO microinjection, lineage tracing, and transgenics. Recent advances in live imaging have enabled researchers to utilize the *Xenopus* model to visualize cardiac development in real time and to use non-invasive electrical recording, Doppler optical cardiograms, and optical coherence tomography to study heart structure, conduction, and blood flow to determine the role of the epicardium in these processes (Bartlett et al., 2004; Mariampillai et al., 2007; Yelin et al., 2007; Kieserman et al., 2010).

In Vivo Imaging of the Developing *Xenopus* Heart

Xenopus embryos are very well-suited for live imaging of dynamic developmental processes due to their large size and external development. Because of the large size of the embryos, individual cells in the embryo are larger, which allows visualization of the subcellular localization and dynamics of a given fluorescent fusion protein. For example, live confocal imaging has been successfully used to demonstrate the dispersal of individual fluorescent myeloid cells throughout the *Xenopus* embryo (Kieserman et al., 2010). A combination of transgenesis and advanced imaging tools makes this type of approach feasible in the living animal.

Yolk opacity in the early *Xenopus* embryo presents a challenge for imaging of deeper tissues. However, cells and/or deep tissues can be visualized easily after microsurgery and subsequent culture of tissue explants. High resolution imaging of the structure and function of the developing myocardium will be critical to complete our understanding of how the heart develops in three and four dimensions, and thus how developmental defects can arise in this system.

Historically, the morphology of the *Xenopus* embryonic heart has been studied in fixed embryos with a combination of confocal microscopy and 3D reconstruction of serial sections through the heart (Kolker et al., 2000; Mohun, 2000). As even slight morphological or dynamic changes in the heart can result in myocardial dysfunction, it is of vital importance to examine these changes *in vivo* in the developing embryo. One area in which this is particularly relevant is in the characterization of defects in the cardiac conduction system. Human CHD is often complicated by atrioventricular conduction abnormalities. However, a thorough understanding of the defects in embryonic heart contraction as they result from a genetic or morphological abnormality is lacking due to the difficulty of examining these defects *in vivo*. It has recently been demonstrated that the *Xenopus* embryo is amenable to noninvasive live video analysis of the conduction system, allowing one to examine the properties of chamber contraction *in vivo* (Bartlett et al., 2004). Moreover, *Xenopus* cardiac electrophysiology shares many characteristics with the human conduction system, making it an ideal model in which to analyze the physiology of cardiac conduction defects. As a proof of principle, this methodology

has been used to examine the microscopic timing of heart contraction in embryos injected with two human *Nkx2.5* mutants and resulted in the identification of a number of conduction defects including a delay in the AV interval and a distinct tachycardia (Bartlett et al., 2007). This type of study, when applied to other human mutations such as those in *Tbx5* that cause Holt-Oram Syndrome, can improve our understanding of these complex human pathologies.

Protein Interactions and Biochemical Function

As discussed previously, transgenesis has primarily been used to study the regulation of gene expression and has revealed much about the transcriptional regulation of cardiac development. However, it has been used relatively little as a tool for isolating protein complexes. Because protein complexes mediate the majority of cellular processes, knowledge of the composition and function of cardiac-specific protein complexes will provide key insights into their tissue-specific activity in the heart. With the advent of proteomics-based approaches to identify endogenous protein complexes, there are a variety of convenient *in vivo* tags such as GFP that can be used to genomically label any protein of interest. Thus, the generation of transgenic *Xenopus* lines that express tagged versions of proteins will provide virtually unlimited material for applications such as mass spectrometry and protein localization studies. Additionally, tagged proteins carrying known CHD-causing mutations could be utilized to characterize changes in their ability to form complexes with other cardiac proteins. As discussed previously, deficiencies in members of cardiac transcriptional complexes often lead to congenital heart

malformations, illuminating the need to investigate the functional role of these complexes during cardiac development.

Genetic Approaches in *Xenopus tropicalis*

To date, most studies that have used *Xenopus* as a model system to examine cardiac development have used the pseudotetraploid species *Xenopus laevis* and have relied upon well-established nucleic acid microinjection techniques for depletion or over-expression of proteins in the developing embryo. As our understanding of the genetic basis of inherited cardiac disease increases, there will be a greater need to use genetic approaches in *Xenopus*. Genetic techniques enable precise experimental manipulation that can be used to gain a deeper understanding not just of individual gene functions, but also of the interconnectivity between genes in genetic networks (through enhancer/suppressor gene interaction studies, for example). These interconnections, coupled with variation in the genetic background, may ultimately explain the range of disease type and severity often observed in patients with particular CHDs (Basson et al., 1994; Newbury-Ecob et al., 1996; Sznajer et al., 2007). The use of loss-of-function or gain-of-function alleles of endogenous genes that are generated by mutagenesis also circumvents the undesirable features of MO-based inhibition and mRNA-based expression that result from the inherent limitations in controlling where and when MOs or mRNAs are active in the embryo. Specifically, the role of mutations that affect the biochemical function of a protein can be examined without inappropriately expressing the mutant protein in cells in which the native protein is not expressed, or at times at which it would not normally be present.

The diploid *Xenopus tropicalis* is much more amenable to genetic analysis than the pseudotetraploid *X. laevis*. Fortunately, the vast majority of reagents and techniques developed by researchers for *X. laevis* can be adapted for use with *X. tropicalis*, primarily due to the extremely close similarities between the two species at the genetic and embryonic levels. Even complex reagents such as microarrays developed in one *Xenopus* species have been shown to be usable in both, although species-specific reagents are becoming increasingly available (Chalmers et al., 2005). A key factor encouraging researchers to adopt *X. tropicalis* is the availability of a high-quality genome sequence and the resources that have stemmed from it, including a simple-sequence repeat map of more than 1,500 polymorphic markers that allows mutations to be mapped to relatively small regions of the genome following their isolation in forward genetic screens (Xu et al., 2008; Hellsten et al., 2010) (http://tropmap.biology.uh.edu/index.html). The first two mutations mapped in *X. tropicalis, Muzak* and *Dicky Ticker*, both affect cardiac function and are located in the myosin heavy chain gene *myh6* and the muscle-specific chaperone gene *unc45b*, respectively (Abu-Daya et al., 2009; Geach and Zimmerman, 2010). These early successes validate *X. tropicalis* as a model in which novel cardiac genes can be identified through phenotype-based forward genetic screens. The primary importance of this work will be to gain a better understanding of the developmental genetics of cardiac cell type differentiation and morphogenesis. However, studying the effects of mutations in disease-associated genes is also likely to advance our understanding of the etiology of congenital heart abnormalities.

Table A1.1. *Xenopus* models of human congenital heart disease.

Gene Name	Disease	Cardiovascular Manifestations	*Xenopus* Model	*Xenopus* Cardiac Phenotype	Refs
Tbx1	DiGeorge Syndrome	TOF, persistent truncus arteriosus	overexpression of dominant negative	unlooped heart, pericardial edema	(Ataliotis et al., 2005)
Tbx5	Holt-Oram Syndrome	ASD, VSD, cardiac conduction system defects	overexpression of dominant negative	unlooped heart	(Horb and Thomsen, 1999)
			protein depletion	unlooped heart, loss of cardiac cells	(Brown et al., 2005)
Tbx20	NA	ASD, VSD, valve disease, pulmonary hypertension, cardiomyopathy, TOF	protein depletion	unlooped heart, pericardial edema, loss of cardiac cells	(Brown et al., 2005)
Nkx2.5	NA	ASD, cardiac conduction system defects	overexpression	enlarged heart	(Cleaver, 1996)
			overexpression of dominant negative	reduced heart	(Fu, 1998; Grow and Krieg, 1998)
			overexpression of mutant mRNA	ASD, cardiac conduction system defects	(Bartlett et al., 2007)
Gata4	NA	ASD	protein depletion	partial fusion of heart fields, cardiac bifida, abnormal cardiac looping	(Haworth et al., 2008)
Shp2	Noonan Syndrome	ASD, VSD, pulmonary stenosis, hypertrophic cardiomyopathy	chemical inhibition	unfused heart fields, loss of cardiac cells	(Langdon et al., 2007)
Zic3	Heterotaxy	cardiac looping defects, ASD, VSD, transposition of the great arteries, double outlet right ventricle, ventricle and aortic arch defects	overexpression	abnormal cardiac looping	(Kitaguchi et al., 2000; Kitaguchi et al., 2002)
Pitx2	Axonfeld-Reiger Syndrome	ASD, pseudotruncus arteriosus, mitral valve and intraventricular septal defects	overexpression	abnormal cardiac looping	(Campione et al., 1999)
			overexpression of dominant negative	abnormal cardiac looping	(Campione et al., 1999)
			protein depletion	abnormal atrial septation, defects in atrial and ventricular chamber position, restriction of ventricular development	(Dagle et al., 2003)
Chd7	CHARGE Syndrome	TOF, atrioventricular canal defects, aortic arch defects	protein depletion	defects in neural crest cell migration	(Bajpai et al., 2010)
			overexpression of mutant mRNA	abnormal positioning of truncus arteriosus and OFT	(Bajpai et al., 2010)

TOF, Tetralogy of Fallot; ASD, atrial septal defects; VSD, ventricular septal defects; NA, Not Applicable; OFT, outflow tract

REFERENCES

Abu-Daya, A., Sater, A. K., Wells, D. E., Mohun, T. J. and Zimmerman, L. B. (2009) 'Absence of heartbeat in the Xenopus tropicalis mutation muzak is caused by a nonsense mutation in cardiac myosin myh6', *Dev Biol*.

Adams, M. E., Hurd, E. A., Beyer, L. A., Swiderski, D. L., Raphael, Y. and Martin, D. M. (2007) 'Defects in vestibular sensory epithelia and innervation in mice with loss of Chd7 function: implications for human CHARGE syndrome', *J Comp Neurol* 504(5): 519-32.

Afouda, B. A., Martin, J., Liu, F., Ciau-Uitz, A., Patient, R. and Hoppler, S. (2008) 'GATA transcription factors integrate Wnt signalling during heart development', *Development* 135(19): 3185-90.

Ai, D., Liu, W., Ma, L., Dong, F., Lu, M. F., Wang, D., Verzi, M. P., Cai, C., Gage, P. J., Evans, S. et al. (2006) 'Pitx2 regulates cardiac left-right asymmetry by patterning second cardiac lineage-derived myocardium', *Dev Biol* 296(2): 437-49.

Akkus, M. N. and Argin, A. (2010) 'Congenital heart defects in two siblings in an Axenfeld-Rieger syndrome family', *Clin Dysmorphol* 19(2): 56-61.

Allen, B. G. and Weeks, D. L. (2005) 'Transgenic Xenopus laevis embryos can be generated using phiC31 integrase', *Nat Methods* 2(12): 975-9.

Allen, B. G. and Weeks, D. L. (2009) 'Bacteriophage phiC31 integrase mediated transgenesis in Xenopus laevis for protein expression at endogenous levels', *Methods Mol Biol* 518: 113-22.

Amaya, E. and Kroll, K. L. (1999) 'A method for generating transgenic frog embryos', *Methods Mol Biol* 97: 393-414.

Amendt, B. A., Semina, E. V. and Alward, W. L. (2000) 'Rieger syndrome: a clinical, molecular, and biochemical analysis', *Cell Mol Life Sci* 57(11): 1652-66.

Andres, A. C., Muellener, D. B. and Ryffel, G. U. (1984) 'Persistence, methylation and expression of vitellogenin gene derivatives after injection into fertilized eggs of Xenopus laevis', *Nucleic Acids Res* 12(5): 2283-302.

Antevil, J., Umakanthan, R., Leacche, M., Brewer, Z., Solenkova, N., Byrne, J. G. and Greelish, J. P. (2009) 'Idiopathic mitral valve disease in a patient presenting with Axenfeld-Rieger syndrome', *J Heart Valve Dis* 18(3): 349-51.

Aramaki, M., Kimura, T., Udaka, T., Kosaki, R., Mitsuhashi, T., Okada, Y., Takahashi, T. and Kosaki, K. (2007) 'Embryonic expression profile of chicken CHD7, the ortholog of the causative gene for CHARGE syndrome', *Birth Defects Res A Clin Mol Teratol* 79(1): 50-7.

Aramaki, M., Udaka, T., Kosaki, R., Makita, Y., Okamoto, N., Yoshihashi, H., Oki, H., Nanao, K., Moriyama, N., Oku, S. et al. (2006) 'Phenotypic spectrum of CHARGE syndrome with CHD7 mutations', *J Pediatr* 148(3): 410-4.

Ariizumi, T., Kinoshita, M., Yokota, C., Takano, K., Fukuda, K., Moriyama, N., Malacinski, G. M. and Asashima, M. (2003) 'Amphibian in vitro heart induction: a simple and reliable model for the study of vertebrate cardiac development', *Int J Dev Biol* 47(6): 405-10.

Ataliotis, P., Ivins, S., Mohun, T. J. and Scambler, P. J. (2005) 'XTbx1 is a transcriptional activator involved in head and pharyngeal arch development in Xenopus laevis', *Dev Dyn* 232(4): 979-91.

Attenhofer Jost, C. H., Connolly, H. M., Edwards, W. D., Hayes, D., Warnes, C. A. and Danielson, G. K. (2005) 'Ebstein's anomaly - review of a multifaceted congenital cardiac condition', *Swiss Med Wkly* 135(19-20): 269-81.

Aysenur Pac, F., Cagdas, D. N. and Necati Demir, M. (2008) 'Axenfeld-Rieger syndrome and pseudotruncus arteriosus', *Int J Cardiol* 126(1): e4-7.

Bajpai, R., Chen, D. A., Rada-Iglesias, A., Zhang, J., Xiong, Y., Helms, J., Chang, C. P., Zhao, Y., Swigut, T. and Wysocka, J. (2010) 'CHD7 cooperates with PBAF to control multipotent neural crest formation', *Nature* 463(7283): 958-62.

Baldini, A. (2004) 'DiGeorge syndrome: an update', *Curr Opin Cardiol* 19(3): 201-4.
Bartlett, H. L., Scholz, T. D., Lamb, F. S. and Weeks, D. L. (2004) 'Characterization of embryonic cardiac pacemaker and atrioventricular conduction physiology in Xenopus laevis using noninvasive imaging', *Am J Physiol Heart Circ Physiol* 286(6): H2035-41.

Bartlett, H. L., Sutherland, L., Kolker, S. J., Welp, C., Tajchman, U., Desmarais, V. and Weeks, D. L. (2007) 'Transient early embryonic expression of Nkx2-5 mutations linked to congenital heart defects in human causes heart defects in Xenopus laevis', *Dev Dyn* 236(9): 2475-84.

Bartlett, H. L. and Weeks, D. L. (2008) 'Lessons from the lily pad: Using Xenopus to understand heart disease', *Drug Discov Today Dis Models* 5(3): 141-146.

Baruch, A. C. and Erickson, R. P. (2001) 'Axenfeld-Rieger anomaly, hypertelorism, clinodactyly, and cardiac anomalies in sibs with an unbalanced translocation der(6)t(6;8)', *Am J Med Genet* 100(3): 187-90.

Basson, C. T., Bachinsky, D. R., Lin, R. C., Levi, T., Elkins, J. A., Soults, J., Grayzel, D., Kroumpouzou, E., Traill, T. A., Leblanc-Straceski, J. et al. (1997) 'Mutations in human TBX5 [corrected] cause limb and cardiac malformation in Holt-Oram syndrome', *Nat Genet* 15(1): 30-5.

Basson, C. T., Cowley, G. S., Solomon, S. D., Weissman, B., Poznanski, A. K., Traill, T. A., Seidman, J. G. and Seidman, C. E. (1994) 'The clinical and genetic spectrum of the Holt-Oram syndrome (heart-hand syndrome)', *N Engl J Med* 330(13): 885-91.

Basson, C. T., Huang, T., Lin, R. C., Bachinsky, D. R., Weremowicz, S., Vaglio, A., Bruzzone, R., Quadrelli, R., Lerone, M., Romeo, G. et al. (1999) 'Different TBX5 interactions in heart and limb defined by Holt-Oram syndrome mutations', *Proc Natl Acad Sci U S A* 96(6): 2919-24.

Batsukh, T., Pieper, L., Koszucka, A. M., von Velsen, N., Hoyer-Fender, S., Elbracht, M., Bergman, J. E., Hoefsloot, L. H. and Pauli, S. (2010) 'CHD8 interacts with CHD7, a protein which is mutated in CHARGE syndrome', *Hum Mol Genet* 19(14): 2858-66.

Bekir, N. A. and Gungor, K. (2000) 'Atrial septal defect with interatrial aneurysm and Axenfeld-Rieger syndrome', *Acta Ophthalmol Scand* 78(1): 101-3.

Belmont, J. W., Mohapatra, B., Towbin, J. A. and Ware, S. M. (2004) 'Molecular genetics of heterotaxy syndromes', *Curr Opin Cardiol* 19(3): 216-20.

Bendig, M. M. and Williams, J. G. (1984) 'Differential expression of the Xenopus laevis tadpole and adult beta-globin genes when injected into fertilized Xenopus laevis eggs', *Mol Cell Biol* 4(3): 567-70.

Benson, D. W., Basson, C. T. and MacRae, C. A. (1996) 'New understandings in the genetics of congenital heart disease', *Curr. Opin. Pediatr.* 8(5): 505-511.

Benson, D. W., Silberbach, G. M., Kavanaugh-McHugh, A., Cottrill, C., Zhang, Y., Riggs, S., Smalls, O., Johnson, M. C., Watson, M. S., Seidman, J. G. et al. (1999) 'Mutations in the cardiac transcription factor NKX2.5 affect diverse cardiac developmental pathways', *J Clin Invest* 104(11): 1567-73.

Bentires-Alj, M., Paez, J. G., David, F. S., Keilhack, H., Halmos, B., Naoki, K., Maris, J. M., Richardson, A., Bardelli, A., Sugarbaker, D. J. et al. (2004) 'Activating mutations of the noonan syndrome-associated SHP2/PTPN11 gene in human solid tumors and adult acute myelogenous leukemia', *Cancer Res* 64(24): 8816-20.

Bill, B. R., Petzold, A. M., Clark, K. J., Schimmenti, L. A. and Ekker, S. C. (2009) 'A primer for morpholino use in zebrafish', *Zebrafish* 6(1): 69-77.

Blum, M., Beyer, T., Weber, T., Vick, P., Andre, P., Bitzer, E. and Schweickert, A. (2009) 'Xenopus, an ideal model system to study vertebrate left-right asymmetry', *Dev Dyn* 238(6): 1215-25.

Boorman, C. J. and Shimeld, S. M. (2002) 'The evolution of left-right asymmetry in chordates', *BioEssays* 24(11): 1004-11.

Bosman, E. A., Penn, A. C., Ambrose, J. C., Kettleborough, R., Stemple, D. L. and Steel, K. P. (2005) 'Multiple mutations in mouse Chd7 provide models for CHARGE syndrome', *Hum Mol Genet* 14(22): 3463-76.

Bowers, P. N., Brueckner, M. and Yost, H. J. (1996) 'The genetics of left-right development and heterotaxia', *Semin Perinatol* 20(6): 577-88.

Branford, W. W., Essner, J. J. and Yost, H. J. (2000) 'Regulation of gut and heart left-right asymmetry by context-dependent interactions between xenopus lefty and BMP4 signaling', *Dev Biol* 223(2): 291-306.

Brassington, A. M., Sung, S. S., Toydemir, R. M., Le, T., Roeder, A. D., Rutherford, A. E., Whitby, F. G., Jorde, L. B. and Bamshad, M. J. (2003) 'Expressivity of Holt-Oram syndrome is not predicted by TBX5 genotype', *Am J Hum Genet* 73(1): 74-85.

Breckenridge, R. A., Mohun, T. J. and Amaya, E. (2001) 'A role for BMP signalling in heart looping morphogenesis in Xenopus', *Dev Biol* 232(1): 191-203.

Brown, D. D., Christine, K. S., Showell, C. and Conlon, F. L. (2007) 'Small heat shock protein Hsp27 is required for proper heart tube formation', *Genesis* 45(11): 667-78.

Brown, D. D., Martz, S. N., Binder, O., Goetz, S. C., Price, B. M. J., Smith, J. C. and Conlon, F. L. (2005) 'Tbx5 and Tbx20 act synergistically to control vertebrate heart morphogenesis', *Development* 132(3): 553-563.

Bruneau, B. G., Nemer, G., Schmitt, J. P., Charron, F., Robitaille, L., Caron, S., Conner, D. A., Gessler, M., Nemer, M., Seidman, C. E. et al. (2001) 'A Murine Model of Holt-Oram Syndrome Defines Roles of the T-Box Transcription Factor Tbx5 in Cardiogenesis and Disease', *Cell* 106(6): 709-721.

Cai, C. L., Zhou, W., Yang, L., Bu, L., Qyang, Y., Zhang, X., Li, X., Rosenfeld, M. G., Chen, J. and Evans, S. (2005) 'T-box genes coordinate regional rates of proliferation and regional specification during cardiogenesis', *Development*.

Calcagni, G., Digilio, M. C., Capolino, R., Dallapiccola, B. and Marino, B. (2006) 'Concordant familial segregation of atrial septal defect and Axenfeld-Rieger anomaly in father and son', *Clin Dysmorphol* 15(4): 203-6.

Campione, M., Steinbeisser, H., Schweickert, A., Deissler, K., van Bebber, F., Lowe, L. A., Nowotschin, S., Viebahn, C., Haffter, P., Kuehn, M. R. et al. (1999) 'The homeobox gene Pitx2: mediator of asymmetric left-right signaling in vertebrate heart and gut looping', *Development* 126(6): 1225-34.

Cha, J. Y., Birsoy, B., Kofron, M., Mahoney, E., Lang, S., Wylie, C. and Heasman, J. (2007) 'The role of FoxC1 in early Xenopus development', *Dev Dyn* 236(10): 2731-41.

Chalmers, A. D., Goldstone, K., Smith, J. C., Gilchrist, M., Amaya, E. and Papalopulu, N. (2005) 'A Xenopus tropicalis oligonucleotide microarray works across species using RNA from Xenopus laevis', *Mech Dev* 122(3): 355-63.

Chapman, D. L., Garvey, N., Hancock, S., Alexiou, M., Agulnik, S. I., Gibson-Brown, J., Cebra-Thomas, J., Bollag, R., Silver, L. M. and Papaionnou, V. E. (1996) 'Expression of the T-box family genes, *Tbx1-Tbx5*, during early mouse development', *Dev. Dynam.* 206: 379-390.

Chen, B., Bronson, R. T., Klaman, L. D., Hampton, T. G., Wang, J. F., Green, P. J., Magnuson, T., Douglas, P. S., Morgan, J. P. and Neel, B. G. (2000) 'Mice mutant for Egfr and Shp2 have defective cardiac semilunar valvulogenesis', *Nat Genet* 24(3): 296-9.

Chen, Y., Mironova, E., Whitaker, L. L., Edwards, L., Yost, H. J. and Ramsdell, A. F. (2004) 'ALK4 functions as a receptor for multiple TGF beta-related ligands to regulate left-right axis determination and mesoderm induction in Xenopus', *Dev Biol* 268(2): 280-94.

Chesneau, A., Sachs, L. M., Chai, N., Chen, Y., Du Pasquier, L., Loeber, J., Pollet, N., Reilly, M., Weeks, D. L. and Bronchain, O. J. (2008) 'Transgenesis procedures in Xenopus', *Biol Cell* 100(9): 503-21.

Choo, B. G., Kondrichin, I., Parinov, S., Emelyanov, A., Go, W., Toh, W. C. and Korzh, V. (2006) 'Zebrafish transgenic Enhancer TRAP line database (ZETRAP)', *BMC Dev Biol* 6: 5.

Christine, K. S. and Conlon, F. L. (2008) 'Vertebrate CASTOR is required for differentiation of cardiac precursor cells at the ventral midline', *Dev Cell* 14(4): 616-23.

Clark, K. L., Yutzey, K. E. and Benson, D. W. (2006) 'Transcription factors and congenital heart defects', *Annu Rev Physiol* 68: 97-121.

Cleaver, O. B., PAtterson, K. D. and Krieg, P. A. (1996) 'Overexpressoin of the *tinman*-related genes XNkx-2.5 and XNkx-2.3 in *Xenopus* embryos results in myocardial hyperplasia.', *Development* 122: 3549-3556.

Cross, S. J., Ching, Y. H., Li, Q. Y., Armstrong-Buisseret, L., Spranger, S., Lyonnet, S., Bonnet, D., Penttinen, M., Jonveaux, P., Leheup, B. et al. (2000) 'The mutation spectrum in Holt-Oram syndrome', *J Med Genet* 37(10): 785-7.

Cunningham, E. T., Jr., Eliott, D., Miller, N. R., Maumenee, I. H. and Green, W. R. (1998) 'Familial Axenfeld-Rieger anomaly, atrial septal defect, and sensorineural hearing loss: a possible new genetic syndrome', *Arch Ophthalmol* 116(1): 78-82.

Dagle, J. M., Sabel, J. L., Littig, J. L., Sutherland, L. B., Kolker, S. J. and Weeks, D. L. (2003) 'Pitx2c attenuation results in cardiac defects and abnormalities of intestinal orientation in developing Xenopus laevis', *Dev Biol* 262(2): 268-81.

Dagle, J. M. and Weeks, D. L. (2001) 'Oligonucleotide-based strategies to reduce gene expression', *Differentiation* 69(2-3): 75-82.

Dale, L. and Slack, J. M. (1987) 'Fate map for the 32-cell stage of Xenopus laevis', *Development* 99(4): 527-51.

Davenport, S. L., Hefner, M. A. and Mitchell, J. A. (1986) 'The spectrum of clinical features in CHARGE syndrome', *Clin Genet* 29(4): 298-310.

Davies, A. F., Mirza, G., Sekhon, G., Turnpenny, P., Leroy, F., Speleman, F., Law, C., van Regemorter, N., Vamos, E., Flinter, F. et al. (1999) 'Delineation of two distinct 6p deletion syndromes', *Hum Genet* 104(1): 64-72.

Delahaye, A., Sznajer, Y., Lyonnet, S., Elmaleh-Berges, M., Delpierre, I., Audollent, S., Wiener-Vacher, S., Mansbach, A. L., Amiel, J., Baumann, C. et al. (2007) 'Familial CHARGE syndrome because of CHD7 mutation: clinical intra- and interfamilial variability', *Clin Genet* 72(2): 112-21.

Di Felice, V. and Zummo, G. (2009) 'Tetralogy of fallot as a model to study cardiac progenitor cell migration and differentiation during heart development', *Trends Cardiovasc Med* 19(4): 130-5.

Durocher, D., Charron, F., Warren, R., Schwartz, R. J. and Nemer, M. (1997) 'The cardiac transcription factors Nkx2-5 and GATA-4 are mutual cofactors', *EMBO J* 16(18): 5687-96.

Eisen, J. S. and Smith, J. C. (2008) 'Controlling morpholino experiments: don't stop making antisense', *Development* 135(10): 1735-43.

Epstein, J. A. (2001) 'Developing models of DiGeorge syndrome', *Trends Genet* 17(10): S13-7.

Eralp, I., Lie-Venema, H., Bax, N. A., Wijffels, M. C., Van Der Laarse, A., Deruiter, M. C., Bogers, A. J., Van Den Akker, N. M., Gourdie, R. G., Schalij, M. J. et al. (2006) 'Epicardium-derived cells are important for correct development of the Purkinje fibers in the avian heart', *Anat Rec A Discov Mol Cell Evol Biol* 288(12): 1272-80.

Essner, J. J., Branford, W. W., Zhang, J. and Yost, H. J. (2000) 'Mesendoderm and left-right brain, heart and gut development are differentially regulated by pitx2 isoforms', *Development* 127(5): 1081-93.

Etkin, L., Pearman, B., Roberts, M. and Bektesh, S. L. (1984) 'Replication, integration and expression of exogenous DNA injected into fertilized eggs of Xenopus laevis', *Differentiation* 26(3): 194-202.

Etkin, L. D. and Pearman, B. (1987) 'Distribution, expression, and germline transmission of exogenous DNA sequences following microinjection into Xenopus eggs', *Development* 99: 15-23.

Etkin, L. D. and Roberts, M. (1983) 'Transmission of integrated sea urchin histone genes by nuclear transplantation in Xenopus laevis', *Science* 221(4605): 67-9.

Evans, S. M., Yelon, D., Conlon, F. L. and Kirby, M. L. (2010) 'Myocardial lineage development', *Circ Res* 107(12): 1428-44.

Feng, G. S. (1999) 'Shp-2 tyrosine phosphatase: signaling one cell or many', *Exp Cell Res* 253(1): 47-54.

Feng, G. S., Shen, R., Heng, H. H., Tsui, L. C., Kazlauskas, A. and Pawson, T. (1994) 'Receptor-binding, tyrosine phosphorylation and chromosome localization of the mouse SH2-containing phosphotyrosine phosphatase Syp', *Oncogene* 9(6): 1545-50.

Foley, A. C. and Mercola, M. (2005) 'Heart induction by Wnt antagonists depends on the homeodomain transcription factor Hex', *Genes Dev* 19(3): 387-96.

Fu, Y., Yan, W., Mohun, T. J., and Evans, S. M. (1998) 'Vertebrate tinman homologues XNkx2-3 and XNkx2-5 are required for heart formation in a functionally redundant manner', *Development* 125: 4439-4449.

Gage, P. J., Suh, H. and Camper, S. A. (1999) 'Dosage requirement of Pitx2 for development of multiple organs', *Development* 126(20): 4643-51.

Galli, D., Dominguez, J. N., Zaffran, S., Munk, A., Brown, N. A. and Buckingham, M. E. (2008) 'Atrial myocardium derives from the posterior region of the second heart field, which acquires left-right identity as Pitx2c is expressed', *Development* 135(6): 1157-67.

Garavelli, L., De Brasi, D., Verri, R., Guareschi, E., Cariola, F., Melis, D., Calcagno, G., Salvatore, F., Unger, S., Sebastio, G. et al. (2008) 'Holt-Oram syndrome associated with anomalies of the feet', *Am J Med Genet A* 146A(9): 1185-9.

Garg, V., Kathiriya, I. S., Barnes, R., Schluterman, M. K., King, I. N., Butler, C. A., Rothrock, C. R., Eapen, R. S., Hirayama-Yamada, K., Joo, K. et al. (2003) 'GATA4 mutations cause human congenital heart defects and reveal an interaction with TBX5', *Nature* 424(6947): 443-7.

Garriock, R. J., D'Agostino, S. L., Pilcher, K. C. and Krieg, P. A. (2005a) 'Wnt11-R, a protein closely related to mammalian Wnt11, is required for heart morphogenesis in Xenopus', *Dev Biol* 279(1): 179-92.

Garriock, R. J., Meadows, S. M. and Krieg, P. A. (2005b) 'Developmental expression and comparative genomic analysis of Xenopus cardiac myosin heavy chain genes', *Dev Dyn* 233(4): 1287-93.

Garrity, D. M., Childs, S. and Fishman, M. C. (2002) 'The heartstrings mutation in zebrafish causes heart/fin Tbx5 deficiency syndrome', *Development* 129(19): 4635-45.

Geach, T. J. and Zimmerman, L. B. (2010) 'Paralysis and delayed Z-disc formation in the Xenopus tropicalis unc45b mutant dicky ticker', *BMC Dev Biol* 10: 75.

Gebbia, M., Ferrero, G. B., Pilia, G., Bassi, M. T., Aylsworth, A., Penman-Splitt, M., Bird, L. M., Bamforth, J. S., Burn, J., Schlessinger, D. et al. (1997) 'X-linked situs abnormalities result from mutations in ZIC3', *Nat Genet* 17(3): 305-8.

Gessert, S. and Kuhl, M. (2009) 'Comparative gene expression analysis and fate mapping studies suggest an early segregation of cardiogenic lineages in Xenopus laevis', *Dev Biol* 334(2): 395-408.

Gittenberger-de Groot, A. C., Vrancken Peeters, M. P., Bergwerff, M., Mentink, M. M. and Poelmann, R. E. (2000) 'Epicardial outgrowth inhibition leads to compensatory mesothelial outflow tract collar and abnormal cardiac septation and coronary formation', *Circ Res* 87(11): 969-71.

Gittenberger-de Groot, A. C., Vrancken Peeters, M. P., Mentink, M. M., Gourdie, R. G. and Poelmann, R. E. (1998) 'Epicardium-derived cells contribute a novel population to the myocardial wall and the atrioventricular cushions', *Circ Res* 82(10): 1043-52.

Goetz, S. C., Brown, D. D. and Conlon, F. L. (2006) 'TBX5 is required for embryonic cardiac cell cycle progression', *Development*.

Gormley, J. P. and Nascone-Yoder, N. M. (2003) 'Left and right contributions to the Xenopus heart: implications for asymmetric morphogenesis', *Dev Genes Evol* 213(8): 390-8.

Grepin, C., Nemer, G. and Nemer, M. (1997) 'Enhanced cardiogenesis in embryonic stem cells overexpressing the GATA-4 transcription factor', *Development* 124(12): 2387-95.

Grepin, C., Robitaille, L., Antakly, T. and Nemer, M. (1995) 'Inhibition of transcription factor GATA-4 expression blocks in vitro cardiac muscle differentiation', *Mol Cell Biol* 15(8): 4095-102.

Grosso, S., Farnetani, M. A., Berardi, R., Vivarelli, R., Vanni, M., Morgese, G. and Balestri, P. (2002) 'Familial Axenfeld-Rieger anomaly, cardiac malformations, and sensorineural hearing loss: a provisionally unique genetic syndrome?', *Am J Med Genet* 111(2): 182-6.

Grow, M. W. and Krieg, P. A. (1998) 'Tinman function is essential for vertebrate heart development: elimination of cardiac differentiation by dominant inhibitory mutants of the tinman-related genes, XNkx2-3 and XNkx2-5', *Dev Biol* 204(1): 187-96.

Grunz, H. (1992) 'Suramin changes the fate of Spemann's organizer and prevents neural induction in Xenopus laevis', *Mech Dev* 38(2): 133-41.

Hamlet, M. R., Yergeau, D. A., Kuliyev, E., Takeda, M., Taira, M., Kawakami, K. and Mead, P. E. (2006) 'Tol2 transposon-mediated transgenesis in Xenopus tropicalis', *Genesis* 44(9): 438-45.

Hammer, S., Toenjes, M., Lange, M., Fischer, J. J., Dunkel, I., Mebus, S., Grimm, C. H., Hetzer, R., Berger, F. and Sperling, S. (2008) 'Characterization of TBX20 in human hearts and its regulation by TFAP2', *J Cell Biochem* 104(3): 1022-33.

Hanafusa, H., Torii, S., Yasunaga, T., Matsumoto, K. and Nishida, E. (2004) 'Shp2, an SH2-containing protein-tyrosine phosphatase, positively regulates receptor tyrosine kinase signaling by dephosphorylating and inactivating the inhibitor Sprouty', *J Biol Chem* 279(22): 22992-5.

Hang, C. T., Yang, J., Han, P., Cheng, H. L., Shang, C., Ashley, E., Zhou, B. and Chang, C. P. (2010) 'Chromatin regulation by Brg1 underlies heart muscle development and disease', *Nature* 466(7302): 62-7.

Harland, R. and Weintraub, H. (1985) 'Translation of mRNA injected into Xenopus oocytes is specifically inhibited by antisense RNA', *J Cell Biol* 101(3): 1094-9.

Harvey, R. P. and Melton, D. A. (1988) 'Microinjection of synthetic Xhox-1A homeobox mRNA disrupts somite formation in developing Xenopus embryos', *Cell* 53(5): 687-97.

Hatcher, C. J., Kim, M. S., Mah, C. S., Goldstein, M. M., Wong, B., Mikawa, T. and Basson, C. T. (2001) 'TBX5 transcription factor regulates cell proliferation during cardiogenesis', *Dev. Biol.* 230(2): 177-188.

Haworth, K. E., Kotecha, S., Mohun, T. J. and Latinkic, B. V. (2008) 'GATA4 and GATA5 are essential for heart and liver development in Xenopus embryos', *BMC Dev Biol* 8: 74.

Heasman, J., Kofron, M. and Wylie, C. (2000) 'Beta-catenin signaling activity dissected in the early Xenopus embryo: a novel antisense approach', *Dev Biol* 222(1): 124-34.

Hellsten, U., Harland, R. M., Gilchrist, M. J., Hendrix, D., Jurka, J., Kapitonov, V., Ovcharenko, I., Putnam, N. H., Shu, S., Taher, L. et al. (2010) 'The genome of the Western clawed frog Xenopus tropicalis', *Science* 328(5978): 633-6.

Hilton, E. N., Manson, F. D., Urquhart, J. E., Johnston, J. J., Slavotinek, A. M., Hedera, P., Stattin, E. L., Nordgren, A., Biesecker, L. G. and Black, G. C. (2007) 'Left-sided embryonic

expression of the BCL-6 corepressor, BCOR, is required for vertebrate laterality determination', *Hum Mol Genet* 16(14): 1773-82.

Hirakow, R. (1992) 'Epicardial formation in staged human embryos', *Kaibogaku Zasshi* 67(5): 616-22.

Hiroi, Y., Kudoh, S., Monzen, K., Ikeda, Y., Yazaki, Y., Nagai, R. and Komuro, I. (2001) 'Tbx5 associates with Nkx2-5 and synergisticallly promotes cardiomyocyte differentiation', *Nature Genetics* 28(3): 276-280.

Hjalt, T. A. and Semina, E. V. (2005) 'Current molecular understanding of Axenfeld-Rieger syndrome', *Expert Rev Mol Med* 7(25): 1-17.

Ho, E. and Shimada, Y. (1978) 'Formation of the epicardium studied with the scanning electron microscope', *Dev Biol* 66(2): 579-85.

Hoffman, J. I. and Kaplan, S. (2002) 'The incidence of congenital heart disease', *J Am Coll Cardiol* 39(12): 1890-900.

Holt, M. and Oram, S. (1960) 'Familial heart disease with skeletal malformations', *Br Heart J* 22: 236-42.

Horb, M. E. and Thomsen, G. H. (1999) 'Tbx5 is essential for heart development', *Development* 126: 1739-1751.

Hurd, E. A., Capers, P. L., Blauwkamp, M. N., Adams, M. E., Raphael, Y., Poucher, H. K. and Martin, D. M. (2007) 'Loss of Chd7 function in gene-trapped reporter mice is embryonic lethal and associated with severe defects in multiple developing tissues', *Mamm Genome* 18(2): 94-104.

Iida, K., Koseki, H., Kakinuma, H., Kato, N., Mizutani-Koseki, Y., Ohuchi, H., Yoshioka, H., Noji, S., Kawamura, K., Kataoka, Y. et al. (1997) 'Essential roles of the winged helix transcription factor MFH-1 in aortic arch patterning and skeletogenesis', *Development* 124(22): 4627-38.

Inui, M., Fukui, A., Ito, Y. and Asashima, M. (2006) 'Xapelin and Xmsr are required for cardiovascular development in Xenopus laevis', *Dev Biol* 298(1): 188-200.

Jacquier, A. and Dujon, B. (1985) 'An intron-encoded protein is active in a gene conversion process that spreads an intron into a mitochondrial gene', *Cell* 41(2): 383-94.

Jahr, M., Schlueter, J., Brand, T. and Manner, J. (2008) 'Development of the proepicardium in Xenopus laevis', *Dev Dyn* 237(10): 3088-96.

Jarvis, L. A., Toering, S. J., Simon, M. A., Krasnow, M. A. and Smith-Bolton, R. K. (2006) 'Sprouty proteins are in vivo targets of Corkscrew/SHP-2 tyrosine phosphatases', *Development* 133(6): 1133-42.

Jerome, L. A. and Papaioannou, V. E. (2001) 'DiGeorge syndrome phenotype in mice mutant for the T-box gene, Tbx1', *Nat. Genet.* 27(3): 286-291.

Jongmans, M. C., Admiraal, R. J., van der Donk, K. P., Vissers, L. E., Baas, A. F., Kapusta, L., van Hagen, J. M., Donnai, D., de Ravel, T. J., Veltman, J. A. et al. (2006) 'CHARGE syndrome: the phenotypic spectrum of mutations in the CHD7 gene', *J Med Genet* 43(4): 306-14.

Kaliakatsos, M., Giannakopoulos, A., Fryssira, H., Kanariou, M., Skiathitou, A. V., Siahanidou, T., Giannikou, K., Makrythanasis, P., Kanavakis, E. and Tzetis, M. (2010) 'Combined microdeletions and CHD7 mutation causing severe CHARGE/DiGeorge syndrome: clinical presentation and molecular investigation by array-CGH', *J Hum Genet*.

Kawakami, K., Imanaka, K., Itoh, M. and Taira, M. (2004) 'Excision of the Tol2 transposable element of the medaka fish Oryzias latipes in Xenopus laevis and Xenopus tropicalis', *Gene* 338(1): 93-8.

Kawakami, K., Shima, A. and Kawakami, N. (2000) 'Identification of a functional transposase of the Tol2 element, an Ac-like element from the Japanese medaka fish, and its transposition in the zebrafish germ lineage', *Proc Natl Acad Sci U S A* 97(21): 11403-8.

Kieserman, E. K., Lee, C., Gray, R. S., Park, T. J. and Wallingford, J. B. (2010) 'High-magnification in vivo imaging of Xenopus embryos for cell and developmental biology', *Cold Spring Harb Protoc* 2010(5): pdb prot5427.

Kirk, E. P., Sunde, M., Costa, M. W., Rankin, S. A., Wolstein, O., Castro, M. L., Butler, T. L., Hyun, C., Guo, G., Otway, R. et al. (2007) 'Mutations in cardiac T-box factor gene TBX20 are associated with diverse cardiac pathologies, including defects of septation and valvulogenesis and cardiomyopathy', *Am J Hum Genet* 81(2): 280-91.

Kitaguchi, T., Mizugishi, K., Hatayama, M., Aruga, J. and Mikoshiba, K. (2002) 'Xenopus Brachyury regulates mesodermal expression of Zic3, a gene controlling left-right asymmetry', *Dev Growth Differ* 44(1): 55-61.

Kitaguchi, T., Nagai, T., Nakata, K., Aruga, J. and Mikoshiba, K. (2000) 'Zic3 is involved in the left-right specification of the Xenopus embryo', *Development* 127(22): 4787-95.
Knudsen, H. and Nielsen, P. E. (1996) 'Antisense properties of duplex- and triplex-forming PNAs', *Nucleic Acids Res* 24(3): 494-500.

Kochilas, L., Merscher-Gomez, S., Lu, M. M., Potluri, V., Liao, J., Kucherlapati, R., Morrow, B. and Epstein, J. A. (2002) 'The role of neural crest during cardiac development in a mouse model of DiGeorge syndrome', *Dev Biol* 251(1): 157-66.

Kochilas, L. K., Potluri, V., Gitler, A., Balasubramanian, K. and Chin, A. J. (2003) 'Cloning and characterization of zebrafish tbx1', *Gene Expr Patterns* 3(5): 645-51.

Kolker, S. J., Tajchman, U. and Weeks, D. L. (2000) 'Confocal imaging of early heart development in Xenopus laevis', *Dev Biol* 218(1): 64-73.

Kosaki, K., Suzuki, T., Muroya, K., Hasegawa, T., Sato, S., Matsuo, N., Kosaki, R., Nagai, T., Hasegawa, Y. and Ogata, T. (2002) 'PTPN11 (protein-tyrosine phosphatase, nonreceptor-type 11) mutations in seven Japanese patients with Noonan syndrome', *J Clin Endocrinol Metab* 87(8): 3529-33.

Koster, M., Dillinger, K. and Knochel, W. (1998) 'Expression pattern of the winged helix factor XFD-11 during Xenopus embryogenesis', *Mech Dev* 76(1-2): 169-73.

Kratz, C. P., Niemeyer, C. M., Castleberry, R. P., Cetin, M., Bergstrasser, E., Emanuel, P. D., Hasle, H., Kardos, G., Klein, C., Kojima, S. et al. (2005) 'The mutational spectrum of PTPN11 in juvenile myelomonocytic leukemia and Noonan syndrome/myeloproliferative disease', *Blood* 106(6): 2183-5.

Krebs, L. T., Iwai, N., Nonaka, S., Welsh, I. C., Lan, Y., Jiang, R., Saijoh, Y., O'Brien, T. P., Hamada, H. and Gridley, T. (2003) 'Notch signaling regulates left-right asymmetry determination by inducing Nodal expression', *Genes Dev* 17(10): 1207-12.

Krenz, M., Yutzey, K. E. and Robbins, J. (2005) 'Noonan syndrome mutation Q79R in Shp2 increases proliferation of valve primordia mesenchymal cells via extracellular signal-regulated kinase 1/2 signaling', *Circ Res* 97(8): 813-20.

Kroll, K. L. and Amaya, E. (1996a) 'Transgenic Xenopus embryos from sperm nuclear transplantations reveal FGF signaling requirements during gastrulation', *Development* 122(10): 3173-83.

Kroll, K. L. and Amaya, E. (1996b) 'Transgenic *Xenopus* embryos from sperm nuclear transplantations reveal FGF signalling requirements during gastrulation', *Development* 122: 3173-3183.

Kumano, G., Ezal, C. and Smith, W. C. (2006) 'ADMP2 is essential for primitive blood and heart development in Xenopus', *Dev Biol* 299(2): 411-23.

Kume, T., Jiang, H., Topczewska, J. M. and Hogan, B. L. (2001) 'The murine winged helix transcription factors, Foxc1 and Foxc2, are both required for cardiovascular development and somitogenesis', *Genes Dev* 15(18): 2470-82.

Kuo, C. T., Morrisey, E. E., Anandappa, R., Sigrist, K., Lu, M. M., Parmacek, M. S., Soudais, C. and Leiden, J. M. (1997) 'GATA4 transcription factor is required for ventral morphogenesis and heart tube formation', *Genes Dev* 11(8): 1048-60.

Lalani, S. R., Safiullah, A. M., Fernbach, S. D., Harutyunyan, K. G., Thaller, C., Peterson, L. E., McPherson, J. D., Gibbs, R. A., White, L. D., Hefner, M. et al. (2006) 'Spectrum of CHD7 mutations in 110 individuals with CHARGE syndrome and genotype-phenotype correlation', *Am J Hum Genet* 78(2): 303-14.

Langdon, Y. G., Goetz, S. C., Berg, A. E., Swanik, J. T. and Conlon, F. L. (2007) 'SHP-2 is required for the maintenance of cardiac progenitors', *Development* 134(22): 4119-30.

Latinkić , B. V., Cooper, B., Smith, S., Kotecha, S., Towers, N., Sparrow, D. and Mohun, T. J. (2004) 'Transcriptional regulation of the cardiac-specific MLC2 gene during Xenopus embryonic development', *Development* 131(3): 669-79.

Latinkić, B. V., Cooper, B., Towers, N., Sparrow, D., Kotecha, S. and Mohun, T. J. (2002) 'Distinct enhancers regulate skeletal and cardiac muscle-specific expression programs of the cardiac alpha-actin gene in Xenopus embryos', *Dev Biol* 245(1): 57-70.

Layman, W. S., McEwen, D. P., Beyer, L. A., Lalani, S. R., Fernbach, S. D., Oh, E., Swaroop, A., Hegg, C. C., Raphael, Y., Martens, J. R. et al. (2009) 'Defects in neural stem cell proliferation and olfaction in Chd7 deficient mice indicate a mechanism for hyposmia in human CHARGE syndrome', *Hum Mol Genet* 18(11): 1909-23.

Lee, Y., Shioi, T., Kasahara, H., Jobe, S. M., Wiese, R. J., Markham, B. E. and Izumo, S. (1998) 'The cardiac tissue-restricted homeobox protein Csx/Nkx2.5 physically associates with the zinc finger protein GATA4 and cooperatively activates atrial natriuretic factor gene expression', *Mol Cell Biol* 18(6): 3120-9.

Lehner, R., Goharkhay, N., Tringler, B., Fasching, C. and Hengstschlager, M. (2003) 'Pedigree analysis and descriptive investigation of three classic phenotypes associated with Holt-Oram syndrome', *J Reprod Med* 48(3): 153-9.

Lepilina, A., Coon, A. N., Kikuchi, K., Holdway, J. E., Roberts, R. W., Burns, C. G. and Poss, K. D. (2006) 'A dynamic epicardial injury response supports progenitor cell activity during zebrafish heart regeneration', *Cell* 127(3): 607-19.

Li, Q. Y., Newbury Ecob, R. A., Terrett, J. A., Wilson, D. I., Curtis, A. R., Yi, C. H., Gebuhr, T., Bullen, P. J., Robson, S. C., Strachan, T. et al. (1997) 'Holt-Oram syndrome is caused by mutations in TBX5, a member of the Brachyury (T) gene family', *Nat. Genet.* 15(1): 21-29.

Liberatore, C. M., Searcy-Schrick, R. D. and Yutzey, K. E. (2000) 'Ventricular expression of tbx5 inhibits normal heart chamber development', *Dev Biol* 223(1): 169-80.

Lie-Venema, H., Eralp, I., Maas, S., Gittenberger-De Groot, A. C., Poelmann, R. E. and DeRuiter, M. C. (2005) 'Myocardial heterogeneity in permissiveness for epicardium-derived cells and endothelial precursor cells along the developing heart tube at the onset of coronary vascularization', *Anat Rec A Discov Mol Cell Evol Biol* 282(2): 120-9.

Lie-Venema, H., van den Akker, N. M., Bax, N. A., Winter, E. M., Maas, S., Kekarainen, T., Hoeben, R. C., deRuiter, M. C., Poelmann, R. E. and Gittenberger-de Groot, A. C. (2007) 'Origin, fate, and function of epicardium-derived cells (EPDCs) in normal and abnormal cardiac development', *ScientificWorldJournal* 7: 1777-98.

Lin, A. E., Ticho, B. S., Houde, K., Westgate, M. N. and Holmes, L. B. (2000) 'Heterotaxy: associated conditions and hospital-based prevalence in newborns', *Genet Med* 2(3): 157-72.

Lin, C. R., Kioussi, C., O'Connell, S., Briata, P., Szeto, D., Liu, F., Izpisua-Belmonte, J. C. and Rosenfeld, M. G. (1999) 'Pitx2 regulates lung asymmetry, cardiac positioning and pituitary and tooth morphogenesis', *Nature* 401(6750): 279-82.

Lindsay, E. A. and Baldini, A. (2001) 'Recovery from arterial growth delay reduces penetrance of cardiovascular defects in mice deleted for the DiGeorge syndrome region', *Hum Mol Genet* 10(9): 997-1002.

Lindsay, E. A., Botta, A., Jurecic, V., Carattini-Rivera, S., Cheah, Y. C., Rosenblatt, H. M., Bradley, A. and Baldini, A. (1999) 'Congenital heart disease in mice deficient for the DiGeorge syndrome region', *Nature* 401(6751): 379-83.

Lindsay, E. A., Vitelli, F., Su, H., Morishima, M., Huynh, T., Pramparo, T., Jurecic, V., Ogunrinu, G., Sutherland, H. F., Scambler, P. J. et al. (2001a) 'Tbx1 haploinsufficiency in the DiGeorge syndrome region causes aortic arch defects in mice', *Nature* 410(6824): 97-101.

Lindsay, E. A., Vitelli, F., Su, H., Morishima, M., Huynh, T., Pramparo, T., Jurecic, V., Ogunrinu, G., Sutherland, H. F., Scambler, P. J. et al. (2001b) 'Tbx1 haploinsufficieny in the DiGeorge syndrome region causes aortic arch defects in mice', *Nature* 410(6824): 97-101.

Liu, C., Liu, W., Palie, J., Lu, M. F., Brown, N. A. and Martin, J. F. (2002) 'Pitx2c patterns anterior myocardium and aortic arch vessels and is required for local cell movement into atrioventricular cushions', *Development* 129(21): 5081-91.

Liu, C., Shen, A., Li, X., Jiao, W., Zhang, X. and Li, Z. (2008) 'T-box transcription factor TBX20 mutations in Chinese patients with congenital heart disease', *Eur J Med Genet* 51(6): 580-7.

Logan, M. and Mohun, T. (1993) 'Induction of cardiac muscle differentiation in isolated animal pole explants of Xenopus laevis embryos', *Development* 118(3): 865-875.

Loh, M. L., Reynolds, M. G., Vattikuti, S., Gerbing, R. B., Alonzo, T. A., Carlson, E., Cheng, J. W., Lee, C. M., Lange, B. J. and Meshinchi, S. (2004) 'PTPN11 mutations in pediatric patients with acute myeloid leukemia: results from the Children's Cancer Group', *Leukemia* 18(11): 1831-4.

Lu, M. F., Pressman, C., Dyer, R., Johnson, R. L. and Martin, J. F. (1999) 'Function of Rieger syndrome gene in left-right asymmetry and craniofacial development', *Nature* 401(6750): 276-8.

Lyons, I., et al. (1995) 'Myogenic and morphogenic defects in the heart tubes of murine embrryos lacking thehomeobox gene Nkx-2.5', *Genes Dev.* 9: 1654-1666.

Maclean, K., Smith, J., St Heaps, L., Chia, N., Williams, R., Peters, G. B., Onikul, E., McCrossin, T., Lehmann, O. J. and Ades, L. C. (2005) 'Axenfeld-Rieger malformation and distinctive facial features: Clues to a recognizable 6p25 microdeletion syndrome', *Am J Med Genet A* 132(4): 381-5.

Maheshwari, M., Belmont, J., Fernbach, S., Ho, T., Molinari, L., Yakub, I., Yu, F., Combes, A., Towbin, J., Craigen, W. J. et al. (2002) 'PTPN11 mutations in Noonan syndrome type I: detection of recurrent mutations in exons 3 and 13', *Hum Mutat* 20(4): 298-304.

Mammi, I., De Giorgio, P., Clementi, M. and Tenconi, R. (1998) 'Cardiovascular anomaly in Rieger Syndrome: heterogeneity or contiguity?', *Acta Ophthalmol Scand* 76(4): 509-12.

Mandel, E. M., Kaltenbrun, E., Callis, T. E., Zeng, X. X., Marques, S. R., Yelon, D., Wang, D. Z. and Conlon, F. L. (2010) 'The BMP pathway acts to directly regulate Tbx20 in the developing heart', *Development* 137(11): 1919-29.

Manner, J. (2000) 'Cardiac looping in the chick embryo: a morphological review with special reference to terminological and biomechanical aspects of the looping process', *Anat Rec* 259(3): 248-62.

Manner, J. (2009) 'The anatomy of cardiac looping: a step towards the understanding of the morphogenesis of several forms of congenital cardiac malformations', *Clin Anat* 22(1): 21-35.

Manner, J., Perez-Pomares, J. M., Macias, D. and Munoz-Chapuli, R. (2001) 'The origin, formation and developmental significance of the epicardium: a review', *Cells Tissues Organs* 169(2): 89-103.

Manner, J., Schlueter, J. and Brand, T. (2005) 'Experimental analyses of the function of the proepicardium using a new microsurgical procedure to induce loss-of-proepicardial-function in chick embryos', *Dev Dyn* 233(4): 1454-63.

Mariampillai, A., Standish, B. A., Munce, N. R., Randall, C., Liu, G., Jiang, J. Y., Cable, A. E., Vitkin, I. A. and Yang, V. X. (2007) 'Doppler optical cardiogram gated 2D color flow

imaging at 1000 fps and 4D in vivo visualization of embryonic heart at 45 fps on a swept source OCT system', *Opt Express* 15(4): 1627-38.

McDermott, D. A., Bressan, M. C., He, J., Lee, J. S., Aftimos, S., Brueckner, M., Gilbert, F., Graham, G. E., Hannibal, M. C., Innis, J. W. et al. (2005) 'TBX5 genetic testing validates strict clinical criteria for Holt-Oram syndrome', *Pediatr Res* 58(5): 981-6.

Melton, D. A. (1985) 'Injected anti-sense RNAs specifically block messenger RNA translation in vivo', *Proc Natl Acad Sci U S A* 82(1): 144-8.

Mercola, M. (1999) 'Embryological basis for cardiac left-right asymmetry', *Semin Cell Dev Biol* 10(1): 109-16.

Merki, E., Zamora, M., Raya, A., Kawakami, Y., Wang, J., Zhang, X., Burch, J., Kubalak, S. W., Kaliman, P., Belmonte, J. C. et al. (2005) 'Epicardial retinoid X receptor alpha is required for myocardial growth and coronary artery formation', *Proc Natl Acad Sci U S A* 102(51): 18455-60.

Merscher, S., Funke, B., Epstein, J. A., Heyer, J., Puech, A., Lu, M. M., Xavier, R. J., Demay, M. B., Russell, R. G., Factor, S. et al. (2001) 'TBX1 is responsible for cardiovascular defects in velo-cardio- facial/DiGeorge syndrome', *Cell* 104(4): 619-29.

Mohun, T. J., Leong, L.M., Weninger, W. J., and Sparrow, D. B. (2000) 'The Morphology of Heart Development in Xenopus laevis', *Developmental Biology* 218: 74-88.

Molkentin, J. D., Lin, Q., Duncan, S. A. and Olson, E. N. (1997) 'Requirement of the transcription factor GATA4 for heart tube formation and ventral morphogenesis', *Genes Dev* 11(8): 1061-72.

Momma, K. (2010) 'Cardiovascular anomalies associated with chromosome 22q11.2 deletion syndrome', *Am J Cardiol* 105(11): 1617-24.

Moody, S. A. (1987) 'Fates of the blastomeres of the 32-cell-stage Xenopus embryo', *Dev Biol* 122(2): 300-19.

Moore, A. W., Schedl, A., McInnes, L., Doyle, M., Hecksher-Sorensen, J. and Hastie, N. D. (1998) 'YAC transgenic analysis reveals Wilms' tumour 1 gene activity in the proliferating coelomic epithelium, developing diaphragm and limb', *Mech Dev* 79(1-2): 169-84.

Morcos, P. A. (2007) 'Achieving targeted and quantifiable alteration of mRNA splicing with Morpholino oligos', *Biochem Biophys Res Commun* 358(2): 521-7.

Moskowitz, I. P., Pizard, A., Patel, V. V., Bruneau, B. G., Kim, J. B., Kupershmidt, S., Roden, D., Berul, C. I., Seidman, C. E. and Seidman, J. G. (2004) 'The T-Box transcription factor

Tbx5 is required for the patterning and maturation of the murine cardiac conduction system', *Development* 131(16): 4107-16.

Moulton, J. D. (2007) 'Using morpholinos to control gene expression', *Curr Protoc Nucleic Acid Chem* Chapter 4: Unit 4 30.

Movassagh, M. and Philpott, A. (2008) 'Cardiac differentiation in Xenopus requires the cyclin-dependent kinase inhibitor, p27Xic1', *Cardiovasc Res* 79(3): 436-47.

Musante, L., Kehl, H. G., Majewski, F., Meinecke, P., Schweiger, S., Gillessen-Kaesbach, G., Wieczorek, D., Hinkel, G. K., Tinschert, S., Hoeltzenbein, M. et al. (2003) 'Spectrum of mutations in PTPN11 and genotype-phenotype correlation in 96 patients with Noonan syndrome and five patients with cardio-facio-cutaneous syndrome', *Eur J Hum Genet* 11(2): 201-6.

Nagao, K., Taniyama, Y., Kietzmann, T., Doi, T., Komuro, I. and Morishita, R. (2008) 'HIF-1alpha signaling upstream of NKX2.5 is required for cardiac development in Xenopus', *J Biol Chem* 283(17): 11841-9.

Newbury-Ecob, R. A., Leanage, R., Raeburn, J. A. and Young, I. D. (1996) 'Holt-Oram syndrome: a clinical genetic study', *J Med Genet* 33(4): 300-7.

Noonan, J. A. (1968) 'Hypertelorism with Turner phenotype. A new syndrome with associated congenital heart disease', *Am J Dis Child* 116(4): 373-80.

Noonan, J. A. (1994) 'Noonan syndrome. An update and review for the primary pediatrician', *Clin Pediatr (Phila)* 33(9): 548-55.

Ogino, H., McConnell, W. B. and Grainger, R. M. (2006) 'Highly efficient transgenesis in Xenopus tropicalis using I-SceI meganuclease', *Mech Dev* 123(2): 103-13.

Pan, F. C., Chen, Y., Loeber, J., Henningfeld, K. and Pieler, T. (2006) 'I-SceI meganuclease-mediated transgenesis in Xenopus', *Dev Dyn* 235(1): 247-52.

Pandur, P., Lasche, M., Eisenberg, L. M. and Kuhl, M. (2002) 'Wnt-11 activation of a non-canonical Wnt signalling pathway is required for cardiogenesis', *Nature* 418(6898): 636-41.

Parinov, S., Kondrichin, I., Korzh, V. and Emelyanov, A. (2004) 'Tol2 transposon-mediated enhancer trap to identify developmentally regulated zebrafish genes in vivo', *Dev Dyn* 231(2): 449-59.

Pehlivan, T., Pober, B. R., Brueckner, M., Garrett, S., Slaugh, R., Van Rheeden, R., Wilson, D. B., Watson, M. S. and Hing, A. V. (1999) 'GATA4 haploinsufficiency in patients with interstitial deletion of chromosome region 8p23.1 and congenital heart disease', *Am J Med Genet* 83(3): 201-6.

Perez-Pomares, J. M., Phelps, A., Sedmerova, M., Carmona, R., Gonzalez-Iriarte, M., Munoz-Chapuli, R. and Wessels, A. (2002) 'Experimental studies on the spatiotemporal expression of WT1 and RALDH2 in the embryonic avian heart: a model for the regulation of myocardial and valvuloseptal development by epicardially derived cells (EPDCs)', *Dev Biol* 247(2): 307-26.

Peterkin, T., Gibson, A. and Patient, R. (2007) 'Redundancy and evolution of GATA factor requirements in development of the myocardium', *Dev Biol* 311(2): 623-35.

Plageman, T. F., Jr. and Yutzey, K. E. (2004) 'Differential expression and function of tbx5 and tbx20 in cardiac development', *J Biol Chem* 279(18): 19026-34.

Pombal, M. A., Carmona, R., Megias, M., Ruiz, A., Perez-Pomares, J. M. and Munoz-Chapuli, R. (2008) 'Epicardial development in lamprey supports an evolutionary origin of the vertebrate epicardium from an ancestral pronephric external glomerulus', *Evol Dev* 10(2): 210-6.

Posch, M. G., Gramlich, M., Sunde, M., Schmitt, K. R., Lee, S. H., Richter, S., Kersten, A., Perrot, A., Panek, A. N., Al Khatib, I. H. et al. 'A gain-of-function TBX20 mutation causes congenital atrial septal defects, patent foramen ovale and cardiac valve defects', *J Med Genet* 47(4): 230-5.

Purandare, S. M., Ware, S. M., Kwan, K. M., Gebbia, M., Bassi, M. T., Deng, J. M., Vogel, H., Behringer, R. R., Belmont, J. W. and Casey, B. (2002) 'A complex syndrome of left-right axis, central nervous system and axial skeleton defects in Zic3 mutant mice', *Development* 129(9): 2293-302.

Qian, L., Mohapatra, B., Akasaka, T., Liu, J., Ocorr, K., Towbin, J. A. and Bodmer, R. (2008) 'Transcription factor neuromancer/TBX20 is required for cardiac function in Drosophila with implications for human heart disease', *Proc Natl Acad Sci U S A* 105(50): 19833-8.

Qu, C. K. (2000) 'The SHP-2 tyrosine phosphatase: signaling mechanisms and biological functions', *Cell Res* 10(4): 279-88.

Raffin, M., Leong, L. M., Rones, M. S., Sparrow, D., Mohun, T. and Mercola, M. (2000) 'Subdivision of the cardiac Nkx2.5 expression domain into myogenic and nonmyogenic compartments', *Dev Biol* 218(2): 326-40.

Ramsdell, A. F., Bernanke, J. M. and Trusk, T. C. (2006) 'Left-right lineage analysis of the embryonic Xenopus heart reveals a novel framework linking congenital cardiac defects and laterality disease', *Development* 133(7): 1399-410.

Raya, A., Kawakami, Y., Rodriguez-Esteban, C., Buscher, D., Koth, C. M., Itoh, T., Morita, M., Raya, R. M., Dubova, I., Bessa, J. G. et al. (2003) 'Notch activity induces Nodal

expression and mediates the establishment of left-right asymmetry in vertebrate embryos', *Genes Dev* 17(10): 1213-8.

Rusconi, S. and Schaffner, W. (1981) 'Transformation of frog embryos with a rabbit beta-globin gene', *Proc Natl Acad Sci U S A* 78(8): 5051-5.

Ryan, A. K., Blumberg, B., Rodriguez-Esteban, C., Yonei-Tamura, S., Tamura, K., Tsukui, T., de la Pena, J., Sabbagh, W., Greenwald, J., Choe, S. et al. (1998) 'Pitx2 determines left-right asymmetry of internal organs in vertebrates', *Nature* 394(6693): 545-51.

Sauka-Spengler, T. and Bronner-Fraser, M. (2008) 'A gene regulatory network orchestrates neural crest formation', *Nat Rev Mol Cell Biol* 9(7): 557-68.

Sauka-Spengler, T., Le Mentec, C., Lepage, M. and Mazan, S. (2002) 'Embryonic expression of Tbx1, a DiGeorge syndrome candidate gene, in the lamprey Lampetra fluviatilis', *Gene Expr Patterns* 2(1-2): 99-103.

Saxton, T. M., Henkemeyer, M., Gasca, S., Shen, R., Rossi, D. J., Shalaby, F., Feng, G. S. and Pawson, T. (1997) 'Abnormal mesoderm patterning in mouse embryos mutant for the SH2 tyrosine phosphatase Shp-2', *EMBO J* 16(9): 2352-64.

Saxton, T. M. and Pawson, T. (1999) 'Morphogenetic movements at gastrulation require the SH2 tyrosine phosphatase Shp2', *Proc Natl Acad Sci U S A* 96(7): 3790-5.

Schneider, V. A. and Mercola, M. (2001) 'Wnt antagonism initiates cardiogenesis in Xenopus laevis', *Genes Dev* 15(3): 304-15.

Schott, J., Benson, D. W., Bassson, C. T., Pease, W., Silberbach, S., Moak, J. P., Maron, B. J., Seidman, C. E. and Seidman, J. G. (1998) 'Congenital Heart Disease Caused by Mutations in the Transcription Factor NKX2-5', *Science* 281: 108-111.

Schweickert, A., Campione, M., Steinbeisser, H. and Blum, M. (2000) 'Pitx2 isoforms: involvement of Pitx2c but not Pitx2a or Pitx2b in vertebrate left-right asymmetry', *Mechanisms of Development* 90(1): 41-51.

Seo, S., Fujita, H., Nakano, A., Kang, M., Duarte, A. and Kume, T. (2006) 'The forkhead transcription factors, Foxc1 and Foxc2, are required for arterial specification and lymphatic sprouting during vascular development', *Dev Biol* 294(2): 458-70.

Seo, S. and Kume, T. (2006) 'Forkhead transcription factors, Foxc1 and Foxc2, are required for the morphogenesis of the cardiac outflow tract', *Dev Biol* 296(2): 421-36.

Sepulveda, J. L., Belaguli, N., Nigam, V., Chen, C. Y., Nemer, M. and Schwartz, R. J. (1998) 'GATA-4 and Nkx-2.5 coactivate Nkx-2 DNA binding targets: role for regulating early cardiac gene expression', *Mol Cell Biol* 18(6): 3405-15.

Serluca, F. C. (2008) 'Development of the proepicardial organ in the zebrafish', *Dev Biol* 315(1): 18-27.

Showell, C., Christine, K. S., Mandel, E. M. and Conlon, F. L. (2006) 'Developmental expression patterns of Tbx1, Tbx2, Tbx5, and Tbx20 in Xenopus tropicalis', *Dev Dyn* 235(6): 1623-30.

Showell, C. and Conlon, F. L. (2007) 'Decoding development in Xenopus tropicalis', *Genesis* 45(6): 418-26.

Siebert, J. R., Graham, J. M., Jr. and MacDonald, C. (1985) 'Pathologic features of the CHARGE association: support for involvement of the neural crest', *Teratology* 31(3): 331-6.

Singh, M. K., Christoffels, V. M., Dias, J. M., Trowe, M. O., Petry, M., Schuster-Gossler, K., Burger, A., Ericson, J. and Kispert, A. (2005) 'Tbx20 is essential for cardiac chamber differentiation and repression of Tbx2', *Development* 132(12): 2697-707.

Sinzelle, L., Vallin, J., Coen, L., Chesneau, A., Du Pasquier, D., Pollet, N., Demeneix, B. and Mazabraud, A. (2006) 'Generation of trangenic Xenopus laevis using the Sleeping Beauty transposon system', *Transgenic Res* 15(6): 751-60.

Sletten, L. J. and Pierpont, M. E. (1996) 'Variation in severity of cardiac disease in Holt-Oram syndrome', *Am J Med Genet* 65(2): 128-32.

Small, E. M. and Krieg, P. A. (2003) 'Transgenic analysis of the atrialnatriuretic factor (ANF) promoter: Nkx2-5 and GATA-4 binding sites are required for atrial specific expression of ANF', *Dev Biol* 261(1): 116-31.

Small, E. M., Warkman, A. S., Wang, D. Z., Sutherland, L. B., Olson, E. N. and Krieg, P. A. (2005) 'Myocardin is sufficient and necessary for cardiac gene expression in Xenopus', *Development* 132(5): 987-97.

Smith, S. J., Ataliotis, P., Kotecha, S., Towers, N., Sparrow, D. B. and Mohun, T. J. (2005) 'The MLC1v gene provides a transgenic marker of myocardium formation within developing chambers of the Xenopus heart', *Dev Dyn* 232(4): 1003-12.

Smith, S. J., Fairclough, L., Latinkic, B. V., Sparrow, D. B. and Mohun, T. J. (2006) 'Xenopus laevis transgenesis by sperm nuclear injection', *Nat Protoc* 1(5): 2195-203.

Sparrow, D. B., Cai, C., Kotecha, S., Latinkic, B., Cooper, B., Towers, N., Evans, S. M. and Mohun, T. J. (2000) 'Regulation of the tinman homologues in Xenopus embryos', *Dev Biol* 227(1): 65-79.

Starr, J. P. (2010) 'Tetralogy of fallot: yesterday and today', *World J Surg* 34(4): 658-68.

Stennard, F. A., Costa, M. W., Elliott, D. A., Rankin, S., Haast, S. J., Lai, D., McDonald, L. P., Niederreither, K., Dolle, P., Bruneau, B. G. et al. (2003) 'Cardiac T-box factor Tbx20

directly interacts with Nkx2-5, GATA4, and GATA5 in regulation of gene expression in the developing heart', *Dev Biol* 262(2): 206-24.

Stennard, F. A., Costa, M. W., Lai, D., Biben, C., Furtado, M. B., Solloway, M. J., McCulley, D. J., Leimena, C., Preis, J. I., Dunwoodie, S. L. et al. (2005) 'Murine T-box transcription factor Tbx20 acts as a repressor during heart development, and is essential for adult heart integrity, function and adaptation', *Development*.

Sucov, H. M., Gu, Y., Thomas, S., Li, P. and Pashmforoush, M. (2009) 'Epicardial control of myocardial proliferation and morphogenesis', *Pediatr Cardiol* 30(5): 617-25.

Summerton, J. E. (2007) 'Morpholino, siRNA, and S-DNA compared: impact of structure and mechanism of action on off-target effects and sequence specificity', *Curr Top Med Chem* 7(7): 651-60.

Sutherland, M. J. and Ware, S. M. (2009) 'Disorders of left-right asymmetry: heterotaxy and situs inversus', *Am J Med Genet C Semin Med Genet* 151C(4): 307-17.

Svensson, E. C., Huggins, G. S., Dardik, F. B., Polk, C. E. and Leiden, J. M. (2000) 'A functionally conserved N-terminal domain of the friend of GATA-2 (FOG-2) protein represses GATA4-dependent transcription', *J Biol Chem* 275(27): 20762-9.

Swiderski, R. E., Reiter, R. S., Nishimura, D. Y., Alward, W. L., Kalenak, J. W., Searby, C. S., Stone, E. M., Sheffield, V. C. and Lin, J. J. (1999) 'Expression of the Mf1 gene in developing mouse hearts: implication in the development of human congenital heart defects', *Dev Dyn* 216(1): 16-27.

Szeto, D. P., Griffin, K. J. and Kimelman, D. (2002) 'HrT is required for cardiovascular development in zebrafish', *Development* 129(21): 5093-101.

Sznajer, Y., Keren, B., Baumann, C., Pereira, S., Alberti, C., Elion, J., Cave, H. and Verloes, A. (2007) 'The spectrum of cardiac anomalies in Noonan syndrome as a result of mutations in the PTPN11 gene', *Pediatrics* 119(6): e1325-31.

Tabin, C. J. and Vogan, K. J. (2003) 'A two-cilia model for vertebrate left-right axis specification', *Genes Dev* 17(1): 1-6.

Takeuchi, J. K., Mileikovskaia, M., Koshiba-Takeuchi, K., Heidt, A. B., Mori, A. D., Arruda, E. P., Gertsenstein, M., Georges, R., Davidson, L., Mo, R. et al. (2005) 'Tbx20 dose-dependently regulates transcription factor networks required for mouse heart and motoneuron development', *Development*.

Tang, T. L., Freeman, R. M., Jr., O'Reilly, A. M., Neel, B. G. and Sokol, S. Y. (1995) 'The SH2-containing protein-tyrosine phosphatase SH-PTP2 is required upstream of MAP kinase for early Xenopus development', *Cell* 80(3): 473-83.

Tartaglia, M., Kalidas, K., Shaw, A., Song, X., Musat, D. L., van der Burgt, I., Brunner, H. G., Bertola, D. R., Crosby, A., Ion, A. et al. (2002) 'PTPN11 mutations in Noonan syndrome: molecular spectrum, genotype-phenotype correlation, and phenotypic heterogeneity', *Am J Hum Genet* 70(6): 1555-63.

Tartaglia, M., Mehler, E. L., Goldberg, R., Zampino, G., Brunner, H. G., Kremer, H., van der Burgt, I., Crosby, A. H., Ion, A., Jeffery, S. et al. (2001) 'Mutations in PTPN11, encoding the protein tyrosine phosphatase SHP-2, cause Noonan syndrome', *Nat Genet* 29(4): 465-8.

Tartaglia, M., Niemeyer, C. M., Fragale, A., Song, X., Buechner, J., Jung, A., Hahlen, K., Hasle, H., Licht, J. D. and Gelb, B. D. (2003) 'Somatic mutations in PTPN11 in juvenile myelomonocytic leukemia, myelodysplastic syndromes and acute myeloid leukemia', *Nat Genet* 34(2): 148-50.

Tevosian, S. G., Deconinck, A. E., Tanaka, M., Schinke, M., Litovsky, S. H., Izumo, S., Fujiwara, Y. and Orkin, S. H. (2000) 'FOG-2, a cofactor for GATA transcription factors, is essential for heart morphogenesis and development of coronary vessels from epicardium', *Cell* 101(7): 729-39.

Toyoizumi, R., Takeuchi, S. and Mogi, K. (2006) 'Subtilisin-like proprotein convertase activity is necessary for left-right axis determination in Xenopus neurula embryos', *Dev Genes Evol* 216(10): 607-22.

Van Vactor, D., O'Reilly, A. M. and Neel, B. G. (1998) 'Genetic analysis of protein tyrosine phosphatases', *Curr Opin Genet Dev* 8(1): 112-26.

Viragh, S. and Challice, C. E. (1981) 'The origin of the epicardium and the embryonic myocardial circulation in the mouse', *Anat Rec* 201(1): 157-68.

Vissers, L. E., van Ravenswaaij, C. M., Admiraal, R., Hurst, J. A., de Vries, B. B., Janssen, I. M., van der Vliet, W. A., Huys, E. H., de Jong, P. J., Hamel, B. C. et al. (2004) 'Mutations in a new member of the chromodomain gene family cause CHARGE syndrome', *Nat Genet* 36(9): 955-7.

Vitelli, F., Taddei, I., Morishima, M., Meyers, E. N., Lindsay, E. A. and Baldini, A. (2002) 'A genetic link between Tbx1 and fibroblast growth factor signaling', *Development* 129(19): 4605-11.

Waldo, K. L., Kumiski, D. H., Wallis, K. T., Stadt, H. A., Hutson, M. R., Platt, D. H. and Kirby, M. L. (2001) 'Conotruncal myocardium arises from a secondary heart field', *Development* 128(16): 3179-88.

Ware, S. M., Peng, J., Zhu, L., Fernbach, S., Colicos, S., Casey, B., Towbin, J. and Belmont, J. W. (2004) 'Identification and functional analysis of ZIC3 mutations in heterotaxy and related congenital heart defects', *Am J Hum Genet* 74(1): 93-105.

Warkman, A. S. and Krieg, P. A. (2006) 'Xenopus as a model system for vertebrate heart development', *Semin Cell Dev Biol*.

Weisschuh, N., Wolf, C., Wissinger, B. and Gramer, E. (2008) 'A novel mutation in the FOXC1 gene in a family with Axenfeld-Rieger syndrome and Peters' anomaly', *Clin Genet* 74(5): 476-80.

Wessels, K., Bohnhorst, B., Luhmer, I., Morlot, S., Bohring, A., Jonasson, J., Epplen, J. T., Gadzicki, D., Glaser, S., Gohring, G. et al. (2010) 'Novel CHD7 mutations contributing to the mutation spectrum in patients with CHARGE syndrome', *Eur J Med Genet*.

Wincent, J., Holmberg, E., Stromland, K., Soller, M., Mirzaei, L., Djureinovic, T., Robinson, K., Anderlid, B. and Schoumans, J. (2008) 'CHD7 mutation spectrum in 28 Swedish patients diagnosed with CHARGE syndrome', *Clin Genet* 74(1): 31-8.

Winnier, G. E., Kume, T., Deng, K., Rogers, R., Bundy, J., Raines, C., Walter, M. A., Hogan, B. L. and Conway, S. J. (1999) 'Roles for the winged helix transcription factors MF1 and MFH1 in cardiovascular development revealed by nonallelic noncomplementation of null alleles', *Dev Biol* 213(2): 418-31.

Winter, E. M. and Gittenberger-de Groot, A. C. (2007) 'Epicardium-derived cells in cardiogenesis and cardiac regeneration', *Cell Mol Life Sci* 64(6): 692-703.

Winter, E. M., Grauss, R. W., Hogers, B., van Tuyn, J., van der Geest, R., Lie-Venema, H., Steijn, R. V., Maas, S., DeRuiter, M. C., deVries, A. A. et al. (2007) 'Preservation of left ventricular function and attenuation of remodeling after transplantation of human epicardium-derived cells into the infarcted mouse heart', *Circulation* 116(8): 917-27.

Winter, E. M., van Oorschot, A. A., Hogers, B., van der Graaf, L. M., Doevendans, P. A., Poelmann, R. E., Atsma, D. E., Gittenberger-de Groot, A. C. and Goumans, M. J. (2009) 'A new direction for cardiac regeneration therapy: application of synergistically acting epicardium-derived cells and cardiomyocyte progenitor cells', *Circ Heart Fail* 2(6): 643-53.

Xu, H., Morishima, M., Wylie, J. N., Schwartz, R. J., Bruneau, B. G., Lindsay, E. A. and Baldini, A. (2004) 'Tbx1 has a dual role in the morphogenesis of the cardiac outflow tract', *Development* 131(13): 3217-27.

Xu, Z., Gutierrez, L., Hitchens, M., Scherer, S., Sater, A. K. and Wells, D. E. (2008) 'Distribution of polymorphic and non-polymorphic microsatellite repeats in Xenopus tropicalis', *Bioinform Biol Insights* 2: 157-69.

Yagi, H., Furutani, Y., Hamada, H., Sasaki, T., Asakawa, S., Minoshima, S., Ichida, F., Joo, K., Kimura, M., Imamura, S. et al. (2003) 'Role of TBX1 in human del22q11.2 syndrome', *Lancet* 362(9393): 1366-73.

Yamagishi, H. and Srivastava, D. (2003) 'Unraveling the genetic and developmental mysteries of 22q11 deletion syndrome', *Trends Mol Med* 9(9): 383-9.

Yang, W., Klaman, L. D., Chen, B., Araki, T., Harada, H., Thomas, S. M., George, E. L. and Neel, B. G. (2006) 'An Shp2/SFK/Ras/Erk signaling pathway controls trophoblast stem cell survival', *Dev Cell* 10(3): 317-27.

Yelin, R., Yelin, D., Oh, W. Y., Yun, S. H., Boudoux, C., Vakoc, B. J., Bouma, B. E. and Tearney, G. J. (2007) 'Multimodality optical imaging of embryonic heart microstructure', *J Biomed Opt* 12(6): 064021.

Yergeau, D. A., Johnson Hamlet, M. R., Kuliyev, E., Zhu, H., Doherty, J. R., Archer, T. D., Subhawong, A. P., Valentine, M. B., Kelley, C. M. and Mead, P. E. (2009) 'Transgenesis in Xenopus using the Sleeping Beauty transposon system', *Dev Dyn* 238(7): 1727-43.

Yergeau, D. A. and Mead, P. E. (2007) 'Manipulating the Xenopus genome with transposable elements', *Genome Biol* 8 Suppl 1: S11.

Zhang, C., Basta, T. and Klymkowsky, M. W. (2005) 'SOX7 and SOX18 are essential for cardiogenesis in Xenopus', *Dev Dyn* 234(4): 878-91.

Zhang, J., Somani, A. K. and Siminovitch, K. A. (2000) 'Roles of the SHP-1 tyrosine phosphatase in the negative regulation of cell signalling', *Semin Immunol* 12(4): 361-78.

Zhou, B., von Gise, A., Ma, Q., Hu, Y. W. and Pu, W. T. (2010) 'Genetic fate mapping demonstrates contribution of epicardium-derived cells to the annulus fibrosis of the mammalian heart', *Dev Biol* 338(2): 251-61.

Zhou, Y., Ching, Y. P., Kok, K. H., Kung, H. F. and Jin, D. Y. (2002) 'Post-transcriptional suppression of gene expression in Xenopus embryos by small interfering RNA', *Nucleic Acids Res* 30(7): 1664-9.

Appendix 2

Immunoisolation of protein complexes from *Xenopus*

Preface

This work was published as an in-depth technical article as part of the series *Xenopus Protocols: Post-Genomic Approaches* (ed. Stefan Hoppler and Peter D. Vize) in the journal *Methods in Molecular Biology*. It is based on a collaboration between our laboratory and Ileana Cristea's group at Princeton University to optimize the immunoisolation of protein complexes from *Xenopus* embryonic tissue. I contributed a western blot demonstrating assessment of isolation efficiency of a GFP-tagged protein and to the writing of the manuscript itself. The article was conceived and finalized by Frank Conlon and Ileana Cristea.

Conlon F.L., Miteva Y., Kaltenbrun E., Waldron L., Greco T.M., and Cristea I.M. (2012) Immunoisolation of protein complexes from *Xenopus*. *Methods in Molecular Biology*, vol 917: 369-390.

ABSTRACT

The immunoaffinity isolation of protein complexes is an essential technique for the purification and concentration of protein complexes from cells and tissues. In this chapter we present the methodologies for the purification of proteins and protein complexes from *Xenopus laevis* and *Xenopus tropicalis.* Specific to this protocol are the techniques for the cryolysis of *Xenopus* cells and tissues, a procedure that limits contamination from yolk proteins while preserving endogenous protein complexes, the methodologies for immunoaffinity purification of proteins using magnetic beads, and the protocols for western blot analysis. In addition, the procedures in this chapter can be extended to use with proteomic analysis of protein complexes as presented in the following chapter.

INTRODUCTION

It is becoming increasingly clear that many forms of human disease are associated with defects in genes that are required for early steps in embryonic development. Moreover, the molecular and cellular pathways through which these genes function can be elucidated using established model systems such as the African clawed frog, *Xenopus*. *Xenopus* has numerous advantages as a model system in which to identify and characterize cellular and developmental processes particularly in regards to proteomic-based approaches. Most critically, unlike the mouse, the *Xenopus* embryo develops externally and the embryo is relatively large and is amenable to surgical manipulations, allowing defined regions to be excised and cultured in simple salt solutions. These classical approaches are complemented

by molecular techniques that allow the ectopic expression, overexpression, or knock-down of specific gene transcripts in the early embryo, and transgenic technologies.

Complementary to these approaches are emerging biochemical approaches. In this regard, *Xenopus* offers a unique model system for the identification and characterization of protein complexes *in vivo*. However, the use of these approaches has been limited due to the lack of optimized protocols for isolation of early stage *Xenopus* tissues and the large abundance of yolk proteins. As shown in Figure A2.1, this chapter describes methods for conducting immuno-precipitation of endogenous protein complexes in *Xenopus laevis* and *Xenopus tropicalis* which combines the cryogenic lysis of tissues with immunoisolation on magnetic beads. An overview of the approach is shown in Figure A2.1. Collectively, these approaches function to preserve endogenous protein complexes, limit problems associated with yolk platelets, and proved a specific isolation of a given protein.

METHODS AND EQUIPMENT

Obtaining *Xenopus laevis* embryonic tissue

1. Fine watchmaker's forceps such as Dumont number 5 forceps.
2. X. *laevis* embryos cultured to desired stage of development (Nieuwkoop, 1994)
3. 10X Modified Barth's Saline (MBS), pH 7.8: 880 mM NaCl, 10 mM KCl, 10 mM $MgSO_4$, 50 mM HEPES pH 7.8, 25 mM $NaHCO_3$. 1X MBS is made by mixing

100 mL of 10X stock solution with 700 µL 1 M $CaCl_2$ and adjusting the volume to 1 L with dH_2O. Store at room temperature.

4. 1% agarose plates for dissections: Weigh 1 g agarose and transfer to 250 mL Erlenmeyer flask containing 100 mL dH_2O. Heat flask in microwave until agarose has completely dissolved. Cool molten agarose until cool enough to hold flask. Pour a layer of agarose into small plastic petri dishes (5 cm). Allow agarose to set. Store plates at 4°C.
5. Plastic transfer pipettes
6. Liquid nitrogen
7. Syringe needle (19G1½)
8. 50 mL conical tubes
9. A dissecting microcope (e.g. Leica MZ6)

Tissue lysis and protein extraction

1. Retsch MM 301 Mixer Mill with 2 X 25 mL jars and 2 X 20 mm (tungsten carbide or stainless steel) grinding balls (Retsch, Newtown, PA).
2. Liquid nitrogen, Styrofoam container and a pair of long forceps
3. Windex
4. Methanol
5. 50 mL conical tubes
6. Ultrapure water

Immunoaffinity purification of protein complexes

Conjugation of magnetic beads

Unless otherwise stated all solutions can be stored at room temperature

1. Dynabeads M-270 Epoxy (Invitrogen).
2. Affinity purified antibodies against a protein of interest or tag (e.g., anti-GFP antibodies as shown below for the isolation of GFP-tagged proteins), or Immunoglobulin G (for isolation of Protein A-tagged proteins).
3. 0.1 M Sodium Phosphate buffer, pH 7.4: Prepare as 19 mM NaH_2PO_4, 81 mM Na_2HPO_4 in water and adjust pH to 7.4, if necessary. Filter sterilize (0.2 µm filter (Millipore)). Store at 4°C.
4. 3 M Ammonium Sulfate: Prepare in 0.1 M Sodium Phosphate buffer, pH 7.4. Filter sterilize (0.2 µm filter (Millipore)).
5. 100 mM Glycine-HCl, pH 2.5: Prepare in water. Adjust pH to 2.5 with HCl. Filter sterilize (0.2 µm filter (Millipore)). Store at 4°C.
6. 10 mM Tris, pH 8.8: Prepare in water. Adjust pH to 8.8 with HCl. Filter sterilize (0.2 µm filter (Millipore)).
7. 100 mM Triethylamine: Prepare fresh in water. CAUTION: toxic and extremely flammable. Must handle in a chemical hood and dispose of appropriately.
8. DPBS, pH 7.4 (Dulbecco's Phosphate-Buffered Saline (1X), liquid), (Invitrogen): Store at 4°C.
9. 0.5% Triton X-100: Prepare in DPBS. Store at 4°C.

10. 0.02% Sodium azide (NaN_3): Prepare in DPBS. Store at 4°C. CAUTION: NaN_3 is a toxic solid compound. Must handle in a chemical hood and dispose of appropriately.
11. Rotator (at 30°C)
12. Magnetic separation tube rack (Invitrogen)
13. Tube shaker (Tomy shaker)
14. Round bottom 2 mL Safe-Lock tubes (Eppendorf)
15. Ultrapure water (e.g., from a Milli-Q Integral Water Purification System)

Immunoaffinity purification

1. Frozen tissue powder (see section *Obtaining Xenopus laevis embryonic tissue*)
2. Optimized lysis buffer (See section *Tissue lysis and protein extraction*) prepared fresh prior to each experiment.
3. Magnetic beads conjugated with antibodies (see section *Conjugation of magnetic beads*)
4. 50 mL conical tubes
5. Polytron for tissue homogenization (e.g., PT 10-35 Polytron from Kinematica)
6. Centrifuge and rotor, compatible with 50 mL conical tubes and capable of 8000 x g at 4°C
7. Tube rotator at 4°C
8. Ultrapure dH_2O
9. Round bottom eppendorf tubes (Fisher)
10. Axygen Maxymum Recovery microcentrifuge tubes, 1.5 mL (VWR)

11. Bar magnets (for conical tubes) and magnetic separation rack (for eppendorf tubes) (Invitrogen)
12. Ammonium hydroxide, 14.8 M (Sigma). Store at 4°C.
13. Base elution buffer: Mix 4.826 mL of ultrapure H_2O, 5 µL of 0.5 M EDTA, pH 8.0, and 169 µL of ammonium hydroxide. Prepare fresh before use.
14. 4X LDS elution buffer: Dissolve 0.666 g of Tris-HCl, 0.682 g of Tris-Base, 0.8 g of LDS, and 0.006 g of EDTA (free acid) in ultrapure dH_2O to a final volume of 10 mL. Aliquot and store at -20°C.
15. 10X Reducing Agent (Invitrogen)
16. 1M iodoacetamide (IAA) (Sigma): Dissolve 0.185 g of iodoacetamide in 1 mL HPLC grade water. Dispense into 50 x 20 ml aliquots and store at -20°C
17. Heat block at 70°C

Assessment of immunoaffinity purification: Sample preparation

1. Reserved fractions (from section *Basic elution of immunoisolates*)
   a. Cell pellet (step 7)
   b. Input Supernatant (step 7)
   c. Flow-through (step 11)
   d. Primary eluate (step 21)
   e. Secondary eluate (step 18)
2. Ultrapure dH_2O
3. Acetone (-20°C)
4. 1.7 mL eppendorf tubes (Fisher)

5. Microcentrifuge
6. NuPAGE 4-12% Bis-Tris pre-cast SDS-PAGE gel, 10 well (Invitrogen)
7. Xcell SureLock Mini-Cell electrophoresis system (Invitrogen)
1. 20X NuPAGE MOPS SDS Running Buffer (Invitrogen)
8. 4X NuPAGE LDS Sample Buffer (Invitrogen)
9. 10X Reducing Agent (Invitrogen)
10. Heat block at 70°C

Assessment of immunoaffinity purification: SDS-PAGE and western blot analysis

1. Prepared fractions (from section *Assessment of immunoaffinity purification: Sample preparation*)
   a. Cell pellet (step 1)
   b. Input supernatant (step 2)
   c. Flow-through (step 3)
   d. Secondary eluate (step 4)
   e. Primary eluate (step 5)
2. NuPAGE 4-12% Bis-Tris gel, 10 well (Invitrogen)
3. Xcell SureLock Mini-Cell electrophoresis system (Invitrogen)
4. 20X NuPAGE MOPS SDS Running Buffer (Invitrogen)
5. 1X Running Buffer: Dilute 20X NuPAGE MOPS SDS Running Buffer in 700 mL of ultrapure water.
6. Precision Plus Protein Dual Color Molecular Weight Standards (BioRad)
7. 4X NuPAGE LDS Sample Buffer (Invitrogen)

8. 10X Reducing Reagent (Invitrogen)
9. PVDF membrane (BioRad)
10. Methanol
11. Transfer apparatus (e.g. Mini Trans-blot Cell from BioRad)
12. 10X Transfer Buffer: Dissolve 144 g glycine and 30.3 g Tris base in final volume of 1 L dH_2O. Prepare 1L of 1X Transfer Buffer containing 20% methanol. Chill at 4°C for 30min before use.
13. 2 x Whatman filter paper and 2 x sponges for transfer
14. 20X TBST: 200 mM Tris-HCl pH 8, 3 M NaCl, 2% Tween-20 in dH_20. Dilute to 1X with dH_20 for use.
15. Blocking Buffer: 5% non-fat dry milk powder in 1X TBST.
16. Appropriate primary and secondary antibodies, diluted in Blocking Buffer
17. Autoradiography cassette (FisherBiotech Cat# FBCA 57)
18. ECL chemiluminescent substrate kit (Thermo Scientific)
19. Autoradiography film (Kodak)

METHODS AND PROCEDURES

Obtaining *Xenopus laevis* embryonic tissue

Of all the proteins in *X. laevis* embryonic tissue, yolk proteins are among the most abundant, especially at earlier developmental stages when the embryo is still dependent on yolk for nutrients. The abundance of yolk proteins can be problematic when performing immunoaffinity purifications, as these proteins can nonspecifically

react with antibodies and mask a less abundant interaction. For this reason, it is desirable to remove as much of the yolk from the embryo as possible.

1. Fill a 1% agarose plate with cold 1X MBS. Transfer *X. laevis* embryos to MBS in agarose plate.
2. Using fine forceps and a dissecting microscope, remove as much of the yolk as possible from the rest of the embryo. Using a plastic transfer pipette, transfer the embryo to a new agarose plate containing fresh 1X MBS. Keep tissue on ice until all dissections are completed. Collect appropriate number of embryos for each immunopurification to be performed (See Note 1).
3. Using a syringe needle, poke 4 holes in the cap of a 50 mL conical tube. Remove cap and secure tube into a rack in a styrofoam cooler. Fill cooler and tube with liquid nitrogen.
4. Using a plastic transfer pipette, drop embryos one by one into liquid nitrogen in conical tube (see Note 4). When finished, replace the cap and screw on tightly. Remove the tube from the cooler (using a paper towel for protection) and invert to remove the liquid nitrogen. Store frozen tissue at -80°C.

Tissue lysis and protein extraction

Tissue lysis can be carried out utilizing several approaches, including homogenization in a detergent-containing lysis buffer, passage through a needle (different needle gauges can be tested for efficiency of lysis), and cryogenic tissue disruption using traditional mortar and pestle or a Mixer Mill. While the procedures

described below for immunoaffinity purification of protein complexes utilize as starting material tissue disrupted cryogenically using a Mixer Mill, the other types of tissue lysis can also be incorporated. We prefer the type of cryogenic disruption described below as it leads to an increased efficiency of extraction (i.e., isolation of the targeted protein) and decreased level of non-specific associations. This method has provided us with a reliable and effective means of cell lysis for isolating varied protein complexes (Cristea et al., 2005; Cristea et al., 2006; Carabetta et al., 2010; Goldberg et al., 2010; Moorman et al., 2010; Greco et al., 2011). In circumstances that require a mild tissue lysis, such as the maintenance of intact organelles or large structures, e.g postsynaptic densities (Selimi et al., 2009), cryogenic disruption may not be the method of choice.

Cryogenic tissue disruption

1. Clean one spatula, the Retsch Mixer Mill jars, and the grinding balls sequentially with ultrapure dH_2O, Windex, ultrapure dH_2O, and 100% methanol. Allow all parts to dry completely in a chemical hood.
2. Cool the jars and balls in liquid nitrogen (e.g., using a Styrofoam container filled with liquid nitrogen). Once cooled (i.e., liquid nitrogen no longer appears to be bubbling) remove them from the liquid nitrogen container using a pair of long forceps and place the frozen tissue into the jar. The tissue can fill up to a maximum of one third of the total volume of the jar for optimal cryogenic grinding (e.g., ~7 g frozen tissue pellets per 25 mL jar). Add the chilled ball on

top of the tissue (use one ball per jar), close the jar, and place it back into the liquid nitrogen container to cool.

3. Place the filled jars in the Retsch Mixer Mill holders. If only one jar contains frozen tissue for grinding, then use the other empty jar (without a ball) as a balance. Grind the tissue using 20 cycles of 2 minutes 30 seconds each at a frequency of 30 Hz. Place the jars in liquid nitrogen in between cycles to cool, and ensure that the jars are still tightly closed.
4. Open the jar and use a chilled spatula to transfer the frozen tissue powder to a 50 mL conical tube kept on dry ice. Work as quickly as possible to avoid thawing of the ground sample. Periodically chill the spatula in liquid nitrogen. Store the powder at -80°C until immunopurification is to be performed.

Optimization of lysis buffer and isolation conditions

Successful isolation of a protein of interest and its interacting partners is dependent on several criteria including protein abundance and subcellular localization, sample amount, affinity of the antibody used for immunoaffinity purification, efficiency of bead conjugation, and lysis buffer conditions for immunoaffinity purification. During the cell lysis and protein isolation steps it is crucial to extract and preserve the targeted protein with its interactions in a soluble fraction. Therefore, the lysis buffer conditions utilized prior and during the affinity purification have to be optimized for each protein of interest before proceeding with larger scale immunoaffinity purifications for proteomics studies. This can be done by performing small scale experiments (i.e., 20 embryos per immunopurification) that

use western blotting to assess 1) the efficiency of protein solubilization (see procedure below) and 2) efficiency of isolation (see section *Assessment of immunoaffinity purification*). It is recommended to compare at least three lysis buffer conditions with varied levels of stringency. Generally, the stringency of a lysis buffer is determined by the concentrations and combinations of detergents and salts. Table A2.1 provides examples of frequently used detergents, and Table A2.2 lists several lysis buffers that differ slightly in their compositions and were successfully utilized in immunoaffinity purifications of protein complexes from varied species.

1. Split cryogenically ground tissue into equal small aliquots (e.g., 0.1 g) (see Note 2). Ensure that the tissue power does not thaw during the weighing.
2. Place the small aliquots on ice (4°C) and add a different lysis buffer (5 mL buffer per 1 g cells) to each sample.
3. Homogenize the tissue powder in the buffer by vortexing for 1 min with intermittent cooling. This step is different than the usual homogenization for immunoaffinity purifications, which uses a polytron and a larger volume for the starting material.
4. Separate the soluble and insoluble fractions by centrifugation at 8000 x g at 4°C for 10 minutes. Recover soluble fraction and label “supernatant”
5. Wash the pellet in water and discard supernatant. Extract pellet by sequential sonication then boiling at 95°C for 5 min in 50 mM Tris-HCl, pH 7.4, containing 2% SDS. Centrifuge at 20,000 x g for 10 min. Recover supernatant and label “Pellet”.

6. Assess the levels of bait protein in the supernatant and pellet fractions (5 – 10% aliquots) using western blotting and antibodies against either the affinity tag (if present) or the endogenous protein.
7. To proceed with a larger scale immunoaffinity purification for proteomics analyses, select the lysis buffer condition that provides the highest proportion of bait protein in the soluble fraction, at the lowest necessary stringency. This will allow for a balance between an efficient extraction of the protein of interest and maintenance of interacting partners (see Note 3).

Immunoaffinity purification of protein complexes

Conjugation of magnetic beads

This protocol has been optimized for conjugation of Dynabeads M-270 Epoxy, however it can also be applied for conjugation of other types of magnetic beads with larger or smaller diameters. In such cases, it is important to adjust the amount of antibody used for conjugation, depending on the bead capacity of binding. This protocol can be utilized for conjugating beads with high-affinity purified in-house developed antibodies as well as commercially available ones, provided their storage buffer doesn't hinder covalent conjugation to Epoxy.

It is best to start this protocol in the late afternoon and perform all washing steps (Step 7-10) in the morning of the following day. Unless otherwise stated all steps should be performed at room temperature. Do not allow the beads to dry out (i.e., do not keep the beads without a washing solution in between the steps).

1. Weigh out the necessary amount of magnetic Dynabeads in a round-bottom tube.
    a. Round-bottom tubes are preferred to avoid the trapping of beads in conical-shape tubes during the conjugation.
    b. The necessary amount of beads is dependent on the purpose of the experiment and the abundance of the protein that will be immunoaffinity purified. An approximate guidance: 1-2 mg beads are appropriate for small-scale optimization experiments, 5-7 mg beads are usually sufficient for performing single immunoaffinity purifications, and 10-20 mg beads are suitable for highly abundant proteins.
2. Add 1 mL Sodium Phosphate buffer pH 7.4 to the beads; mix by vortexing for 30 sec, followed by 15 min on a tube shaker (vigorous setting).
3. Place the tube on a magnetic rack. After all the beads settle towards the magnetic side, discard the buffer.
4. Remove the tube from the rack. Add 1 mL Sodium Phosphate buffer pH 7.4. Mix by vortexing for 30 sec and remove the buffer in the same manner as above.
5. Remove the tube from the rack. Add, in this order, the necessary amount of antibodies, Sodium Phosphate buffer, and Ammonium Sulfate solution.
    a. The optimal total volume during the beads conjugation (that includes the antibody, Sodium Phosphate buffer, and Ammonium Sulfate solution) is ~ 20 µl/mg beads

b. As a guideline of amounts of antibodies or IgG that we routinely use: 8-10 µg Ab/mg beads for commercially available antibodies and IgG, and 3-5 µg Ab/mg beads for purified high-affinity antibodies (e.g., in-house developed anti-GFP antibodies).

c. The 3 M Ammonium Sulfate solution is added last and will be one third of total volume to give a final concentration of 1 M.

d. For example, to conjugate 18 mg beads, use a total volume of 360 µL. For this, add 54 µg antibody to beads (if using 3 µg Ab/mg beads), then add 0.1 M Sodium Phosphate Buffer (volume 0.1 M Sodium Phosphate Buffer = 360 µL – volume of antibody used – 66.7 µL 3M Ammonium Sulfate), then add 66.7 µL of 3 M Ammonium Sulfate.

6. Secure the tube with parafilm and rotate bead slurry overnight on rotator at 30°C.

7. The next morning, place the tube with bead slurry on a magnetic rack. Remove and reserve the supernatant to assess the efficiency of bead conjugation by SDS-PAGE (See Note 4).

8. Wash the beads sequentially with the following buffers. For each wash, gently resuspend the beads in 1 mL of the buffer, then place the tube on the magnet and remove buffer. “FAST” indicates that buffer should not be in contact with beads for longer than it takes to resuspend them:

   a. 1 mL of Sodium Phosphate buffer

   b. 1 mL 100 mM Glycine-HCl, pH 2.5 (FAST)

   c. 1 mL 10 mM Tris-HCl pH 8.8

d. 1 mL 100 mM Triethylamine solution (FAST)

e. 4 x 1 mL DPBS

f. 1 mL DPBS containing 0.5% Triton X-100. Leave the tube on a Tomy shaker (gentle setting) for 15 min.

g. 1 mL DPBS

9. Beads can be used immediately or stored at 4°C in DPBS containing 0.02% NaN_3. For beads stored for future use, measure the final volume of the bead slurry (the bead size will contribute to the final volume) and make a note of the volume required for one mg beads as this will permit known aliquots of beads to be removed for multiple immunoaffinity purifications. Beads should be used within 2 weeks of conjugation. After 1 month of storage, their efficiency for isolation decreases by approximately 40%.

Immunoaffinity purification: Basic elution of immunoisolates

It is important to prepare all necessary reagents beforehand. Carry out all procedures on ice unless otherwise noted. At several steps during the protocol aliquots of samples (indicated with "RESERVE") are taken to assess bait protein extraction and isolation efficiency (see section *Assessment of immunoaffinity purification*).

Day 1

1. Prepare appropriate volume of optimized lysis buffer as determined in section 3.2.2. Pre-cool to 4°C. Add protease inhibitors just before use. Prepare 10 mL

of wash buffer per sample (used in steps 6, 11 – 13), which is usually identical in composition to the optimized lysis buffer, except protease and phosphatase inhibitors cocktails are not included.

2. Incubate the frozen tissue powder on ice for 1 - 2 min, but do not thaw. Proceed immediately to step 3.
3. Resuspend the frozen tissue powder in appropriate volume of lysis buffer by first adding a small amount of lysis buffer and swirling homogenate to solubilize pellet. Continue to add lysis buffer and gently mixing by hand until tissue powder has been completely solubilized (see Note 5).
4. Run Polytron 10 sec in ultrapure dH_2O to wash. Ensure that the tissue homogenate occupies ≤ 1/3 of the conical tube volume. Subject tissue lysates to Polytron homogenization for 2 x 15 second (speed = 22.5k), resting the sample on ice for a few minutes between homogenizations. If processing additional samples, rinse and run Polytron in ultrapure dH_2O to wash out excess lysate. When finished, perform a final rinse with methanol.
5. Centrifuge the lysate at 8000 x g at 4°C for 10 minutes.
6. During centrifugation, place tube containing antibody-conjugated magnetic beads on a magnetic rack for 30 – 60 secs. Discard the storage buffer and wash with 3 x 1 mL wash buffer by gently pipeting up and down to resuspend the beads. Do not vortex antibody-conjugated beads. Suspend beads in 100 – 200 mL of wash buffer.
7. Carefully pour the clarified lysates (supernatant) into new 50 mL conical tubes (see Note 6). RESERVE (i) the cell pellet and (ii) 40 mL of the input

supernatant (See section *Assessment of immunoaffinity purification* for analysis).

8. Gently flick tube of antibody-conjugated beads to mix beads in solution. Pipet the appropriate amount of beads into the clarified lysates.
9. Rotate the lysates with beads on a rotator at 4°C for 1 hour. Do not use longer incubation times as this promotes the accumulation of non-specific binding and loss of weak interacting partners.
10. During incubation, prepare base elution buffer and 1X LDS elution buffer (see Note 7).
11. Attach a bar magnet to the lysates/bead suspension tube using a rubber band. Incubate on ice for 5 min. RESERVE the flow-through (unbound) fraction by pouring the supernatant into a clean conical tube (see section *Assessment of immunoaffinity purification* for analysis)
12. Resuspend the beads in 1 mL of wash buffer and transfer the bead slurry to a round-bottom eppendorf tube.
13. Place on a magnetic rack for 30 sec to pellet the beads and discard wash buffer. Perform this procedure between all subsequent wash steps.
14. Wash the beads 3 x 1 mL wash buffer. On the third wash, transfer the bead slurry to a clean round-bottom eppendorf tube, then pellet beads and discard wash buffer.
15. Wash the beads 2 x 1 mL with wash buffer.

16. Add 1 mL DPBS to beads and transfer slurry to clean round-bottom eppendorf tube. Repeat wash once with 1 mL of DPBS to remove residual detergent. Quantitatively remove DPBS wash.
17. Add 750 ml of base elution buffer. Incubate at RT for 20 min while shaking (see Note 8).
18. Place the tube on the magnetic rack and transfer the eluate to an Axygen microcentrifuge tube. Freeze primary eluate in liquid nitrogen and evaporate to dryness overnight by vacuum centrifugation.
19. Perform a second elution from the beads by suspending the beads in 40 µL of 1X LDS elution buffer containing 50 mM DTT, incubating at 70°C for 10 min, and then at RT for 10 min while shaking. Place the tube on a magnetic rack and transfer the eluate to a clean microcentrifuge tube. RESERVE 10% (4 µl) of the secondary eluate in a clean microcentrifuge tube (see section *Assessment of immunoaffinity purification* for analysis). Freeze remaining 90% of secondary eluate in liquid nitrogen and store at -20°C.
20. Proceed to *Assessment of immunoaffinity purification* to prepare reserved samples for Western blot analysis. Continue with step 21 the following day.

Day 2

21. Remove dried eluate from the Speedvac.
    a. If performing SDS-PAGE-in-gel digestion (see Note 4), suspend dried eluate in 40 mL of 1X NuPAGE sample buffer containing 1X reducing agent and heat at 70°C for 10 min. RESERVE 10% (4 µl) of the eluate in a clean

microcentrifuge tube. Add 4 ml of 1 M iodoacetamide to remaining 90% of primary eluate and incubate 30 min at RT protected from light. Freeze in liquid nitrogen and store at -20°C or proceed immediately to proteomic analysis (see (Greco et al., 2012)

b. If in-solution digestion is to be performed (see Note 4), suspend dried eluate in 40 mL of 1X LDS elution buffer containing 50 mM DTT and heat at 70°C for 10 min. RESERVE 10% (4 µl) of the eluate in a clean microcentrifuge tube. Freeze remaining 90% of primary eluate in liquid nitrogen and store at -20°C or proceed immediately to proteomic analysis (see (Greco et al., 2012).

Immunoaffinity purification: Alternate procedure (detergent elution of immunoisolates; see Note 7)

Day 1

1. Perform steps 1 – 16 as described above, except preparation of base elution buffer can be omitted (step 10).
2. Add 40 µl of 1X LDS elution buffer to beads. Incubate 10 min at 70°C, then 10 min at RT while shaking.
3. Pellet beads on magnetic rack and transfer primary eluate to an Axygen microcentrifuge tube.
4. Repeat Steps 2 and 3, transferring secondary eluate to an Axygen microcentrifuge tube.
5. Add 2.0 mL of 1 M DTT to primary and secondary eluates. Heat at 70°C for 10 min. RESERVE 10% (4 µl) of eluates in clean microcentrifuge tubes.

6. If performing in-gel digestion (see Note 8), add 4 µl of 1 M iodoacetamide to remaining 90% of eluates and incubate at RT for 30 min protected from light. If performing in-solution digestion (see Note 8), proceed directly to step 7.
7. Freeze remaining 90% of eluates in liquid nitrogen and store at -20°C or proceed immediately to proteomic analysis (see (Greco et al., 2012).

Assessment of immunoaffinity purification: Sample preparation

Reserved sample aliquots from section *Immunoaffinity purification* are prepared for SDS-PAGE and Western blot analysis. The recommended amount of each aliquot analyzed is provided as a starting point, and may need further optimization for differences in input material and bait protein abundance.

1. Cell Pellet
    a. Wash the cell pellet with 1.0 mL dH_2O. Homogenize washed cell pellet in 1.0 mL of 2% SDS, transfer to microcentrifuge tube, and heat at 70°C for 10 min. Centrifuge at maximum speed for 5 minutes at RT (see Note 9).
    b. Remove aliquot of SDS-soluble pellet fraction that corresponds to an identical percent of the input supernatant. For example, assuming a 40 µL aliquot of input supernatant was reserved from a total lysis volume of 10 mL, a 4 µL aliquot of the pellet sample should be removed.
    c. Dilute aliquot of SDS-soluble pellet fraction to a final volume of 60 µL containing 1X NuPAGE LDS Sample Buffer/1X Reducing Agent.
2. Input Supernatant

a. Dilute 40 µL of reserved input supernatant to a final volume of 60 µL containing 1X NuPAGE LDS Sample Buffer/1X Reducing Agent.

3. Flow-through (see Note 10)
   a. Transfer 10% of flow-through to clean tube. Slowly add 4 volumes of -20°C acetone. Vortex briefly. Incubate at -20°C for at least 1 hr.
   b. Centrifuge at 3000 x g at 4°C for 10 min. Pour off supernatant
   c. Briefly wash pellet with 4 volumes of 80% acetone/20% dH_2O and discard.
   d. Air dry pellet for 5 min, then partially solubilize in 40 µL of 1X NuPAGE LDS Sampler Buffer/1X Reducing Agent by gentle agitation.
4. Secondary Eluate
   a. Dilute 4 µL (10%) of the secondary eluate into a final volume of 40 µL 1x NuPAGE LDS Sample Buffer/1X Reducing Agent.
5. Primary Eluate (prepared the following day, see Note 11)
   a. Dilute 4 µL (10%) of the primary eluate into a final volume of 40 µL 1x NuPAGE LDS Sample Buffer/1X Reducing Agent.
6. Heat all samples at 70°C for 10 minutes. Freeze the samples at -20°C until ready to proceed with SDS-PAGE and western blot analysis.

Assessment of immunoaffinity purification: SDS-PAGE and western blot analysis

In this protocol the efficiency of immunoaffinity isolation of the bait protein is assessed by comparing 5 samples reserved at progressing stages of the immunoaffinity purification procedure: 1) cell pellet, 2) input supernatant, 3) flow-through, 4) secondary eluate, and 5) primary eluate (see section *Immunoaffinity*

purification). While the amount of sample prepared (see section *Sample preparation*) is sufficient for duplicates analyses, the protocol below details a single experiment. A representative western blot is shown below (Figure A2.2A) indicating efficient isolation (no protein remaining in the flow-through) and recovery of the intended GFP-tagged bait protein (a majority of the protein was in the primary eluate).

1. Set up the Xcell SureLock Mini-Cell electrophoresis system:
    a. Remove the white strip and the upper comb from the NuPAGE 4-12% Bis-Tris pre-cast SDS-PAGE gel and rinse wells with ultrapure dH_20. Place the gel in the apparatus, using a buffer dam for the opposing side, then lock the assembly in place.
    b. Fill the inner chamber with 200 mL and the outer chamber with 500 mL of 1X Running Buffer.
2. Thaw fractions if previously frozen and load into wells as follows: Lane 2, 10 µL Molecular Weight Standards; Lane 3, 30 µl of input supernatant; Lane 4, 30 µl of cell pellet; Lane 5, 20 µl of primary eluate; Lane 6, 20 µl of secondary eluate; Lane 8, 20 µl of flow-through; Empty lanes, 20 µL of 1X LDS Sample Buffer.
3. Electrophorese for 5 min at 100 V, then 45 - 50 min at 200 V, or until the dye front has migrated all the way down the gel.
4. While the gel is running, cut 2 pieces of Whatman filter paper and one PVDF membrane to the appropriate gel size. Always handle the membrane with tweezers.

5. Pre-wet PVDF in methanol and soak along with 2 transfer sponges, 2 filter papers, in pre-cooled 1X Transfer Buffer at least 15 min at 4°C.
6. Open gel cassette to expose gel and discard the wells. Working with wet gloves, transfer gel (by the thick ridge at the bottom) into a plastic tray containing 1X Transfer buffer. Remove bottom ridge.
7. Assemble a WB "sandwich" in the tray with pre-soaked items. Layer them in a transfer cassette as follows, starting from the clear side of the cassette: sponge, filter paper, PVDF membrane, SDS-PAGE gel, filter paper (gently roll out any bubbles using a 15ml conical tube), sponge. Close the sandwich and place into transfer apparatus with black side of cassette (gel side) facing black (anode) side transfer core. Place ice tray and stir bar into apparatus. Pour ice-cold 1X Transfer Buffer into the apparatus until it covers fully the cassette.
8. Transfer at 100 V for 1.5 hrs at 4°C while stirring.
9. Open transfer cassette and discard the filter papers and gel. Verify the pre-stained Molecular Weight Standards transferred to the membrane.
10. Wash PVDF membrane with 1X TBST, discard, then add Blocking Buffer and incubate for 1 hour at RT on a rocking platform. Do not let the membrane dry.
11. Discard Blocking Buffer and add the primary antibody diluted in Blocking Buffer. Incubate for 1-2 hours at RT or overnight at 4°C.
12. Wash the membrane 3 x 20 mL in 1X TBST for 5 min while rocking at RT.
13. Add the secondary horseradish peroxidase-conjugated antibody diluted in Blocking Buffer. Incubate for 1 hour at RT.
14. Wash the membrane 4 x 20 mL in 1X TBST for 5 min while rocking at RT.

15. Mix ECL chemiluminescence substrates in 1:1 ratio (a total volume of 1 mL is usually sufficient to cover the membrane). Using tweezers, place the membrane on a dry plastic surface and apply the ECL solution, incubating for 1 minute. Blot off the excess substrate and place the membrane between a sheet protector or Saran-wrap and tape into a film cassette.
16. Carefully place a piece of autoradiography film on top of the membrane and close the cassette avoiding any film shifts as this will result in smeared bands. An initial exposure of 30 sec will indicate whether subsequent exposures of longer or shorter duration are required.

Appropriate controls

To assess the specificity of immunoaffinity isolation it is critical to have a control sample analyzed in parallel, beginning from tissue lysis through the isolation of the target protein. The controls described below account for non-specific binding of proteins to magnetic beads, antibody, and affinity tag (when present).

GFP-tagged

Often the bait protein is expressed as a GFP fusion protein. Here, parallel isolations of the GFP-tagged protein and GFP alone are highly desirable. If the GFP-tagged protein is stably overexpressed by mRNA injection into embryos, it is necessary to generate a GFP-only tissue/animal in the same manner as the GFP fusion protein, i.e. mRNA injection of a GFP-only expression construct. Moreover, all treatment conditions and experimental variables, such as lysis buffer composition,

should be identical between the two isolations. Thus both the tag alone and the fusion protein can be immunoaffinity purified using identical preparations of antibody-conjugated magnetic beads. If lysis buffer conditions or other isolation variables are altered, such as incubation time of sample with antibody, an additional control should be performed.

FLAG-tagged

If the bait protein is tagged with FLAG, then a more appropriate control (compared to the GFP tag), is the respective cell/tissue/animal but under wild type conditions. For both FLAG-tagged and wild-type conditions, magnetic beads conjugated with an antibody against the FLAG tag should be utilized. Although this doesn't control for proteins that bind non-specifically to FLAG itself, non-specificity due to the antibody and beads can be determined.

Endogenous, non-tagged protein

In many experiments it is essential to immunoaffinity purify the bait protein at an endogenous level of expression (under its native promoter). Here, the control sample will use the identical cell/tissue/animal as for the experimental condition. In contrast to an affinity tag, the beads for the negative control are conjugated with either non-specific IgG or an IgG that lacks reactivity towards the endogenous bait protein. The control protein isolation will reveal interactions that bind non-specifically to the antibody and magnetic beads. A representative western blot from an

immunoisolation of endogenous Shp2 from *X. tropicalis* embryos is shown in Figure A2.2B.

NOTES

1. The number of embryos needed for each immunopurification is dependent on a number of criteria including protein abundance and solubility as well as the affinity of the antibody used for immunoisolation. For this reason, the optimal number of embryos and resulting amount of tissue must be optimized individually for each protein studied. Generally, 20-50 embryos per immunoisolation is a good starting point for small-scale experiments and may be scaled up for larger immunoaffinity purifications for proteomics studies.

2. If starting directly with a small amount of tissue, the sample could be ground using round-bottom eppendorf tubes or used directly for incubation with the various lysis buffers. While performing the cryogenic grinding is preferred to mimic the conditions that will be utilized for protein isolation, direct resuspension in lysis buffer is an alternative that can adequately guide selection of an optimal buffer composition.

3. The balance between extraction efficiency and maintenance of interacting partners can be further optimized by increasing the stringency of the buffer used to wash the magnetic beads relative to the buffer used for tissue homogenization.

4. To test the efficiency of bead conjugation, prepare the following samples for SDS-PAGE analysis: 1) Dilute ≥1 µg neat antibody with 2.5 µL 10x Reducing Agent and 6.25 µL 4x NuPAGE LDS Sample Buffer. Bring the sample to 25 µL total volume with dH_2O. 2) Calculate the amount of bead supernatant that is equivalent to the amount of neat antibody in the previous sample, assuming that no antibody successfully conjugated to the beads. Dilute this amount with 2.5 µL 10X Reducing Agent and 6.25 µL 4X NuPAGE LDS Sample Buffer. Bring sample to 25 µL with ultrapure H_2O. Heat samples for 10 minutes at 70°C. Centrifuge the samples at 20,000 x g for 3 minutes at room temperature and load onto an SDS-PAGE gel. Stain the gel with SimplyBlue SafeStain and look for a reduction in the amount of antibody in the lane containing the bead supernatant. Refer to Cristea *et al.* 2005 (Cristea et al., 2005) for the expected amount of unbound antibody resulting from differing amounts of antibody used in the conjugation.

5. After suspending tissue powder in lysis buffer, the solution may be slightly turbid, but should be devoid of tissue “clumps”. Do not proceed to Polytron (step 4) until a homogenous suspension is observed. If necessary, additional rotation for 10 – 20 min at 4°C can be performed.

6. If insoluble particles are present in supernatant after centrifugation, a pipet can be used to selectively transfer supernatant to clean 50 mL conical tube.

7. The base elution buffer is preferred as significantly less background protein contamination is observed under these elution conditions. However, if low recovery of bait protein is observed, e.g. when a high affinity antibody is used, an “Alternate Procedure” can be followed that uses a harsher detergent-based elution buffer (see above).

8. The selection of an in-gel or in-solution digestion approach depends largely on the properties and nature of the proteins within the samples, e.g. pI, molecular weight, hydrophobicity, complexity, dynamic range, and total yield. In general, for high complexity and large yield and/or dynamic range of protein abundances, an in-gel approach is often desired. For further discussion, see (Greco et al., 2012).

9. For viscous samples, brief sonication can be used to aid solubilization of cell pellet.

10. As the flow-through fraction often has higher protein concentration, the percent of material analyzed may need to be adjusted to prevent overloading of the SDS gel. For NuPAGE gels of 1.0 mm thickness, between 100 – 150 mg is recommended.

11. If base elution buffer is used, processing of the primary eluate and its reserved fraction is not performed until the day after the immunoisolation was started (see section *Immunoaffinity purification: Base elution*, step 20).

Figure A2.1. Immunoisolation of protein complexes from *Xenopus*.

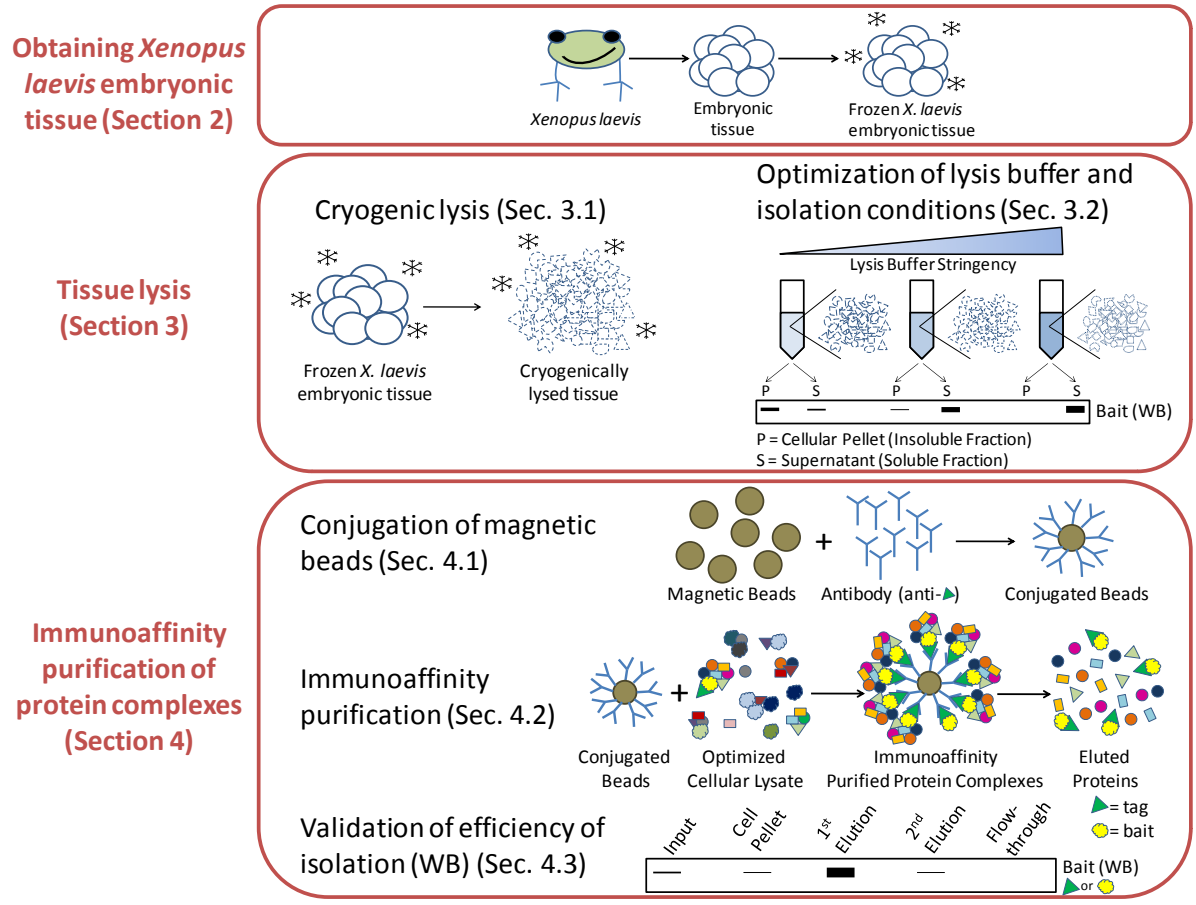

Figure A2.2. Assessment of isolation efficiency and specificity of immunoaffinity purification. (A) A GFP-tagged bait protein was isolated and eluted with the alternate detergent-based procedure. 10% of the following fractions were analyzed to assess the efficiency of isolation: FT, flow-through; PE, primary eluate; SE, secondary eluate. The majority of bait protein was found in the primary eluate. (B) Immunoaffinity purification of endogenous Shp2 protein from 100 stage 40 *Xenopus tropicalis* whole embryos. As a control for the specificity of the Shp2 antibody, a second immunopurification was performed using anti-V5 antibody-conjugated beads.

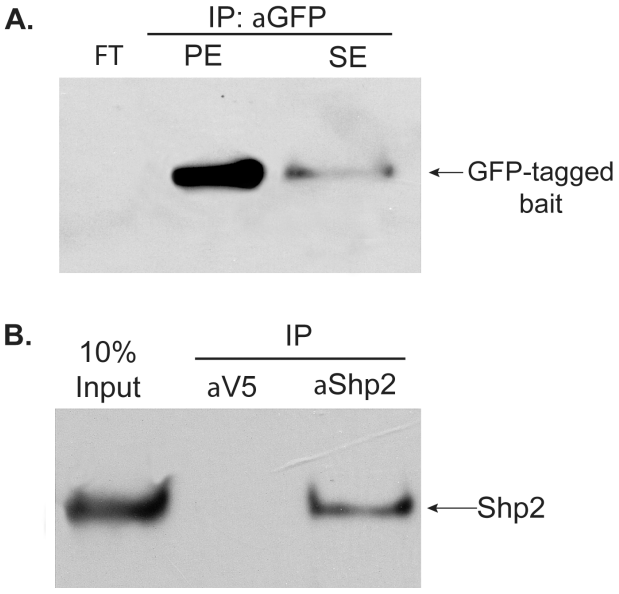

Table A2.1. Examples of detergents commonly used for cell lysis and their properties.

Detergent	Properties	Notes
Triton X-100	• Nonionic detergent • pH 6.0 to 8.0 (5% aqueous solution) • Critical micelle concentration (CMC): 0.22-24 mM • Soluble at 25°C in all proportions; Soluble in water, benzene, toluene, xylene, trichloroethylene, ethylene glycol, ethyl ether, ethanol, isopropanol, ethylene dichloride	• Depending on the utilized concentration, Triton is considered a relatively mild, non-denaturing detergent. Many enzymes remain active in 0.1%-0.5% Triton X-100 solution (e.g. Proteinase K is still active in 1% solution). • Can be used to preserve protein-lipid interactions
Sodium deoxycholate (DOC)	• Anionic detergent • pH 5.0 to 9.0 (1% aqueous solution) • CMC: 2-6 mM (0.083 to 0.249%, w/v). Micelle Molecular Weight: 2000 g (average), at concentrations above 2 mM • Soluble at 20°C; Soluble in water in less than 5% solution	• Common component of RIPA lysis buffer. • Suitable for isolating membrane associated proteins, and liposome preparation. Disrupts protein-lipid interactions.
Digitonin	• Nonionic detergent • pH: data not available • CMC: <0.5 mM, at 20-25°C. Micelle Molecular Weight: 70,000 g (average) • Soluble in water at ~5% (w/v); Must be heated to 95-98°C first, then cooled to room temperature. Soluble in ethanol at 10 mg/mL	• Suitable for analyzing membrane-bound proteins and solubilizing lipids.
Octyl-beta-glucoside	• Nonionic detergent • pH: data not available • CMC: 23-25 mM (0.6716 to 0.7300%, w/v); Micelle Molecular Weight: 8000 g • Soluble in water	• Suitable for studying membrane-associated proteins • Readily integrated with mass spectrometry studies (i.e.., does not interfere as much as other detergents with ionization in MALDI MS experiments)
Nonidet P-40	• Nonionic detergent • pH 5.0 to 8.0 (5% aqueous solution) • CMC: 0.059 mM (20-25C) • Soluble in water	• Milder alternative to Triton X-100; depending on the concentration it may not penetrate nuclear membranes.

Table A2.2. Examples of lysis buffers used for immunoaffinity purification of protein complexes.

Bait (GFP-tagged)	Description & Localization	Species & Sample type	Optimized Lysis Buffer	Ref.
Apl1	beta-adaptin of AP-2 complex; cellular membrane	*S. cerevisiae* cells	20 mM K-HEPES, pH 7.4, 110 mM KOAc, 2 mM $MgCl_2$, 0.1% Tween, 0.4% Triton, 200 mM NaCl, 1/100 (v/v) protease inhibitor mixture (20 mg/mL PMSF + 0.4 mg/mL pepstatin A), and 1/200 (v/v) protease inhibitor cocktail)	(Cristea et al., 2005)
Nup37	Member of nuclear pore complex; subunit of Nup107-160 subcomplex	*Homo sapiens* cells	20 mM K-HEPES, pH 7.4, 110 mM KOAc, 2 mM $MgCl_2$, 0.1% Tween, 0.5% Triton, 200 mM NaCl, 1/100 (v/v) protease inhibitor mixture (20 mg/mL PMSF + 0.4 mg/mL pepstatin A), and 1/200 (v/v) protease inhibitor cocktail)	(Cristea et al., 2005)
HDAC5	Histone deacetylase 5; Nucleus and Cytoplasm	*Homo sapiens* cells	20 mM HEPES-KOH, pH 7.4, 0.1 M potassium acetate, 2 mM $MgCl_2$, 0.1% Tween-20, 1 µM $ZnCl_2$, 1 µM $CaCl_2$, 0.5% Triton X-100, 250 mM NaCl, 4 µg/mL DNase, 1/100 (v/v) protease and phosphatase inhibitor cocktails	(Greco et al., 2011)
PAP I	poly(A) polymerase I; Cytoplasm and inner membrane	*Escherichia coli* cells	20 mM HEPES, pH 7.4, 0.11 M KOAc, 2 mM $MgCl_2$, 0.1% Tween-20 (v/v), 1 µM $ZnCl_2$, 1 µM $CaCl_2$, 1% Triton X-100, 0.5% Deoxycholate, 150 mM NaCl, 1:100 protease inhibitor cocktail, 1:200 phenylmethylsulphonyl fluoride	(Carabetta et al., 2010)
H3	Histone 3 isoforms; Nucleus	*Mus musculus* ES cells	20 mM K-HEPES, pH 7.4, 110 mM K-acetate, 0.1% Tween 20, 0.5% Triton, 300 mM NaCl, and 1/100 (v/v) protease inhibitor cocktail	(Goldberg et al., 2010)
nsP3	Sindbis nonstructural protein 3; Cytoplasm	Sindbis-infected *Rattus Norvegicus* cells	20 mM K-HEPES, pH 7.4, 110 mM KOAc, 2 mm $MgCl_2$, 0.1% Tween 20, 1% Triton, 0.5% deoxycholate, 500 mM NaCl, 25 units/mL DNase, 1/100 (v/v) protease inhibitor mixture	(Cristea et al., 2006)
PSD (via VGluRδ2)	postsynaptic densities; cerebellar excitatory synapses	*Mus musculus* tissue	10 mM HEPES, pH 7.4, 2 mM $CaCl_2$, 132 mM NaCl, 3 mM KCl, 2 mM $MgSO_4$, 1.2 mM NaH_2PO_4, 0.5% Triton X-100, 1/100 (v/v/) protease inhibitor cocktail	(Selimi et al., 2009)

REFERENCES

Carabetta, V. J., Silhavy, T. J. and Cristea, I. M. (2010) 'The response regulator SprE (RssB) is required for maintaining poly(A) polymerase I-degradosome association during stationary phase', *J Bacteriol* 192(14): 3713-21.

Cristea, I. M., Carroll, J. W., Rout, M. P., Rice, C. M., Chait, B. T. and MacDonald, M. R. (2006) 'Tracking and elucidating alphavirus-host protein interactions', *J Biol Chem* 281(40): 30269-78.

Cristea, I. M., Williams, R., Chait, B. T. and Rout, M. P. (2005) 'Fluorescent proteins as proteomic probes', *Mol Cell Proteomics* 4(12): 1933-41.

Goldberg, A. D., Banaszynski, L. A., Noh, K. M., Lewis, P. W., Elsaesser, S. J., Stadler, S., Dewell, S., Law, M., Guo, X., Li, X. et al. (2010) 'Distinct factors control histone variant H3.3 localization at specific genomic regions', *Cell* 140(5): 678-91.

Greco, T. M., Miteva, Y., Conlon, F. L. and Cristea, I. M. (2012) 'Complementary proteomic analysis of protein complexes', *Methods in molecular biology* 917: 391-407.

Greco, T. M., Yu, F., Guise, A. J. and Cristea, I. M. (2011) 'Nuclear import of histone deacetylase 5 by requisite nuclear localization signal phosphorylation', *Mol Cell Proteomics* 10(2): M110 004317.

Moorman, N. J., Sharon-Friling, R., Shenk, T. and Cristea, I. M. (2010) 'A targeted spatial-temporal proteomics approach implicates multiple cellular trafficking pathways in human cytomegalovirus virion maturation', *Mol Cell Proteomics* 9(5): 851-60.

Nieuwkoop, P., Faber, J. (1994) *Normal Table of Xenopus laevis*, New York: Garland Publishing.

Selimi, F., Cristea, I. M., Heller, E., Chait, B. T. and Heintz, N. (2009) 'Proteomic studies of a single CNS synapse type: the parallel fiber/purkinje cell synapse', *PLoS Biol* 7(4): e83.